AD-A090 827 BIRMINGHAM UNIV (ENGLAND) DEPT OF TRANSPORTATION AND--ETC F/G 13/2
FLEXIBLE PAVEMENT ANALYSIS.(U)
MAY 80 M S SNAITH, D MCMULLEN DA-ERO-78-G-125
UNCLASSIFIED NL

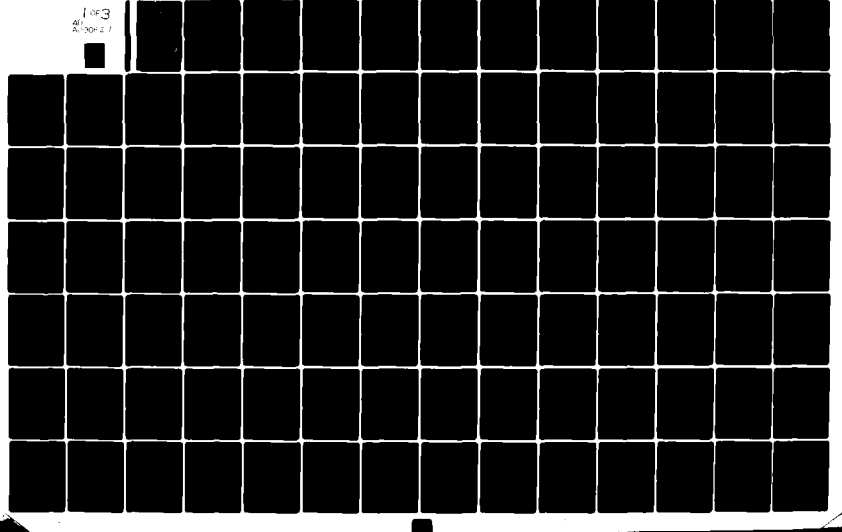

LEVEL II (12)

AD A090027

FLEXIBLE PAVEMENT ANALYSIS

FINAL TECHNICAL REPORT

by

M S SNAITH
D McMULLEN
R J FREER-HEWISH
A SHEIN

DDC FILE COPY

Contractor UNIVERSITY OF BIRMINGHAM
DEPARTMENT OF TRANSPORTATION
AND ENVIRONMENTAL PLANNING

DTIC ELECTE OCT 28 1980 S D A

EUROPEAN RESEARCH OFFICE
United States Army

GRANT NO DAERO-78-G-125

DISTRIBUTION STATEMENT A
Approved for public release;
Distribution Unlimited

MAY 1980

80 10 27 011

Approved for public release, distribution unlimited

UNCLASSIFIED

SECURITY CLASSIFICATION OF THIS PAGE (When Data Entered)

REPORT DOCUMENTATION PAGE

READ INSTRUCTIONS BEFORE COMPLETING FORM

1. REPORT NUMBER
2. GOVT ACCESSION NO. AD-A090827
3. RECIPIENT'S CATALOG NUMBER

4. TITLE (and Subtitle)
Flexible Pavement Analysis

5. TYPE OF REPORT & PERIOD COVERED
Final Technical Report.
Dec 78 — May 80

6. PERFORMING ORG. REPORT NUMBER

7. AUTHOR(s)
M. S. Snaith D. McMullen
R. J. Freer-Hewish A. Shein

8. CONTRACT OR GRANT NUMBER(s)
DAERO-78-G-125

9. PERFORMING ORGANIZATION NAME AND ADDRESS
Department of Transporation & Environmental Planning - University of Birmingham
Birmingham B15 2TT, England

10. PROGRAM ELEMENT, PROJECT, TASK AREA & WORK UNIT NUMBERS
6.1102A 1T161102BH57-01

11. CONTROLLING OFFICE NAME AND ADDRESS
U. S. Army Research , Development & Standardization Group - United Kingdom
Box 65, FPO NY 09510

12. REPORT DATE
May 1980

13. NUMBER OF PAGES
203

14. MONITORING AGENCY NAME & ADDRESS(if different from Controlling Office)

15. SECURITY CLASS. (of this report)
None

15a. DECLASSIFICATION/DOWNGRADING SCHEDULE

16. DISTRIBUTION STATEMENT (of this Report)
Approved for public release; distribution unlimited

17. DISTRIBUTION STATEMENT (of the abstract entered in Block 20, if different from Report)

18. SUPPLEMENTARY NOTES

19. KEY WORDS (Continue on reverse side if necessary and identify by block number)
Flexible pavements, soil mechanics, pavement analysis, pavement performance, transient deflection, crack propagation

20. ABSTRACT (Continue on reverse side if necessary and identify by block number)
Part I describes the pavement analysis program DEFPAV. The development of pavement models for two sections of road is described in detail; they predict the values of transient deflection and rut depth growth. The use of the program in analyzing the effect of surface temperature on transient deflections is described. An investigation of the effect of crack propagation through a bituminous surface layer is also reported.

(continued)

DD FORM 1 JAN 73 1473 EDITION OF 1 NOV 65 IS OBSOLETE

UNCLASSIFIED

SECURITY CLASSIFICATION OF THIS PAGE (When Data Entered)

Part II describes a method of overlay thickness selection for flexible pavements. A rational selection of bituminous overlay may be made with the aid of a transient deflection measurement and a single computational procedure which is suitable for use on a modern programmable calculation.

ABSTRACT

The report describes work undertaken at the Queens University of Belfast and the University of Birmingham in the area of flexible pavement analysis.

The first part deals with the enhanced pavement analysis program DEFPAV, which is now suitable for use by a practising Engineer as well as the researcher. The development of pavement models for two sections of road in Northern Ireland is described in detail. These models have been used with considerable success to predict the values of transient deflection and rut depth growth in the field. The program has also been used to investigate the effect of surfacing temperature on transient deflection and to compare deflection measurements made with the use of a Standard Benkelman Beam lorry and the first British built Deflectograph. An investigation of the effect of crack propagation through a bituminous layer has been carried out. Other applications of the program considered were the derivation of axle equivalence factors and the effect of fabric inclusions in a pavement structure.

The second part describes a method of overlay thickness selection for flexible pavements suitable for developing countries where the minimum technical infrastructure is available. The method makes use of the expertise developed on the contract together with advances reported by a number of research centres working in similar fields. It is shown that a rational selection of bituminous overlay may be made with the aid of a transient deflection measurement and a simple computational procedure which is suitable for mounting on a modern programmable calculator.

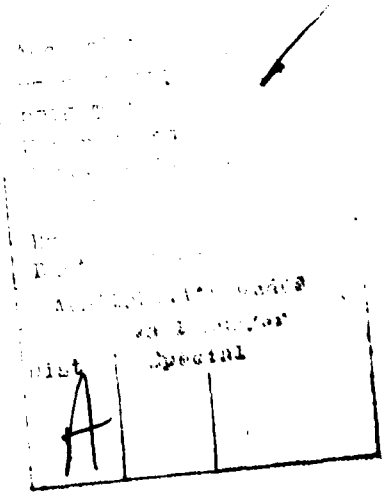

TABLE OF CONTENTS

PART ONE
COMPUTER AIDED FLEXIBLE PAVEMENT ANALYSIS

CHAPTER 1 INTRODUCTION 1

CHAPTER 2 THE COMPUTER PROGRAM DEFPAV 3

2.1 INTRODUCTION 3

2.2 THE PAVEMENT MODEL 3

2.3 OUTPUT FROM THE PROGRAM 4

2.4 CREEP CHARACTERIZATION 4

2.5 ENGINEER'S VERSION 4

2.6 OPTION VERSION 5

2.7 PROGRAM VERIFICATION 7

2.8 SENSITIVITY STUDY 8

2.8.1 Finite element Grid Configuration 8

2.8.2 Simulation of the Wheel Load 9

2.8.3 Specification of Material Properties 10

2.9 LIMITATIONS 11

2.10 CONCLUSIONS 12

CHAPTER 3 DEVELOPMENT OF THE PAVEMENT MODELS 13

3.1 INTRODUCTION 13

3.2 MATERIAL CHARACTERIZATION 14

3.3 THE CONCEPT OF BACK ANALYSIS 15

3.4 MODELLING THE PAVEMENT AT THE HILLSBOROUGH TEST SECTION 16

3.4.1 Estimation of Layer Properties 16

3.4.2 Simulation of the Rear Wheel Load of the Benkelman Beam Vehicle 17

3.4.2 Calibration of the Models for Transient Deflection 17

3.4.4 Simulation of the Standard Axle Wheel Load 18

3.4.5 Calibration of the Models for Rutting 19

3.5 MODELLING THE PAVEMENT AT THE M1 MOTORWAY TEST SECTION 20

3.5.1 Estimation of Layer Properties 20

	3.5.2 Calibration of the Model for Transient Deflection	20
	3.5.3 Calibration of the Model for Rutting	20
3.6	CONCLUSION	21
CHAPTER 4	PREDICTION OF OVERLAY REQUIREMENTS	22
4.1	INTRODUCTION	22
4.2	DEVELOPMENT OF AN OVERLAY DESIGN CHART FOR THE HILLSBOROUGH TEST SECTION	23
4.3	DEVELOPMENT OF AN OVERLAY DESIGN CHART FOR THE M1 MOTORWAY TEST SECTION	24
4.4	DISCUSSION	24
4.5	CONCLUSION	25
CHAPTER 5	PAVEMENT TEMPERATURE STUDIES	26
5.1	INTRODUCTION	26
5.2	USE OF UNCORRECTED DEFLECTIONS	26
5.3	MEASUREMENT OF PAVEMENT TEMPERATURES AT THE HILLSBOROUGH TEST SECTION	27
5.4	SIMULATION OF TEMPERATURE VARIATIONS IN THE BITUMINOUS LAYER	28
5.5	INFLUENCE OF TEMPERATURE ON TRANSIENT DEFLECTION	28
5.6	USE OF TEMPERATURE MEASURED AT A DEPTH OF 40mm	29
5.7	DISCUSSION	29
5.8	CONCLUSION	30
CHAPTER 6	CORRELATION OF BENKELMAN BEAM AND DEFLECTOGRAPH DEFLECTIONS	32
6.1	INTRODUCTION	32
6.2	NEED FOR A CORRELATION	32
6.3	METHOD OF CORRELATION	33
6.4	PREDICTION OF DEFLECTIONS MEASURED BY THE BENKELMAN BEAM	34
6.5	CORRECTION FOR INFLUENCE OF DEFLECTION BOWLS ON BENKELMAN BEAM SUPPORTS	35
6.6	PREDICTION OF DEFLECTIONS MEASURED BY THE DEFLECTOGRAPH	35
6.7	CORRECTION FOR INFLUENCE OF DEFLECTION BOWLS ON DEFLECTOGRAPH BEAM ASSEMBLY SUPPORTS	36
6.8	CORRELATION OF PREDICTED DEFLECTIONS	36
6.9	DISCUSSION	37

	6.9.1 Modelling Assumptions	37
	6.9.2 Influence of Deflection Bowls on Beam Assembly Supports	37
	6.9.3 Practical Correlation Exercise	38
6.10	CONCLUSIONS	38
CHAPTER 7	AN INVESTIGATION OF STRUCTURAL FAILURE PHENOMENA	40
7.1	INTRODUCTION	40
7.2	RUTTING AND CRACKING	41
7.3	PREDICTIONS OF PERMANENT DEFORMATION GROWTH	42
	7.3.1 Rut Depth Predictions at the Hillsborough Test Section	42
	7.3.2 Rut Depth Predictions at the M1 Motorway Test Section	42
	7.3.3 Discussion	43
	7.3.4 Conclusion	44
7.4	INVESTIGATION OF THE CRACKING PHENOMENON	44
	7.4.1 Simulation of Crack Propagation	44
	7.4.2 Influence of Cracking on Transient Deflection	45
	7.4.3 Influence of Cracking on Pavement Stresses and Strains	45
	7.4.4 Discussion	46
	7.4.5 Conclusion	47
CHAPTER 8	OTHER APPLICATIONS OF THE COMPUTER PROGRAM DEFPAV	48
8.1	DERIVATION OF LOAD EQUIVALENCE FACTORS	48
	8.1.1 Introduction	48
	8.1.2 Load Equivalence Factors by Analysis	49
	8.1.3 Discussion	51
	8.1.4 Conclusion	51
8.2	USE OF FABRICS IN PAVEMENT CONSTRUCTION	52
	8.2.1 Introduction	52
	8.2.2 Effect of a Fabric Inclusion Between the Granular Layer and the Subgrade	52
	8.2.3 Discussion	53
	8.2.4 Conclusion	53
CHAPTER 9	SUMMARY OF WORK DONE	54

PART TWO
AN OVERLAY DESIGN SYSTEM FOR DEVELOPING COUNTRIES

CHAPTER 10 INTRODUCTION 57

10.1 STRUCTURAL RESPONSE MODEL OF A PAVEMENT 57

10.2 STRUCTURAL DISTRESS MODEL OF PAVEMENT 58

10.3 OUTLINE OF THE PROPOSED METHOD 60

CHAPTER 11 DETERMINATION OF IN-SITU LAYER MODULI 61

11.1 INTRODUCTION 61

11.2 SUBGRADE LAYER MODULUS FROM CALIFORNIA BEARING RATIO 61

11.3 UNBOUND LAYER MODULUS FROM SUBGRADE LAYER MODULUS 61

11.4 BITUMINOUS LAYER MODULUS FROM BENKELMAN BEAM DEFLECTION 61

11.4.1 Method of Equivalent Thicknesses 62

11.4.2 Computation of Bituminous Layer Modulus 63

11.4.3 Adjustment for Loading Time Differences 64

CHAPTER 12 DETERMINATION OF CRITICAL STRAINS 66

12.1 SELECTION OF THE METHOD 66

12.2 PREDICTION MODELS FOR CRITICAL STRAINS 66

12.3 COMPUTATION OF CRITICAL STRAINS FROM MULTI-LAYER ELASTIC THEORY 67

12.3.1 Factorial Design of Pavement Response Computation 68

12.4 MULTIPLE REGRESSION ANALYSIS 68

CHAPTER 13 DETERMINATION OF OVERLAY THICKNESS 70

13.1 PHENOMENOLOGICAL THEORY OF CUMULATIVE DAMAGE 70

13.2 COMPUTATION OF ALLOWABLE CRITICAL STRAINS 72

13.3 COMPUTATION OF OVERLAY THICKNESS 75

CHAPTER 14 OVERLAY DESIGN EXAMPLE BY THE PROPOSED METHOD 77

14.1 OVERLAY DESIGN EXAMPLE 77

14.2 OVERLAY DESIGN BY OTHER METHODS 79

14.3 REMARKS 79

CHAPTER 15 SUMMARY OF WORK DONE 80

ACKNOWLEDGEMENTS 81

REFERENCES 82

APPENDIX 1 - TABLES 88

APPENDIX 2 - FIGURES 119

PART ONE

COMPUTER AIDED FLEXIBLE PAVEMENT ANALYSIS

CHAPTER ONE

INTRODUCTION

Recent advances (1) in the development of structural design procedures for flexible pavements have placed considerable emphasis on the use of computer programs for multi-layer analysis. The development of these computer programs has facilitated the prediction of load induced stresses and strains throughout any specific pavement structure. One such program is DEFPAV (2,3), which, in addition to computing the elastic stresses and strains in a multi-layer pavement, can be used to predict the lateral surface permanent deformation profile after any specified number of wheel passes.

The computer program DEFPAV was produced in 1975 by Kirwan and Snaith, and has been described in a previous report to the E.R.O. (4). The program was developed as the successor to the program DYNASTCO, which was produced by Kirwan and Glynn (5) in 1969.

In 1976 the program DEFPAV was modified (6) so that it could be used more easily by the road engineer. This involved considerable simplification to the input data and resulted in the 'Engineer's Version of DEFPAV'. Further improvements have been implemented during 1977 as part of the present research programme. An option has been incorporated within the program which enables the user to decide whether to specify a finite element grid or to use one which is generated automatically. The current version is known as the 'Option Version of DEFPAV'. This version has been made available to other pavement research centres, including Trinity College, Dublin, and the University of Nottingham.

The 'Option Version of DEFPAV' has been used extensively at the Queen's University of Belfast (Q.U.B.) in an effort to demonstrate the application of multi-layer analysis to the assessment of pavement performance and the prediction of maintenance requirements. The work, described in this report, represents one facet of a continuing programme of research into the maintenance of flexible pavements.

The construction details needed to model specific in-service pavements were made available by the Roads Service of the Department of the Environment for Northern Ireland (D.O.E.(N.I.)). Furthermore, it has been possible to check various predictions made using DEFPAV, by comparison with pavement condition survey data collected for two joint D.O.E.(N.I.)/Q.U.B. research projects (7,8) which ran concurrently with the work under discussion.

This report shows how the program DEFPAV has been used to model specific in-service pavements in Northern Ireland and its application to the following problems:

(a) Prediction of overlay requirements.

(b) Investigation of the influence of pavement temperature on measured deflections.

(c) Correlation of Benkelman Beam and Deflectograph deflections.

(d) Prediction of the growth of permanent deformation.

(e) Investigation of the effect of crack propagation through the bituminous layer.

(f) Derivation of load equivalence factors.

(g) Investigation of the effect of a fabric inclusion.

It is hoped that the application of the program to the problems listed will show that the use of computer aided pavement analysis can bring about substantial savings in both time and money. In many cases, full scale road tests could be replaced by an appropriate theoretical analysis followed by small scale trials to verify the results.

CHAPTER TWO

THE COMPUTER PROGRAM DEFPAV

2.1. Introduction

This Chapter provides a brief description of the program DEFPAV (4). The modifications leading to the 'Engineer's Version' and 'Option Version' are listed. Furthermore, the results of a sensitivity study are presented, showing the effect on computed surface transient deflections of changes in various input parameters.

2.2. The Pavement Model

The case of a wheel load acting on a multilayer road pavement is considered as an axially symmetric problem. As shown in Fig. 1, the pavement layers (including the subgrade) are modelled as a three-dimensional finite element grid. Each layer is subdivided into a system of elements, which are connected at the nodes.

The wheel load is specified as a uniformly distributed pressure over a circular contact area. This is applied by the program in the form of a set of concentrated loads acting at the relevant nodes. For this reason the finite element grid should be constructed so that a node is situated at the boundary of the uniform load.

The boundary conditions are set automatically; i.e. the lateral boundaries are restrained horizontally, whilst the base of the model is restrained in both the horizontal and vertical directions.

Material properites (*Resilient Modulus, M_r, and Poisson's Ratio, υ) are specified for each layer of the structure. The resilient modulus may be either linear or dependent on any one of a number of stress regimes. Fig. 2 summarizes the input to the program.

---

* Resilient Modulus is defined as the applied dynamic deviator stress divided by the total recoverable strain measured between successive applications of stress (9).

2.3. Output from the Program

The elastic analysis (5) employes the successive over relaxation technique to obtain the stresses in each element of the finite element grid. When the elastic analysis is completed, a non-iterative procedure makes use of the computed stress values and 'creep equations' (see Section 2.4) to calculate the vertical permanent strain independently for each element. The strains are then converted to deformations, and summed for each column of elements to give the overall surface permanent deformation, or rut depth (Fig. 3).

This approach is similar to that used by Barksdale (10) and Romain (11). The suitability of such a method for inclusion in a finite element program had been proposed by Croney and Thompson (12).

Hence the full solution contains the elastic deflections at each node, the stresses in each element, and the expected lateral surface permanent deformation profile after any number of wheel passages.

2.4. Creep Characterization

The creep equations used in the non-iterative procedure following the elastic analysis have been derived from the results of either repeated-load triaxial or creep tests on specific construction materials. Each equation relates the induced permanent strain to the imposed stresses. Those incorporated in the current version of DEFPAV are as follows:

Equation 1 : Dublin boulder clay, after Kirwan and Snaith (13).

Equation 2 : Dense bitumen macadam, after Kirwan and Snaith (4).

Equation 3 : Dense bitumen macadam, after Brown and Snaith (14).

Equation 7 : Keuper Marl, after Kirwan et al (2).

2.5. Engineer's Version

The 1975 version of DEFPAV was modified (6) so that it could be used more easily by the road engineer. The main changes are listed below (6):

(a) Expansion of the program to cope with a maximum of nineteen layers.

(b) Automatic horizontal and vertical grid generation.

(c) Automatic boundary setting.

(d) No deflection input.

(e) Output of up to fifteen plastic solutions from only one generation of the element stresses.

(f) Improved output format.

The result of these changes was the 'Engineer's Version of DEFPAV'.

2.6. Option Version

Further improvements have been implemented during the course of the current research programme. These were as follows:

(a) Incorporation of a Grid Option

The Engineer's Version used only an automatic grid, so it was decided to introduce a grid option whereby the user would decide whether to use the automatic grid generation, or to specify his own grid. The former would be suitable for the road engineer, and the latter would be more appropriate for research purposes.

The option was introduced near the start of the subroutine DATAIN, and was implemented by specifying either zero or unity for a variable named 'GRID'. Thus if GRID was specified as zero, control passed to the automatic grid generation sequence, and if specified as unity, control passed to the grid specification sequence.

A maximum of five layers can be catered for using the automatic grid generator. With the grid specification option, up to nineteen layers are permitted.

(b) Expansion of Automatic Grid Size

The boundary conditions assumed when modelling a pavement with the program are that the lateral boundaries are restrained horizontally, whilst the base of the model is restrained both horizontally and vertically. To improve the validity of these

assumptions, both the automatic horizontal and automatic vertical grids were expanded. This was achieved by changing the original automatic grid generator.

The lateral position of the nodes was based on the radius of the loaded area, and the horizontal grid was generated so that there were five element columns of equal width under the loaded area. This ensured that a column of nodes was located at the boundary of the uniform load. The sixth element had the same width, and thereafter the element widths were increased by a certain factor (either 2, 2.25, or 4.5, depending on the number of layers in the pavement). Different factors were required as the total number of nodes should not exceed 225, and the maximum number of horizontal and vertical nodes is 16 and 20 respectively.

The automatic vertical grid was generated so that there were four element rows per layer until the subgrade was reached, and then the remaining nodes were used. Within each layer of the pavement (excluding the subgrade), the vertical grid was generated as a cubic function, based on the layer thickness. This ensured that a row of nodes coincided with the layer interfaces. The vertical position of the nodes within the subgrade was based on the thickness of the layer immediately above it, and varied as a cubic function. A separate sequence has been included for the case of a 'one-layer pavement'. The vertical grid for this case uses ten element rows, and is generated as a square function, based on the layer thickness. A typical automatic grid generation for a three-layer pavement is shown in Fig. 4.

(c) Incorporation of a Calibration Factor in the Creep Solution

It has been noted elsewhere (2) that rut depths predicted using the program were consistently within an order of magnitude of those measured. However, it is possible to introduce a 'weighting factor' so that the computed values agree with those observed. This has been termed a 'calibration factor', and may be specified for any layer of the pavement structure. The effect is that the permanent strain values for that layer are multiplied by the factor before the deformation values are summed over all the layers.

(d) Compatibility with other Computers

The successor to the 'Engineer's Version' is known as the 'Option Version' of DEFPAV, and was developed in the ICL 1900 card code. The program was demonstrated at the Fourth International Conference on the Structural Design of Asphalt Pavements at Ann Arbor, Michigan, in August 1977 (2), after conversion to suit the computer system in operation. The 'Option Version' is currently available in the ICL 1900 and EBCDIC card codes.

2.7. Program Verification

With the increasing use of computer 'packages' in structural analysis, it is important that the engineer should be wary of accepting the output as an instant solution to his problems. The results must be viewed in the light of the simplifying assumptions made in the formulation of the mathematical model. In the case of DEFPAV, this includes those assumptions made when assigning material properties to each layer.

However, successful verification will enable the user to accept the results with more confidence. It has been stated (15) that the best method of testing computer program results is to compare the computer analysis with laboratory model studies or field test results. Another approach is to use two or more programs to analyse a particular problem.

The accuracy of the elastic solution obtained using the program DYNASTCO has been tested by Kirwan and Glynn (5). Cases considered included a four-layer pavement with non-linear elastic properties, subjected to a single wheel load. This had been analysed by Duncan et al (16). In each case satisfactory agreement was obtained between the finite element and a closed solution.

The accuracy of the creep computation obtained using DEFPAV has been verified by Kirwan et al (2), who compared the computer analyses with results from laboratory models. Cases considered were a triaxial specimen of Dublin boulder clay, the Shell test track (17), and the Nottingham test pit (18).

2.8. Sensitivity Study

A brief investigation has been carried out into the sensitivity of the program DEFPAV to changes in various input parameters. These include the form of the finite element grid, the simulation of the wheel load, and the specification of the layer properties. The pavement models used are typical of those adopted for later analyses.

2.8.1. Finite Element Grid Configuration

The boundary conditions assumed by the program are shown in Fig. 1. As the effect of the applied load decreases with increasing distance from its area of application, an increase in the overall size of the pavement model will improve the validity of the various simplifying assumptions shown in the figure. However, due to the limitation on the total number of elements (225 maximum), the overall model size must not be excessive. This may result in a grid composed of relatively large elements which do not adequately simulate the behaviour of the pavement structure.

To determine suitable dimensions for the pavement model, the distance from the axis of symmetry to the lateral boundary was varied

whilst the depth to the base of the model was kept constant. Fig. 5 shows the resulting variation in transient deflection for a model having a depth of 15 metres. There is a definite convergence as the distance to the lateral boundary is increased. After further use of this trial and error procedure, a model having an overall width of 10 metres and depth 15 metres was adopted.

The internal form of the finite element grid was determined largely by judgement. The smallest elements were used in the vicinity of the applied load, and their aspect ratio (ratio of the larger dimension of the element to the smaller dimension) kept close to unity. As a general rule, four or five element columns of equal width were used under the loaded area. Typical finite element configurations are shown in Figs 6 and 7.

2.8.2. Simulation of the Wheel Load

The Benkelman Beam vehicle has a rear axle load of 6350 kg (19), equally divided between the twin wheel assemblies at each end of the axle. The wheel load may be modelled using either a twin wheel assembly or a single wheel assembly.

If a twin wheel assembly (Fig. 6) is adopted, the applied load is assumed to be one quarter of the overall axle load. The contact pressure is assumed to be equal to the specified tyre inflation pressure of 590 kN/m^2 (19). The value of the computed surface transient deflection at the position of the Benkelman Beam shoe is doubled to take account of the other wheel in the assembly.

In the case of the single wheel assembly (Fig. 7), the applied load is assumed to be one half of the axle load, and the contact pressure again taken as 590 kN/m^2. The required surface deflection is that at the axis of symmetry.

In both cases the load is applied uniformly over a circular contact area, and the radius of the loaded area deduced from the wheel

load and contact pressure. Table 1 summarizes the loading details for the two types of wheel assembly. The general shape of the respective deflection bowls is shown in Fig. 8. That for the twin wheel assembly was derived by superposition of the separate bowls for each wheel in the assembly. The deflection bowl for the single wheel assembly was considered a better representation of the deflected pavement profile, and this assembly was adopted for all further analyses.

The variation of transient deflection with the magnitude of the wheel load has been investigated. As shown in Fig. 9, the computer deflection is directly proportional to the applied load. To establish this relationship, the contact pressure was kept constant at 690 kN/m^2 for all values of load. (In each case the finite element configuration was generated automatically by the program.) An approximately linear relationship between transient deflection and wheel load has been observed in practice (20,21,22).

The effect of variations in contact pressure at constant load has also been considered. Fig. 10 shows the variation of transient deflection whilst the wheel load has a fixed value of 3175 kg. It may be seen that, over the range of practical tyre inflation pressures for heavy vehicles, there is negligible change in deflection. (The finite element configurations used in the derivation of this relationship were generated automatically by the program.) This trend has also been observed in practice (22).

2.8.3. Specification of Material Properties

The sensitivity of the program to changes in the elastic parameters M_r and υ has been investigated.

The effect of variations in the value assigned to the resilient modulus of the surface layer, M_{r_1} (in a typical three-layer pavement construction), will be considered in Chapter Three (Figs. 17 and 23). It will be seen that as the resilient modulus increases there is a marked reduction in deflection.

Fig. 11 shows how the transient deflection is influenced by changes in the CBR value of the subgrade. As the CBR value rises there is a corresponding fall in computed deflection. As noted in Chapter Three, a factor of 10 has been used to convert the subgrade CBR value to the corresponding resilient modulus (M_{r_3}), and a modular ratio of 2.5 adopted to deduce the resilient modulus for the granular layer (M_{r_2}).

The influence of Poisson's Ratio on the computer transient deflection is shown in Fig. 12. It may be seen that only the value assigned to the surface layer (υ_1) has any significant effect.

Similar trends have been reported by Bleyenberg et al (23) who observed the effect of variations in material properties and test conditions on calculated strains, soil pressures and deflections.

2.9. Limitations

The main limitation with the program is that, for the calculation of the permanent strains in the pavement model, the lateral strain of one column of elements is prevented from affecting the adjoining column. However, it is hoped that a suitable mathematical solution will be found to allow the iterative procedure used for the elastic solution to be employed in the permanent deformation solution, and hence overcome this deficiency (2).

As the pavement under load is considered as an axially symmetric problem (Fig. 1), difficulties may arise when considering the case of a wheel load close to the edge of an unpaved shoulder (5). The pavements considered herein (Chapter three) have paved shoulders which are of lighter construction than the pavement itself. A sensitivity study (Fig. 5) has shown that the effect of the boundary is insignificant beyond 3 metres (measured from the axis of symmetry). As wheel tracking is generally 4 metres from the outer edge of the paved shoulder, this is considered acceptable.

2.10. Conclusion

The 'Option Version of DEFPAV' may be used by the road engineer to compute the elastic stresses and strains induced in a road pavement by a single wheel load. Furthermore, the lateral surface permanent deformation profile may be estimated after any number of wheel passages. The program has been verified for both the elastic and creep solutions. It should be added, however, that any computations will only be as good as the values assigned to the elastic parameters, and the validity of the creep equations selected for each layer.

CHAPTER THREE

DEVELOPMENT OF THE PAVEMENT MODELS

3.1. Introduction

To gain confidence in the use of computer-aided pavement analysis, it is essential that existing roads should be modelled, so that the predicted performance can be compared with that which is observed. To this end, two pavement sections in Northern Ireland have been modelled using the computer program DEFPAV. These were:

(i) Hillsborough Test Section

The Hillsborough By-pass is a dual two-lane carriageway forming part of Route A1 which runs from the Sprucefield interchange off the M1 Motorway, to Newry. The test section considered is a 150 m length of the by-pass, and is located two miles from the Sprucefield interchange. Only the North-bound carriageway was considered in the analyses.

Because of the variability in measured deflections at this section (Fig. 13), two test lengths were considered. Model A represented conditions over a 20 m test length (Ch. 0.970 to Ch. 0.990 km), and Model B represented conditions over the complete 150 m test section (Ch. 0.910 to Ch. 1.060 km).

(ii) M1 Motorway Test Section

The M1 Motorway is a dual two-lane carriageway which links Belfast and Dungannon. The test section considered is 300 m long (Fig. 14), and is situated between the Moira and Lurgan interchanges. Only the West-bound carriageway was considered for analysis (Ch. 3.120 to Ch. 3.420 km).

Conditions over the test sections should not be considered as representative of the complete lengths of the respective routes. The test

sections modelled were selected for the following reasons:

(i) The Hillsborough test section was overlaid in several stages, and a deflection survey had been carried out between successive overlay applications. This provided the necessary data to compare deflections measured after overlaying with those predicted using the computer program DEFPAV.

(ii) Severe rutting and some 'alligator' cracking had occurred on the M1 Motorway test section. Consequently test pits had been constructed by the Roads Service of the Department of the Environment (Northern Ireland) for investigation of the subgrade. To date, this pavement has not been overlaid.

This chapter describes the methods used to assign material properties to each layer in the pavement models, and the subsequent calibration procedure.

3.2. Material Characterization

As noted in Chapter Two, the program DEFPAV performs an elastic analysis to produce the transient deflections and stresses throughout the pavement structure, and then makes use of 'creep equations' to estimate the long term behaviour (rutting). It is clear that effective use of the elastic analysis depends on the specification of appropriate values for the elastic parameters (M_r,υ) used to define the constituent materials. Moreover, use of the 'long term' analysis depends on the selection (or specification) of a suitable creep equation. Thus a major problem in modelling in-service pavements is the ability to characterize the constituent materials. Ideally the materials should be tested either in situ or in the laboratory, but unfortunately this was beyond the scope of the current research programme. A review of literature relevant to the characterization of the common pavement materials is presented elsewhere (24).

In view of the lack of direct test results for the pavements under consideration, it was decided to select material characteristics initially

from research data (9,25-27). This involved some laboratory testing of the subgrade material and is discussed more fully in Sections 3.4 and 3.5. Consequently, a back analysis procedure was adopted in order to calibrate the pavement models. This is discussed in Section 3.3. The lack of direct test results for material properties emphasizes the need for such a procedure.

3.3. The Concept of Back Analysis

The pavement model may be calibrated for transient deflection by using a back analysis procedure to modify the values assigned to the layer properties. The method is summarized in Fig. 15.

Simply, the pavement configuration is deduced from records, and a three-layer structure defined (i.e. bituminous layer, granular layer, and subgrade). The properties of each layer are selected initially from research data (9,25-27) and the results of laboratory tests. The pavement model is then loaded with a standard (3175 kg) wheel load, and the transient deflection, analagous to the Benkelman Beam deflection, is computed. This value is compared with that measured on the road pavement before overlaying. (The assumption is made that the Benkelman Beam gives an absolute measure of transient deflection.) The properties of the model layers are then varied until a close correlation is obtained. The model is then considered to be calibrated for transient deflection. (It should be noted that the measured deflections used in the back analysis procedure were not corrected to a standard temperature. This is discussed in Chapter Five.)

Furthermore, the model may be calibrated for rutting as shown in Fig. 16. Using a chart proposed by Brown (28) the material properties of the bituminous layer are modified to take account of average vehicle speeds, which are much higher than the creep speed associated with the Benkelman Beam vehicle. A 'creep equation' (Section 2.4) is then assigned to each layer which is considered to contribute to the overall permanent deformation.

(Evidence of permanent deformation in the bituminous layer may be found by taking cores across the pavement.) The pavement model is then loaded with a standard (4100 kg) wheel load, and the rut depth computed after a specified number of wheel passages (i.e. an estimate of the number of Standard Axle passages up to the date of the pavement survey). The computed rut depth is compared with the measured value, and close correlation obtained by altering the value of the 'calibration factor' (Section 2.6(c)) associated with each creep equation. The model is then calibrated for rutting.

3.4. Modelling the Pavement at the Hillsborough Test Section

3.4.1. Estimation of Layer Properties

The pavement configuration obtained from records (29) was simplified to a three-layer structure for the computer analyses. The methods used to assign values for the Resilient Modulus (M_r) and Poisson's Ratio (υ) to each layer are summarized below.

Layer 3 - Subgrade

A site investigation was carried out to obtain subgrade samples for CBR and compaction tests. A test pit was located on an embankment section adjacent to the North-bound carriageway (Ch 0.979 km). Disturbed subgrade samples were obtained for identification and compaction tests. A CBR mould was used to collect an 'undisturbed' sample for determination of the CBR value, the in situ moisture content and dry density. The laboratory results are given in Table 2.

A value for the resilient modulus of the subgrade (M_{r_3}) was obtained by two different methods. The first made use of a correlation established by Heukelom and Klomp (26) between the dynamic elastic modulus of the subgrade and its CBR value. The second approach employed a chart produced by Kirwan and Snaith (9) which related resilient modulus to the in situ dry density and moisture content. Table 2 summarizes the results obtained. The value

for Poisson's Ratio was taken to be 0.45, as suggested by Pell and Brown (27).

Layer 2 - Crushed Rock Base

It has been shown (26) that the modular ratio between an unbound granular layer and the underlaying subgrade may be considered constant, with a value of 2.5. This enabled a value to be assigned to the resilient modulus of the crushed rock base (Table 3). The value assigned to Poisson's Ratio was 0.3 (27).

Layer 1 - D.B.M. Surface Layer

The value used initially for the resilient modulus of the bituminous layer was 3720 MN/m^2, after Snaith (25). However, it was necessary to calibrate the pavement model for transient deflection, and this was achieved by use of the back analysis procedure (Section 3.3) to modify the value assigned to the resilient modulus. The procedure is described in Section 3.4.3.

The value assigned to Poisson's Ratio was 0.4 (27).

A summary of the values of Resilient Modulus and Poisson's Ratio used to characterize the test lengths on the Hillsborough test section is given in Table 3.

3.4.2. Simulation of the Rear Wheel Load of the Benkelman Beam Vehicle

The rear wheel load of the Benkelman Beam vehicle was simulated using a single wheel assembly (Section 2.8.2). The assumed contact pressure was 590 kN/m^2, uniformly distributed over an area of 130 mm radius.

3.4.3. Calibration of the Models for Transient Deflection

The computer model for each test length was calibrated by use of a back analysis procedure to find a particular value for the surface layer modulus (M_{r_1}) corresponding to a calibration deflection. The calibration deflection was taken as the mean value of the measured deflections before overlaying.

A relationship (Fig. 17) between the computed transient deflection and the surface layer modulus was established using the finite element configuration shown in Fig. 18. This relationship was used to find the value of M_{r_1} corresponding to the calibration deflection for each test length. The values obtained are given in Table 3.

It may be seen (Fig. 17) that the calibration deflection for Model B is 16 per cent less than that for Model A, resulting in a corresponding increase of 20 per cent in the value of the surface layer modulus. Although the surface layer was nominally identical for both test lengths, the difference in surface layer modulus values between the two test lengths was considered acceptable.

Only the modulus value assigned to the surface layer has been modified in the calibration procedure, as least was known about the properties of this layer. It must be stated, however, that the variation in the mean deflection values between the two test lengths could be interpreted as being due to different subgrade or base conditions, or some combination of these.

3.4.4. Simulation of the Standard Axle Wheel Load

The Standard Axle, which has a specified load of 8200 kg (30), was assumed to have a single (4100 kg) wheel assembly at each end. The contact pressure was taken as 620 kN/m^2, and the radius of the loaded area was 144 mm.

The traffic flow over the Hillsborough test section (before overlaying) was defined in terms of the cumulative number of standard (8200 kg) axles which had passed over it between the opening date (November 1974) and the completion of overlaying (November 1976). Data obtained from records (29) indicated that, at the nearest census point, the average daily flow of vehicles in each direction was 5500 in August 1974. The cumulative number of standard axles which had passed over the test section during the two year period before overlaying was estimated to be 0.47 million.

3.4.5. Calibration of the Models for Rutting

Only Model B (Ch. 0.910 to Ch. 1.060 km) was used to model the Hillsborough test section for rutting. Model A (Ch. 0.970 to Ch. 0.990 km) was not used because only three measured rut depth values were available.

The layer properties used when modelling the passage of the Benkelman Beam vehicle have been evaluated in Section 3.4.1. To model the passage of the standard (8200) kg) axle, the resilient modulus of the bituminous layer was modified, to take account of higher vehicle speeds. This was achieved by adapting a chart propsed by Brown (28) as shown in Fig. 19, giving a value of 6000 MN/m^2.

The model was calibrated for rutting by finding a value for the 'calibration factor' which corresponded to a calibration rut depth. (The concept of a calibration factor has been described in Section 2.6(c)). The calibration rut depth was taken as the mean value of the measured rut depths before overlaying. This was assumed to be due to the passage of 0.47 million standard axles.

The pavement section (Fig. 20) obtained from cores indicated that there was negligible permanent deformation in the bituminous bound layer (29). In the first instance (Model B1), it was assumed that no permanent deformation occurred in the granular layer, and a creep equation was specified only for the subgrade layer. Of the creep equations available (Section 2.4), that for Keuper Marl was considered most appropriate.

A relationship (Fig. 21) between the computer rut depth (after 0.47 million passes of a standard axle wheel load) and the subgrade calibration factor was established using the finite element configuration shown in Fig. 22. This relationship was used to find the value of the subgrade calibration factor corresponding to the calibration rut depth. The value obtained was 0.5.

A second model was established, based on the assumption that permanent deformation occurred in both the granular layer and the subgrade (i.e. Layers 2 and 3 in Table 4). The creep equation for Keuper Marl was specified for both layers, and each had the same calibration

factor applied. This model was similarly calibrated (Fig. 21), and the resulting calibration factors are shown in Table 4.

3.5. Modelling the Pavement at the M1 Motorway Test Section

3.5.1. Estimation of Layer Properties

The pavement configuration obtained from records (29) was simplified to a three-layer structure for the computer analyses. The methods used to assign values for the Resilient Modulus (M_r) and Poisson's Ratio (υ) to each layer are similar to those adopted for the Hillsborough test section. The values are summarized in Table 5 and Table 6.

3.5.2. Calibration of the Model for Transient Deflection

The pavement model was calibrated for transient deflection using the procedure outlined in Section 3.3. As the M1 Motorway test section has not to date been overlaid, the calibration deflection was based on the results of the deflection survey carried out in April 1976, after a life of ten years.

Fig. 23 shows the relationship established between the computed transient deflection and the surface layer modulus. The finite element configuration used is given in Fig. 24, and the results of the calibration are presented in Table 6.

3.5.3. Calibration of the Model for Rutting

The cumulative number of standard (8200 kg) axles which had passed over the test section during its ten year life up to April 1976 has been estimated at 3.4 million (31).

The layer properties used to simulate the passage of the Benkelman Beam vehicle have been evaluated in Section 3.5.1. To model the passage of the standard (8200 kg) axle, the resilient modulus of the bituminous layer was modified to take account of higher vehicle speeds. The value

obtained was 3200 MN/m^2 (Fig. 25), using a chart proposed by Brown (28).

Evidence (29) from bituminous cores indicated that, as at the Hillsborough test section, negligible permanent deformation had occurred in the bituminous layer. Again, two models were created. Model 1 was based on the assumption that permanent deformation occurred only in the subgrade, as with Model 2 it was assumed that both the granular layer and the subgrade contributed to overall permanent deformation. The creep equation for Keuper Marl (Section 2.4) was considered the most appropriate for both layers.

Fig. 26 shows the variation of computer rut depth (after 3.4 million passes of a standard axle wheel load) with calibration factor, obtained using the finite element configuration given in Fig. 27. The resulting calibration factors are presented in Table 7.

3.6. Conclusion

Computer models have been established for the pavements at the Hillsborough and M1 Motorway test sections. The models have been calibrated for transient deflection and for rutting. Their application is described in the ensuing chapters.

CHAPTER FOUR

PREDICTION OF OVERLAY REQUIREMENTS

4.1. Introduction

It is known that the application of a bituminous overlay to a flexible pavement increases its structural strength and reduces the value of the Benkelman Beam deflection. To be effective, the overlay must be applied before the pavement reaches the 'critical' condition, which has been defined (32) in terms of the observed levels of rutting and cracking.

Examination of a typical deflection criterion curve (32) shows that the transient deflection remains relatively constant for the greater part of a pavement's life. As the 'critical' condition is approached, a rapid increase in deflection occurs, indicating that maintenance is required. It has been found (19) that if the pavement is overlaid before the critical condition is reached, the overlaid structure will behave as a new pavement, with its potential life a function of the new early life deflection.

To ensure that the pavement never passes the critical condition, a continual road assessment programme such as that proposed by the Marshall Committee (33) must be undertaken, together with a deflection survey.

Having decided that the pavement is approaching the critical condition, the engineer can use a deflection criterion curve to find the required new early life deflection for future traffic volumes. The thickness of overlay needed may be found either by a trial and error procedure of adding layers of bituminous material until the measured deflection is adequate, or by use of overlay design charts derived by the T.R.R.L. (19). Alternatively, a theoretical elastic analysis may be used, with the aid of a computer program such as DEFPAV. The application of such a method to two pavement sections in Northern Ireland is described in this chapter.

4.2. Development of an Overlay Design Chart for the Hillsborough Test Section

The pavement at the Hillsborough test section was overlaid in three stages, as shown in Fig. 20. Using the pavement models (A and B) described in Section 3.4, the transient deflection caused by a standard Benkelman Beam wheel load was predicted for each stage of the overlay procedure. (i.e. after cumulative overlay thicknesses of 30, 83 and 116 mm, representing the regulating course, surface layer base course, and surface layer wearing course stages respectively.) It was assumed that the properties of the overlay material (known to be hot rolled asphalt) were the same as those of the underlying bituminous layer.

Fig. 28 shows, for Model A, a comparison of the predicted deflection after completion of overlaying and the corresponding measured values. (The finite element configuration used is given in Fig. 29). It may be seen that good agreement was obtained. A comparison of predicted and measured deflections after each stage of overlaying is given in Fig. 30. A similar comparison for Model B is presented in Fig. 31.

As the predicted deflection after completion of overlaying (for each test length) corresponded closely with the mean of the measured values, further back analysis using the measured deflections after overlaying to obtain a modulus value for the overlay material was considered unnecessary.

By using models A and B, two curves (Figs. 30 and 31) have been obtained which relate deflection to overlay thickness. As defined in Chapter three, models A and B represent the 20 m and 150 m test lengths respectively, and their only distinguishing feature is the value assigned to the surface layer modulus (i.e. modulus value assumed for the bituminous layer). Hence by choosing various values for the surface layer modulus a family of curves may be plotted (Fig. 32), each representing the condition where the pavement has a deflection before overlaying as indicated. For each curve, the value given to the surface layer modulus was obtained from Fig. 17, which shows the variation of deflection with modulus value. The

modulus values used in the derivation of the overlay chart are given in Table 8.

The overlay design chart presented may be used directly to estimate overlay requirements for any particular test length on the Hillsborough test section.

4.3. Development of an Overlay Design Chart for the M1 Motorway Test Section

An overlay design chart has been derived for the M1 Motorway test section in a similar manner to that for the Hillsborough test section.

Using the pavement model described in Section 3.5, the Benkelman Beam deflection was predicted for various overlay thicknesses. By choosing different values for the surface layer modulus (using Fig. 23), several curves were plotted, each one representing a specified value of deflection before overlaying. (The modulus values used are given in Table 9).

The resulting overlay design chart is presented in Fig. 33. (Fig. 34 shows a typical finite element representation.)

4.4. Discussion

Considering the Hillsborough test section, it may be seen that for both models A and B, the computed value for the deflection after completion of overlaying compares favourably with the corresponding measured value. However, the values predicted for the regulating course (30 mm overlay) and base course (83 mm overlay) are lower than the corresponding measured values (Figs. 30 and 31). This may be explained by the fact that the regulating course has been considered as a layer in its own right, with a thickness equal to the mean value of the maximum depths measured over the test length.

The curves contained in the proposed overlay design chart (Fig. 32) are steeper than those proposed by the T.R.R.L. (19). This means that, of the two charts, that derived using DEFPAV will be less conservative.

In the case of the M1 Motorway, the chart derived using DEFPAV gives a more conservative estimate of the effect of overlay than the T.R.R.L.

design chart (19). The chart derived using DEFPAV has recently been used (34) to predict deflection levels after an overlay of 40mm depth was placed over a 50m length of carriageway. A comparison of the predicted and measured deflections is given in Fig. 35. It may be seen that close agreement was obtained. Fig. 35 also shows the deflection values predicted using the T.R.R.L. design chart (19). It is clear that, for the range of overlay thickness from zero to forty millimetres, the DEFPAV chart gives a less conservative estimate of the effect of overlay than the T.R.R.L. chart.

4.5 Conclusion

The computer program DEFPAV has been used to prepare overlay design charts for two pavements in Northern Ireland. In both cases, good correlation has been obtained between predicted and measured deflections. Whilst these results are encouraging, further full scale trials are needed to verify the method.

CHAPTER FIVE

PAVEMENT TEMPERATURE STUDIES

5.1 Introduction

It is known that the stiffness of a bituminous layer changes with the temperature of the binder. A rise in temperature will cause the resilient modulus to decrease in value, so reducing the load spreading capabilities of the layer. It is therefore reasonable to expect that the stresses and strains induced by traffic loads will be temperature dependent.

However, deflections measured (29) at two pavements in Northern Ireland suggested that there was no marked dependence on temperature. This prompted a study of the deflection/temperature relationship.

This chapter describes the methods used to monitor the temperature variation through the bituminous bound layer of the pavement at the Hillsborough test section. The measurements were made periodically from sunrise to sunset on June 21, September 15 and December 5, 1977, and on April 19, 1978. The influence of pavement temperature on transient deflection is investigated using the computer program DEFPAV, and the validity of a temperature correction proposed by the T.R.R.L. (19) is discussed.

5.2 Use of Uncorrected Deflections

Studies of measured, uncorrected deflections (29) at the Hillsborough By-pass and M1 Motorway pavements in Northern Ireland have suggested that the deflections were not strongly influenced by temperature. Fig. 36 shows the variation of deflection (uncorrected) with temperature (T_{40}) for different sections of the Hillsborough By-pass. A similar relationship for the M1 Motorway is given in Fig. 37. (T_{40} denotes the temperature measured at a depth of 40mm below the road surface).

It was therefore decided that the temperature correction suggested by the T.R.R.L. (19) should not be applied to the measured Benkelman Beam

deflections used in the back analysis procedure (Section 3.3).

5.3 Measurement of Pavement Temperatures at the Hillsborough Test Section

To observe the temperature variation through the bituminous bound layer, thermocouples (Type K : Nickel chromium/Nickel aluminium) were installed separately at depths of 0, 40, 124, 165 and 214 mm from the surface, as shown in Fig. 38. (The pavement had been overlaid at this time.) The temperature values were obtained using a Comark (Type 1602) electronic thermometer.

It was considered that the plastic filler used to secure the thermocouple wires to the pavement had some influence on the readings taken using the thermocouple at the road surface. Hence the road surface temperature was measured by placing a mercury thermometer on the pavement, close to the kerb.

Pavement temperatures have been recorded over the period from sunrise to sunset on June 21, September 15, and December 5, 1977, and on April 19, 1978. The temperature variation observed on each date is shown in Figs. 39 to 42 respectively. The temperature gradients through the bituminous layer on June 21 and September 15, 1977 are presented in Figs. 43 and 44. The gradients measured on the other two dates were negligible.

It may be seen that the temperatures measured at the road surface correspond closely with those recorded at a depth of 40 mm, which is the recommended depth at which temperatures are measured during a deflection survey (19).

As expected, the largest range of surface temperature occurred during the summer months (Fig. 39). This range decreases progressively with depth, and at the bottom of the bituminous layer the temperature variations are very small over a given period from sunrise to sunset. At any depth in the pavement, there is a daily cyclic variation of temperature, with the maximum surface temperature occurring around 1.00 p.m. With

increasing depth, there is a marked phase lag between the peak temperatures (Figs. 39 and 40).

Figs. 43 and 44 indicate that the largest temperature gradients also occur in the summer months. It may be seen that there is generally a marked fall in temperature near the surface of the pavement. This suggests that the pavement surface is cooling down, although the effect may be due to the method of temperature measurement at the surface. It was noted that the presence of cloud could alter the surface temperature by $4^{o}C$.

5.4 Simulation of Temperature Variations in the Bituminous Layer

The pavement models used in the analysis were those for the 20 m test length (Model A) and the 150 m test length (Model B) of the Hillsborough test section, after overlaying. For each model, the bituminous layer was divided into five sub-layers, and the temperature at the centre of each sub-layer found by interpolation from the temperature records.

A relationship between resilient modulus and temperature was obtained from the results of laboratory tests reported by Snaith (25), as shown in Fig. 45. It was assumed that the modulus values for the bituminous layer found by back analysis (Section 3.4.3) represented conditions at $20^{o}C$.

Hence it was possible to assign a modulus value to each of the bituminous sub-layers, based on its representative temperature value. Table 10 summarizes the values obtained using the data for June 21, 1977. Also included are the temperatures recorded at a depth of 40 mm, T_{40}.

5.5 Influence of Temperature on Transient Deflection

Using the 'modulus profiles' (Table 10) derived for the bituminous layer, an individual model was created for each observation of temperatures. A standard (3175 kg) load, representing the rear wheel of the Benkelman Beam vehicle, was applied in each case (e.g. Fig. 46), and the induced transient deflection computed (Table 10). The predicted deflections were plotted against the corresponding values for T_{40}, as shown in Fig. 47.

increasing depth, there is a marked phase lag between the peak temperatures (Figs. 39 and 40).

Figs. 43 and 44 indicate that the largest temperature gradients also occur in the summer months. It may be seen that there is generally a marked fall in temperature near the surface of the pavement. This suggests that the pavement surface is cooling down, although the effect may be due to the method of temperature measurement at the surface. It was noted that the presence of cloud could alter the surface temperature by $4^{o}C$.

5.4 Simulation of Temperature Variations in the Bituminous Layer

The pavement models used in the analysis were those for the 20 m test length (Model A) and the 150 m test length (Model B) of the Hillsborough test section, after overlaying. For each model, the bituminous layer was divided into five sub-layers, and the temperature at the centre of each sub-layer found by interpolation from the temperature records.

A relationship between resilient modulus and temperature was obtained from the results of laboratory tests reported by Snaith (25), as shown in Fig. 45. It was assumed that the modulus values for the bituminous layer found by back analysis (Section 3.4.3) represented conditions at $20^{o}C$.

Hence it was possible to assign a modulus value to each of the bituminous sub-layers, based on its representative temperature value. Table 10 summarizes the values obtained using the data for June 21, 1977. Also included are the temperatures recorded at a depth of 40 mm, T_{40}.

5.5 Influence of Temperature on Transient Deflection

Using the 'modulus profiles' (Table 10) derived for the bituminous layer, an individual model was created for each observation of temperatures. A standard (3175 kg) load, representing the rear wheel of the Benkelman Beam vehicle, was applied in each case (e.g. Fig. 46), and the induced transient deflection computed (Table 10). The predicted deflections were plotted against the corresponding values for T_{40}, as shown in Fig. 47.

The deflection/temperature relationship suggested by the T.R.R.L. (19) is also given.

It may be seen that the predicted curves are slightly steeper, thus implying a stronger dependence on temperature.

5.6 Use of Temperature Measured at a Depth of 40 mm

If the temperature at a depth of 40 mm (T_{40}) is assumed to be representative of the entire depth of the bituminous layer, Fig. 45 may be used to obtain a corresponding modulus value for each observation of T_{40} (Table 11).

A standard (3175 kg) wheel load was applied in each case (e.g. Fig. 48), and a second deflection/temperature relationship derived (Fig. 49). This exhibits a much stronger dependence on temperature than that established using five sub-layers to model the bituminous material (Fig. 47). A comparison of the deflection/temperature relationships is given in Fig. 50.

5.7 Discussion

At the outset to this investigation, it was considered that temperature had little influence on measured deflection values (Figs. 36 and 37). At the Hillsborough By-pass, pavement temperatures in the range $10^{o}C$ to $38^{o}C$ have been recorded, with no apparent variation in measured deflection. The aim of the theoretical analysis was to verify the supposition that the transient deflections were not strongly dependent on pavement temperature. The data used in the analysis was that for June 21, 1977, as a reasonable range of values was observed on this date.

The use of five sub-layers to model the bituminous material is considered more realistic than a single layer, as it is possible to take account of the temperature gradient through the layer. Hence the relationship (Fig. 47) derived using the former model should be more reliable. Some scatter was observed in this relationship. This may be explained by

the fact that for any value of T_{40}, a number of temperature profiles are possible. The predicted relationship is similar to that reported by the T.R.R.L. (19).

If the proposed relationship (Fig. 47) is compared with that obtained using a single bituminous layer, (Fig. 50), it may be seen that the latter is much steeper. The implication is that the temperature measured at a depth of 40 mm is not truly representative of the effective pavement temperature.

Nevertheless, the measurement of pavement temperature at this fixed depth provides a relatively quick assessment of a typical pavement temperature which has been found to correlate with measured deflections (19). Furthermore, good correlation has been observed getween T_{40} and stresses measured in the subgrade (35). It has been stated (32) that errors inherent in the procedure are minimized by restricting deflection studies to periods when the surfacing temperature is between $10^{o}C$ and $30^{o}C$.

The predicted deflection/temperature relationship (Fig. 47) is much steeper than that observed (Fig. 36) at the Hillsborough By-pass. It would appear, therefore, that the bituminous material at the Hillsborough test section is much less temperature susceptible than pavements in Great Britian (19) and indeed bituminous samples tested under laboratory conditions (25). This view is supported by other research findings (7). The deflection/temperature relationship proposed by Bailie (7), which is currently used in Northern Ireland to correct deflection measurements to a standard temperature of $20^{o}C$, exhibits much less dependence on temperature than that suggested by the T.R.R.L. (19).

5.8 Conclusion

Studies of deflections measured over a range of temperatures have indicated no marked dependence on the temperature value. A theoretical investigation, using measured temperaturevalues in conjunction with laboratory test results, has suggested a deflection/temperature relationship similar to that proposed by the T.R.R.L.

It is concluded that the bituminous layer at the Hillsborough test section is much less temperature susceptible than pavements in Great Britain and indeed bituminous samples tested under laboratory conditions. Some explanation for this effect may be found by testing cores from the pavement in question. It is evident that the temperature correction proposed by the T.R.R.L. is not applicable to pavement deflections measured in Northern Ireland.

CHAPTER SIX

CORRELATION OF BENKELMAN BEAM AND DEFLECTOGRAPH DEFLECTIONS

6.1 Introduction

Research (32) has shown that the magnitude of the transient deflection of a road pavement under a standard wheel load may be related to its long term performance. This provides a relatively quick and simple method of predicting maintenance requirements.

Pavement deflections may be measured using the Benkelman Beam or the Deflectograph. The construction and operation of these are described elsewhere (36,37). To date, most deflection measurements in the United Kingdom have been made using the Benkelman Beam. However, with the introduction of the Deflectograph, some correlation between the two methods of measurement is needed if existing design recommendations (19,38) are to be adopted. This chapter describes the use of the computer program DEFPAV to study the way in which the beam support points associated with each of the measuring systems are influenced by the deflection bowls of the respective vehicles. The resulting effect on measured deflections is investigated, and a correlation established between the two methods of measurement.

6.2 Need for a Correlation

As used in the United Kingdom, the Benkelman Beam and the Deflectograph employ the same rear wheel load (3175 kg). The two methods would indicate the same deflection if the tyre spacing and contact area of the tyres were identical for the two types of wheel assembly used, and if during the measuring cycle, the beam support points in the two methods were influenced in the same manner by the movement of the wheels of the vehicle.

Dealing with the first point, significant differences in tyre spacing and contact area have been reported (19). Regarding the second point, neither method gives an absolute measure of deflection since the

beam assembly supports are influenced by the deflection of the pavement under the action of both the front and rear wheels of the vehicle.

With the Benkelman Beam, the front wheels are sufficiently remote to have only a small influence on the beam supports, and the rear wheels have a decreasing effect as the vehicle moves forward. In the case of the Deflectograph, the beam assembly supports tend to pass out of the influence of the front wheels and into the influence of the rear wheels during the measuring cycle.

For each vehicle, the magnitudes of the front and rear wheel loads have been measured using a portable weighbridge (39). Details of these and relevant dimensions are given in Table 12.

6.3 Method of Correlation

The computer program DEFPAV has been used to model the passage of both the Benkelman Beam vehicle and the Deflectograph over the Hillsborough test section. The front and rear wheel loads were simulated using single wheel assemblies. Details are given in Table 12. The deflection bowls associated with each wheel load were established, so that a deflection contour plan could be drawn for each vehicle.

By superimposing a plan view of the Benkelman Beam on the appropriate contours, it was possible to obtain the computed absolute (true) deflection at the shoe and beam supports, for each stage of the measuring cycle. If the supports were influenced by the deflection pattern, a correction was applied to give the apparent (measured) deflection. Having obtained the apparent shoe deflection at each stage of the measuring cycle, the nett deflection was easily deduced.

By a similar procedure, the corresponding Deflectograph deflection was found using a deflection contour plan for the Deflectograph.

The pavement model used for the analysis was that for the Hillsborough test section, after overlaying. To simulate a wide range of pavement temperature conditions (i.e. to obtain a range of corresponding deflections

for the correlation), the value assigned to the surface layer modulus (M_{r_1}) was varied between 500 MN/m^2 and 5000 MN/m^2.

Fig. 51 summarizes the procedure used to predict the corresponding Benkelman Beam and Deflectograph deflections.

6.4 Prediction of Deflections Measured by the Benkelman Beam

By applying the Benkelman Beam vehicle wheel loads to the pavement model, the deflection bowls associated with the front and rear wheels were deduced. Fig. 52 shows a typical finite element representation. For each value assigned to M_{r_1}, a deflection contour plan (e.g. Fig. 53) was drawn. Hence, for each stage of the measuring cycle, the absolute deflections at the shoe and the beam supports were determined. This is illustrated in Fig. 53, for the case M_{r_1} = 750 MN/m^2.

In a few cases it was found that the front supports of the beam were influenced by the deflection pattern. This occurred only at the initial stage of the measuring cycle, and in these cases a correction (Section 6.5) was applied to obtain the apparent deflection.

Having found the apparent deflection for each stage of the measuring cycle, the nett deflection was deduced using the relationship:

$$\text{Nett deflection} = \delta_{max} - \delta_{i/2} - \delta_{f/2}$$

where δ_i = apparent shoe deflection at initial stage of measuring cycle.

δ_{max} = apparent maximum shoe deflection.

δ_f = apparent shoe deflection at final stage of measuring cycle.

This relationship was derived from that which is used in practice, i.e.,

$$\text{Nett deflection} = 2\Delta_{max} - \Delta_i - \Delta_f$$

where Δ = corresponding displacement measured at the dial gauge.

Table 13 shows the nett deflections predicted for various values of surface layer modulus (M_{r_1}).

6.5 Correction for Influence of Deflection Bowls on Benkelman Beam Supports

Deflections measured using the Benkelman Beam are influenced by any vertical displacement of the front legs. The nett effect of a downward displacement is a reduction in the measured deflection. The apparent deflection may be estimated as follows:

If δ_{S_L} = equivalent deflection of shoe S due to a vertical displacement δ_L at the front legs,

then, referring to Fig. 54.

Apparent shoe deflection = Absolute shoe deflection - 2.8 δ_L.

This relationship may be used to predict the measured deflection whenever the front legs of the beam lie inside the deflection bowl. The relationship corresponds closely to that reported by the Canadian Good Roads Association (40).

6.6 Prediction of Deflections Measured by the Deflectograph

The deflection bowls associated with the front and rear wheels of the Deflectograph were computed by applying the appropriate wheel load (Table 12) to the pavement model. For each value of M_{r_1} used, a deflection contour plan (e.g Fig. 55) was drawn. Hence, for each stage of the measuring cycle, the absolute deflections at the shoe and the beam assembly supports were obtained. An example is shown in Fig. 55, for the case M_{r_1} = 750 MN/m^2.

In those cases where the beam assembly supports were influenced by the deflection pattern, a correction (Section 6.7) was applied to obtain the apparent deflection. Having found the apparent deflection for each stage of the measuring cycle, the nett deflection was deduced as follows:

$$\text{Nett deflection} = \delta_{max} - \delta_i$$

where δ_i = apparent shoe deflection at initial stage of measuring cycle

δ_{max} = apparent maximum shoe deflection.

Table 14 summarizes the nett deflections predicted for various values of surface layer modulus (M_{r_1}).

6.7 Correction for Influence of Deflection Bowls on Deflectograph Beam Assembly Supports

Deflections measured using the Deflectograph are influenced by any vertical displacement at the supports. Referring to Fig. 55, the deflection measured using beam assembly BG will be altered by any vertical displacement at supports B or C. (It is assumed that there is no relative movement between supports B and A.) The nett effect of a downward displacement at either B or C is a reduction in the measured deflection. The apparent deflection may be estimated as follows:

If δ_{G_B} = equivalent deflection at shoe G due to a vertical displacement δ_B at support B.

δ_{G_C} = equivalent deflection at show G due to a vertical displacement δ_C at support C.

then,

Apparent shoe deflection = Absolute shoe deflection - δ_{G_B} - δ_{G_C}.

The evaluation of the terms δ_{G_B} and δ_{G_C} is presented in Figs 56 and 57 respectively.

Thus

Apparent shoe deflection = Absolute shoe deflection - δ_B - 0.7 δ_C.

6.8 Correlation of Predicted Deflections

The predicted Benkelman Beam deflections were plotted against the corresponding Deflectograph values, as shown in Fig. 58. Using the computer program CURFIT (41), both a straight line and a second degree polynomial were fitted to the points. The latter was considered the better representation, and this held the relationship:

$$y = 7.16 + 0.69x + 0.0052\ x^2$$

where x = Deflectograph value.

y = Benkelman Beam value.

It may be seen (Fig. 58) that the correlation derived using the program DEFPAV corresponds closely to that reported by the T.R.R.L. (19) for pavements with unbound bases and hot rolled asphalt surfacing.

6.9 Discussion

6.9.1 Modelling Assumptions

The development of the pavement models for each vehicle has involved the use of certain simplifying assumptions.

The rear wheel load of each vehicle was simulated using a single wheel assembly, whereas in practice a twin wheel assembly is employed. It has been noted (Section 2.8.2) that use of a single wheel assembly will give higher computer deflections. However, as the single wheel model has been used for the rear wheels of both vehicles, the correlation will not be affected to any significant extent.

In practice, the contact area associated with the rear wheel of the Deflectograph is larger than that of the Benkelman Beam vehicle (19). However, in the respective pavement models the contact area was deduced from the wheel load and the contact pressure. As the contact pressure associated with the rear wheel of the Deflectograph was greater than that of the Benkelman Beam vehicle, the former was assigned a smaller contact area. This should not adversely affect the correlation, however, as a sensitivity study (Section 2.8.2) has shown that variations in contact pressure over this range whilst keeping the overall load constant gives minimal change in the computed deflection.

6.9.2 Influence of Deflection Bowls on Beam Assembly Supports

It has been noted that, for both vehicles, the front wheels were sufficiently remote to have no effect on the beam assembly supports.

In the case of the Benkelman Beam vehicle, the rear wheels had a decreasing effect on the position of the beam supports as the vehicle

moved forward. The correction for influence of the deflection bowls on the front legs was applied in only two of the cases considered.

Considering the Deflectograph, the beam assembly supports moved into the influence of the rear wheels during the measuring cycle. It was noted that the deflection at the T-frame support (support C in Fig. 55) held the same value for both the initial and maximum stages of the measuring cycle. Thus, when the nett deflection (i.e. $\delta_{max} - \delta_i$) was calculated, the correction for displacement at this support had no effect. Additionally, the correction for influence of the deflection bowls on the recording head support (support B in Fig. 55) was applied in only one of the cases considered.

6.9.3. Practical Correlation Exercise

A correlation between Benkelman Beam and Deflectograph deflections measured in Northern Ireland has been established by other researchers (42), as part of a joint project between the Department of the Environment for Northern Ireland and the Queen's University of Belfast (D.O.E./Q.U.B.). The location chosen for the practical correlation exercise was the South-bound carriageway of the M1 Motorway between the Moira and Lurgan inter-changes, as this provided a wide range of deflection values.

The results of the exercise were significantly different from both the DEFPAV and the T.R.R.L. correlations (Fig. 59). They suggest that, in general, the Deflectograph gives higher deflection readings than the Benkelman Beam. It must be noted that the DEFPAV correlation was derived by modelling the pavement at the Hillsborough test section. However, both this pavement and that at the M1 Motorway are of similar construction, and the correlation proposed by the T.R.R.L. should apply in each case.

6.10. Conclusion

A second degree polynomial relationship exists between the predicted

Benkelman Beam and Deflectograph deflections. This has the form:

$$y = 7.16 + 0.69x + 0.0052\ x^2$$

where x = Deflectograph value.

y = Benkelman Beam value.

This correlation corresponds closely with that proposed by the T.R.R.L. for pavements with unbound bases and hot rolled asphalt surfacing.

CHAPTER SEVEN

AN INVESTIGATION OF STRUCTURAL FAILURE PHENOMENA

7.1 Introduction

The failure criteria which are generally considered appropriate for analytical pavement design have been listed (43) as follows:

(a) Tensile strain in the extreme fibre of the bituminous layer.

(b) Compressive strain at the top of the subgrade.

(c) Tensile strain in the extreme fibre of the granular layer.

These are shown diagrammatically in Fig. 60. The corresponding modes of failure are fatigue of the bituminous bound layer, excessive permanent deformation in the subgrade, and tensile failure of the sub-base. Criteira (a) and (b) have been adopted in several analytically based design systems reported to the Fourth International Conference on the Structural Design of Asphalt Pavements (1).

The failure criteria which are used in practice in Great Britain have been defined by Croney (44). The 'failure' condition is the state at which major structural repair is required, and the 'critical' condition is the state at which overlaying would ensure continued satisfactory performance. These criteria were developed directly by observations on existing roads (45) in conjunction with the maintenance procedures of typical road authorities.

Croney (44) has reported that, with the base and surfacing materials commonly used in Great Britain, permanent deformation was accepted by engineers as the principal indication of failure. Major reconstruction was generally undertaken when the rut depth in the wheel track of the slow lane was approximately 20mm, measured with a 1.8m straight edge. At this level of deformation some cracking was generally apparent where rolled asphalt wearing courses were used. It was thought that the subsequent ingress of water was responsible for the relatively rapid deterioration occurring where rut depths exceeded 20mm.

The critical condition was considered (44) to occur when rut depths were in the range from 10 to 20mm, because it was at this level of rutting that overlays were being applied in practice. At this condition there was generally little evidence of cracking, and if present it was usually confined to longitudinal hair cracks along the edge of the wheel paths.

To ensure that the pavement never passes the critical condition, a continual road assessment programme, such as that proposed by the Marshall Committee (33), should be undertaken.

This chapter describes the use of the computer program DEFPAV to investigate the two phenomena of rutting and cracking. Rut depth predictions have been made for the pavements at the Hillsborough and M1 Motorway test sections. The effect of crack propagation through the bituminous layer at the Hillsborough test section has been investigated.

7.2 Rutting and Cracking

From the preceding section, it is clear that the phenomena of rutting and cracking may be regarded as the two outward signs of pavement deterioration.

Wheel track rutting is caused by a build-up of the minute irrecoverable deformations that occur in each layer of a pavement every time a wheel load passes. The danger of rutting lies in the fact that water may pond in the longitudinal trough and then lead to aquaplaning or reduced visibility by spray generation.

With the climatic conditions in the United Kingdom, cracking in flexible pavements is generally a fatigue phenomenon. As a wheel load passes over the pavement, the extreme fibres of the bituminous layer undergo a cyclic variaton of strain. It has been shown (46,47) that this may lead to the formation of fatigue cracks at the base of the bound layer. With further load applications the cracks propagate towards the road surface, progressively weakening the structure finally, resulting in 'chicken-wire' or 'alligator' (20) cracking, which is characterized by a network of cracks over the road surface. With further load applications, surface disintegration in the form of pot-holing may occur.

It has been recommended (33) that the extent of both rutting and cracking should be measured in any survey system. In the United Kingdom rutting is expressed as the maximum depth of rut measured under a 2m straight edge (33). The extent of cracking may be measured by either an estimate of the cracked area (expressed as a percentage of the area of wheel path or carriageway) or an assessment of the type of cracks seen (e.g. single, interconnected, longitudinal). The severity of both rutting and cracking may be used to classify the conditon of the pavement (32).

7.3 Predictions of Permanent Deformation Growth

7.3.1 Rut Depth Predictions at the Hillsborough Test Section

Using the pavement models (B1 and B2) detailed in Section 3.4.5, the development of rut depth on the overlaid pavement has been predicted after a specified number of standard (8200 kg) axle passes.

With each model, the thickness of the surface layer was increased by the depth of overlay, known to be 116 mm of hot rolled asphalt. The assumption was made that the properties of the overlay material were the same as those of the underlying bituminous layer.

A commercial vehicle growth rate of 4 per cent was considered appropriate (29) for the Hillsborough test section. Hence the passage of 0.25, 0.51, 0.78 and 1.06 million standard axles correspond to periods of 1,2,3 and 4 years respectively after overlaying (Fig. 61).

The predicted growth of rut depth is presented in Fig. 61. (The finite element configuration used is given in Fig. 62). It may be seen that the growth curve derived using Model B2 lies closer to the measured (March 1978) value than that obtained with Model B1. Model B1 overestimated the measured value by a factor of four, whilst Model B2 overestimated by a factor of two.

7.3.2 Rut Depth Predictions at the M1 Motorway Test Section

The pavement models (1 and 2) described in Section 3.5.3 have been

used to estimate the future growth of permanent deformation at the M1 Motorway test section. (This pavement has not to date been overlaid.)

The assumed commercial vehicle growth rate was 4 per cent. Values for the cumulative numbers of standard axles used to represent expired life are given in Fig. 63, which shows the estimated development of rut depth on the existing pavement. (The finite element configuration used is given in Fig. 27). Both models 1 and 2 give a similar prediction.

The effect of overlaying the pavement at this test section has been considered. It was assumed that the properties of the overlay material were the same as those of the underlying bituminous layer. A typical finite element configuration is shown in Fig. 64. The date of overlaying was taken as September 1978, and the estimated growth in the number of standard axles over an eight year period is given in Fig. 63, which shows the predicted growth of rut depth after the application of various overlay thicknesses. It may be seen that, using either model, a 50 mm overlay would allow an eight year period to elapse before the rut depth reaches a value of 13 mm.

7.3.3 Discussion

Considering the Hillsborough test section, the rut depth predictions for the overlaid pavement were overestimated within a factor of four of the measured (March 1978) values. It was unfortunate that the rut depth was measured on only one occasion after overlaying. Consequently it is not known whether the growth curve should incorporate a compaction phase immediately after overlaying.

In the case of the M1 Motorway test section, it remains to be seen how accurate the predictions are, as no measurements have been made since 1976.

The accuracy of any rut depth predictions made using the program DEFPAV depends on the validity of the creep equations and material properties specified for each layer of the pavement. For the two test sections considered, the creep equation for Keuper Marl has been applied to both the granular layer and the subgrade. Clearly, this is an optimistic assumption.

It has been established from bituminous cores that, for both pavement sections, negligible permanent deformation occurred in the bituminous layer. This behaviour is not typical of pavements observed in Great Britain. Lister and Kennedy (38) have reported that most or all pavement layers and the subgrade contribute to the deformation. Furthermore, Lister (48) has stated that in a pavement having a crushed stone base at Conington Lodge, deformation occurred in all layers including the subgrade. The major contribution came from the base and surfacing. It is thought that the behaviour of the two test sections under consideration may be influenced strongly by their relatively weak subgrades.

7.3.4 Conclusion

Predictions regarding the growth of rut depth have been made for two pavement sections. It is considered that, whilst the method shows promise, better creep characterization of the pavement materials is required before more accurate predictions can be made.

7.4 Investigation of the Cracking Phenomenon

7.4.1 Simulation of Crack Propagation

The pavement model used in the analysis was that for the 20 m test length (Model A) of the Hillsborough test section (Section 3.4), both before and after overlaying. It was assumed that this model represented conditions at a temperature of 20°C. To simulate conditions at temperatures of 10°C and 30°C, the resilient modulus of the bituminous layer was modified using results obtained by Snaith (25), as shown in Fig. 65.

The propagation of cracks through the bituminous layer was simulated by the introduction of a zone of weaker (cracked) material with a thickness equal to the depth of cracking (Fig. 66). It was assumed that, as the 'family' of cracks propagated upwards, the thickness of the cracked zone increased uniformly across the bituminous layer. This is an over-simplification, as

in reality cracking will only occur in the vicinity of the wheel paths.

Thus the bituminous material was treated as two separate layers, with an assumed modular ratio of five between the 'uncracked' and 'cracked' zones. The value assigned to Poisson's Ratio was the same for both zones.

The 'cracking ratio' was defined as the ratio of the depth of cracked zone to the overall layer thickness.

7.4.2 Influence of Cracking on Transient Deflection

A standard (3175 kg) wheel load was applied to the pavement model (e.g. Fig. 67). The transient deflection, analagous to the Benkelman Beam deflection, was computed for values of cracking ratio varying from zero (i.e. no cracking) to 100 per cent (i.e. cracking fully developed). The results are shown in Fig 68.

It may be seen that, as the cracks propagate towards the surface, the transient deflection increases by a factor of between two and three. Temperature appears to have only a slight influence on the rate of deflection increase, even though the method of simulating temperature variation is considered to over estimate its effect (Chapter Five).

7.4.3 Influence of Cracking on Pavement Stresses and Strains

The failure parameters appropriate for theoretical pavement analysis have been noted in Section 7.1. To study the influence of crack propagation within the bituminous layer on these parameters, a standard (4100 kg) wheel load was applied to the pavement model (Fig. 69). The resilient modulus of the bituminous layer was modified to take account of average vehicle speeds, using the chart proposed by Brown (28). The value obtained was 6000MN/m^2 (Fig. 19 will apply to Model A). This was assumed to represent conditions at a temperature of 20°C.

Fig. 70 shows the variation of ϵ_r, ϵ_z and σ_r with cracking ratio. It may be seen that, as cracking progresses, there is a corresponding increase in each of the parameters considered. The effect of overlay is

clearly seen, as a considerable reduction in the values is achieved.

Reference to Fig. 70 indicates that, as cracking proceeds, there is an increased likelihood of failure by either excessive permanent deformation in the subgrade, tensile failure of the sub-base, or some combination of these. The mode of failure adopted will depend on the critical values of the respective failure parameters.

The computed values for each of the above mentioned parameters have been plotted against the corresponding computed Benkelman Beam deflections, as shown in Fig. 71. (Table 15 summarizes the deflections, stresses, and strains computed for various values of cracking ratio.) In each case it may be seen that a definite correlation exists. This suggests that where there is progressive cracking of the bituminous layer, the magnitude of the Benkelman Beam deflection reflects the structural integrity of the pavement.

7.4.4. Discussion

It has been observed (32) that as a road pavement reaches its 'critical' condition, there is a rapid increase in the surface transient deflection. Clearly, this may be due to the propagation of fatigue cracks in the bottom of the bound layer.

Where pavement deterioration is initiated by fatigue cracking, it is possible that the subsequent weakening of the pavement structure may induce a different mode of failure, such as excessive permanent deformation in the subgrade or tensile failure of the sub-base. Thus the concept of pavement deterioration is a complex one, with the probable interaction of several failure mechanisms during the life of the pavement. It is fortunate that a simple measure of transient deflection will adequately infer the condition of the structure.

It is possible that the effects of crack propagation have been overestimated, due to the model adopted for crack simulation. This assumed that cracking occurs across the entire width of carriageway, whereas this is likely only in those areas adjacent to the wheel paths.

7.4.5 Conclusion

The computer program DEFPAV has been used to simulate the propagation of fatigue cracks through the bituminous layer of the pavement at the Hillsborough test section. It has been shown that there is a marked rise in deflection as cracking progresses, and that the weakening effect on the structure may induce other modes of failure. It is concluded that, for the fatigue mode of failure, a measure of the transient deflection adequately reflects the structural integrity of the road pavement.

CHAPTER EIGHT

OTHER APPLICATIONS OF THE COMPUTER PROGRAM DEFPAV

8.1 Derivation of Load Equivalence Factors

8.1.1 Introduction

One aim of the A.A.S.H.O. Road Test (49,50) was to assess the relative damaging power of a wide range of axle loads. The number of passages of a standard (8160 kg) axle required to cause the same damage as one passage of a specified axle load was expressed as an 'equivalence factor'. Typical values are quoted in Table 16 (19). It may be seen that one passage of a standard axle will induce as much damage as 100 passages of a 2720 kg axle. Similarly, 15 passages of a standard axle will do as much damage as one passage of a 16320 kg axle. The values indicate that the damaging effect of an axle is approximately related to the fourth power of its load.

The equivalence factors derived from the A.A.S.H.O. Road Test are incorporated in current design recommendations (30) in the United Kingdom. Thus traffic of mixed composition may be expressed in terms of an equivalent number of standard axles. However, some doubt has been expressed (51) regarding the applicability of these factors to pavements in climatic conditions other than those found at the location of the A.A.S.H.O. Test.

As an alternative to a full scale test, the pavement construction may be modelled using a computer program such as DEFPAV, and a set of equivalence factors deduced for the prevailing climate. A small scale test could then be instituted to verify the findings. This concept has previously been reported by Kirwan et al (2).

Section 8.1 describes the analytical derivation of load equivalence factors for the Hillsborough and M1 Motorway test sections. The pavement model used for the Hillsborough test section was Model B2 (Section 3.4.5), after overlaying. The creep equation associated with Keuper Marl was applied to both the granular layer and the subgrade, with a calibration

factor of 2.4. The model used for the MI Motorway test section was Model 2 (Section 3.5.3). The creep equation for Kent Marl was applied to the granular layer and the subgrade, with a calibration factor of 0.404.

The critical condition has been defined in two different ways. Firstly, a limiting value of 13 mm was placed on the rut depth (33), and secondly the limiting number of wheel passages was expressed as the fatigue life of the bituminous layer, derived from Pell's experimental relationship (52)

8.1.2. Load Equivalence Factors by Analysis

(a) Critical Condition Defined by Rutting

In the United Kingdom the condition of a road pavement is defined principally in terms of the measured rut depth (44, 32). The number of passages of various wheel loads required to produce a limiting rut depth of 13 mm (33) has been found using the program DEFPAV. Figs. 72 and 73 show the computer growth of rut depth at the Hillsborough and MI Motorway test sections. Typical finite element configurations, which were generated using the 'automatic grid' option (Chapter Two), are given in Figs. 74 and 75.

The equivalence factor for any axle load (A_i) may be expressed as:

$$\text{Load equivalence factor} = \frac{N_s}{N_i}$$

where N_s = number of passages of a standard (4100 kg) wheel load required to produce a rut depth of 13 mm

N_i = number of passages of any wheel load (L_i) required to produce a rut depth of 13 mm

and $L_i = \frac{A_i}{2}$

This has been evaluated for a number of axle loads. Table 17 summarizes the values obtained. For each test section, the deduced factors were plotted against the corresponding axle

loads, and a relationship of the form:

$$\text{Load equivalence factor} = \left(\frac{\text{Axle load (kg)}}{8200}\right)^{A}$$

fitted to the points. Figs. 76 and 77 refer to the Hillsborough and M1 Motorway test sections respectively. The value of the power 'A' was found to be 3.8 for the Hillsborough test section, and 2.0 for the M1 Motorway test section.

(b) Critical Condition Defined by Fatigue

Pell (52) has shown that the fatigue life (i.e. number of load applications to failure, N) of a bituminous mix may be expressed in terms of the maximum tensile strain, ε_m, as follows:

$$N = c\left(\frac{1}{\varepsilon_m}\right)^{n}$$

where c and n are factors which depend on the composition and properties of the mix. The value assigned to n was 5. This was obtained from values quoted by Pell and Brown (27) for various mixes. It has been suggested (53) that a factor of 100 be used to increase the laboratory life to that achieved in practice.

Thus

$$N = k\left(\frac{1}{\varepsilon_m}\right)^{5}$$

where $k = 100c$

Hence the equivalence factor for any axle load (A_i) may be expressed as:

$$\text{Load equivalence factor} = \frac{N_s}{N_i} = \left(\frac{\varepsilon_i}{\varepsilon_s}\right)5$$

where N_s = fatigue life associated with a standard (4100 kg) wheel load

N_i = fatigue life associated with any wheel load (L_i)

ε_s = maximum tensile strain in bituminous layer under a standard (4100 kg) wheel load

ε_i = maximum tensile strain in bituminous layer under any wheel load (L_i)

and $L_i = \frac{A_i}{2}$.

Thus by computing the maximum tensile strain in the bituminous layer for a number of wheel loads, it is possible to deduce a set of equivalence factors. (The maximum tensile strain was found to occur at the extreme fibre of the layer.) This has been done for the pavements at the Hillsborough and M1 Motorway test sections (Figs. 74 and 75). The results are summarized in Table 17. For each test section, the deduced factors were plotted against the corresponding axle loads (Figs. 76 and 77), and a relationship of the form:

$$\text{Load equivalence factor} = \left(\frac{\text{Axle load (kg)}}{8200}\right)^{A}$$

fitted to the points. The value of the power 'A' was found to be 4.0 for the Hillsborough test section and 3.4 for the M1 Motorway test section.

8.1.3 Discussion

The equivalence factors deduced for the Hillsborough test section (Fig. 76) are in close agreement with those derived from the A.A.S.H.O. Road Test. The two modes of failure considered (i.e. wheel track rutting and fatigue of the bituminous layer) have produced similar results. In both cases the induced damage is approximately related to the fourth power of the axle load.

Considering the M1 Motorway test section (Fig. 77), it may be seen that the induced damage in terms of rutting is related to the square of the axle load, whilst the damage in terms of fatigue is proportional to the axle load raised to the power 3.4. Although fatigue failure may seem more likely in this case, the ultimate failure mode will depend on the critical values of the respective failure parameters.

8.1.4 Conclusion

The computer program DEFPAV has been used to derive load equivalence factors for the pavements at the Hillsborough and M1 Motorway test sections.

This provides an alternative to a full scale road test, although a small scale test would be required to verify the findings.

8.2 Use of Fabrics in Pavement Construction

8.2.1 Introduction

During the last few years there has been a considerable increase in the use of fabrics in pavement construction. Their chief applications include soil drainage, embankment reinforcement, and subgrade/sub-base separation. It has been claimed (54) that the functions of a fabric in subgrade/sub-base separation are as follows:

(a) By separation, 'down punching' of the sub-base and loss of fines are prevented.

(b) By filtration, the upward pumping of fines from the subgrade to the sub-base is minimized.

(c) The fabric gives reinforcement by absorbing transient tensile loads and maintains the integrity of the sub-base.

Section 8.2 describes the use of the program DEFPAV to model a pavement construction both with and without a fabric inclusion.

8.2.2 Effect of a fabric Inclusion Between the Granular Layer and the Subgrade

Details of the pavement constructions (55) modelled are given in Figs. 78 and 79. The modulus values assigned to the granular layer and the subgrade are summarized in Table 18. The respective creep equations applied to the bituminous layer and the subgrade were those for dense bitumen macadam (4) and Dublin boulder clay (13).

The fabric has been modelled using a layer of 6 mm thickness, subdivided into three element rows. It was considered that, in practice, local reinforcing of the soil structure occurs in the vicinity of the fabric. Consequently transitional layers were introduced both above

and below the fabric 'layer' in the model. This reduced the abrupt change in resilient modulus between the fabric and its adjacent layers.

A 13 kN single wheel load was applied to each model. Table 19 summarizes the computed values of stress and strain at various positions in the pavement directly under the wheel load.

8.2.3. Discussion

It may be seen that, for the pavement under consideration, the inclusion of a fabric between the granular layer and the subgrade causes a reduction of 30 per cent in the value of the surface transient deflection. The inclusion of the fabric has no significant influence on the computed rut depth.

It must be noted that the fabric has been modelled using a layer having a depth of 6 mm. This is unreasonably high for any of the light weight fabrics, but is necessary if the aspect ratio of the elements under the loaded area is to be kept near unity. The value assigned to the resilient modulus of the fabric (1200 MN/m^2) is also optimistic.

Thus the effect of the fabric inclusion may be over estimated. Field tests would be required to verify the findings. Nevertheless, it may be seen that a program such as DEFPAV may be used to predict the effect of a fabric inclusion in a specific pavement construction.

8.2.4. Conclusion

The computer program DEFPAV has been used to study the influence of a fabric inclusion between the granular layer and the subgrade on the behaviour of the pavement under load. A 30 per cent reduction in transient deflection was predicted, but this is considered an overestimate of the effect of the fabric.

CHAPTER NINE

SUMMARY OF WORK DONE

Computer-aided flexible pavement analysis has proved to be a useful tool in the development of rational methods of pavement design (1). However, it is hoped that the work described in the preceding chapters has shown that structural analysis may also be applied to the assessment of pavement performance. To demonstrate this, an attempt has been made to predict the behaviour of specific in-service pavements in Northern Ireland. The results of the analyses have been compared with observations made at the pavements in question.

The predictions made concerning transient deflections (Section 4.2) and rut depths (Section 7.3.1) after overlaying at the Hillsborough test section may be classified according to Lambe (56). These correspond to 'Type C' predictions (i.e. predictions made after the event, and the results not known when the predictions are made). Lambe regards 'Type C' predictions as autopsies, but acknowledges that autopsies can contribute to our knowledge. In the case of the M1 Motorway test section, the predictions made for the overlaid pavement fall into 'Type A' (i.e. predictions made before the event), as this pavement has not to date been overlaid.

As noted in Chapter two, the program DEFPAV performs an elastic analysis to produce the transient deflections and stresses throughout the pavement structure, and then makes use of 'creep equations' to estimate the long term behaviour (rutting). It is clear that effective use of the elastic analysis depends on the specification of appropriate values for the elastic parameters (M_r, ν) used to define the constituent materials. Moreover, use of the 'long term' analysis depends on the selection (or specification) of a suitable creep equation. Thus a major problem in modelling in-service pavements is the ability to characterize the constituent materials. Ideally, the materials should be tested either in situ or in the laboratory, but unfortunately this was beyond the scope of the current research programme.

As a result of the preceding analyses, the following conclusions can be drawn:

1. Overlay design charts have been prepared for the pavements at the Hillsborough and M1 Motorway test sections. The change in Benkelman Beam deflection due to the addition of overlay at the Hillsborough test section was predicted with a fair degree of accuracy. The overlay chart for the M1 Motorway test section has been used (34) with some success to predict the effect of a 40mm overlay over a 50m length of carriageway.

2. The bituminous layer at the Hillsborough test section is much less temperature susceptible than pavements in Great Britain and indeed bituminous samples tested under laboratory conditions. It is concluded that the temperature correction proposed by the T.R.R.L. is not applicable to pavement deflections measured in Northern Ireland.

3. A second degree polynomial relationship exists between the predicted Benkelman Beam and Deflectograph deflections at the Hillsborough test section. This has the form:

$$y = 7.16 + 0.69x + 0.0052\ x^2$$

where x = Deflectograph value

y = Benkelman Beam value

This correlation corresponds closely with that proposed by the T.R.R.L. for pavements with an unbound base and hot rolled asphalt surfacing.

4. Theoretical considerations have shown that, as fatigue cracks propagate upwards through the bituminous layer at the Hillsborough test section, there is a corresponding rise in the surface transient deflection. The weakening effect on the structure may induce other modes of failure. It is concluded that, for the fatigue mode of failure, a measure of the transient deflection adequately reflects the structural integrity of the road pavement.

5. Predictions regarding the growth of rut depth at the Hillsborough test section after overlaying were within a factor of four of the measured value.

6. Load equivalence factors have been derived for the pavements at the Hillsborough and M1 Motorway test sections. The failure modes considered were wheel track rutting and fatigue of the bituminous layer. In the case of the Hillsborough test section, the damage was approximately related to the fourth power of the axle load for both modes of failure. In the case of the M1 Motorway test section, the induced damage in terms of rutting was related to the square of the axle load, whilst the damage in terms of fatigue was proportional to the axle load raised to the power 3.4.

7. A preliminary study of the affect of a fabric inclusion between the granular layer and subgrade in a test pavement has indicated that a 30 per cent reduction in transient deflection can be achieved. However, this is considered an overestimate of the effect of the fabric.

It is worth noting that the T.R.R.L. recommendations for overlay design contained in LR 571 (19) have recently been updated in LR 833 (57). In the later publication, Kennedy and Lister present a comprehenisve relationship connecting overlay thickness with the deflection before overlay and the required extension of life, for a range of pavement types. The new publication also contains updated charts for the 'temperature correction' and 'deflectograph correlation' reported in Chapters Five and Six respectively.

PART TWO

AN OVERLAY DESIGN SYSTEM FOR DEVELOPING COUNTRIES

CHAPTER TEN

INTRODUCTION

The application of multi-layer analysis to the problem of overlay design has been demonstrated in Part One (Chapter Four). This approach adopted the surface transient deflection as the basic design criterion.

Part Two of this report describes an overlay design system in which the design criteria are the horizontal tensile strain in the extreme fibre of the bituminous layer and the vertical compressive strain at the top of the subgrade. The method has been developed at the University of Birmingham (58) and is presented as an overlay system suitable for use in developing countries.

The main features of the system are as follows:

(i) it is based on fundamental structural response and distress models of the pavement, following the current school of thought;

(ii) a simple, cheap apparatus, such as the Benkelman Beam, is required to measure the surface deflection under a moving wheel load;

(iii) a simple calculation is needed to predict the necessary overlay thickness, which can be accomplished in a small amount of time using an electronic calculator.

10.1 Structural Response Model of a Pavement

The adoption of suitable pavement models has been influenced by the constant conflict between the desire to represent the pavement structure by a comprehensive and realistic model and the considerable difficulties encountered in solving the equations for stress and strain as the complexity of the model increases. Much early work on flexible pavement design was seriously inhibited by mathematical and computational problems and only since electronic computers became widely available has it been possible to adopt fairly representative models. Even at the present time there can be problems,

not so much of a methematical nature, but arising from the time and cost of the computations required and from the accessibility to a suitable computer, (59).

Modern flexible pavements consist of three main layers, bituminous surfacing, roadbase and sub-base, (Figure 80(a)). The surfacing is generally sub-divided into a wearing course and a base course, laid separately. The road-base may be bituminous, cement-bound or unbound granular base. The sub-base is usually of unbound granular material. The soil foundation for the pavement structure is termed the subgrade. To present this flexible pavement structure, the following analytical model, (Figure 80(b)) has been adopted.

(i) the pavement structure is regarded as a three-layer system. The lowest layer, semi-infinite in the vertical direction, represents the subgrade. The middle layer represents the unbound base or sub-base layer. The top layer represents all the bituminous layers:-

(ii) these layers are considered to have complete friction between them;

(iii) the materials in the layers are linearly elastic, isotropic and homogeneous;

(iv) the load is assumed to be uniformly distributed over a circular area at the surface of the top layer.

On the basis of this model, the calculation of all stresses, strains and displacements at any point in the system can be done. The general response of a flexible pavement subjected to a traffic load can be shown schematically as in Figure 81.

10.2 Structural Distress Model of Pavement

The structural distress or damage of a pavement structure, associated with traffic loads, is usually divided into two parts:

(i) Fatigue fracture

(ii) Rutting distortion

Fatigue fracture from repeated traffic loading develops in the bituminous layer of the structure and the radial tensile strain at the bottom of that layer has been used as a criterion for limiting fatigue fracture. Rutting deformation from repeated traffic loading can develop in all layers of the structure and the vertical compressive strain at the top of the subgrade has been extensively used as an overall criterion for limiting deformation of the whole pavement, (53). Thus these strain responses are termed 'critical strains', and for normal loading conditions, both maximum values are found on the vertical axis through the centre of the loaded area, (Figure 82).

The majority of the fatigue investigations to date suggest that the response of bituminous material to repetitive loading can be defined by a relationship of the following form, (53,59):

$$N = C \left(\frac{1}{\varepsilon_r}\right)^m \qquad (10.1)$$

in which ε_r = tensile strain repeatedly applied;

N = no. of applications to failure;

C,m = material coefficients.

The relation between the number of strain repetitions and the permissible compressive strain in the subgrade, developed by Edwards and Valkering, (60), is of the same form as above:

$$N = K \left(\frac{1}{\varepsilon_z}\right)^n \qquad (10.2)$$

in which ε_z = compressive strain repeatedly applied:

N = no. of applications to failure;

K,n = material coefficients.

As seen above, the forms of both distress models are identical. Thus the relationship between the critical strains and the number of load applications to failure, i.e., the strain-life, (ε-N) relationship for

both distress (damage) modes can be collectively represented by one model as:

$$N = A \left(\frac{1}{\varepsilon}\right)^b \qquad (10.3)$$

in which ε = the critical strain

N = the life associated with it

A,b= coefficients depending on the type of distress and materials.

Using the distress model given by Equation (10.3) the life associated with the particular damage mode can be found once the critical strain response is calculated using the structural response model.

10.3 Outline of the Proposed Method

The outline of the proposed method is as shown by the flow chart in Figure 83.

(i) the Benkelman beam deflection and in situ C.B.R of subgrade are measured, from which the resilient modulus of each layer is derived.

(ii) the critical strains in the existing pavement are computed.

(iii) from the values of critical strains, the distress lives of the existing pavement can be known. Using the information, together with the present and future traffic, the allowable values of critical strains in the overlaid pavement are determined by applying the cumulative damage theory.

(iv) the required thickness of overlay for each distress mode is computed and the greater one is taken as the design thickness.

CHAPTER ELEVEN

DETERMINATION OF IN SITU LAYER MODULI

11.1 Introduction

The methods used to assign values of resilient modulus to the subgrade and unbound layers are similar to those presented in Part One (Chapter Three). The resilient modulus for the bituminous layer is deduced from the measured Benkelman beam deflection using the Method of Equivalent Thicknesses.

11.2 Subgrade Layer Modulus from California Bearing Ratio

An empirical relationship between the dynamic elastic modulus of the subgrade (M_{r_3}) and its CBR value has been established by Heukelom and Klomp (26):

$$M_{r_3}\ (MN/m^2) = 10 \times CBR \qquad (11.1)$$

11.3 Unbound Layer Modulus from Subgrade Layer Modulus

It has been shown (26) that the modulus of the unbound base layer (M_{r_2}) depends on its thickness (H_2) and the modulus of the underlying subgrade (M_{r_3}), according to the relationship (60,61):

$$M_{r_2} = K_2\ M_{r_3} \qquad (11.2)$$

where $K_2 = 0.2H_2^{0.45}$

H_2 expressed in mm and $2<K_2<4$

11.4 Bituminous Layer Modulus from Benkelman Beam Deflection

The surface deflection under a moving wheel load, measured by the Benkelman Beam, may be used to find the resilient modulus of the bituminous layer. This section describes the procedure which may be used to calculate the surface deflection, from which the resilient modulus of the bituminous layer is derived. As the resilient modulus depends on the loading time, the procedure used to obtain the modulus value corresponding to typical design speeds is presented.

11.4.1 Method of Equivalent Thicknesses

Elastic solutions for multi-layered systems can be obtained by simple approximate calculations using the method of equivalent thicknesses, (62,63,64,65). It is stated, (64,65), that solutions obtained by these methods are in good agreement with rigorous analysis.

Fundamentally the solution involves two steps:

(i) Transformation of the multi-layered system into a single layer with equivalent thickness.

(ii) use of the solutions for distributed loads on the surface of a linear elastic semi-infinite mass.

Transformation into a single layer

To change a system consisting of layers having different moduli into an elastic half-space, it is necessary to calculate an equivalent thickness for each layer. The principle behind the calculation of an equivalent thickness H_e of a layer with thickness H_1, modulus M_{r_1} and Poisson's ratio ν_1 in relation to a material with modulus M_{r_2} and Poisson's ratio ν_2 (Figure 84), is that the equivalent layer must have the same stiffness as the original layer, so as to give the same pressure distribution underneath the layer. This consideration leads to:

$$H_e^3 \times \frac{M_{r_2}}{1-\nu_2^2} = H_1^3 \times \frac{M_{r_1}}{1-\nu_1^2}$$

or

$$H_e = H_1 \left\{ \frac{M_{r_1}}{M_{r_2}} \times \frac{1-\nu_2^2}{1-\nu_1^2} \right\}^{1/3} \qquad (11.3)$$

If the value of Poisson's ratio is the same for both materials, the expression reduces to

$$H_e = H_1 \left\{ \frac{M_{r_1}}{M_{r_2}} \right\}^{1/3} \qquad (11.4)$$

Solutions for Deflections in a Linear Elastic Semi-Infinite Mass

The deflection and stresses at a point (r,z) of a linear elastic semi-infinite mass, loaded at the surface by a point load P (Figure 85(a))

was given by Boussinesq, (66). The deflection and stresses which arise when an area is loaded, as distinct from a point, can be deduced from the Boussinesq analysis by replacing the loaded area with an equivalent system of point loads. The effect of each of these loads is then compounded by a process of integration. For a uniform vertical loading on a circular area, the deflection $\delta(z)$ at any depth (z) on the axis (Figure 85(6)), is given (64,65) by

$$\delta(z) = \frac{(1+\nu)pa}{M_r}\left[\frac{1}{(1+(z/a)^2)^{\frac{1}{2}}} + (1-2\nu)((1+(z/a)^2)^{\frac{1}{2}}-z/a)\right] \qquad (11.5)$$

In calculating pavement stresses and deflections resulting from the passage of traffic, it is usual to assume that the load carried by the wheel is uniformly distributed over a circular area, as mentioned in Section 10.1.

11.4.2 Computation of Bituminous Layer Modulus

Using the method of equivalent thicknesses, it is possible to determine the modulus of the bituminous layer once the surface deflection and the moduli of granular and subgrade layers are known.

Before starting the computational procedure, it is essential to know the components of a surface deflection. As illustrated in Figure 86(a), the surface deflection, S_{surf}, is the sum of the subgrade deflection, S_{subg}, and the elastic deformations of the upper two layers, c_1 and c_2.

The deflection of the subgrade can be found after transforming the upper two layers into equivalent subgrade thickness and calculating the deflection at depth H_{e3} in the elastic half-space with modulus M_{r_3} (Figure 86(b)). The elastic deformation of the granular layer can be obtained after transforming the bituminous layer into an equivalent granular layer thickness and calculating the deflections at depths H_{e2} and $(H_{e2} + H_2)$ in the elastic half-space with modulus M_{r2} (Figure 86(c)). The difference between the deflection values is the elastic deformation of the granular layer. The elastic deformation of the bituminous layer is

the difference between the deflections at the surface and at the depth H_1 in the elastic half space with modulus M_{r_1} (Figure 86(d)).

The algorithm for finding the modulus of the bituminous layer from the measured deflection can be stated as below:

Algorithm:

(1) Take a first approximation of M_{r_1}.

(2) Compute $H_{e2} = H_1\left[\frac{M_{r_1}}{M_{r_2}} \times \frac{1-\nu_2^2}{1-\nu_1^2}\right]^{1/3}$; $H_{e3} = \sum_{i=1}^{2} H_i\left[\frac{M_{r_i}}{M_{r_3}} \times \frac{1-\nu_3^2}{1-\nu_i^2}\right]^{1/3}$

(3) Compute $\delta(H_{e3})$ with M_{r_3} using Eqn. 11.5.

Obtain $\delta_{subg} = \delta(H_{e3})$

(4) Compute $\delta(H_{e2})$ and $\delta(H_{e2} + H_2)$ with M_{r_2} using Eqn. 11.5

Obtain $c_2 = \delta(H_{e2}) - \delta(H_{e2} + H_2)$

(5) Compute $\delta(0)$ and $\delta(H_1)$ with M_{r_1} using Eqn. 11.5

Obtain $c_1 = \delta(0) - \delta(H_1)$

(6) Compute $\delta_{surf} = \delta_{subg} + c_2 + c_1$

(7) If $| \delta_{surf} - \delta_{measured} | < 0.05 (\delta_{measured})$

then take M_{r_1}, otherwise assume another value for M_{r_1} and repeat from step (2).

Using a scientific electronic calculator, the time taken to get one surface deflection value is about six minutes. After finding a minimum of three deflection values and plotting them down on graph paper, it is possible to estimate the required modulus value. A check calculation is done with that estimated value. Thus the required modulus value can be found within half an hour. A simple computer program in FORTRAN has been written for deflection calculation based on this method (58).

11.4.3 Adjustment for Loading Time Differences

As the bituminous material is viscoelastic in nature, the resilient modulus depends on the duration of loading time. The modulus value derived from the Benkelman beam deflection is associated with the loading time corresponding to the speed of the Benkelman beam vehicle, whose speed is

about 3 km/hr. The speed of commerical vehicles may be taken for design purposes as 80 km/hr. An adjustment for loading time difference is thus necessary. This can be accomplished by using the Modulus-Time-Temperature relationship, developed by Brown, (28), as given below.

$$\log_{10}M_r=\log_{10}(aT^2-bT+c)-10^{-4}(dT^2+eT+f)(0.5H-0.2-0.94\log_{10}V) \qquad (11.6)$$

where M_r = resilient modulus, MN/m^2

T = temperature, ^oC

H = bituminous layer thickness, metres.

V = vehicle speed, km/hr.

a,b,c,d,e,f, = constants that depend on the material

Values of the constants for the two materials investigated, (28), are given in Table 20. Using this equation, values of modulus can be calculated for different values of the three basic variables, temperature, layer thickness and vehicle speed. For a given layer thickness and keeping the temperature constant at the standard for Benkelman beam measurement, 20^oC, the ratio of the moduli at vehicle speeds 3 km/hr and 80 km/hr can be calculated. The ratio is then applied to the modulus value at a speed of 3 km/hr to give the modulus at 80 km/hr.

CHAPTER TWELVE

DETERMINATION OF CRITICAL STRAINS

12.1 Selection of the Method

The calculation of stresses and strains in a pavement structure can be done in a number of ways. There are tables and charts of influence values available in the literature that can be used to solve two and three layer systems, (67,68). A difficulty with the tabular solution is the amount of interpolation required for normal analyses. Most of the more recent work has been presented in the form of computer programs. Modern computer programs are characterised by BISAR (69), DEFPAV, (2,3) and others, (70). Solutions in the form of computer programs are very useful and capable of great versatility provided ready access to a suitable computer is available. However, this is not always so. An alternative approach is the use of a prediction equation, (71), developed for specific responses, e.g. critical strains. Elastic layer and finite element computer programs are used to compute fundamental pavement responses for inputs to the prediction equations. Multiple regression analyses are then used to develop models to estimate the required responses. The result is simple, approximate equations capable of estimating the specific response from standard design inputs for many alternatives in a very small amount of computer (or preferably pocket scientific calculator) time. As the basic aspect of the method is to be simple and straightforward in use, the prediction method approach is selected for the determination of critical strains.

12.2 Prediction Models for Critical Strains

The procedure required to develop prediction models can be stated briefly as follows:

(i) sensitivity analyses of the structural design variables with respect to the response under consideration are conducted using computer programs.

(ii) through these sensitivity analyses , some design variables are eliminated, or combined into each other without significantly

affecting the computed response.

(iii) a factorial arrangement is set up to compute the specific response for a typical range of designs with selected variables.

(iv) the data obtained is then used in a multiple regression analysis to produce a response prediction model.

Due to the amount of time available, it was not possibly to develop such models in this project. Instead, the two strain prediction models developed by Meyer et al., (71) are taken for the purpose. After taking the models as they are, the recalibration is done by using the computer program, DEFPAV. The forms of the two models are given by Equations 12.1 and 12.2.

Bituminous Layer Tensile Strain

$$\ln(\varepsilon_r) = a_1 + a_2 H_1 + a_3 \ln(M_{r_2}) + a_4 M_{r_3} \ln(H_1) + a_5 M_{r_1} \ln(H_1) + a_6 H_2 M_{r_2} + a_7 H_1 \ln(M_{r_2}) \quad (12.1)$$

where $\varepsilon_r = \frac{mm}{mm} \times 10^{-3}$; M_{r_1} - MN/m^2 ÷ 700

H_1 - mm ÷ 25 ; M_{r_2} - MN/m^2 ÷ 70

H_2 - mm ÷ 250 ; M_{r_3} - MN/m^2 ÷ 7

Subgrade Soil Layer Compressive Strain

$$\ln(\varepsilon_z) = b_1 + b_2 \ln(EAT.M_{r_1}) + B_3 \ln(M_{r_1}.M_{r_3}) + b_4 \ln(EAT.M_{r_1}.M_{r_3}) \quad (12.2)$$

where $\varepsilon_z = \frac{mm}{mm}$; M_{r_1} - MN/m^2 ÷ 7000

EAT - mm ÷ 250 ; M_{r_3} - MN/m^2 ÷ 70

EAT means Equivalent Asphalt Thickness and is calculated by

$$EAT = H_1 + H_2 \left[\frac{M_{r_2}}{M_{r_1}} \times \frac{1-\nu_1^2}{1-\nu_2^2} \right]^{1/3}$$

(The factors behind the units associated with each input, result from the direct conversion of F.P.S. units in the reference op.cit. to S.I. Units).

12.3 Computation of Critical Strains from Multi-Layer Elastic Theory

The values of critical strain which are necessary for input into the multiple regression analysis are computed by using the computer program DEFPAV, described in Part One (Chapter Two). The automatic grid generation

option was adopted.

12.3.1 Factorial Design of Pavement Reponse Computation

A factorial arrangement was set up for the calculation of critical strains for a typical range of three-layered systems, (Table 21). The set used in a specific calculation is identified by a number as shown. The 80 kN standard axle is characterized by a wheel load of 40 kN, tyre pressure of 500 kN/m^2 and radius of loaded area 160 mm. The results obtained from this computation are listed in Table 22.

12.4 Multiple Regression Analysis

The multiple regression analysis was performed by using the Statistical Package for the Social Sciences (S.P.S.S.) (Version 5), available on the ICL.1906A at Birmingham University Computer Centre, (72). The Fixed Multiple Regression subprogram was used. The data for the regression analysis was prepared from the structural parameters and the strains computed as mentioned in the preceding section, according to Equations 12.1 and 12.2.

From these analyses, the following prediction equations were obtained:

$$\ln(\varepsilon_r) = -0.95696 - 0.11386\, H_1 - 0.98535 \ln(M_{r_2}) + 0.04200\, M_{r_3} \ln(H_1) - 0.04540\, M_{r_1} \ln(H_1) + 0.11244\, H_2\, M_{r_2} + 0.01361\, H_1 \ln(M_{r_2}) \quad (12.3)$$

$$\ln(\varepsilon_z) = -8.78713 - 0.35892 \ln(EAT.M_{r_1}) + 0.84628 \ln(M_{r_1}.M_{r_3}) - 1.10612 \ln(EAT.M_{r_1}.M_{r_3}) \quad (12.4)$$

The multiple correlation coefficient squared (R^2) associated with Equation 12.3 is 0.92306. The F-Value is 35.99198 which is significant at one per cent level of significance, i.e.

$$F = 35.99198 > F_{0.01} = 4.01$$

with $\nu_1 = 6$, $\nu_2 = 18$.

The R^2 associated with Equation 12.4 is 0.95282 and the F-value is 141.35295 which is significant at one per cent level of significance, i.e.

$$F = 141.35295 > F_{0.01} = 4.87$$

with $\nu_1 = 3$, $\nu_2 = 21$.

Thus the prediction accuracy measured by R^2 - values (73), are quite good for both regression equations, and the assumed regression equations are statistically significant as determined by the F-tests, (74).

CHAPTER THIRTEEN

DETERMINATION OF OVERLAY THICKNESS

At any instant in time, there is a certain amount of accumulated damage done to an existing pavement by repeated traffic loading. Together with this, there is also a certain amount of remaining damage which the existing pavement can undergo before failure. The magnitude of damage caused by each repeated traffic loading (usually expressed in terms of its equivalent number of standard axles) depends on the structural strength of the existing pavement. If the magnitude of the critical strains is reduced, then the existing pavement can carry a larger number of standard axle loads. Thus the function of an overlay is to reduce the magnitude of these critical load induced strains. In the following sections the concept of damage and the theory of cumulative damage is discussed together with the determination of allowable critical strains which control fatigue and rutting damage. Finally, the computation of required overlays corresponding to the allowable critical strains is discussed.

13.1 Phenomenological Theory of Cumulative Damage

The phenomenological theory of cumulative damage can be outlined as follows:

Let n_i = number of applications at stress or strain level i

N_i = number of applications to failure at stress or strain level i

D_i = damage due to n_i number of applications at stress or strain level i

Then the damage, D_i, is defined as the stress or strain cycle ratio, i.e.

$$D_i = \frac{n_i}{N_i} \tag{13.1}$$

It is obvious that failure will occur when $D_i = 1$.

Let r = number of different stress or strain levels involved.

D = cumulative damage due to number of applications at different stress or strain levels.

Then the cumulative damage, D, is stated as the linear summation of cycle ratios, i.e.,

$$D = \sum_{i=1}^{r} b_i = \sum_{i=1}^{r} \frac{n_i}{N_i} \qquad (13.2)$$

The hypothesis states that the failure will occur when D = 1, i.e.

$$\sum_{i=1}^{r} \frac{n_i}{N_i} = 1 \qquad (13.3)$$

This phenomenological theory of cumulative damage (75) was advanced by Miner (76) to predict the fatigue life of metals subjected to fluctuating stress amplitudes. Monismith, et al., (77), have suggested that it might be used to estimate the fatigue life of the bituminous layer in the pavement structure. Since then, it has been utilized by a number of investigators (78) and appears to be acceptable as a useful design relationship, at this time, for fatigue life estimation, since anything more complex does not appear warranted.

As mentioned in Section 10.2, (also Part One, Chapter Seven) the structural damage suffered by a pavement structure is usually divided into two parts that are not necessarily independent of each other: fatigue fracture and rutting distortion. Fatigue fracture from repeated traffic loading develops in the bituminous layer of the structure and the radial tensile strain at the bottom of that layer has been used as a criterion for limiting fatigue fracture. Rutting deformation from repeated traffic loading can develop in all layers of the structure and the vertical compressive strain at the top of the subgrade has been extensively used as an overall criterion for limiting deformation of the whole pavement.

In both forms of damage the relationship between strain levels and number of cycles to failure, (strain-life relationship) is given by equation 10.3:

$$N = A \left(\frac{1}{\varepsilon}\right)^b$$

Thus, it seems possible to apply the cumulative damage theory to rutting distortion too. Furthermore, as indicated by Equation 10.3, strain

would be the appropriate criterion when one applies the cumulative damage theory to pavement materials to predict fatigue and rutting damages.

The accumulation of damage from repeated application at various strain levels can be illustrated diagramatically as shown in Figure 87. In Figure 87(a), the strain-life diagram, the strain-life curve is shown as the line 1 - k, with life N_1 corresponding to strain ε_1 and so on. The lines a - b, c - d, and so on represent n_1 applications at strain ε_1, n_2 applications at strain ε_2 and so on. In other words these lines, represented by arrows, can be called damage paths. The dashed lines b - c, d - e and so on can be called iso-damage lines and in fact, the line 1 - k is also in iso-damage line at which failure occurs. As the amounts of damage at b and c are the same, then

$$\frac{n'}{N_2} = \frac{n_1}{N_1}$$

or $n' = N_2 \times \frac{n_1}{N_1}$, and similarly n'' and n''' can be found. Thus, the damage process can be shown on the strain-life diagram accordingly.

A more simple presentation is possible when the process is shown on the damage-life diagram as shown in Figure 87(b). The scale of the damage axis ranges from 0 to 1. The corresponding lines from Figure 87(a) are included. It is worth noting that the values of n', nn'' and so on can be found on the damage-life diagram itself. Finally the damage paths can be shown continuously when they are plotted in the damage-path diagram as shown in Figure 87(c) where the vertical axis represents the amount of damage and the horizontal axis, the number of applications at any strain level. In this way, the cumulative damage arising from repeated applications at different strain levels can be depicted in diagrammatic form.

Computation of Allowable Critical Strains

For practical design purposes, the variation in axle loads is converted to an equivalent number of standard (8200 kg)

axles, and it is also normal practice to use representative values for environmental inputs such as temperature conditions. Therefore the magnitudes of critical strains remain constant for a given pavement structure, unless the structural condition of the pavement itself changes. When a pavement is overlaid, its structural condition is changed and so are the critical strains, Figure 88. The number of strain levels involved throughout the life of the pavement is equal to the number of applications of overlay plus one. The total damage caused to the pavement can then be assessed by applying the cumulative damage theory.

To illustrate the damage process, the case of a pavement structure with a single application of overlay (i.e. two levels of strain involved) before it finally fails, will be considered. The damage process for this overlay problem (which can also be regarded as two-stage construction problem) is shown in Figure 89.

Let ε_1 = strain level before overlay

ε_2 = strain level after overlay

n_1 = number of applications at strain level ε_1 (i.e. number of accumulated standard axles up to the present).

n_2 = number of applications at strain level ε_2 (i.e. number of future accumulated standard axles up to the failure of pavement).

The magnitude of ε_1 can be calculated from the geometry and structural properties of the existing pavement structure as mentioned in Section 12.2. The traffic history gives the value of n_1 and the traffic forecasting the value of n_2. The problem is to find the value of ε_2 so that the pavement can undergo further n_2 number of standard axles before it finally fails.

According to Equation 13.3 failure occurs when

$$\frac{n_1}{N_1} + \frac{n_2}{N_2} = 1$$

or

$$N_2 = \frac{n_2 \; N_1}{(N_1 - n_1)}$$

and from equation 10.3

$$A\left(\frac{1}{\varepsilon_2}\right)^b = \frac{n_2}{N_1 - n_1}$$

$$\varepsilon_2 = \left[\frac{A\,(N_1 - n_1)}{n_2 N_1}\right]^{1/b} \qquad (13.4)$$

The process of obtaining the value of ε_2 can be shown on Figure 89. From the knowledge of ε_1 and n_1, the first damage path 1-2 can be plotted on all diagrams, Figure 89 (a), (b) and (c). Then on the damage path diagram (c), the damage path 3-4 can be drawn with the knowledge of the value of n_2. It is now possible to draw the iso-strain line ε_2 on the damage-life diagram (b), as it is paralled to the second damage path 3-4 on diagram (c). The point where the iso-strain line ε_2 cuts the failure line, D=1, gives the value of life N_2. Projecting this point vertically upward to the strain-life diagram (a) above will give the required value of ε_2.

The principle discussed above can also be generalized to cases which involve a number of applications of overlay, (or when considering stage construction, cases involving several stages of construction) as follows:

Let D_1 = cumulative damage due to compound strain applications up to the present.

D_2 = incremental damage expected after overlay due to n_2 applications at single strain level ε_2.

D_T = total cumulative damage (equals unity at failure).

According to Equations 13.1 and 13.2,

$$D_2 = \frac{n_2}{N_2}$$

and $D_T = D_1 + D_2$

$$\text{thus} N_2 = \frac{n_2}{D_T - D_1}$$

and from Equation 10.3,

$$A\left(\frac{1}{\varepsilon_2}\right)^b = \frac{n_2}{D_T - D_1}$$

yielding $$\varepsilon_2 = \left[\frac{A(D_T - D_1)}{n_2}\right]^{1/b} \qquad (13.5)$$

If failure occurs after damage D_2, the value of D_T is unity. These equations are, of course, common for both critical strains (i.e. radial tensile strain, ϵ_r, and vertical compressive strain, ϵ_z), and so the value of the material constants, A and b, depend on which allowable strain is being sought. Once the magnitude of strain after overlay is known, the thickness and type of overlay can be calculated as discussed in the following section.

13.3 Computation of Overlay Thickness

The function of an overlay is to reduce the amount of damage caused by each application of standard axle load so that the pavement can carry more standard axle loads before it finally fails. The amount of damage, in turn, depends on the magnitude of critical strains in the pavement structure. Fatigue fracture damage depends on the radial tensile strain at the bottom of the bituminous layer and rutting damage on the vertical compressive strain on the top of subgrade. The prediction equations for these strains have been derived in Chapter Twelve and are given by Equations 12.3 and 12.4 respectively.

From the preceding section, the allowable critical strains after overlay can be calculated. Thus the values of the strains in Equation 12.3 and 12.4 are known and the problem is to find the values of H_1 and EAT which would satisfy these equations. The two equations can be re-written implicitly in terms of H_1 and EAT as

$$f(H_1) = 0 \text{ and } g(EAT) = 0.$$

The solutions to these non-linear equations can be obtained by a trial and error approach, or more systematically by a numerical method, such as the Newton-Raphson method.

The difference between the new H_1 (H_1 after overlay) and the old H_1 (existing H_1) gives the necessary overlay thickness to preclude fatigue fracture. Similarly the difference between the new and old EAT gives

the required overlay thickness to preclude rutting distortion. The greater one is taken as the required overlay thickness. If the resilient modulus of the overlay material is different from that of the existing bituminous bound material, the required overlay thickness can be adjusted accordingly by using the equivalent thickness principle.

CHAPTER FOURTEEN

OVERLAY DESIGN EXAMPLE BY THE PROPOSED METHOD

In this chapter, an example of an overlay design by the proposed method is presented. The objective is two-fold:

(i) to illustrate to the user the essential steps in applying the principles of the design procedure to real, practical overlay problems

(ii) to assess the validity of the proposed design procedure by comparing the results obtained by the proposed method and by other methods.

14.1 Overlay Design Example

The design example which is used by Normal et al., (19) to demonstrate the T.R.R.L. Deflection Method, is given in Table 23, and can be stated as follows: A road has the following construction: 100 mm of two-course rolled asphalt surfacing, 125 mm of rolled asphalt roadbase and 300 mm of type 2 subbase material on a subgrade of C.B.R. 4%. The present cumulative traffic is equivalent to 2.2 mSA and the future cumulative traffic equivalent to 9.7 mSA. The deflection survey of the road gives three representative deflections along the road, corrected to an equivalent deflection beam reading at 20°C: 38 x 10^{-2} mm, 43 x 10^{-2} mm, 57 x 10^{-2} mm, to be known as cases 1 - 3 respectively. It is required to know the thicknesses of overlays necessary along the road. The type of material specified for the overlay is rolled asphalt.

Determination of In Situ Layer Moduli

Prior to the determination of in situ layer moduli, the existing pavement structure has to be reduced to a three-layered system. In this problem, the rolled asphalt surfacing layer and the rolled asphalt roadbase are combined to form a 225 mm bituminous layer. After reduction to a three-layered system, the procedure outlined in Chapter Eleven is applied for the calculation of in situ layer moduli. The moduli of the bituminous layer corresponding to each of the deflection values are given in Table 24

together with those of the other two layers.

Determination of Critical Strains

In order to assess the amount of cumulative damage done to the existing pavement by the present traffic, the magnitude of the critical strains in the pavement structure is required. These are determined by using the prediction equations, Equations 12.3 and 12.4, developed in Chapter Twelve. The values of the input parameters to the prediction equations are presented in Table 25 along with the computed critical strains for all three cases. The fatigue law (ε_r - N Line) for a typical rolled asphalt mix, (80) is given by Equation 14.1. The rutting law, (ε_z - N Line) for British conditions (81) which has been obtained by analysis of a range of structures taken from Road Note 29, (30) is given by Equation 14.2.

$$N = 8.9 \times 10^{-13} \times \left(\frac{1}{\varepsilon_r}\right)^{4.9} \qquad (14.1)$$

$$N = 1.1 \times 10^{-6} \times \left(\frac{1}{\varepsilon_z}\right)^{3.6} \qquad (14.2)$$

Using the above equations the lives of the pavement in terms of both types of damages can be found, (Table 25), and hence, with the knowledge of the present cumulative traffic, the amount of damage already done to the pavement can be estimated. From the calculation, it is found that for all cases except case 3, both the fatigue and rutting lines of the existing pavement is greater than the required total life of 11.9 mSA. It means that no overlay is required for Cases 1 and 2. For Case 3, both fatigue and rutting lines are smaller than the required total life and so the overlay is necessary.

Determination of Overlay Thickness

Once the amount of damage suffered by the existing pavement is ascertained, the cumulative damage theory is applied to determine the allowable critical strains that will give the required extension of pavement life for future traffic. Equation 13.4 is used for computing the allowable strains. When the values of these strains are obtained, the

new values of H_1 and EAT are calculated from Equations 12.3 and 12.4 by a trial and error method. Finally the overlay thicknesses to preclude both damage modes are obtained and the larger thickness is taken as the necessary overlay thickness for the pavement. If the resilient modulus taken for the newly laid overlay material is different from that of the existing bituminous layer, the overlay thickness is adjusted accordingly. The results are summarized in Table 26. In this design example, no overlay is needed for Cases 1 and 2, and the fatigue fracture controls the required overlay thickness in Case 3.

14.2 Overlay Design by Other Methods

The design example is solved by the T.R.R.L. Deflection Method, (57), and the results are summarised in Table 27. Two levels of probabilities (0.5 and 0.9) are used and these results are compared with those of the proposed method in Table 28.

14.3 Remarks

(i) The calculated resilient modulus of the bituminous layer from the measured deflections are typical for rolled asphalt, which would indicate that the use of the Method of Equivalent Thicknesses in calculating the deflection of a pavement structure is reasonable.

(ii) Considerable engineering judgement is required in the modelling of the in situ pavement structure into an idealised three-layered system.

(iii) Table 28 indicates that the fatigue law for a typical rolled asphalt mix and the compressive strain criteria for rutting give reasonable predictions of the structural condition of the pavement.

CHAPTER FIFTEEN

SUMMARY OF WORK DONE

Research work carried out at a number of centres has been drawn together to provide the basis for a rational overlay thickness design procedure. It was intended that this method should be applicable in developing countries where there is a relatively poorly developed engineering infrastructure. Consequently the entire procedure may be performed in the field with only a Benklman Beam and a hand held electronic calculator.

ACKNOWLEDGEMENTS

The authors wish to thank the staff of both the Queens University of Belfast, Civil Engineering Department and the University of Birmingham, Department of Transportation and Environmental Planning for their help with this research and particularly Professor Wells F.R.S. and Professor Long of the former Institution and Professor Kolbuszewski and Dr. Lees of the latter who have allowed the full facilities of their Departments to be employed.

Mr. T.A.N. Prescott, Director of the Department of the Environment (Northern Ireland) Roads Service, is thanked for his cooperation and assistance as are Mr. E. Stewart, Mr. H.J.H. Bailie and Mr. D.M. Orr of the Roads Service Intelligence Unit who were responsible for much of the pavement testing.

Mention should also be made of the advice and help given in consultations with Professor R. Kirwan and Mr. E. Farrell of Trinity College, Dublin, Mr. N.W. Lister of the Transport and Road Research Laboratory, and Dr. S.F. Brown of the University of Nottingham.

The support, both financial and practical, given so freely by the European Research Office of the United States Army particularly by Mr. H. Lemons and Mr. W. Grabau, is gratefully acknowledged as is the assistance offered by the personnel of the U.S. Army Waterways Experiment Station.

Mention should also be made that partial funding for this research was obtained from the Department of Education (Northern Ireland).

Finally the authors wish to thank Miss J. Glacken for her splendid work in deciphering their various scripts for inclusion in this report.

REFERENCES

1. "PROCEEDINGS OF THE 4TH INT. CONF. ON THE STRUCT. DESIGN OF ASPHALT PAVEMENTS", Vol. I, Ann Arbor, Michigan, 1977.

2. KIRWAN, R.W., SNAITH, M.S. and GLYNN, T.E., "A Computer Based Subsystem for the Prediction of Pavement Deformation", Proc. 4th Int. Conf. on the Struct. Design of Asphalt Pavements, Vol. I, Ann Arbor, Michigan, 1977, pp 509-518.

3. SNAITH, M.S. and KIRWAN, R.W., "System for Summation of Load-Induced Pavement Strains to Produce a Rut Profile", Transportation Research Record, No. 616, 1976, pp 31-33.

4. KIRWAN, R.W. and SNAITH, M.S., "Further Investigations Towards a Rational Method of Design for Flexible Pavements, Part II", Internal Report to Sponsors, European Research Office of U.S. Army, April 1975.

5. KIRWAN, R.W. and GLYNN, T.E., "Experimental and Theoretical Investigation of Pavement Deflections", Internal Report to Sponsors, European Research Office of U.S. Army, November 1969.

6. McBRIDE, B.W., "The Computer Program DEFPAV - An Aid to Practical Road Design", B.Sc. Dissertation, Department of Civil Engineering, Queen's University of Belfast, 1976.

7. BAILIE, H.J.H., "The Use of Transient Deflections for the Structural Maintenance of Road Pavements in Northern Ireland", M.Sc. Thesis, Queen's University of Belfast, 1978.

8. ORR, D.M., "The Use of Transient Deflections for the Structural Maintenance of Road Pavements in Northern Ireland", M.Sc. Thesis, Queen's University Belfast, 1978.

9. KIRWAN, R.W. and SNAITH, M.S., "A Simple Chart for the Prediction of Resilient Modulus", Geotechnique 26, No. 1, 1976, pp 212-215.

10. BARKSDALE, R.D., "Laboratory Evaluation of Rutting in Base Course Materials", Proc. 3rd Int. Conf. on the Struct. Design of Asphalt Pavements, Vol. I, London, 1972, pp 161-174.

11. ROMAIN, J.E., "Rut Depth Prediction in Asphalt Pavements", Proc. 3rd Int. Conf. on the Struct. Design of Asphalt Pavements, Vol. I, London, 1972, pp 705-710.

12. CRONEY, D. and THOMPSON, P.D., "Moderators' Summary Report of papers prepared for discussion at Section IV", Proc. 3rd Int. Conf. on the Struct. Design of Asphalt Pavements, Vol. II, London, 1972, pp 206-215.

13. KIRWAN, R.W. GLYNN, T.E., and SNAITH, M.S., "Further Investigations Towards a Rational Method of Design for Flexible Pavements, Part I", Internal Report to Sponsors, European Research Office of U.S. Army, April 1974.

14. BROWN, S.F. and SNAITH, M.S., "The Permanent Deformation Characteristics of a Dense Bitumen Macadam subjected to Repeated Loading", Proc. Assn. Asphalt Paving Technologists, Vol. 43, 1974, pp 224-252.

15. ABDELMIGID, E.E., "Engineering Responsibilities of Stress Analysis by Computer", Proc. Instn. Civil Engineers, Vol. 58, 1975, pp 629-630.

16. DUNCAN, J.M., MONISMITH, C.L. and WILSON, E.L., "Finite Element Analyses of Pavements", Highway Research Board, No. 228, 1968, pp 18-33.

17. HOFSTRA, A. and KLOMP, A.J.G., "Permanent Deformation of Flexible Pavements under Simulated Road Traffic Conditions", Proc. 3rd Int. Conf. on the Struct. Design of Asphalt Pavements, Vol. I, London, 1972, pp 613-621.

18. BROWN, S.F., BELL, C.A. and BRODRICK, B.V., "Permanent Deformation of Flexible Pavements", Internal Report to Sponsors, European Research Office of U.S. Army, November 1974.

19. NORMAN, P.J., SNOWDON, R.A. and JACOBS, J.C., "Pavement Deflection Measurements and Their Application to Structural Maintenance and Overlay Design", T.R.R.L. Report 571, Transport and Road Research Laboratory, Crowthorne, 1973.

20. HVEEM, F.N., "Pavement Deflections and Fatigue Failures", Highway Research Board, Bull. 114, 1955, pp 43-87.

21. HVEEM, F.N., ZUBE, E., BRIDGES, R. and FORSYTH, R., "The Effect of Resilience - Deflection Relationship on the Structural Design of Asphaltic Pavements", Proc. Int. Conf. on the Struct. Design of Asphalt Pavements, Ann Arbor, Michigan, 1962, pp 649-666.

22. DEHLEN, G.L., "Flexure of a Road Surfacing, its Relation to Fatigue Cracking, and Factors Determining its Severity", Highway Research Board, Bull. 321, 1962, pp 26-39.

23. BLEYENBERG, W.G., CLAESSEN, A.I.M., van GORKUM, F., HEUKELOM, W. and and PRONK, A.C., "Fully Monitored Motorway Trials in the Netherlands corroborate Linear Elastic Design Theory". Proc. 4th Int. Conf. on the Struct. Design of Asphalt Pavements, Vol. I, Ann Arbor, Michigan, 1977, pp 75-98.

24. McMULLEN, D., "Computer-aided flexible pavement analysis", M.Sc. Thesis, Queen's University of Belfast, 1978.

25. SNAITH, M.S., "Deformation Characteristics of Dense Bitumen Macadam subjected to Dynamic Loading", Ph.D. Thesis, University of Nottingham, 1973.

26. HEUKELOM, W. and KLOMP, A.J.G., "Dynamic Testing as a Means of Controling Pavements During and After Construction", Proc. Int. Conf. on the Struct. Design of Asphalt Pavements, Ann Arbor, Michigan, 1962, pp 667-679.

27. PELL, P.S. and BROWN, S.F., "The Characteristics of Materials for the Design of Flexible Pavement Structures", Proc. 3rd Int. Conf. on the Struct. Design of Asphalt Pavements, Vol. I, London, 1972, pp 326-342.

28. BROWN, S.F., "Determination of Young's Modulus for Bituminous Materials in Pavement Design", Highway Research Record, No. 431, 1973, pp 38-49.

29. BAILIE, H.J.H., Private communication.

30. ROAD RESEARCH LABORATORY, "Guide to the Structural Design of Pavements for New Roads", Road Note 29, Third Edition, H.M.S.O., London, 1970.

31. BAILIE, H.J.H. and SNAITH, M.S., "Interim Report on the Use of Transient Deflections for Maintenance of Roads in Northern Ireland", Internal Report of the Joint D.O.E./Q.U.B. Research Project, Department of Civil Engineering, Queen's University of Belfast, 1977.

32. LISTER, N.W., "Deflection Criteria for Flexible Pavements", T.R.R.L. Report LR 375, Transport and Road Research Laboratory, Crowthorne, 1972.

33. MINISTRY OF TRANSPORT. "The Marshall Committee's Recommendations for Standards of Highway Maintenance and for a Maintenance Rating System", R.R.L. Report LR 367, Road Research Laboratory, Crowthorne, 1970.

34. McCULLOUGH, L.M., Private communication.

35. TROTT, J.J., "An Apparatus for Recording the Duration of Various Temperatures in Roads", Roads and Road Construction, Vol. 41, No.491, 1963, pp 342-345.

36. KENNEDY, C.K., FEVRE, P., and CLARKE, C.S., "Pavement deflection: equipment for measurement in the United Kingdom", T.R.R.L. Report LR 834, Transport and Road Research Laboratory, Crowthorne, 1978.

37. KENNEDY, C.K., "Pavement deflection: operating procedures for use in the United Kingdom", T.R.R.L. Report LR 835, Transport and Road Research Laboratory, Crowthorne, 1978.

38. LISTER, N.W. and KENNEDY, C.K., "A System for the Prediction of Pavement Life and Design of Pavement Strengthening", Proc. 4th Int. Conf. on the Struct. Design of Asphalt Pavements, Vol. I, Ann Arbor, Michigan, 1977, pp 629-648.

39. SNAITH, M.S., "A Digital Portable Weighbridge", Journ. Instn. Highway Engineers, Vol. 25, No. 7, 1978, pp 9-12.

40. CANADIAN GOOD ROADS ASSOCIATION, "Pavement Evaluation Studies in Canada", Proc. Int. Conf. on the Struct. Design of Asphalt Pavements, Ann Arbor, Michigan, 1962, pp 137-218.

41. QUEEN'S UNIVERSITY OF BELFAST, "CUFIT", Manual prepared by The Computer Centre, Queen's University of Belfast, July 1975.

42. SHAW, P., BAILIE, H.J.H. and SNAITH, M.S., "Correlation of Deflection Beam and Deflectograph", Internal Report of the Joint D.O.E./Q.U.B. Research Project, Department of Civil Engineering, Queen's University of Belfast, 1977.

43. KIRWAN, R.W., GLYNN, T.E. and SNAITH, M.S., "A Structural Approach to the Design of Flexible Pavements", Irish Engineers, Journ. Instn. of Engineers of Ireland, Vol. 28, No. 8, 1975, pp 24-31.

44. CRONEY, D., "Failure Criteria for Flexible Pavements", Proc. 3rd Int. Conf. on the Struct. Design of Asphalt Pavements, Vol. I, London, 1972, pp 608-612.

45. LEE, A.R. and CRONEY, D., "British Full-Scale Pavement Design Experiments", Proc. Int. Conf. on the Struct. Design of Asphalt Pavements, Ann Arbor, Michigan, 1962, pp 114-136.

46. PELL, P.S., "Fatigue of Bituminous Materials in Flexible Pavements", Proc. Instn. Civil Engineers, Vol. 31, 1965, pp 283-312.

47. MOAVENZADEH, F., "Causes and Distress in Highway Pavements", Highway Research Board, Special Report 126, 1971 pp 114-139.

48. LISTER, N.W., "The Transient and Long Term Performance of Pavements in Relation to Temperature", Proc. 3rd Int. Conf. on the Struct. Design of Asphalt Pavements, Vol. 1, London, 1972, pp 94-100.

49. HIGHWAY RESEARCH BOARD, "The A.A.S.H.O. Road Test", Report 7, Summary Report, Special Report 61G, Washington D.C., 1962.

50. LIDDLE, W.J., "Application of A.A.S.H.O. Road Test Results to the Design of Flexible Pavement Structures", Proc. Int. Conf. on the Struct. Design of Asphalt Pavements, Ann Arbor, Michigan, 1962, pp 42-51.

51. HUANG, E.Y., "Prepared Discussion, Session 1, Proc. Int. Conf. on the Struct. Design of Asphalt Pavements, Ann Arbor, Michigan, 1962, pp 9-11.

52. PELL, P.S., "Fatigue Characteristics of Bitumen and Bituminous Mixes" Proc. Int. Conf. on the Struct. Design of Asphalt Pavements, Ann Arbor, Michigan, 1962, pp 310-323.

53. BROWN, S.F., "Material characteristics for analytical pavement design", Chapter 2, in 'Developments in Highway Pavement Engineering - 1', P.S. Pell (ed), Applied Science Publishers, London, 1978.

54. NIXON, J.A. and McKEAND, E., "Fabric Included Pavement Design" Symposium on Road Improvement in Ireland, Instn. of Engineers of Ireland, Dublin, 1978, pp 117-129.

55. RUDDOCK, E.O., Private communication.

56. LAMBE, T.W., "Predictions in Soil Engineering", Geotechnique 23, No. 2, 1973, pp 149-202.

57. KENNEDY, C.K. and LISTER, N.W., "Prediction of pavement performance and the design of overlays", T.R.R.L. Report LR 833, Transport and Road Research Laboratory, Crowthorne, 1978.

58. SHEIN, A., "A method for the determination of overlay thicknesses for flexible pavements", M.Sc. Dissertation, Department of Transportation and Environmental Planning, University of Birmingham, 1979.

59. PEATTIE, K.R., "Flexible Pavement Design. "Chapter 1, in 'Developments in Highway Pavement Engineering - 1', P.S. Pell (ed), Applied Science Publishers, London, 1978.

60. EDWARDS, J.M. and VALKERING, C.P., "Structural design of asphalt pavements for road vehicles - the influence of high temperatures", Highways and Road Construction, February, 1974.

61. DORMAN, G.M. and METCALF, C.T., "Design curves for flexible pavements based on layered system theory", H.R.B. 71, Washington, 1965.

62. PALMER, L.A. and BARKAN, P.S., "Soil Displacement under a Circular Loaded Area." Proc. High Res. Board. Vol. 23, 1940, pp 279-286.

63. ODEMARK, N., "Investigations as to the Elastic Properties of Soils and Design of Pavements According to the Theory of Elasticity." Statens Vaeginstitut. Stockholm, Sweden. 1949.

AD-A090 827 BIRMINGHAM UNIV (ENGLAND) DEPT OF TRANSPORTATION AND--ETC F/G 13/2
FLEXIBLE PAVEMENT ANALYSIS.(U)
MAY 80 M S SNAITH, D MCMULLEN DA-ERO-78-G-125
UNCLASSIFIED NL

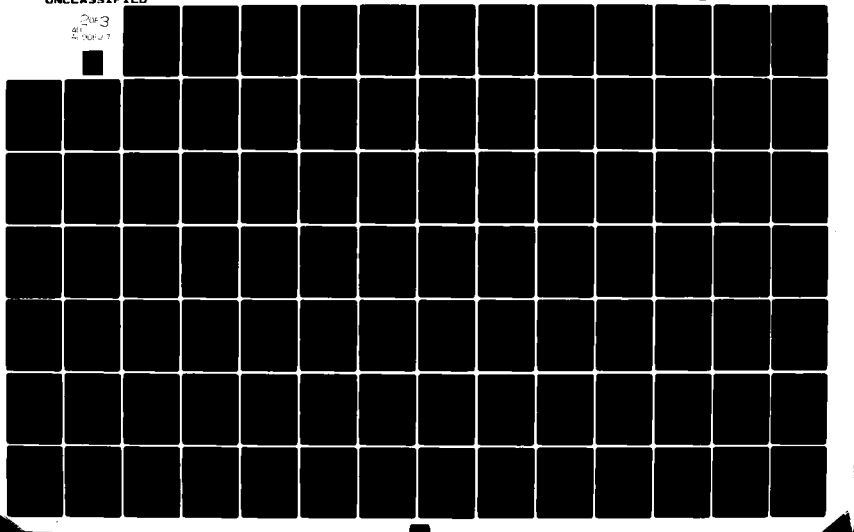

64. ULLIDTZ, P. "Some Simple Methods of Determining the Critical Strains in Road Structures". Dr. Techn. dissertation, The Technical University of Denmark, 1974.

65. POULOS, H.G. and DAVIS E.H., "Elastic Solutions for Soil and Road Mechanics". New York, 1974. (John Wiley & Sons, Inc.).

66. BOUSSINESQ, V.J., "Application des potentiels a l'etude de l'equilibre et du mouvement des solides elastiques avec des Notes Etendues sur divers Points de Physique, Mathematique et d'Analyse". Paris, 1885, (Gauthier-Villais).

67. JONES, A. "Tables of stresses in three-layer Elastic Systems", Highway Research Board, Bulletin 342, Washington, D.C., 1962, (National Research Council).

68. PEATTIE, K.R., "Stresses and Strain Factors for three-layer Elastic Systems", Highway Research Board, Bulletin 342, Washington, D.C., 1962.

69. DeJONG, D.L., PEUTZ M.G.F. and KORSWAGEN A.R., "Computer Program Layered Systems under Normal and Tangential Surface Loads". Koninklzjke/Shell-Laboratorium, Amsterdam, External Report, A.M.S.R. 0006.73, 1973.

70. BARKSDALE, R.D. and HICKS R.G. "Material characterization and Layered Theory for Use in Fatigue Analysis", H.R.B. Special Report, 140. 1973.

71. MEYER, F.R.P., CHEETHAM A. and HASS R.C.G., "A co-ordinated Method for Structural Distress Prediction in Asphalt Pavements, Proc. Assoc. of Asphalt Paving Technologist", Vol. 47. Lake Buena Vista, Fl., 1978, pp.160-189.

72. NIE, N.H., BENT D.H. and HULL C.H., "Statistical Package for the Social Sciences", New York, 1970. (McGraw-Hill).

73. DANIEL, C. and WOOD F.S., "Fitting Equations to Data," New York, 1971, (Wiley-Interscience).

74. NEVILLE, A.M. and KENNEDY J.B., "Basic Statistical Methods for Engineers and Scientists". London, 1968. (International Textbook Co. Limited).

75. MOAVENZADEH, F. "Damage and Distress in Highway Pavements". Highway Research Board Special Report 126. 1971, pp.114-139.

76. MINER, M.A. "Cumulative Damage in Fatigue". Journal of Applied Mechanics, American Society of Mechanical Engineers, Vol. 66, 1945. pp.A159-A164.

77. MONISMITH, C.L., SECOR K.E. and BLACKMER E.W. "Asphaltic Mixture Behaviour in Repeated Flexure". Proc. Assoc. of Asphalt Paving Technologists. Vol. 30, Mineapolis, Mina., 1961. pp.188-215.

78. MONISMITH, C.L. and FINN F.N. "Moderators' Summary Report of Papers Prepared for Discussion at Session III", Proc. Third Int. Conf. on the Struct. Design of Asphalt Pavements, London, 1972. (University of Michigan, Ann Arbor, Michigan, U.S.A.), Vol. II. pp.144-170.

79. TREYBIG, H.J., McCULLOUGH,B.F., FINN, F.N., McCOMB, R., and HUDSON, W.R., "Design of Asphalt Concrete Overlays Using Layer Theory", Proc. 4th Int. Conf. on the Struct. Design of Asphalt Pavements, Vol. I, Ann Arbor, Michigan, 1977, pp.589-628.

80. BROWN, S.F., PELL, P.S. and STOCK, A.F., "The Application of Simplified, Fundamental Design Procedures for Flexible Pavements", Proc. 4th Int. Conf. on the Struct. Design of Asphalt Pavements, Vol. I, Ann Arbor, Michigan, 1977, pp.327-341.

81. VERSTRAETEN, J. "Moduli and Critical Strains in repeated Bending of Bituminous Mixes, Application to Pavement Design". Proc. Third. Int. Conf. of the Struct. Design of Asphalt Pavement, London, 1972 (Univ. of Michigan,) Vol. I. pp.729-38.

APPENDIX 1

TABLES

Layer No.	Material	Thickness (mm)	M_r (MN/m^2)	ν
1	Bituminous	100	2750	0.4
2	Crushed rock	485	31.25	0.3
3	Subgrade	∞	12.5	0.45

Details of pavement model

Wheel Assembly	Twin	Single
Tyre loading (kg)	1588	3175
Contact pressure (kN/m^2)	590	590
Radius of loaded area (mm)	92	130
Required deflection (mm x 10^{-2})	38	57

Loading details

SIMULATION OF SINGLE AND TWIN WHEEL ASSEMBLIES

TABLE 1

IDENTIFICATION TESTS

Description of sample	Soft light brown sandy clay
In situ moisture content	21%
Bulk density	2008 kg/m^3 (125 lb/ft^3)
Dry density	1660 kg/m^3 (104 lb/ft^3)
Liquid limit (using cone penetrometer)	25%
Plastic limit	20%

CBR TEST

CBR (top of sample)	2%
CBR (bottom of sample)	2%

MODIFIED A.A.S.H.O. COMPACTION TEST

Maximum dry density	1870 kg/m^3 (117 lb/ft^3)
Optimum moisture content	12%

RESILIENT MODULUS OF SUBGRADE (M_{r_3})

(i) M_{r_3} (MN/m^2) = 10 x CBR, after Heukelom and Klomp (26).

Thus M_{r_3} = 20 MN/m^2.

(ii) Relative compaction (R_C) = 0.89

Relative moisture content (R_W) = 1.75

Thus M_{r_3} = 12.5 MN/m^2, after Kirwan and Snaith (9).

Value used for analysis : M_{r_3} = 12.5 MN/m^2.

SUMMARY OF LABORATORY TEST RESULTS

(SUBGRADE MATERIAL - HILLSBOROUGH TEST SECTION)

TABLE 2

Layer No.	Material	Thickness (mm)	Source for M_r determination	Initial value M_r (MN/m^2)	Value after back analysis M_r (MN/m^2)		Source for ν determination	ν
				Models A & B	Model A	Model B		
1	Bituminous	100	Snaith (25)	3720	2750	3300	Pell & Brown (27)	0.4
2	Crushed rock	485	Heukelom & Klomp (26)	31.25	31.25	31.25	Pell & Brown (27)	0.3
3	Subgrade	∞	Kirwan & Snaith (9) and laboratory tests	12.5	12.5	12.5	Pell & Brown (27)	0.45

TABLE 3

MATERIAL PROPERTIES USED TO MODEL THE HILLSBOROUGH TEST SECTION FOR TRANSIENT DEFLECTION

Layer No.	Layer details (Model B)				Model B1		Model B2	
	Material	Thickness (mm)	Mr (MN/m^2)	ν	Creep Equation No.	Calibration Factor	Creep Equation No.	Calibration Factor
1	Bituminous	100	6000	0.4	-	-	-	-
2	Crushed rock	485	31.25	0.3	-	-	7	2.4
3	Subgrade	00	12.5	0.45	7	15.9	7	2.4

MATERIALS PROPERTIES USED TO MODEL THE HILLSBOROUGH TEST SECTION FOR RUTTING

IDENTIFICATION TESTS

Description of sample	Soft dark brown clay
In situ moisture content	23%
Bulk density	2110 kg/m^3 (132 lb/ft^3)
Dry density	1715 kg/m^3 (107 lb/ft^3)
Liquid limit (using cone penetrometer)	34%
Plastic limit	18%

CBR TEST

CBR (top of sample)	4%
CBR (bottom of sample)	6%

MODIFIED A.A.S.H.O. COMPACTION TEST

Maximum dry density	1940 kg/m^3 (121 lb/ft^3)
Optimum moisture content	12.5%

RESILIENT MODULUS OF SUBGRADE (M_{r_3})

(i) M_{r_3} (MN/m^2) = 10 x CBR, after Heukelom and Klomp (26).

Thus M_{r_3} = 40 MN/m^2

(ii) Relative compaction (R_C) = 0.88

Relative moisture content (R_W) = 1.84

Thus M_{r_3} = 12.5 MN/m^2, after Kirwan and Snaith (9).

Value used for analysis : M_{r_3} = 40 MN/m^2.

SUMMARY OF LABORATORY TEST RESULTS

(SUBGRADE MATERIAL - M1 MOTORWAY TEST SECTION)

TABLE 5

Layer No.	Material	Thickness (mm)	Souce for M_r determination	Initial value M_r (MN/m^2)	Value after back analysis M_r (MN/m^2)	Source for ν determination	ν
1	Bituminous	180	Snaith (25)	3720	1400	Pell & Brown (27)	0.4
2	Crushed rock	485	Heukelom & Klomp (26)	100	100	Pell & Brown (27)	0.3
3	Subgrade	∞	Heukelom & Klomp (26)	40	40	Pell & Brown (27)	0.45

MATERIAL PROPERTIES USED TO MODEL THE M1 MOTORWAY TEST SECTION

FOR TRANSIENT DEFLECTION

TABLE 6

Layer No.	Layer details				Model 1		Model 2	
	Material	Thickness (mm)	Mr (MN/m^2)	ν	Creep Equation No.	Calibration Factor	Creep Equation No.	Calibration Factor
1	Bituminous	180	3200	0.4	-	-	-	-
2	Crushed rock	485	100	0.3	-	-	7	0.404
3	Subgrade	00	40	0.45	7	1.23	7	0.404

TABLE 7

MATERIAL PROPERTIES USED TO MODEL THE M1 MOTORWAY TEST SECTION FOR RUTTING

Deflection before overlaying ($mm \times 10^{-2}$)	40	50	60	70	80	90	100
Surface layer modulus M_{r_1} (MN/m^2)	4050	3200	2600	2150	1800	1550	1300

Layer No.	Material	Thickness (mm)	M_r (MN/m^2)	ν
1	Bituminous	varied	as shown	0.4
2	Crushed rock	485	31.25	0.3
3	Subgrade	∞	12.5	0.45
Loading details: Radius of loaded area 130 mm Uniform loading of 590 kN/m^2				

DETAILS OF PAVEMENT MODEL USED IN THE DERIVATION OF AN OVERLAY DESIGN CHART FOR THE HILLSBOROUGH TEST SECTION

TABLE 8

Deflection before overlaying ($mm \times 10^{-2}$)	20	30	40	50	60
Surface layer modulus M_{r_1} (MN/m^2)	4450	2450	1450	900	550

Layer No	Material	Thickness (mm)	M_r (MN/m^2)	ν
1	Bituminous	varied	as shown	0.4
2	Crushed rock	485	100	0.3
3	Subgrade	∞	40	0.45
Loading details: Radius of loaded area 130 mm Uniform loading of 590 kN/m^2				

DETAILS OF PAVEMENT MODEL USED IN THE DERIVATION OF AN OVERLAY DESIGN CHART FOR THE M1 MOTORWAY TEST SECTION

TABLE 9

Observation No.	Time (hr. min.)	T_{40} (^{o}C)	Depth (mm)	Temp. (^{o}C)	Resilient modulus values for bituminous layer (MN/m^2)		Computed deflection (mm x 10^{-2})	
					Model A	Model B	Model A	Model B
1	4.15 a.m.	12	20	10.75	5550	6300	20	18
			60	13.00	4750	5500		
			100	14.50	4300	5000		
			140	16.25	3750	4400		
			188	17.25	3500	4150		
2	5.00 a.m.	11	20	9.25	6100	7000	19	17
			60	12.25	5000	5800		
			100	14.25	4400	5100		
			140	15.50	4000	4650		
			188	17.00	3550	4200		

TABLE 10
Contd/

3	6.00 a.m.	11	20	9.50	6000	6850	19	17
			60	12.00	5100	5850		
			100	14.00	4450	5150		
			140	15.25	4050	4750		
			188	16.75	3650	4300		
4	7.00 a.m.	15	20	14.50	4300	5000	24	20
			60	15.50	4000	4650		
			100	16.50	3700	4350		
			140	17.50	3400	4050		
			188	18.75	3050	3700		
5	8.00 a.m.	14.5	20	14.00	4450	5150	22	19
			60	14.50	4300	5000		
			100	14.75	4200	4900		
			140	15.50	4000	4650		
			188	17.00	3550	4200		

TABLE 10
Contd/

6	9.00 a.m.	16.5	20	16.75	3650	4300	24	21
			60	16.50	3700	4350		
			100	16.25	3750	4400		
			140	16.50	3700	4350		
			188	17.25	3500	4150		
7	11.00 a.m.	24.5	20	23.50	1900	2450	32	27
			60	23.50	1900	2450		
			100	19.50	2900	3500		
			140	18.50	3150	3750		
			188	18.50	3150	3750		
8	1.00 p.m.	31.5	20	31.50	550	900	50	40
			60	29.25	850	1250		
			100	24.50	1700	2200		
			140	22.00	2250	2800		
			188	20.25	2700	3250		

TABLE 10
Contd/

9	2.00 p.m.	31	20	28.50	1000	1400	49	39
			60	30.00	750	1100		
			100	26.00	1400	1900		
			140	22.50	2150	2700		
			188	20.50	2600	3200		
10	3.00 p.m.	31.5	20	30.00	750	1100	52	42
			60	30.00	750	1100		
			100	26.50	1300	1800		
			140	23.25	2000	2500		
			188	21.00	2500	3050		
11	5.30 p.m.	30	20	28.50	1000	1400	51	41
			60	29.50	800	1200		
			100	26.75	1300	1750		
			140	24.25	1750	2250		
			188	21.75	2300	2850		

TABLE 10
Contd/

12	8.00 p.m.	26	20	25.00	1600	2100	44	35
			60	25.75	1450	1950		
			100	24.50	1700	2200		
			140	23.75	1850	2400		
			188	22.50	2150	2700		
13	11.00 p.m.	20	20	18.00	3300	3900	33	28
			60	21.00	2500	3050		
			100	22.00	2250	2800		
			140	22.50	2150	2700		
			188	22.00	2250	2800		

PREDICTION OF TRANSIENT DEFLECTION AT DIFFERENT TEMPERATURES, USING DATA FOR JUNE 21, 1977

(BITUMINOUS MATERIAL MODELLED AS FIVE SUB-LAYERS)

TABLE 10

Observation No.	Time (hr. min.)	T_{40} (^{o}C)	Resilient modulus for bituminous layer (MN/m^2)		Computed deflection (mm x 10^{-2})	
			Model A	Model B	Model A	Model B
1	4.15 a.m.	12	5100	5850	17	15
2	5.00 a.m.	11	5450	6200	16	15
3	6.00 a.m.	11	5450	6200	16	15
4	7.00 a.m.	15	4150	4800	21	18
5	8.00 a.m.	14.5	4300	5000	20	18
6	9.00 a.m.	16.5	3700	4350	23	20
7	11.00 a.m.	24.5	1700	2200	45	37
8	1.00 p.m.	31.5	550	900	96	71
9	2.00 p.m.	31	600	950	91	69
10	3.00 p.m.	31.5	550	900	96	71
11	5.30 p.m.	30	750	1100	80	62
12	8.00 p.m.	26	1400	1900	52	41
13	11.00 p.m.	20	2750	3300	30	26

PREDICTION OF TRANSIENT DEFLECTION AT DIFFERENT TEMPERATURES, USING DATA FOR JUNE 21, 1977 (BITUMINOUS MATERIAL MODELLED AS ONE LAYER)

TABLE 11

Details	Benkelman Beam vehicle		Deflectograph	
	Front	Rear	Front	Rear
Axle load (kg)	2960	6350	4750	6350
Wheel load (kg)	1480	3175	2375	3175
Contact pressure (kN/m^2)	552	590	690	690
Radius of loaded area (mm)	92	130	104	120
Wheel track (mm)	1800	1800	1830	1830
Wheel base (mm)	3200		4500	

DETAILS OF SINGLE WHEEL ASSEMBLIES USED TO SIMULATE THE FRONT AND REAR WHEELS OF THE BENKELMAN BEAM VEHICLE AND THE DEFLECTOGRAPH

TABLE 12

M_{r_1} (MN/m^2)	Absolute deflection ($mmx10^{-2}$)						Apparent deflection ($mmx10^{-2}$)			Nett deflection ($mmx10^{-2}$)
	Initial		Maximum		Final		$\delta_S - 2.8\ \delta_L$			
	δ_S	δ_L	δ_S	δ_L	δ_S	δ_L	Initial (δ_i)	Maximum (δ_{max})	Final (δ_f)	$\delta_{max} - \delta_i/2 - \delta_f/2$
500	8	6	101	-	-	-	-8.8	101	-	105
750	6	2	80	-	-	-	0.4	80	-	80
1000	4	-	66	-	-	-	4	66	-	64
1500	3	-	49	-	-	-	3	49	-	48
2000	2	-	39	-	-	-	2	39	-	38
2750	2	-	29	-	-	-	2	29	-	28
5000	1	-	17	-	-	-	1	17	-	17
where δ_S = deflection at shoe, δ_L = deflection at front leg supports										

TABLE 13

PREDICTION OF BENKELMAN BEAM DEFLECTIONS

M_{r_1} (MN/m^2)	Absolute deflection (mmx10^{-2})						Apparent deflection (mmx10^{-2})		Nett deflection (mmx10^{-2})
	Initial			Maximum			$\delta_G - \delta_B - 0.7\,\delta_C$		
	δ_G	δ_B	δ_C	δ_G	δ_B	δ_C	Initial (δ_i)	Maximum (δ_{max})	$\delta_{max} - \delta_i$
500	13	-	30	103	5	30	-8	77	85
750	10	-	24	81	-	24	-6.8	64.2	71
1000	8	-	20	67	-	20	-6	53	59
1500	7	-	16	49	-	16	-4.2	37.8	42
2000	5	-	10	39	-	10	-2	32	34
2750	4	-	8	30	-	8	-1.6	24.4	26
5000	3	-	6	17	-	6	-1.2	12.8	14

where δ_G = deflection at shoe, δ_B = deflection at recording head support, δ_C = deflection at T-frame support

TABLE 14

PREDICTION OF DEFLECTOGRAPH DEFLECTIONS

Cracking ratio (%)	Computed Benkelman Beam deflection (mm x 10^{-2})	ϵ_r (4100 kg load) in bituminous layer (microstrain)	ϵ_z (4100 kg load) in subgrade (microstrain)	σ_r (4100 kg load) in granular layer (kN/m^2)
0	57	327	202	3.2
20	72	520	244	4.1
40	89	717	298	5.2
60	109	890	371	6.5
80	131	1003	484	8.1
100	176	1180	788	12.0

(a) Before Overlaying

SUMMARY OF DEFLECTIONS, STRESSES AND STRAINS COMPUTED FOR VARIOUS VALUES OF CRACKING RATIO (TEMPERATURE = 20°C)

TABLE 15(a)

Cracking ratio (%)	Computed Benkelman Beam deflection (mm x 10^{-2})	ε_r (4100 kg load) in bituminous layer (microstrain)	ε_z (4100 kg load) in subgrade (microstrain)	σ_r (4100 kg load) in granular layer (kN/m^2)
0	30	107	110	1.4
25.9	41	187	148	2.1
44.4	51	243	185	2.7
63.0	62	300	226	3.3
81.5	74	353	273	3.9
100.0	96	433	409	5.3

(b) After Overlaying

SUMMARY OF DEFLECTIONS, STRESSES AND STRAINS COMPUTED FOR VARIOUS VALUES OF CRACKING RATIO (TEMPERATURE = $20^{o}C$)

TABLE 15(b)

Axle Load		Equivalence Factor
lb	kg	
2000	910	0.0002
4000	1810	0.0025
6000	2720	0.01
8000	3630	0.03
10000	4540	0.09
12000	5440	0.19
14000	6350	0.35
16000	7260	0.61
18000	8160	1.0
20000	9070	1.5
22000	9980	2.3
24000	10890	3.2
26000	11790	4.4
28000	12700	5.8
30000	13610	7.6
32000	14520	9.7
34000	15420	12.1
36000	16320	15.0
38000	17230	18.6
40000	18140	22.8

LOAD EQUIVALENCE FACTORS OBTAINED FROM THE RESULTS OF THE A.A.S.H.O. ROAD TEST (AFTER NORMAN ET AL (19))

TABLE 16

Axle load (kg)	Equivalence Factors				
	Hillsborough Test Section		M1 Motorway Test Section		Typical A.A.S.H.O.
	Rutting	Fatigue	Rutting	Fatigue	
2720	0.008	0.012	0.021	0.015	0.01
6350	0.30	0.39	0.41	0.48	0.35
8200	1.0	1.0	1.0	1.0	1.0
10890	3.0	3.4	2.1	2.8	3.2
12700	5.4	5.9	2.5	4.5	5.8
15420	10.4	12.2	3.4	8.7	12.1

TABLE 17

LOAD EQUIVALENCE FACTORS DEDUCED USING THE COMPUTER PROGRAM DEFPAV, AND TYPICAL A.A.S.H.O. VALUES

M_r (MN/m^2)	103	137.3	171.5	205.8	240
σ_3 (kN/m^2)	0	35	70	105	140

Granular Layer (σ_3: minor principal stress)

M_r (MN/m^2)	30	25.5	21	16.5	12
σ_1 (kN/m^2)	20	30	40	50	60

Subgrade (σ_1: major principal stress)

VALUES OF RESILIENT MODULUS ASSIGNED TO THE GRANULAR LAYER AND THE SUBGRADE

TABLE 18

Computed Value	Without Fabric	With Fabric
Surface transient deflection (mm x 10^{-2})	48	32
Horizontal tensile strain at bottom of bituminous layer (microstrain)	510	600
Vertical compressive strain at top of subgrade (microstrain)	638	658
Horizontal tensile stress at bottom of granular layer (kN/m^2)	28	20
Rut depth after 2 x 10^4 load applications (mm)	1.4	1.4

ANALYSIS OF A PAVEMENT BOTH WITH AND WITHOUT A FABRIC INCLUSION

TABLE 19

Material	a	b	c	d	e	f
Dense Bitumen Macadam	10.2	557	8120	1.8	36.0	1470
Rolled Asphalt	20.2	793	10360	0	51.5	1200

Table 20 : CONSTANTS FOR DETERMINING BITUMINOUS LAYER MODULUS USING EQUATION 11.6 (After Brown (28))

L = 40 kN, p = 500 kN/m^2, a = 160 mm

M_{r_3} (MN/m^2)	M_{r_2} (MN/m^2)	H_2 (mm)	M_{r_1} (MN/m^2) / H_1 (mm)	200(0.4)			4000(0.4)			7000(0.4)			9000(0.4)		
				100	300	500	100	300	500	100	300	500	100	300	500
20 (.48)	50 (0.4)	200				1		2			3	4			5
		500		6						7			8		
50 (0.4)	125 (0.3)	200			9			10	11			12		13	
		500					14			15			16		
70 (0.4)	175 (0.3)	200			17	18			19		20			21	22
		500		23			24						25		

Note : Numerals within brackets are values of Poisson's Ratio.

TABLE 21 FACTORIAL DESIGN OF PAVEMENT RESPONSE COMPUTATION

Set No.	ε_r Microstrain	ε_z Microstrain
1	60.0	141.8
2	73.3	156.0
3	46.9	120.5
4	20.5	80.3
5	15.0	64.1
6	535.5	399.5
7	238.7	341.1
8	192.3	315.5
9	107.3	242.4
10	64.5	135.9
11	29.7	74.5
12	18.0	53.3
13	32.1	84.2
14	236.5	165.8
15	172.0	179.4
16	145.3	177.6
17	73.4	209.3
18	45.4	99.5
19	26.4	64.5
20	37.6	91.4
21	30.9	78.5
22	13.9	31.1
23	221.4	218.2
24	185.6	207.8
25	124.4	175.5

TABLE 22: RESULTS OF STRAIN CALCULATION

PAVEMENT DETAILS			TRAFFIC	DEFLECTION
Road layer	Thickness (mm)	Material	mSA	@ 20°C, 3 km/hr mm x 10^{-2}
Surfacing	100	2 course rolled asphalt	Present 2.2	(1) 38
Road base	125	Rolled asphalt	Future 9.7	(2) 43
Sub base	300	Type 2		(3) 57
Subgrade	00	C.B.R. 4%		

Table 23 : DESIGN EXAMPLE

Case	Deflection @ 20°C 3 km/hr mm x 10^{-2}	Subgrade		Unbound layer		Bituminous Layer		
		H_3 mm	M_{r_3} MN/m^2	H_2 mm	M_{r_2} MN/m^2	H_1 mm	M_{r_1}@20°C 3 km/hr MN/m^2	M_{r_1}@20°C 80 km/hr MN/m^2
1	38	00	40	300	104	225	2750	5500
2	43						2000	4000
3	57						950	1900

TABLE 24 : DETERMINATION OF IN SITU LAYER MODULI

Case	Mode of Damage	H_1	H_2	EAT	M_{r_1}	M_{r_2}	M_{r_3}	ε_1	N_1	Required N
		mm ÷ 25	mm ÷ 250	-	MN/m^2 ÷ 700	MN/m^2 ÷ 70	MN/m^2 ÷ 7	micro strain	MSA	MSA
1	Fatigue Fracture	9.0	1.2	-	7.85714	1.48571	5.71429	92.62	51.59	11.9
2					5.71429			114.69	18.10	
3					2.71429			154.70	4.18	
		-	-	mm ÷ 250	MN/m^2 ÷ 7000	-	MN/m^2 ÷ 70	micro strain		
1	Rutting Distor-tion	-	-	1.21970	0.78571	-	0.57143	153.25	59.42	11.9
2				1.25550	0.57143			178.88	34.05	
3				1.35563	0.27143			253.39	9.72	

Table 25 : DETERMINATION OF CRITICAL STRAINS

Case	Damage Mode	ε_2	H_1	Overlay	Adjusted Overlay
		μ strain	mm ÷ 25	mm	mm
1	Fatigue Fracture	-	-	0	0
2		-	-	0	0
3		111.84	12.3	82.5	60
			EAT mm ÷ 250		
1	Rutting Distortion	-	-	0	0
2		-	-	0	0
3		236.10	1.42	16.8	11.8

TABLE 26 : DETERMINATION OF OVERLAY THICKNESS

Case	Existing Life (mSA)		Overlay (mm)	
	Probability 0.5	Probability 0.9	Probability 0.5	Probability 0.9
1	8.3	6.8	40	40
2	5.9	4.8	40	60
3	3.6	2.6	70	110

TABLE 27: DESIGN EXAMPLE BY T.R.R.L. METHOD

Case	OVERLAY (mm)			
	TRRL METHOD		PROPOSED METHOD	
	Probability 0.5	Probability 0.9	Fatigue	Rutting
1	40	40	0	0
2	40	60	0	0
3	70	110	60	12

TABLE 28 : COMPARISON OF RESULTS

APPENDIX 2

FIGURES

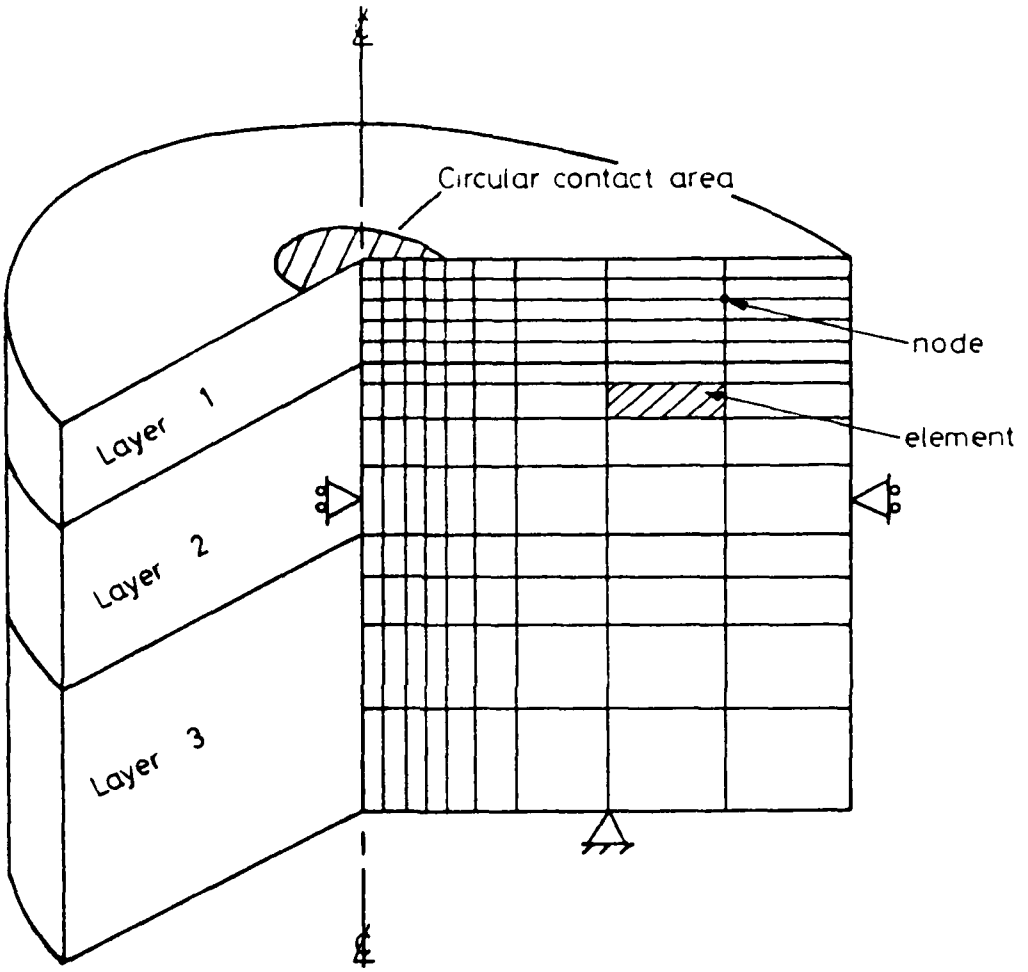

AXIALLY SYMMETRIC CASE OF A UNIFORM CIRCULAR LOAD ON A THREE-LAYER PAVEMENT

FIG. 1

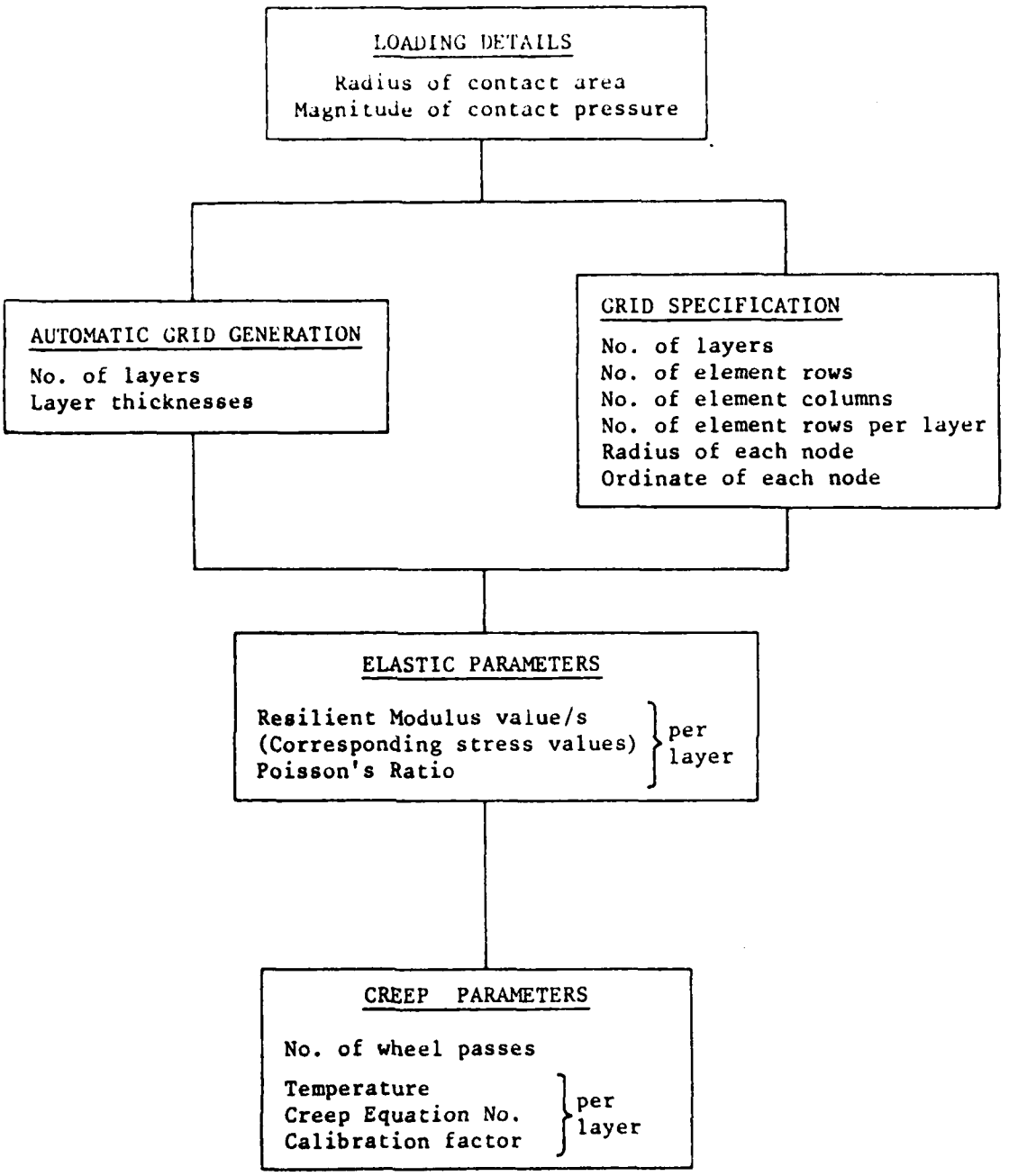

INPUT TO THE COMPUTER PROGRAM DEFPAV (OPTION VERSION)

FIG. 2

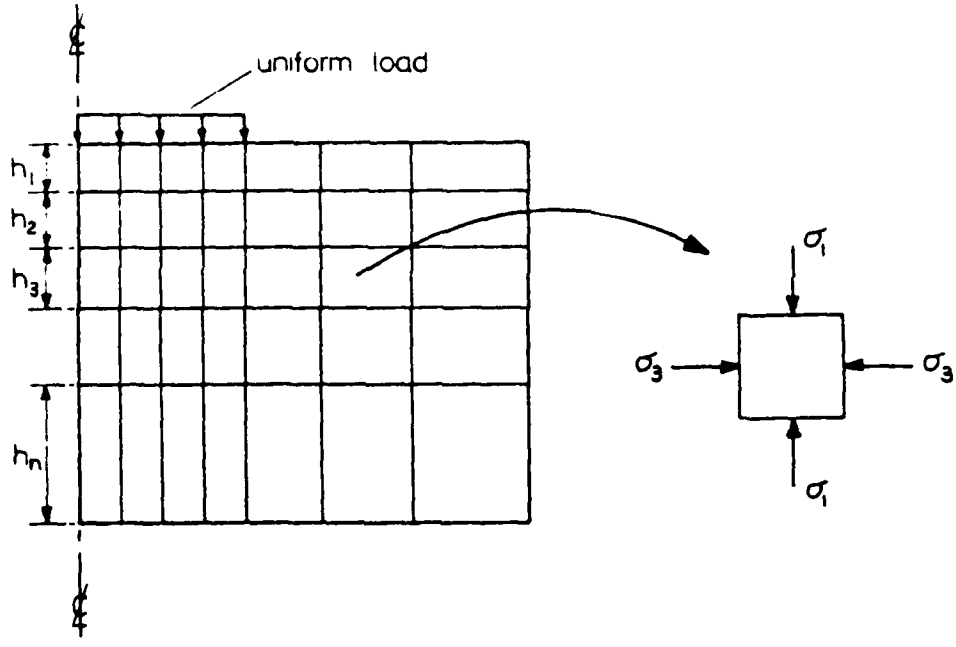

For each column of elements

$$\Delta = \sum_{i=1}^{n} \varepsilon_i h_i$$

where Δ = *total permanent* deformation (rut depth)

ε = permanent vertical strain in an element

h = thickness of element

n = number of elements in the element column

COMPUTATION OF PERMANENT DEFORMATION

(AFTER BARKSDALE (10))

FIG. 3

```
*****************************************
*                                       *
*          DYNASTOR (VERSION 3)         *
*    FLEXIBLE PAVEMENT SYSTEM ANALYSIS  *
*                                       *
*  DEVELOPED,MAINTAINED AND OPERATED BY *
*       COMPUTER SYSTEMS RESEARCH       *
*          TRINITY COLLEGE,DUBLIN       *
*                                       *
*                          SEPT 1970    *
*****************************************

*****************************************
*                                       *
*          DESIGN MODIFICATION          *
*        ROAD ENGINEERS EDITION         *
*                                       *
*              D E F P A V              *
*                                       *
*       QUEENS UNIVERSITY,BELFAST       *
*                                       *
*                          AUG 1976     *
*****************************************

     SAMPLE DATA FOR 3 LAYER PAVEMENT,USING AUTOMATIC GRID,          DATA  2

USING AUTOMATIC GRID GENERATION OPTION (GRID = 0)
************************************************

NUMBER OF LAYERS:-  3
NUMBER OF COLUMNS:- 14

RADIUS OF NODES IN EACH COLUMN:-

        0.000   0.029   0.058   0.086   0.115   0.144   0.173   0.230   0.346   0.576   1.037   1.958
        3.802   7.488  14.861

GRID GENERATED HAS 4 ROWS PER LAYER FOR ALL LAYERS EXCEPT SUBGRADE,LAYER  3

SPECIFIED LAYER THICKNESSES IN ORDER FROM TOP LAYER,BUT EXCLUDING BOTTOM (SUBGRADE) LAYER:-

        0.100   0.485

NUMBER OF NODES AVAILABLE FOR SUBGRADE = NSELECT =  56

LAYER  3 HAS  4 ROWS

VERTICAL ORDINATE OF NODES IN EACH ROW:-

        0.000   0.013   0.038   0.056   0.100   0.161   0.244   0.381   0.585   0.908   2.000   4.586
        9.638

NUMBER OF ELEMENT ROWS IN GRID = 12

TOTAL NUMBER OF NODES USED IN GRID = 196
```

FIG. 4 EXTRACT FROM DEFPAV OUTPUT SHOWING AUTOMATIC GRID GENERATED FOR A TYPICAL THREE - LAYER PAVEMENT (Radius of loaded area = 0.144 m)

Layer No.	Material	Thickness (mm)	M_r (MN/m^2)	ν
1	Bituminous	100	1000	0.4
2	Crushed rock	485	31.25	0.3
3	Subgrade	∞	12.5	0.45
Loading details: Radius of loaded area 130 mm Uniform loading of 590 kN/m^2				

Details of pavement model

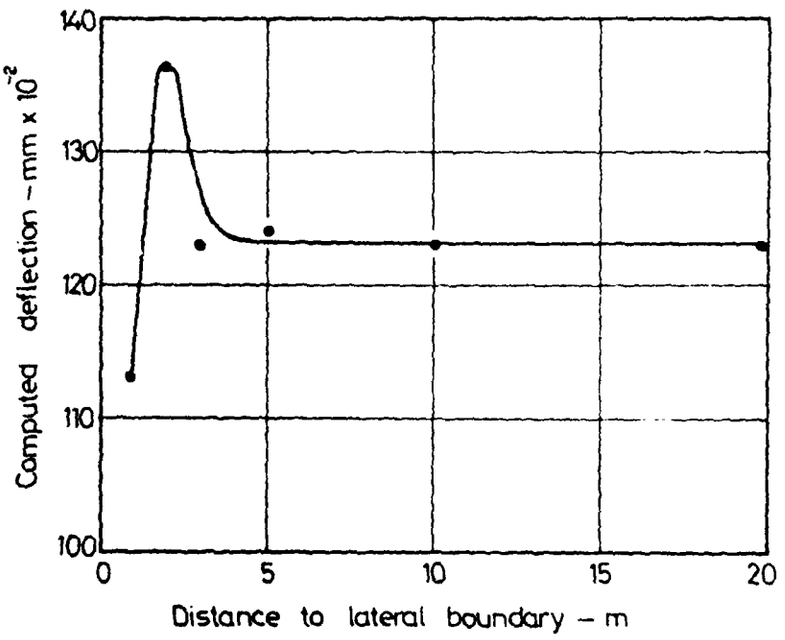

EFFECT OF INCREASING DISTANCE TO LATERAL BOUNDARY ON COMPUTED SURFACE TRANSIENT DEFLECTION

FIG. 5

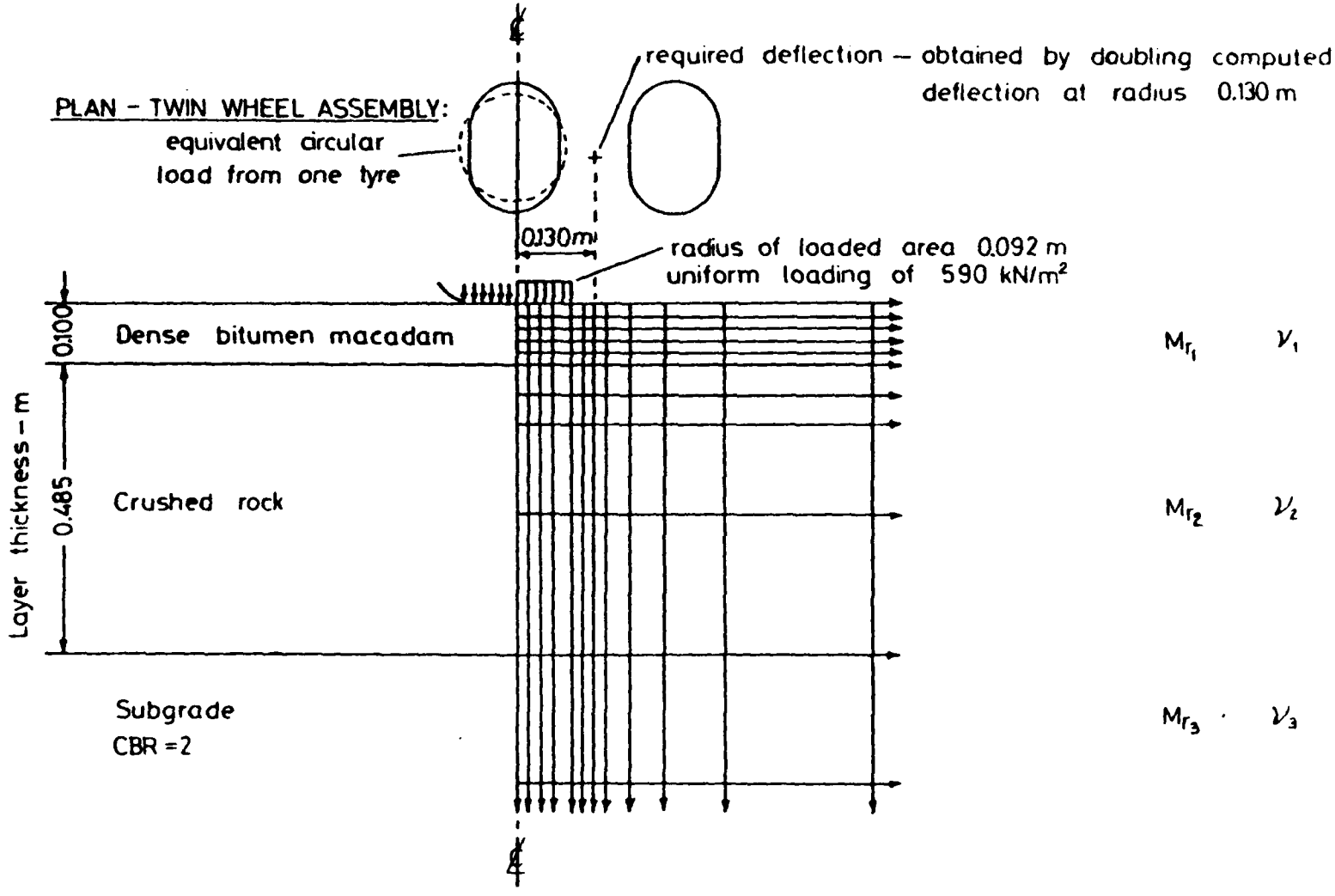

FIG. 6

SIMULATION OF REAR WHEEL LOAD OF BENKELMAN BEAM VEHICLE USING A TWIN WHEEL ASSEMBLY

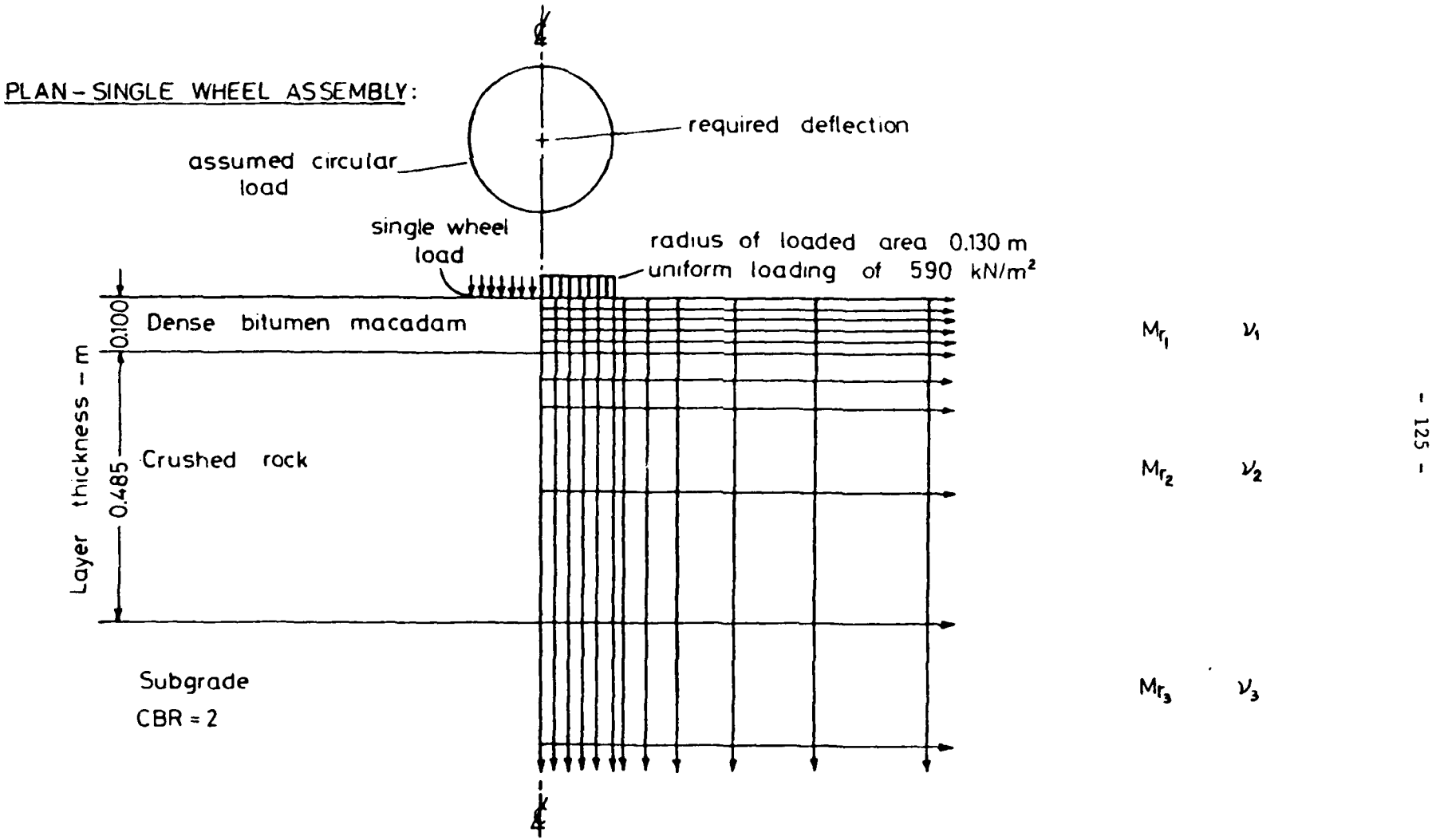

FIG. 7

SIMULATION OF REAR WHEEL LOAD OF BENKELMAN BEAM VEHICLE USING A SINGLE WHEEL ASSEMBLY

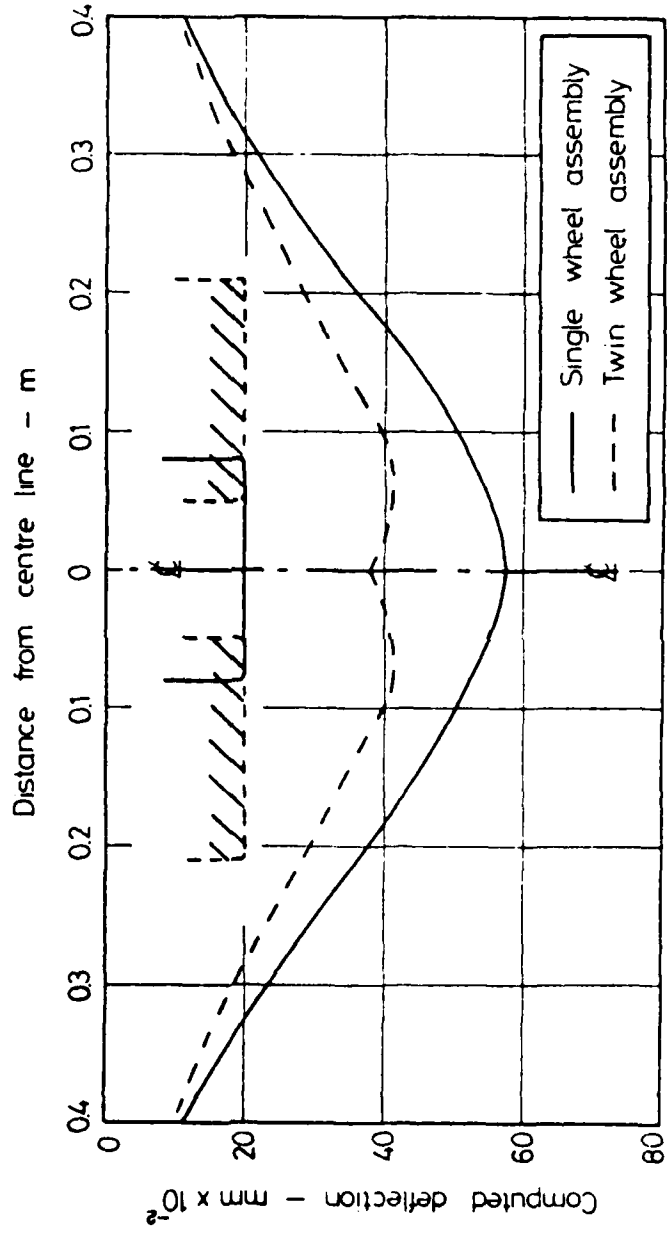

DEFLECTION BOWLS UNDER SINGLE AND TWIN WHEEL ASSEMBLIES

FIG. 8

Layer No.	Material	Thickness (mm)	M_r (MN/m^2)	ν
1	Bituminous	216	2750	0.4
2	Crushed rock	485	31.25	0.3
3	Subgrade	∞	12.5	0.45

Loading details: Contact pressure = 690 kN/m^2
Radius of loaded area deduced from wheel load and contact pressure.

Details of pavement model

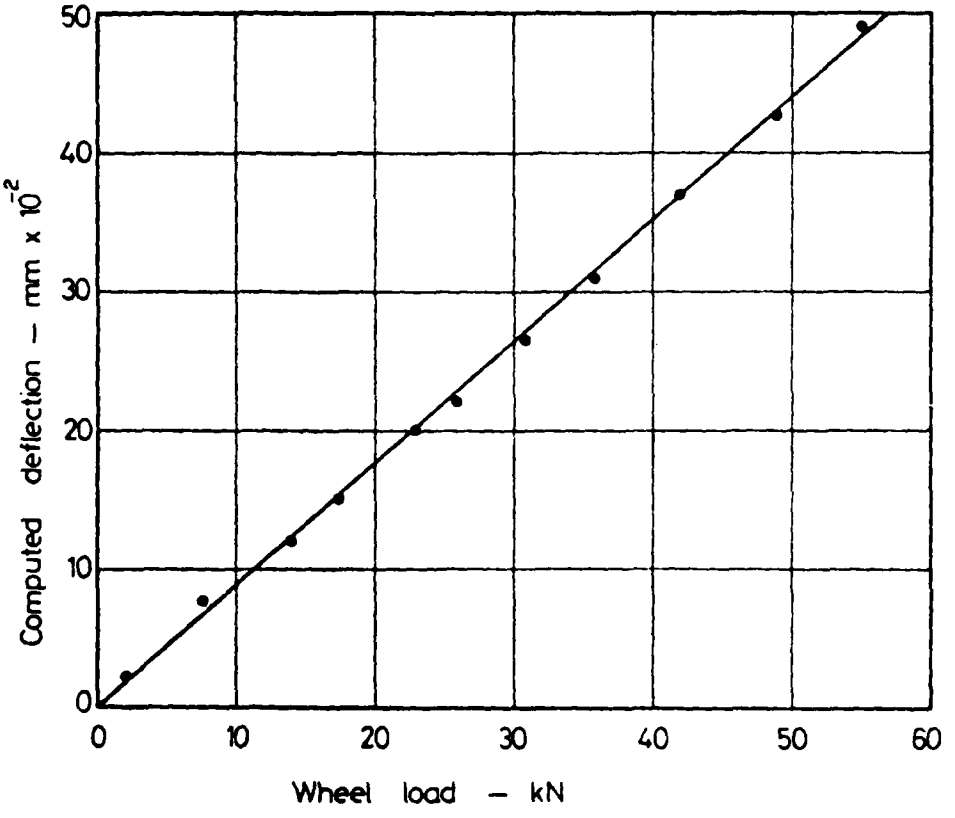

VARIATION OF COMPUTED SURFACE TRANSIENT DEFLECTION WITH MAGNITUDE OF WHEEL LOAD

FIG. 9

Layer No.	Material	Thickness (mm)	M_r (MN/m^2)	ν
1	Bituminous	216	2750	0.4
2	Crushed rock	485	31.25	0.3
3	Subgrade	∞	12.5	0.45

Details of pavement model

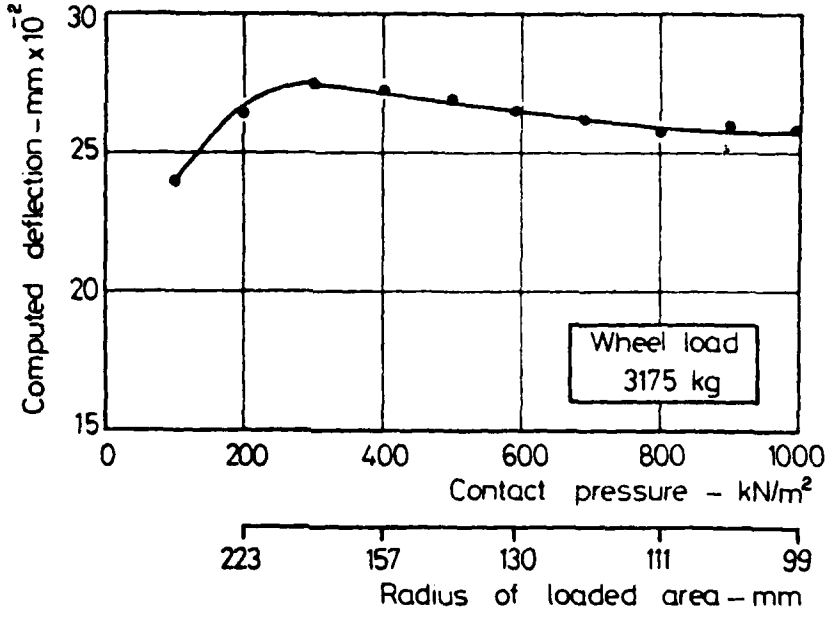

VARIATION OF COMPUTED SURFACE TRANSIENT DEFLECTION WITH CONTACT PRESSURE

FIG. 10

Layer No.	Material	Thickness (mm)	M_r (MN/m^2)	ν
1	Bituminous	180	1400	0.4
2	Crushed rock	485	$M_{r_2} = 2.5\ (M_{r_3})$	0.3
3	Subgrade	∞	$M_{r_3} = 10\ (CBR)$	0.45
Loading details: Radius of loaded area 130 mm Uniform loading of 590 kN/m^2				

Details of pavement model

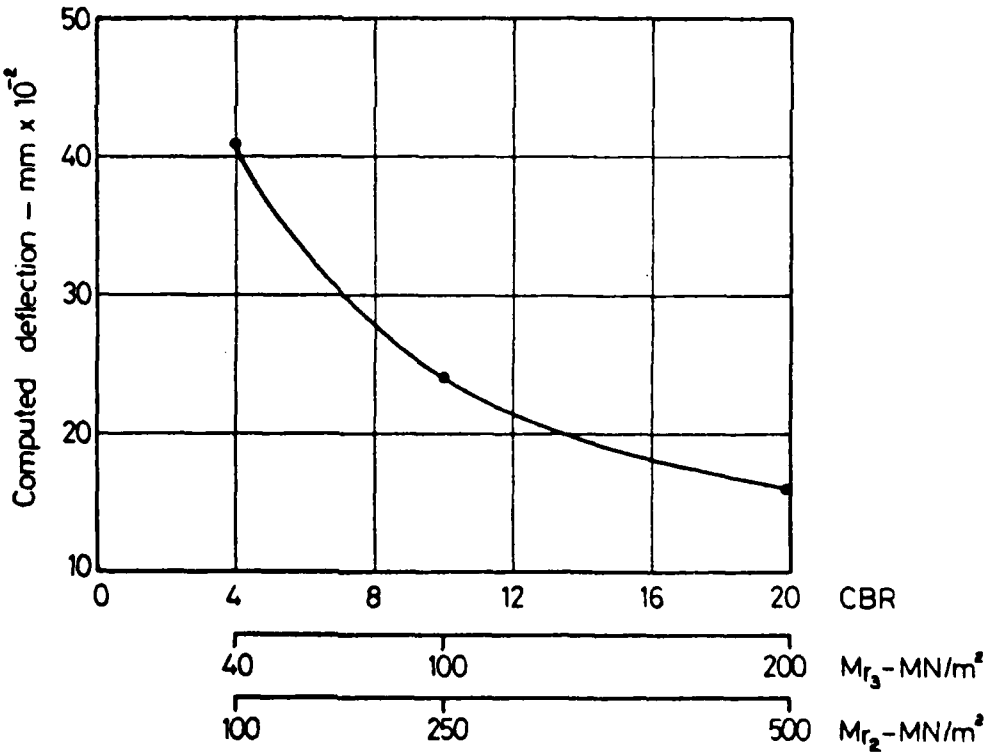

VARIATION OF COMPUTED SURFACE TRANSIENT DEFLECTION WITH CBR VALUE OF THE SUBGRADE

FIG. 11

Layer No.	Material	Thickness (mm)	M_r (MN/m^2)	Poisson's Ratio (ν)		
				Varying ν_1	Varying ν_2	Varying ν_3
1	Bituminous	216	2750	-	0.4	0.4
2	Crushed rock	485	31.25	0.3	-	0.3
3	Subgrade	∞	12.5	0.45	0.45	-
Loading details: Radius of loaded area 130 mm Uniform loading of 590 kN/m^2						

Details of pavement model

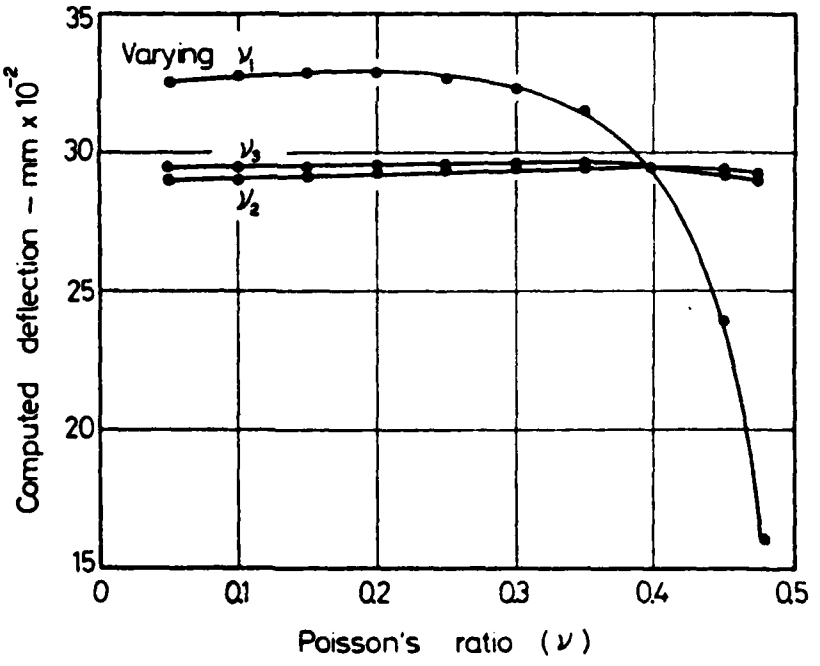

VARIATION OF COMPUTED SURFACE TRANSIENT DEFLECTION WITH POISSON'S RATIO

FIG. 12

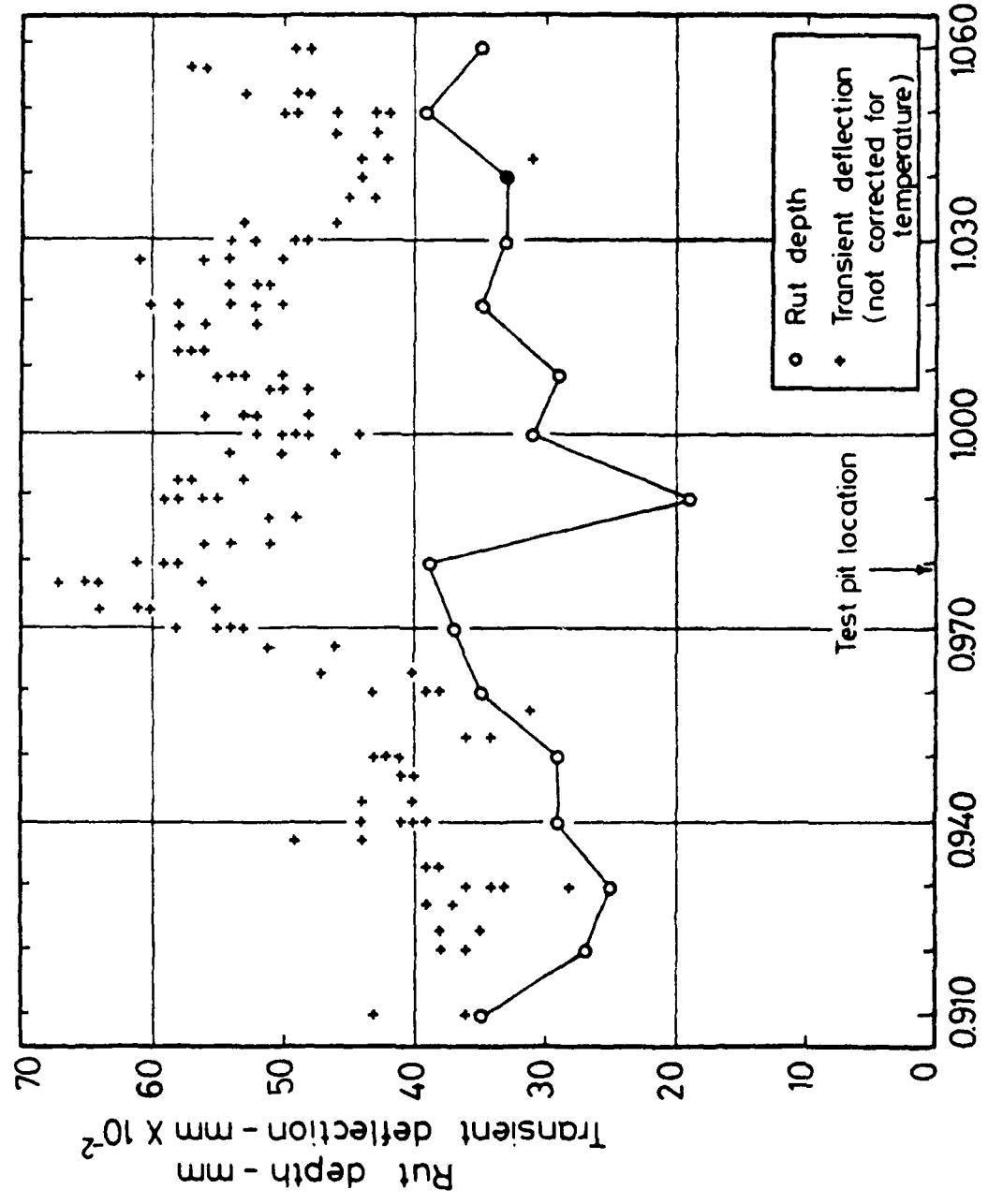

PAVEMENT CONDITION SURVEY RESULTS, OCT. 1976.

HILLSBOROUGH TEST SECTION, BEFORE OVERLAYING.

FIG. 13

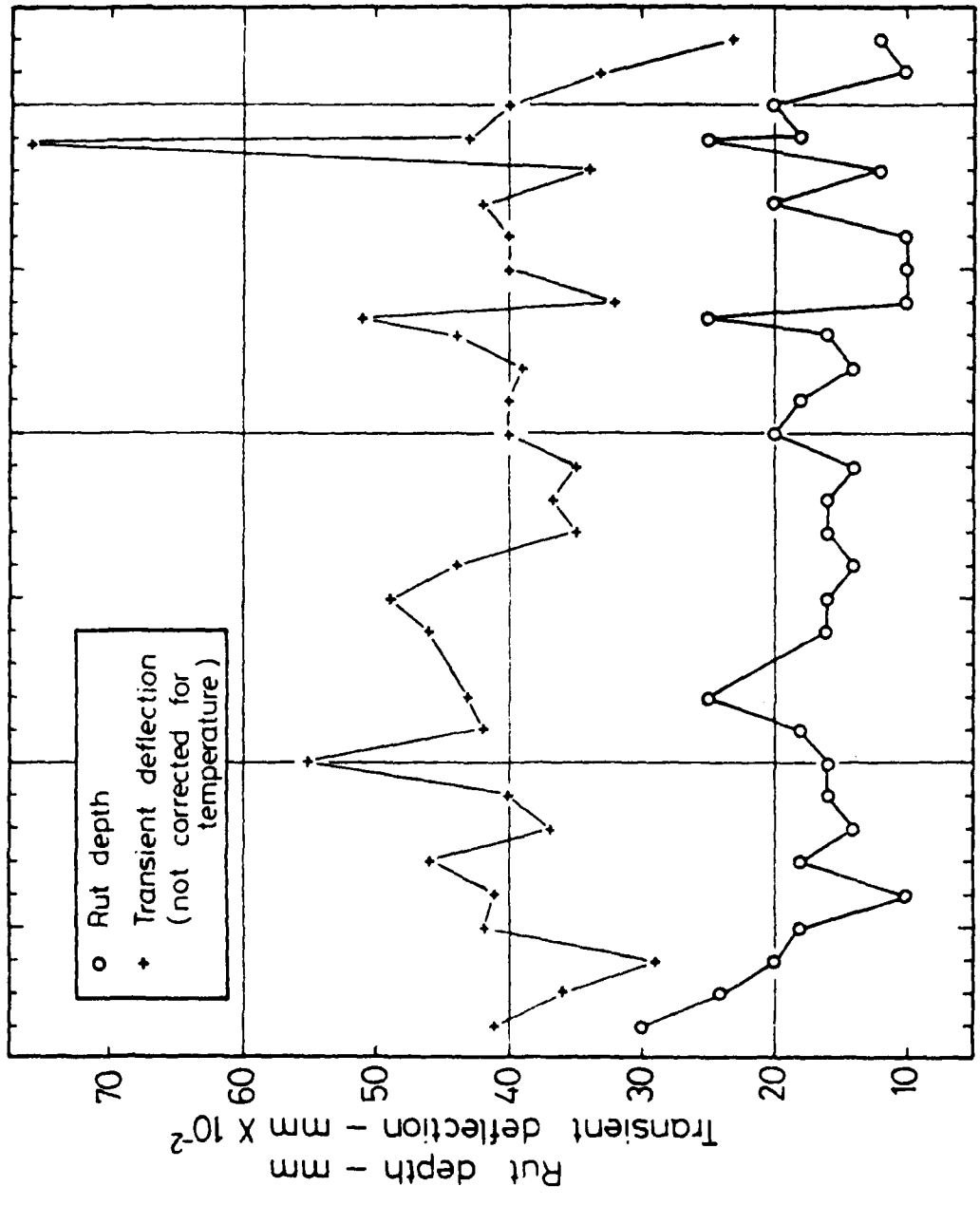

PAVEMENT CONDITION SURVEY RESULTS, APRIL 1976
M1 MOTORWAY TEST SECTION.

FIG. 14

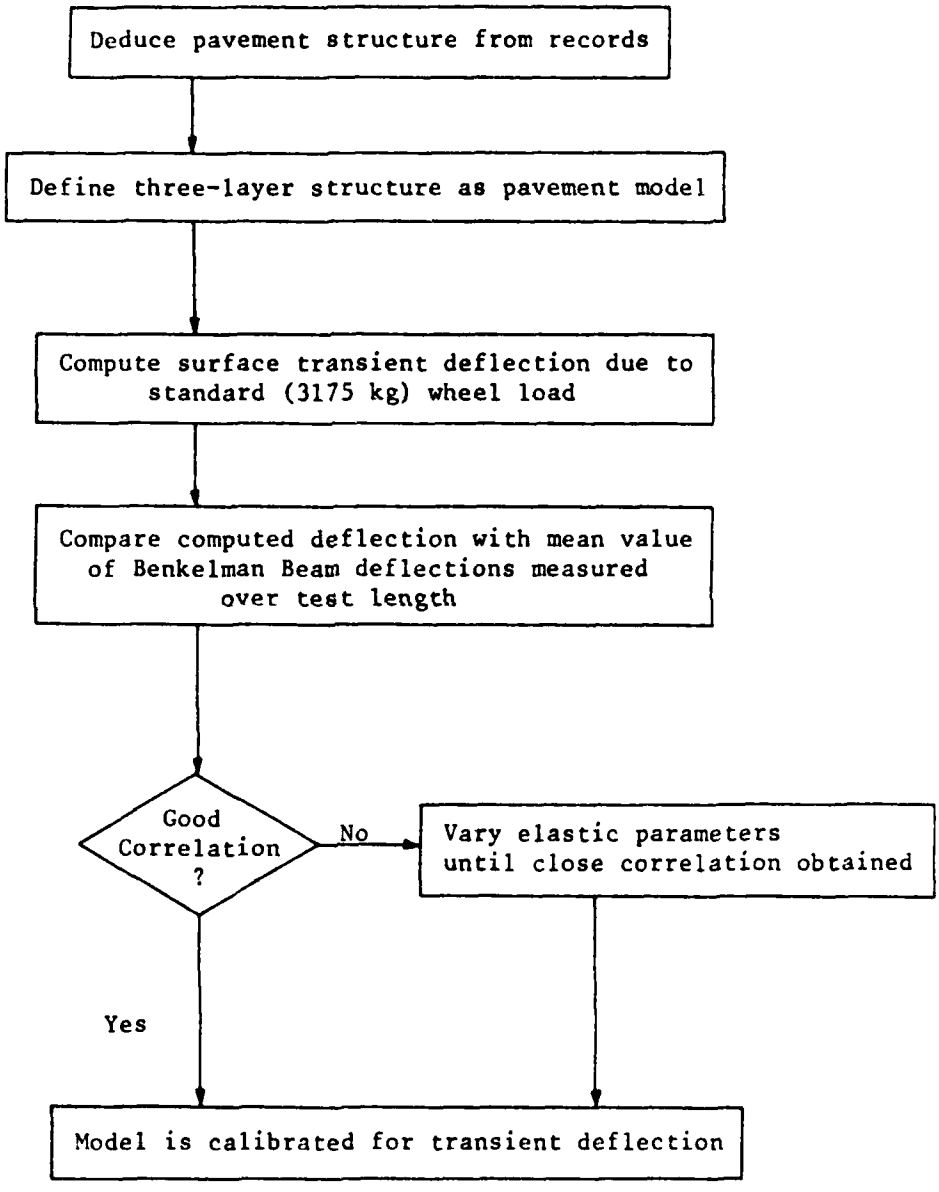

BACK ANALYSIS PROCEDURE TO CALIBRATE THE PAVEMENT MODEL FOR TRANSIENT DEFLECTION

FIG. 15

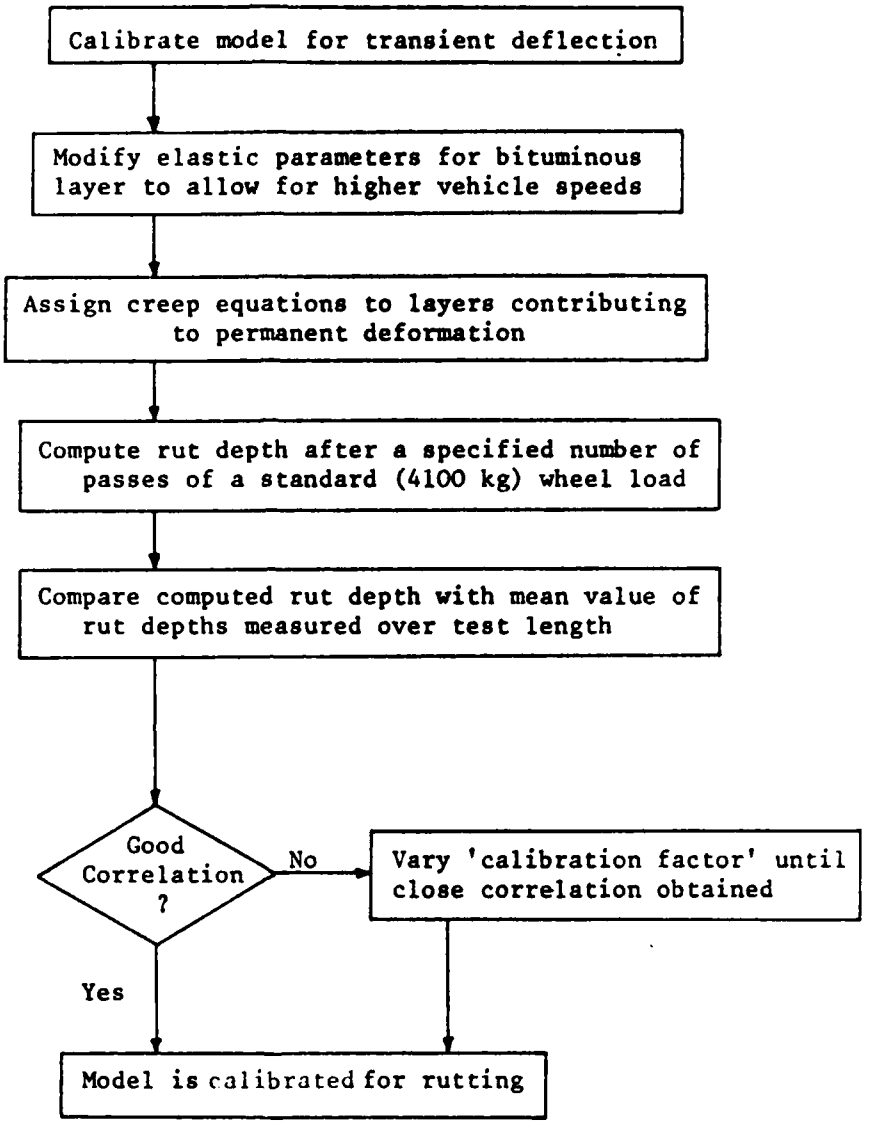

BACK ANALYSIS PROCEDURE TO CALIBRATE THE PAVEMENT MODEL FOR RUTTING

FIG. 16

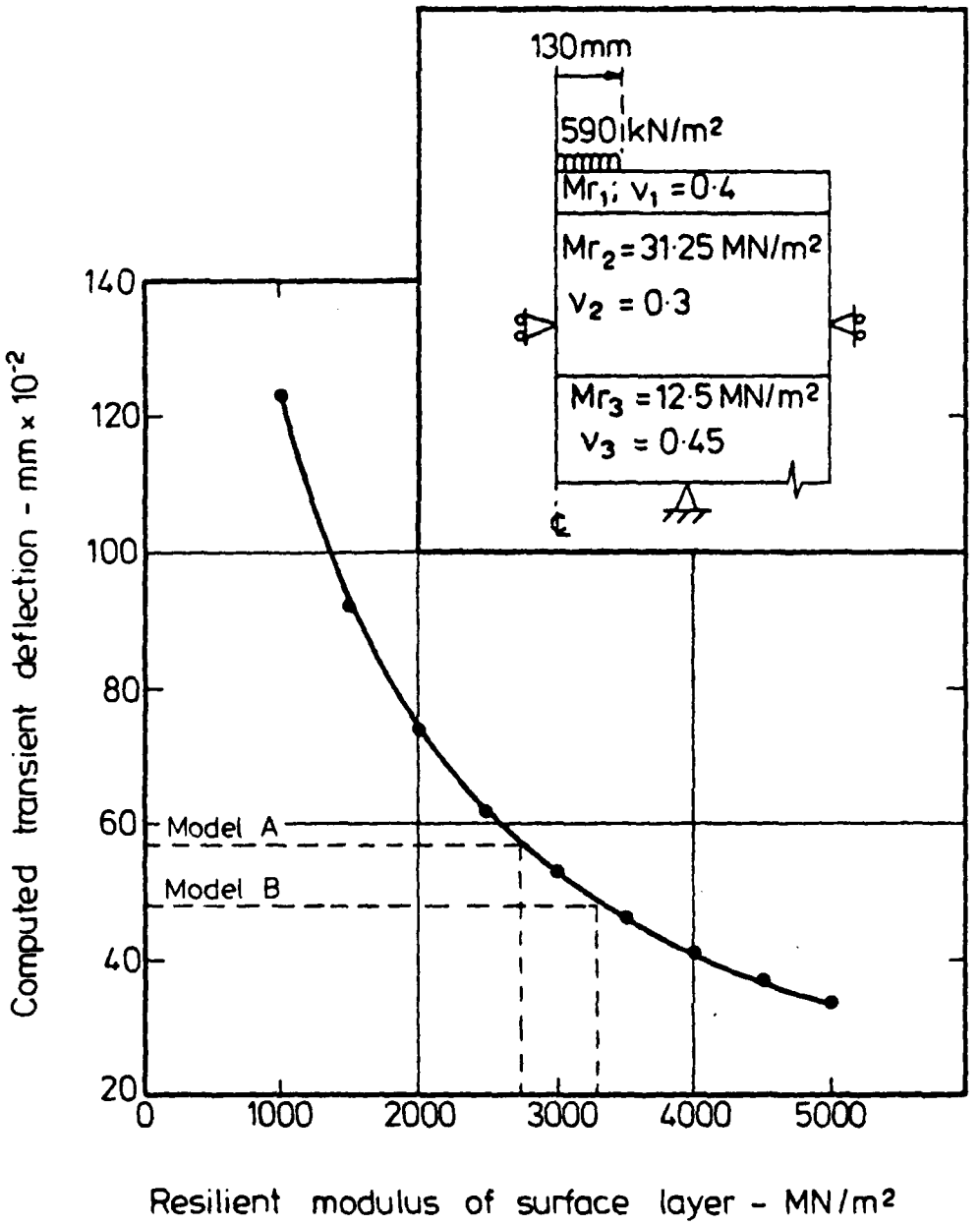

VARIATION OF COMPUTED SURFACE TRANSIENT DEFLECTION WITH SURFACE LAYER MODULUS (HILLSBOROUGH TEST SECTION, BEFORE OVERLAYING)

FIG. 17

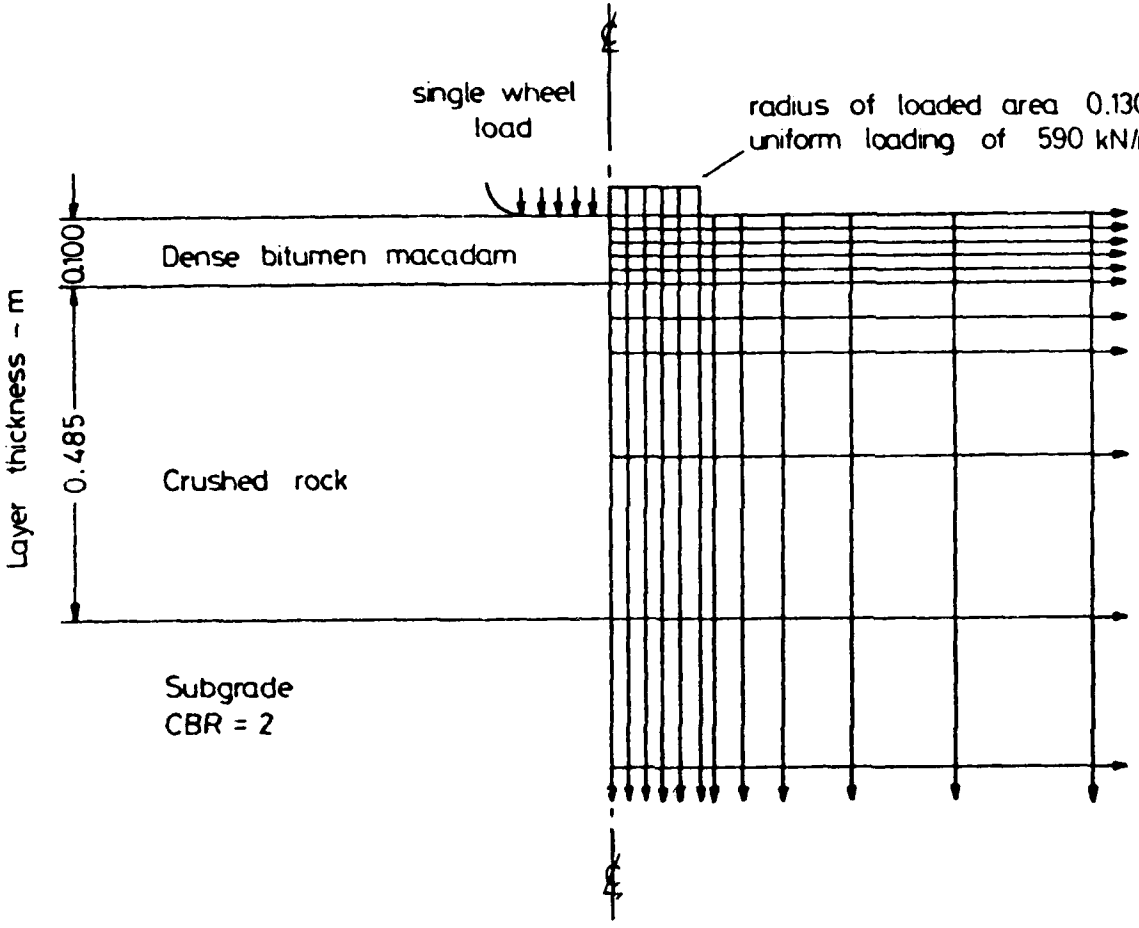

FINITE ELEMENT REPRESENTATION OF HILLSBOROUGH TEST SECTION BEFORE OVERLAYING - SIMULATING REAR WHEEL LOAD OF BENKELMAN BEAM VEHICLE

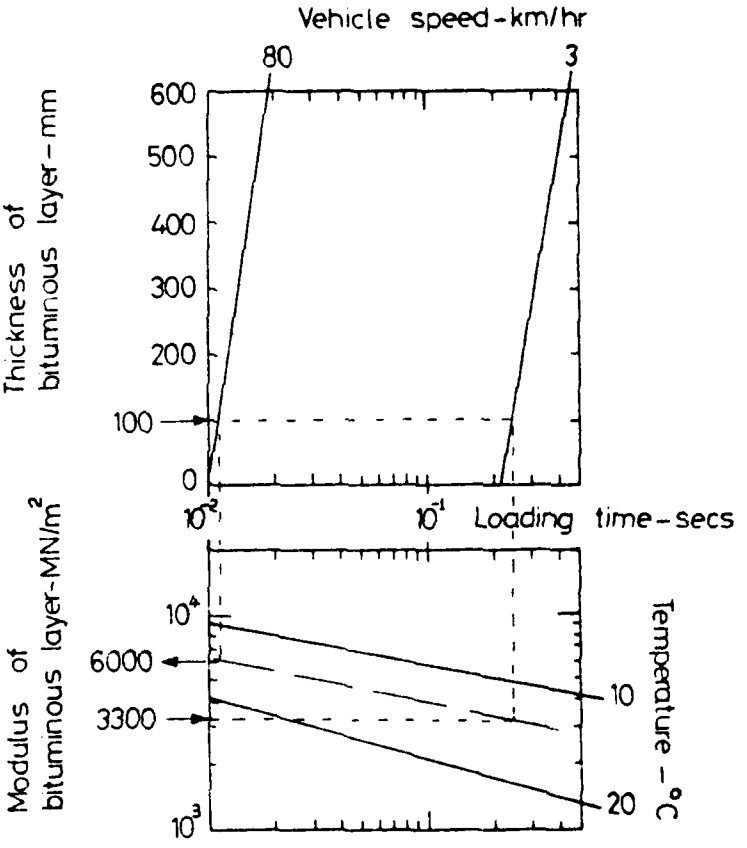

CHART USED TO CALIBRATE SURFACE LAYER MODULUS FOR RUTTING (AFTER BROWN (28)). -HILLSBOROUGH TEST SECTION

FIG. 19

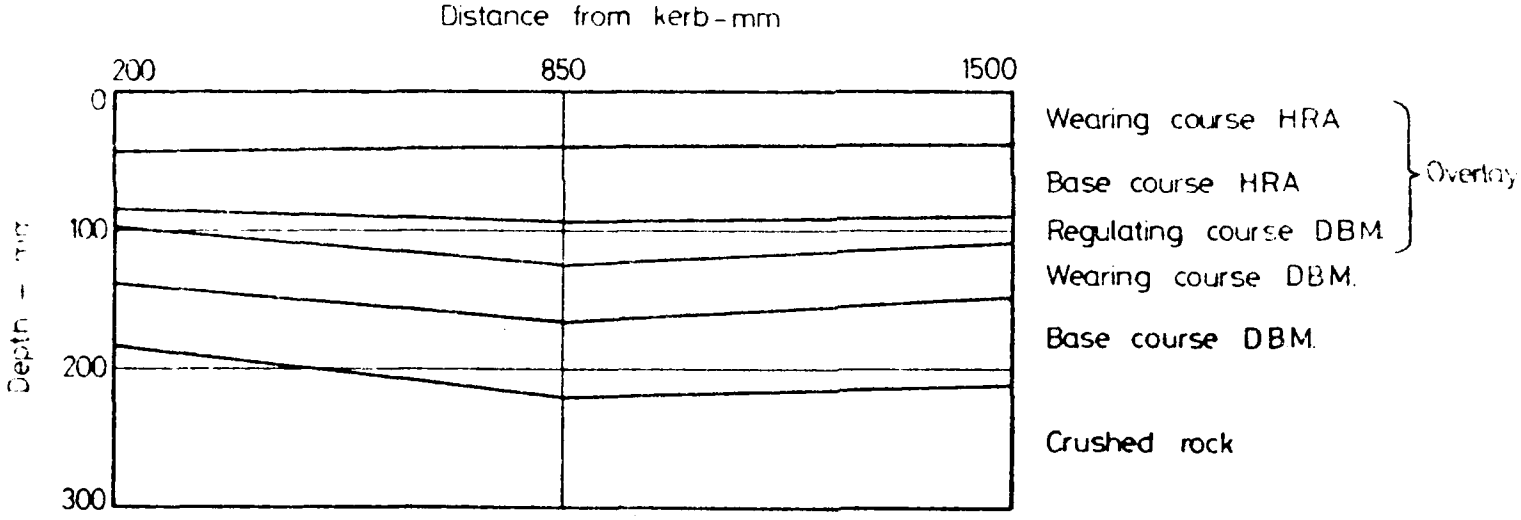

FIG. 20

PAVEMENT SECTION OBTAINED FROM CORES TAKEN AT DISTANCES OF 200, 850, AND 1500 mm FROM THE KERB AT CH 0.980 km ON THE HILLSBOROUGH TEST SECTION (MAY 24, 1977)

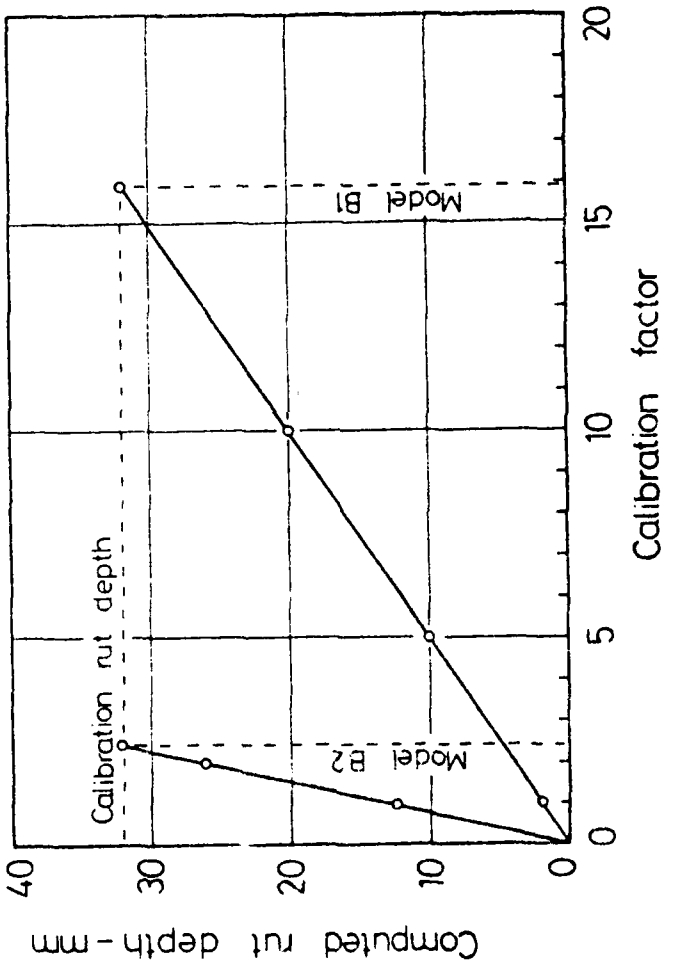

VARIATION OF COMPUTED RUT DEPTH WITH CALIBRATION FACTOR
(HILLSBOROUGH TEST SECTION - BEFORE OVERLAYING)

FIG. 21

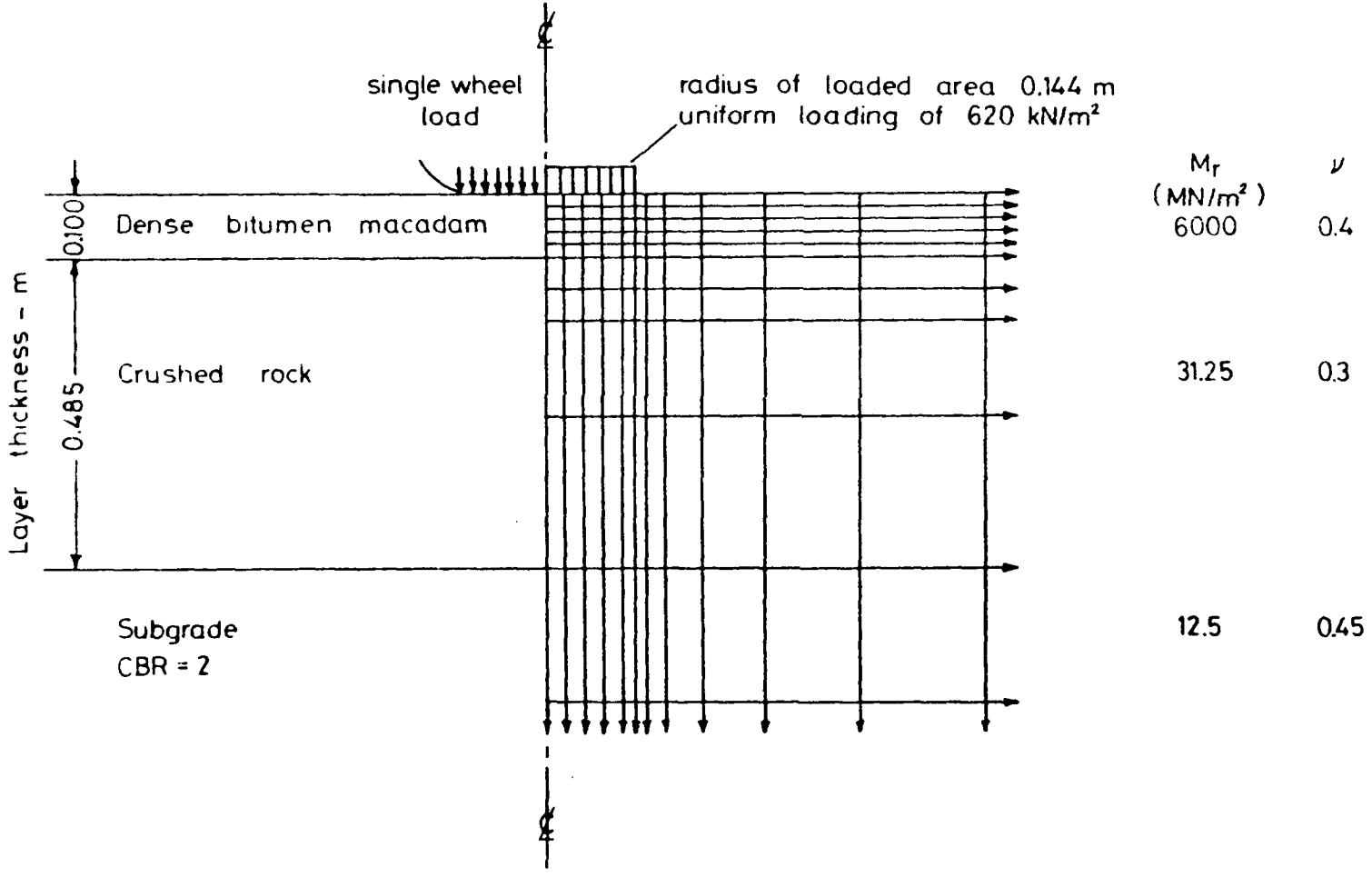

FIG. 22

FINITE ELEMENT REPRESENTATION OF HILLSBOROUGH TEST SECTION BEFORE OVERLAYING (MODEL B - 150 m TEST LENGTH) - SIMULATING STANDARD AXLE WHEEL LOAD

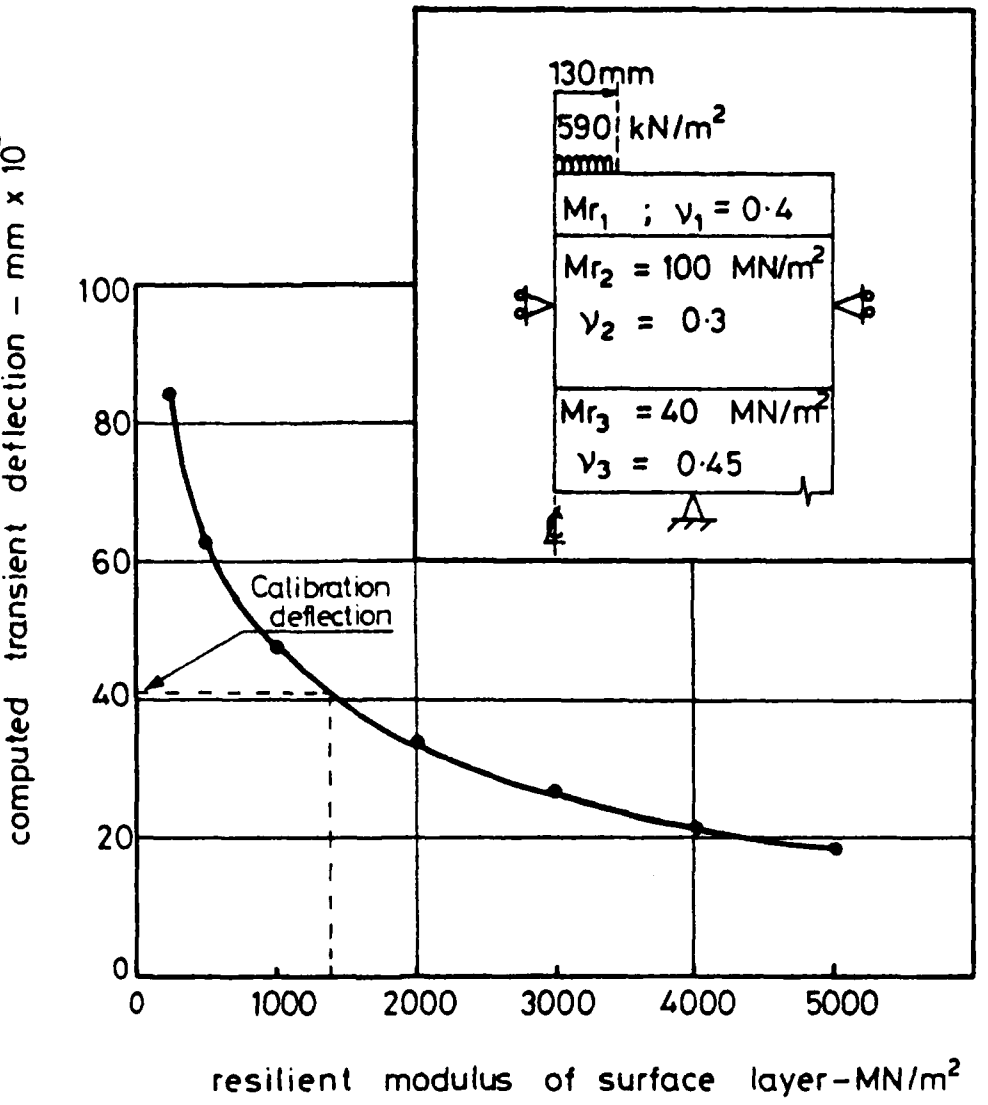

VARIATION OF COMPUTED SURFACE TRANSIENT DEFLECTION WITH SURFACE LAYER MODULUS.
(M1 MOTORWAY TEST SECTION).

FIG. 23

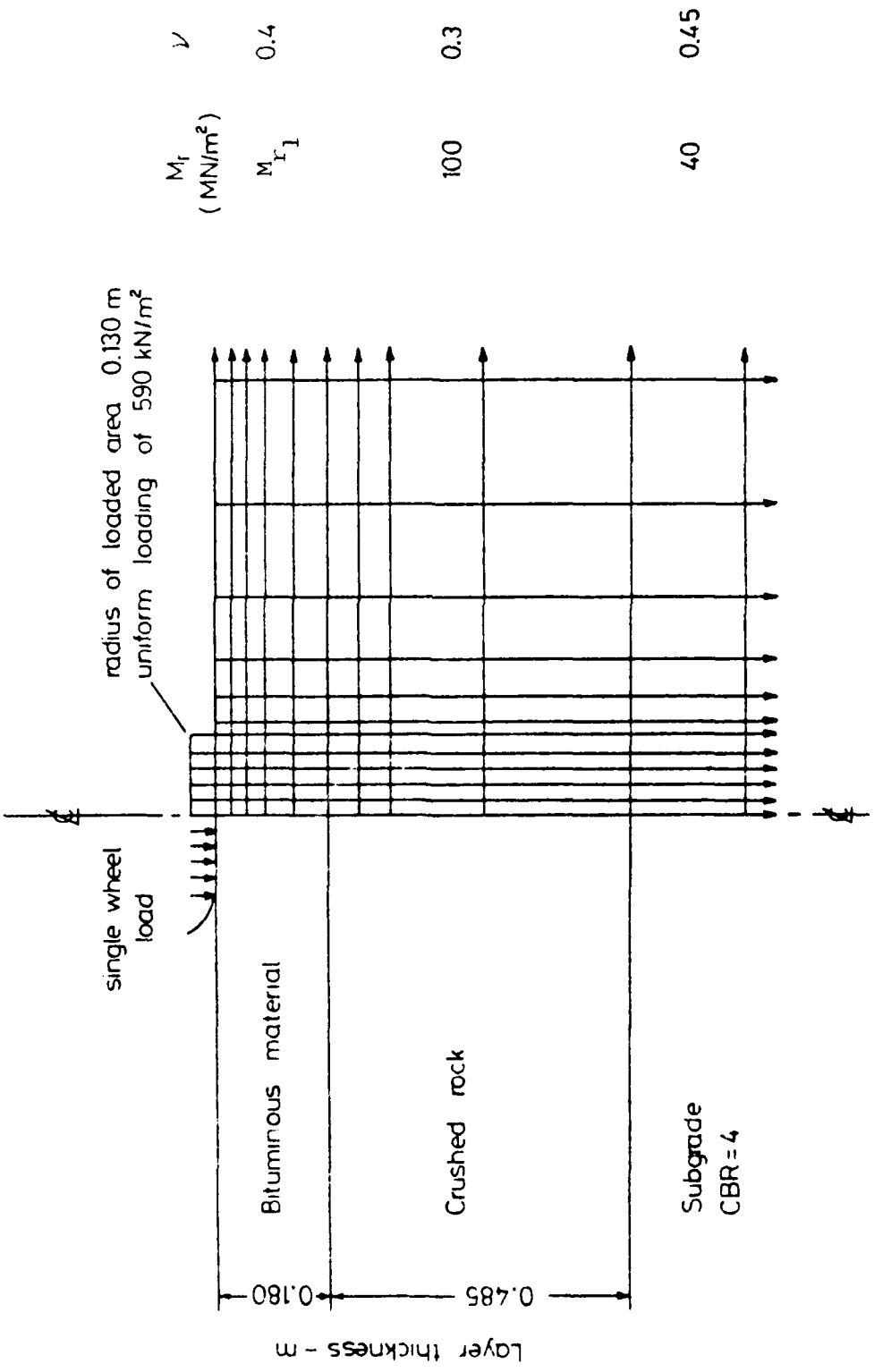

FINITE ELEMENT REPRESENTATION OF M1 MOTORWAY TEST SECTION - SIMULATING REAR WHEEL LOAD OF BENKELMAN BEAM VEHICLE

FIG. 24

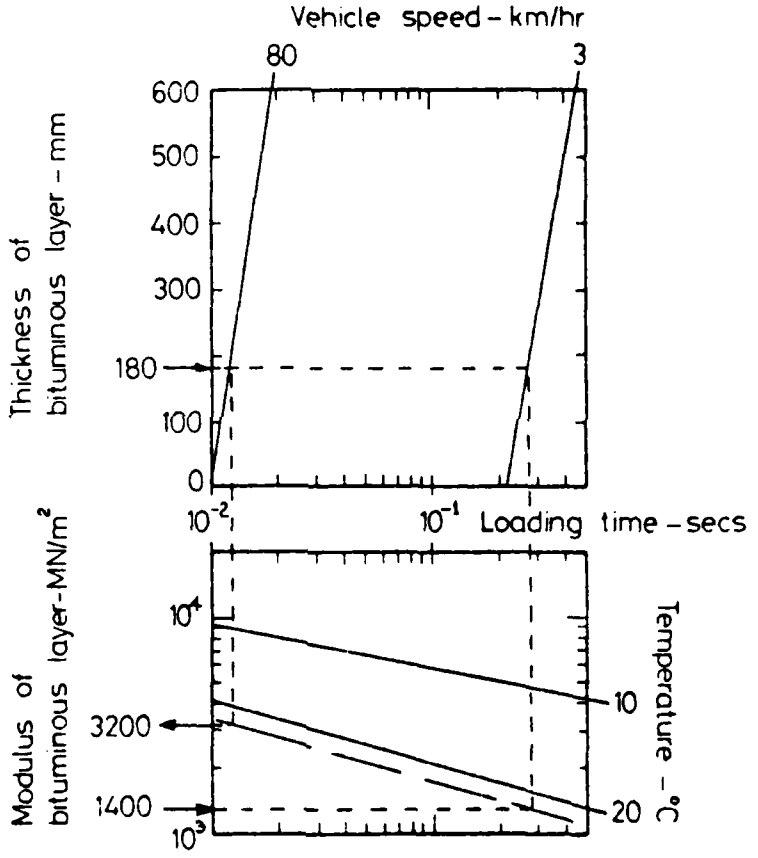

CHART USED TO CALIBRATE SURFACE LAYER MODULUS FOR RUTTING (AFTER BROWN (28)) - M1 MOTORWAY TEST SECTION

FIG. 25

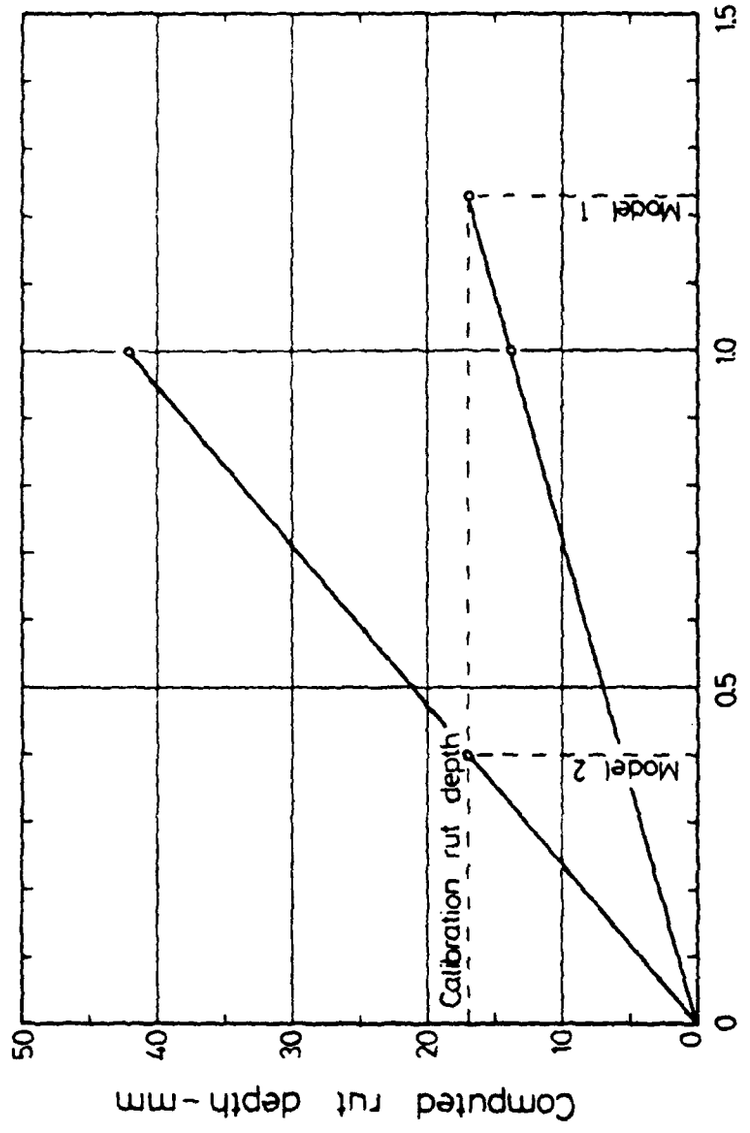

VARIATION OF COMPUTED RUT DEPTH WITH CALIBRATION FACTOR
M1 MOTORWAY TEST SECTION - EXISTING PAVEMENT)

FIG. 26

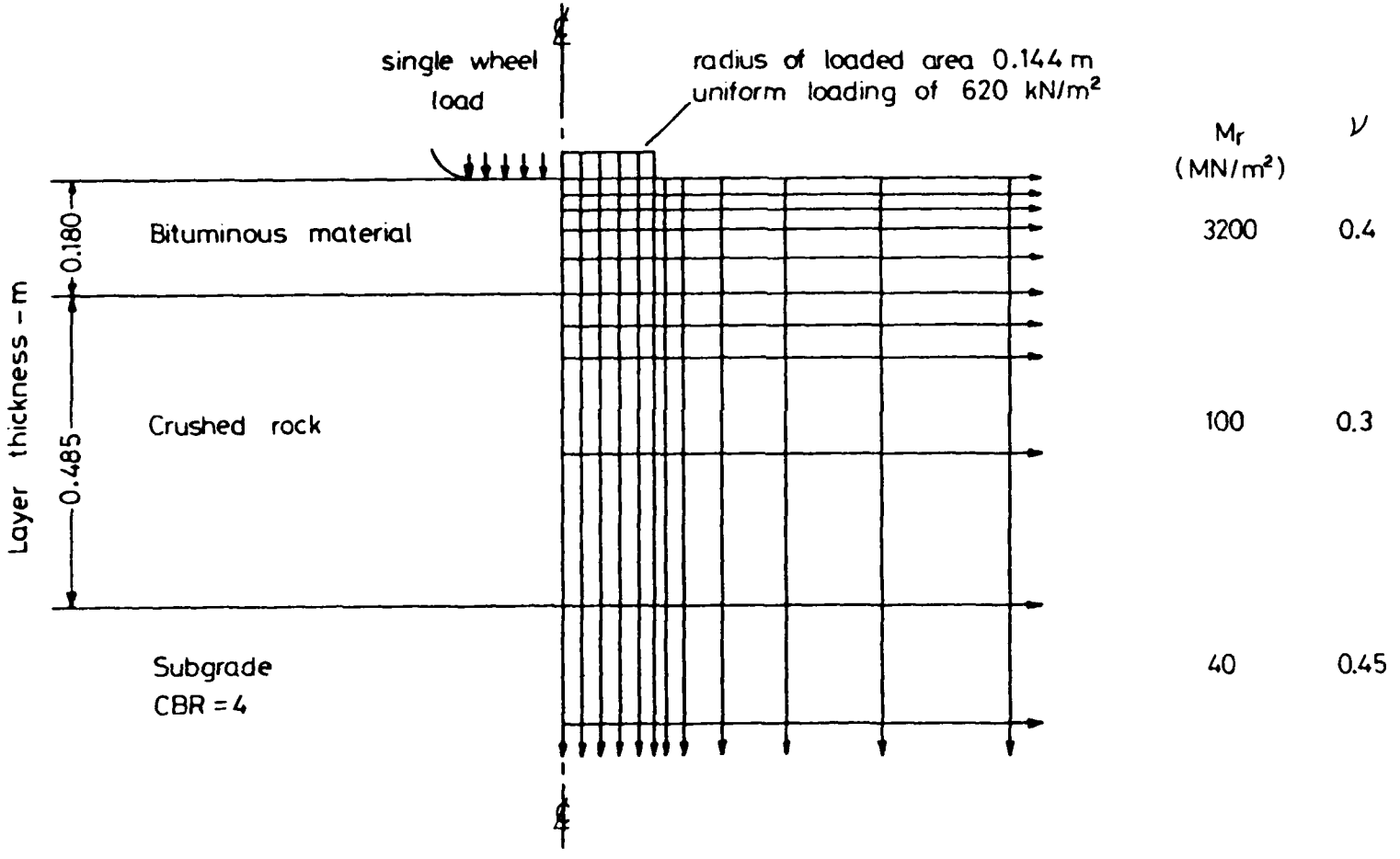

FIG. 27

FINITE ELEMENT REPRESENTATION OF M1 MOTORWAY TEST SECTION - SIMULATING STANDARD AXLE WHEEL LOAD

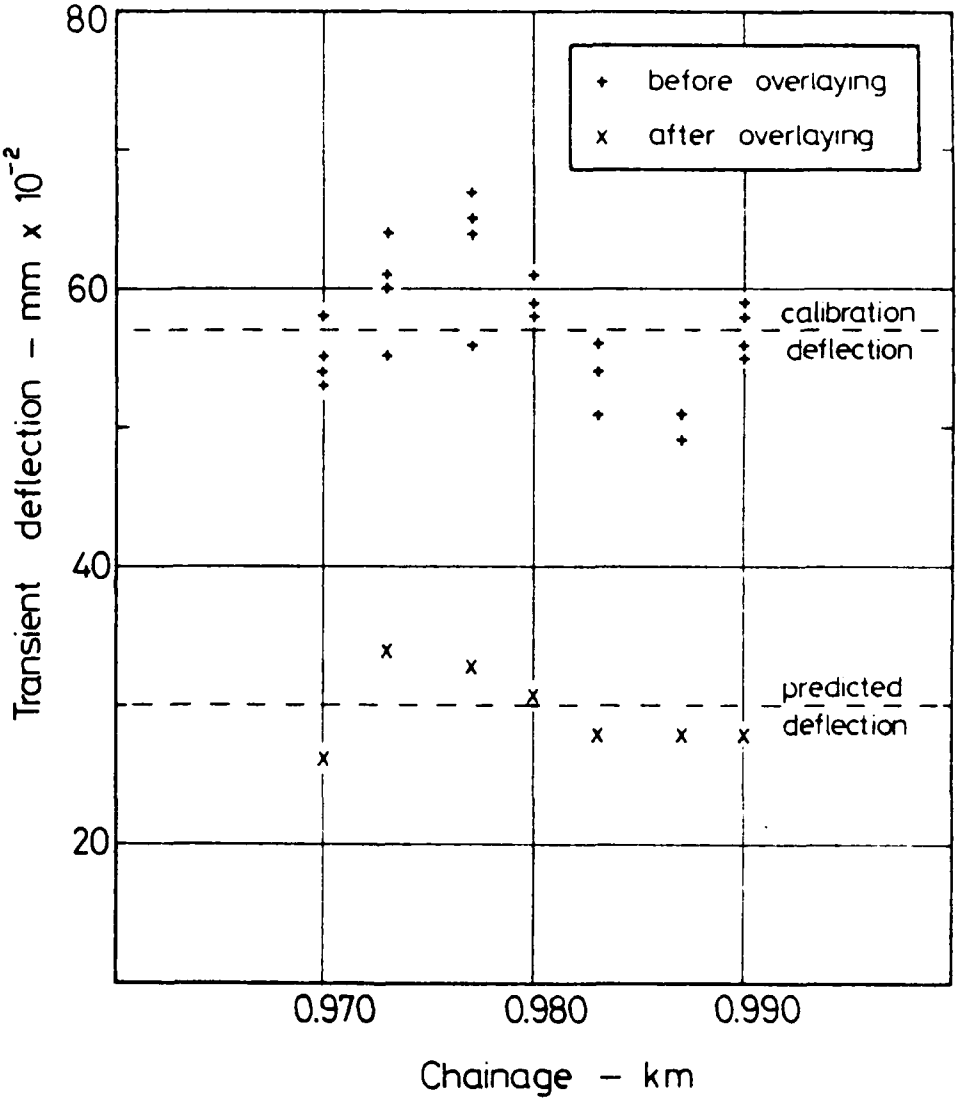

PREDICTION OF TRANSIENT DEFLECTION AFTER OVERLAYING AT HILLSBOROUGH TEST SECTION (MODEL A - 20m TEST LENGTH)

FIG. 28

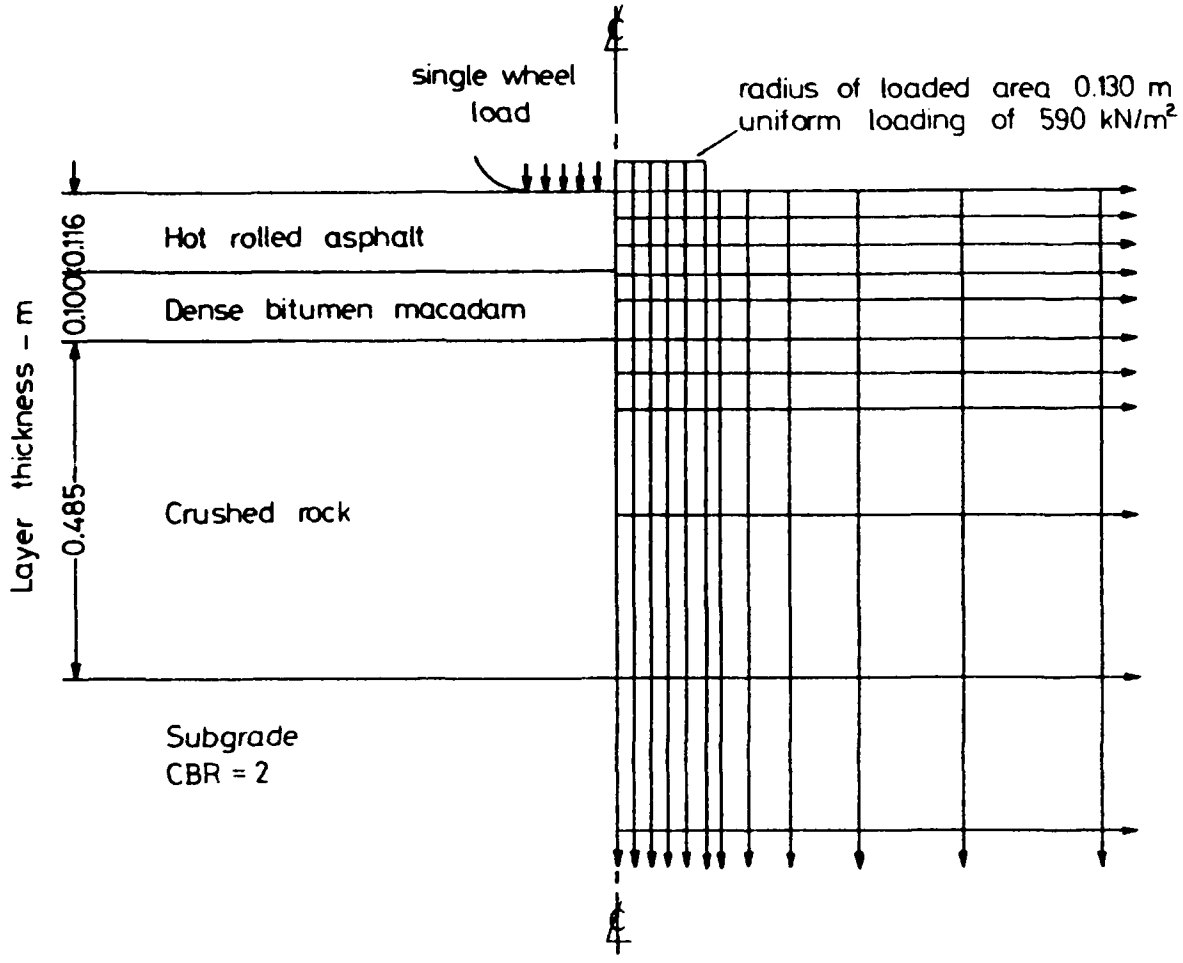

FIG. 29

FINITE ELEMENT REPRESENTATION OF HILLSBOROUGH TEST SECTION AFTER OVERLAYING. (MODEL A - 20m TEST LENGTH) - SIMULATING REAR WHEEL LOAD OF BENKELMAN BEAM VEHICLE.

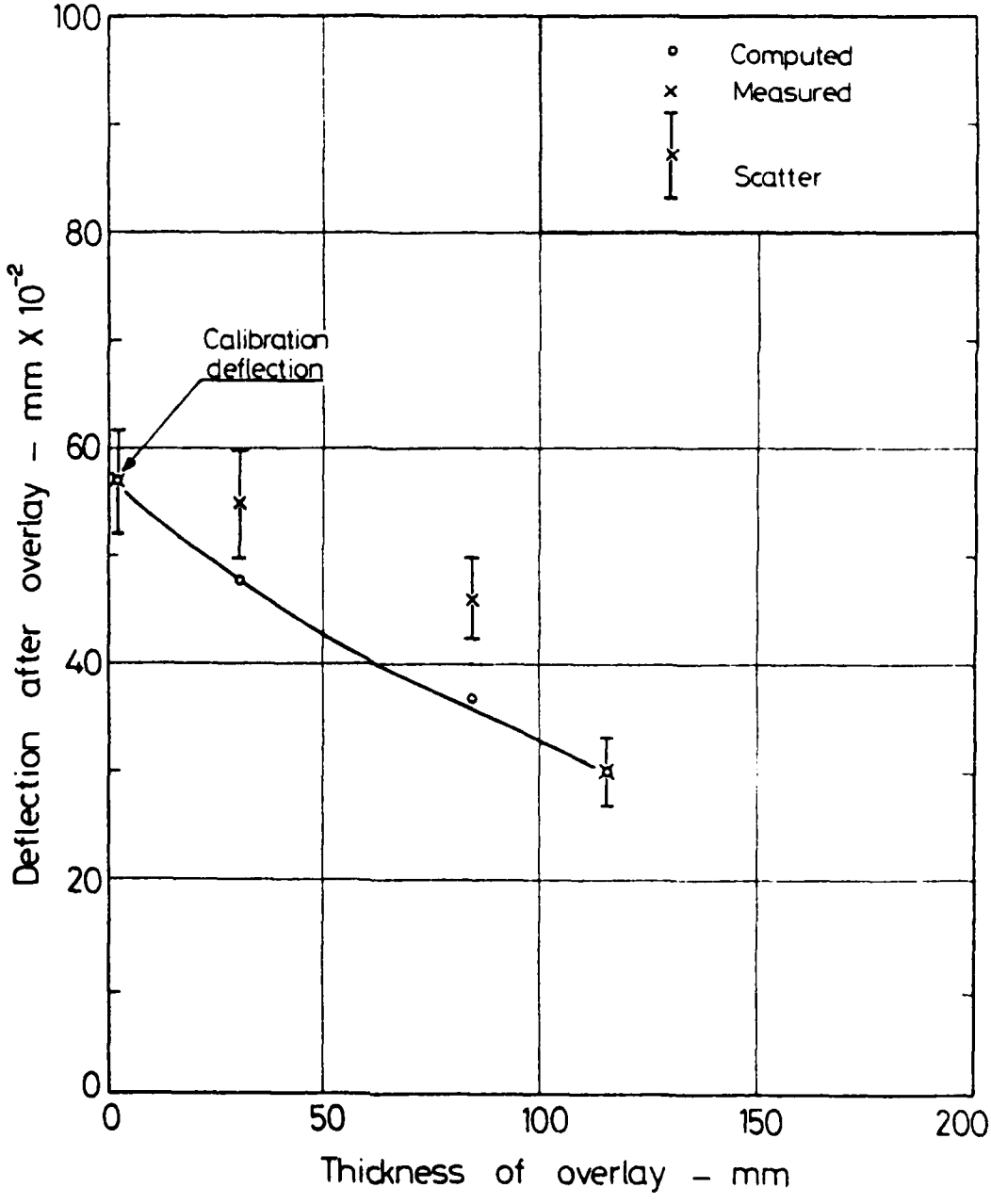

PREDICTION OF TRANSIENT DEFLECTIONS AFTER OVERLAYING AT HILLSBOROUGH TEST SECTION (MODEL A - 20 m TEST LENGTH)

FIG. 30

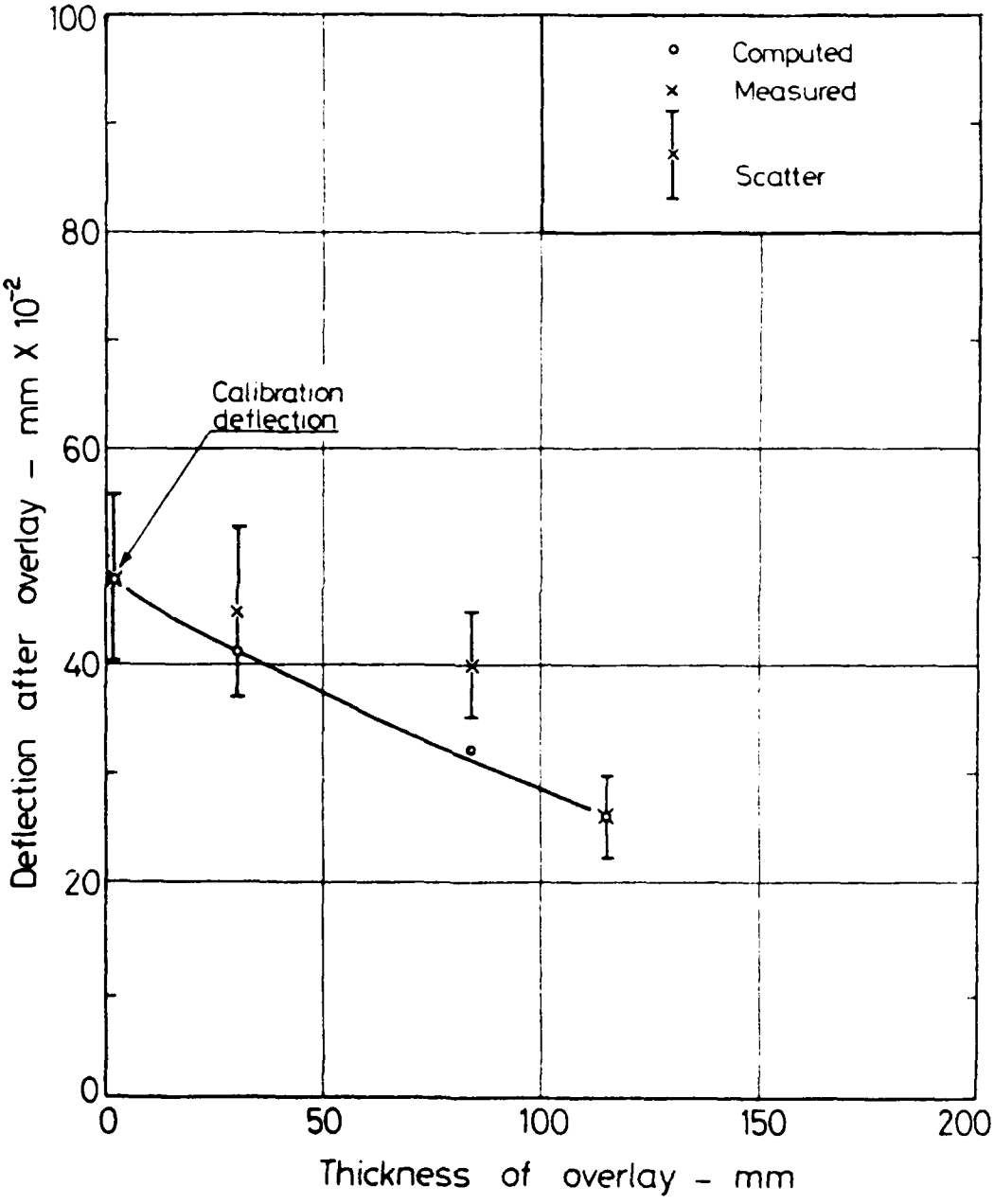

PREDICTION OF TRANSIENT DEFLECTIONS AFTER OVERLAYING AT HILLSBOROUGH TEST SECTION (MODEL B -150 m TEST LENGTH)

FIG. 31

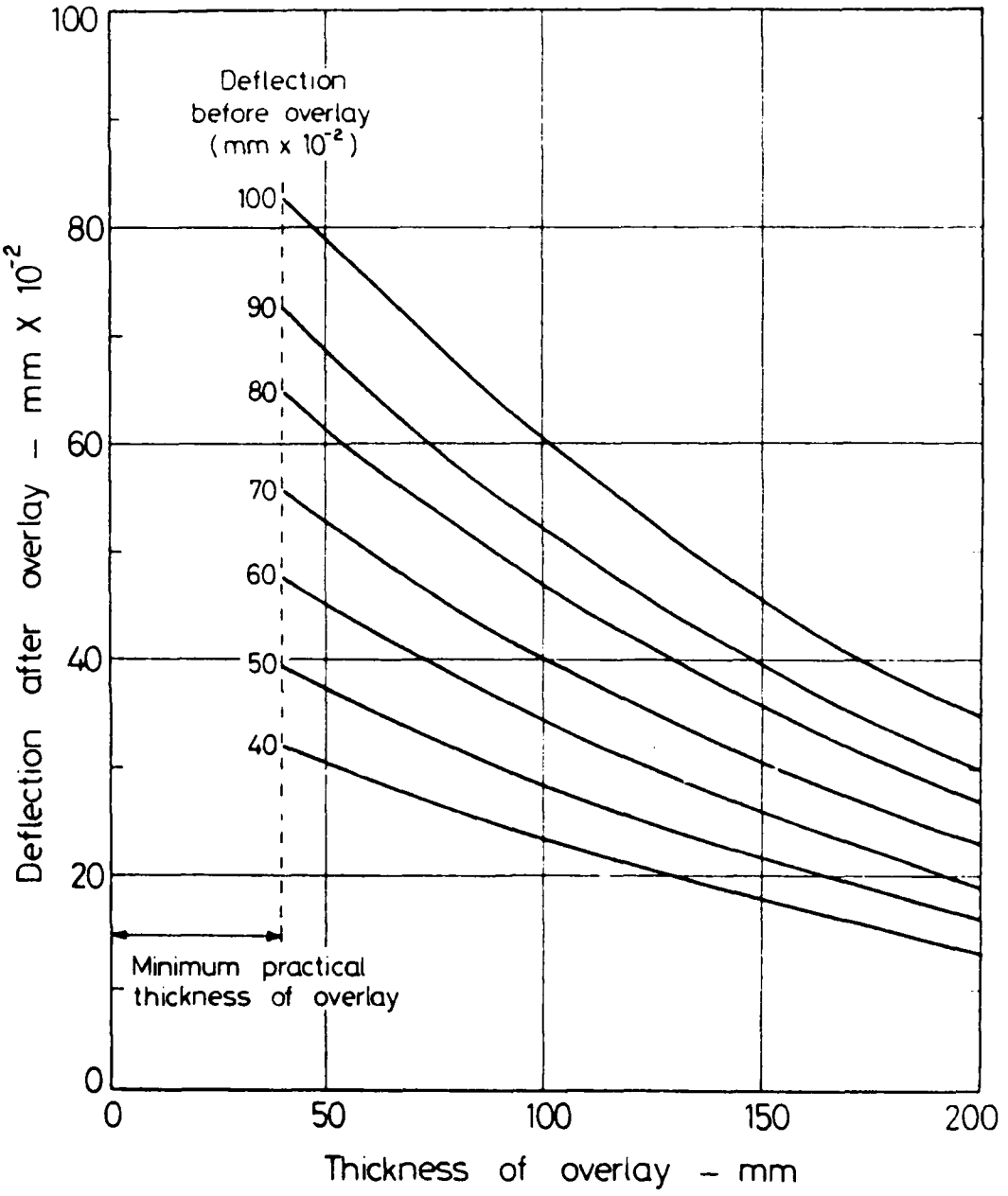

OVERLAY DESIGN CHART DERIVED USING THE COMPUTER PROGRAM DEFPAV (HILLSBOROUGH TEST SECTION)

FIG. 32

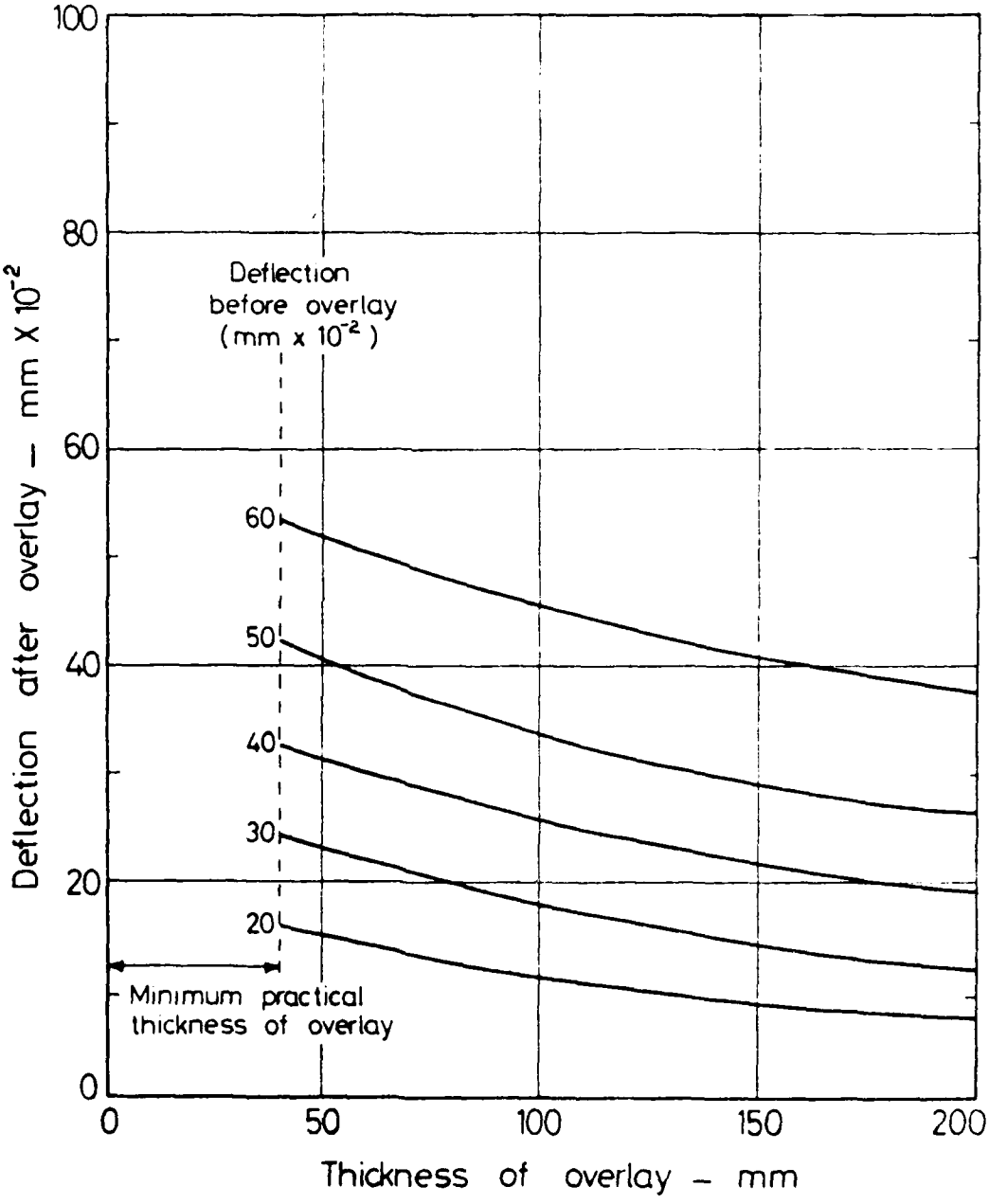

OVERLAY DESIGN CHART DERIVED USING THE COMPUTER PROGRAM DEFPAV (M1 MOTORWAY TEST SECTION)

FIG. 33

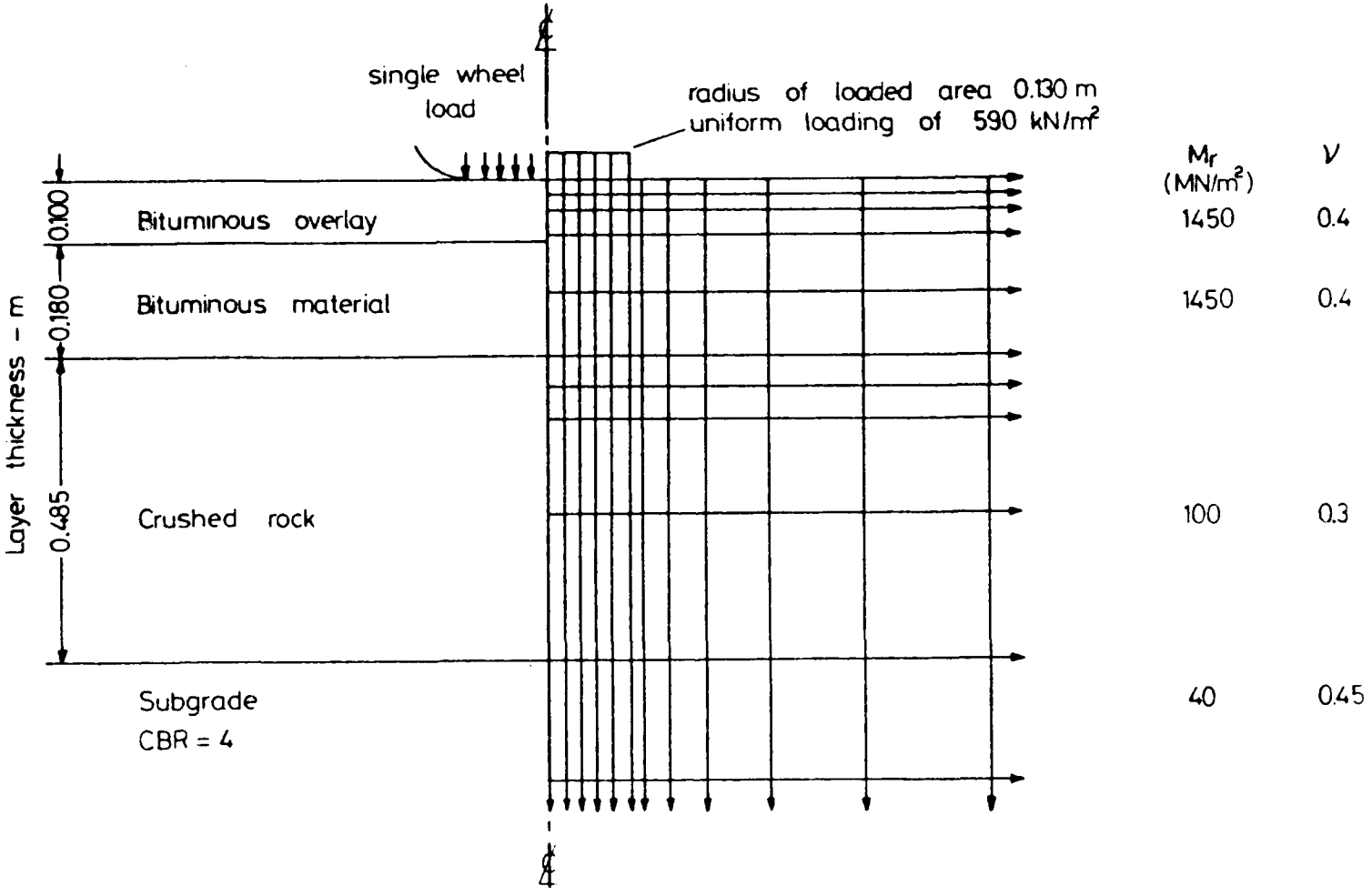

FIG. 34

FINITE ELEMENT REPRESENTATION OF M1 MOTORWAY TEST SECTION WITH OVERLAY THICKNESS OF 100 mm – SIMULATING REAR WHEEL LOAD OF BENKELMAN BEAM VEHICLE

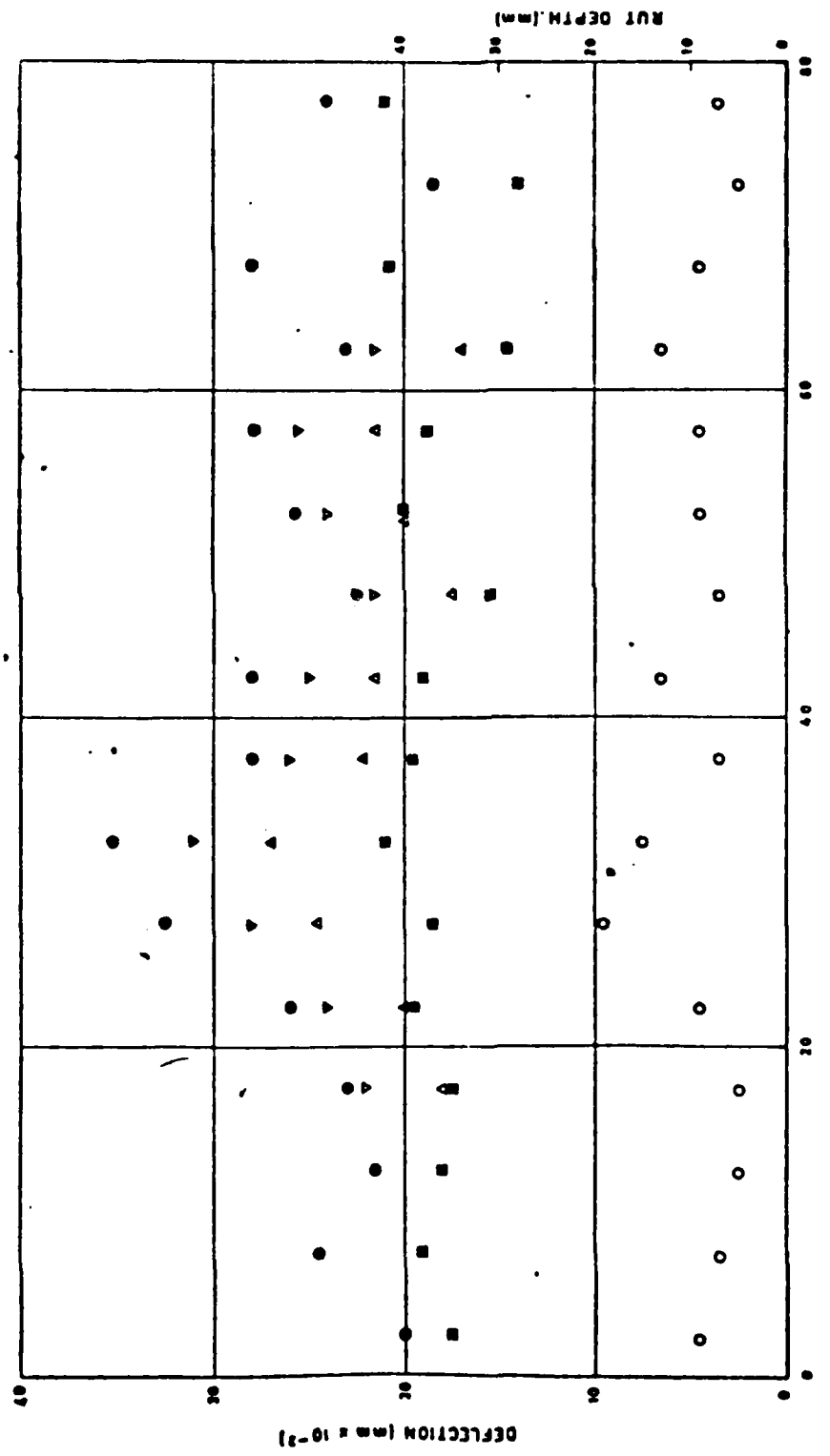

DEFLECTION SURVEY OF NEARSIDE WHEEL TRACK
BEFORE AND AFTER OVERLAY (NOMINAL THICKNESS 40mm)
(After McCullough 34))

FIG. 35

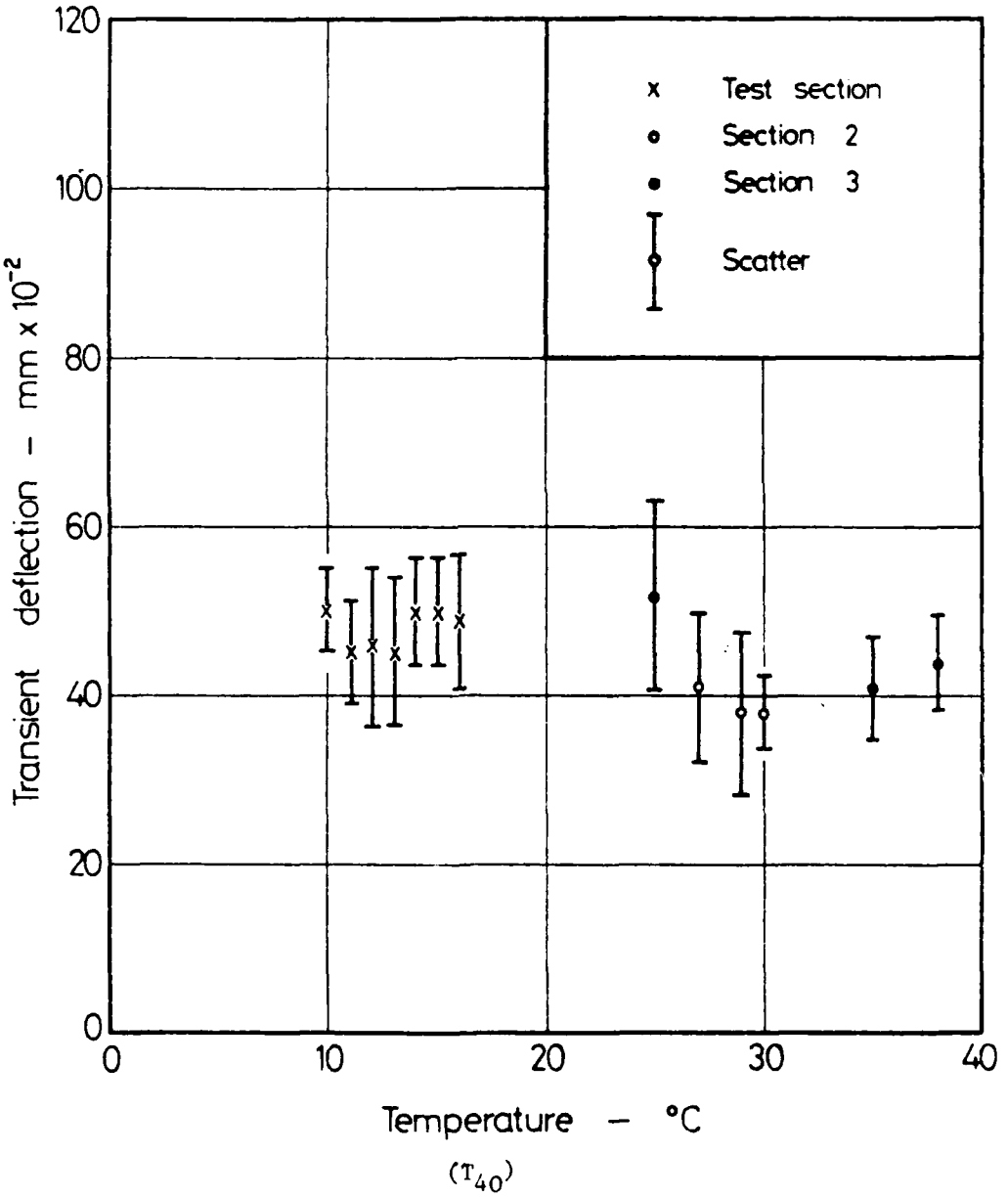

INFLUENCE OF TEMPERATURE ON MEASURED DEFLECTIONS AT HILLSBOROUGH BY-PASS

FIG. 36

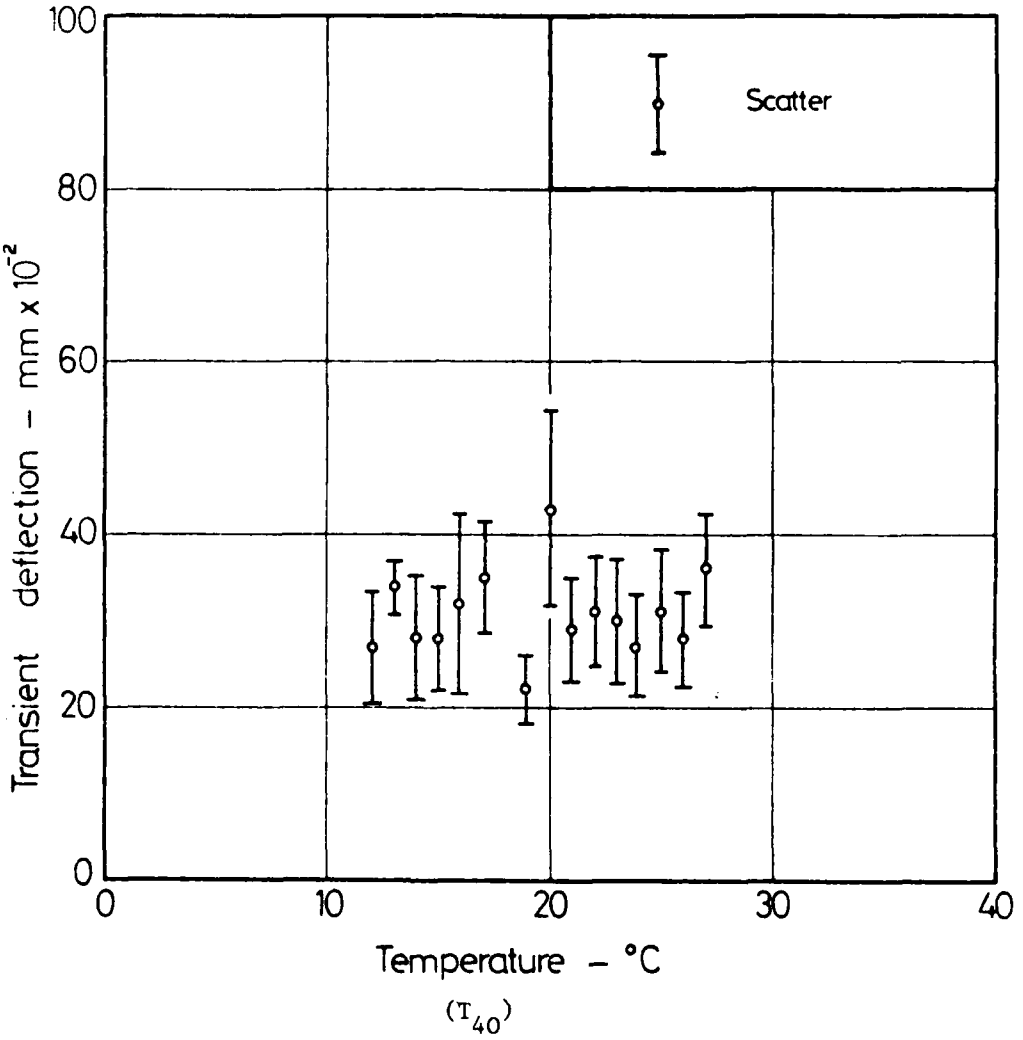

INFLUENCE OF TEMPERATURE ON MEASURED DEFLECTIONS AT M1 MOTORWAY (MOIRA - LURGAN)

FIG. 37

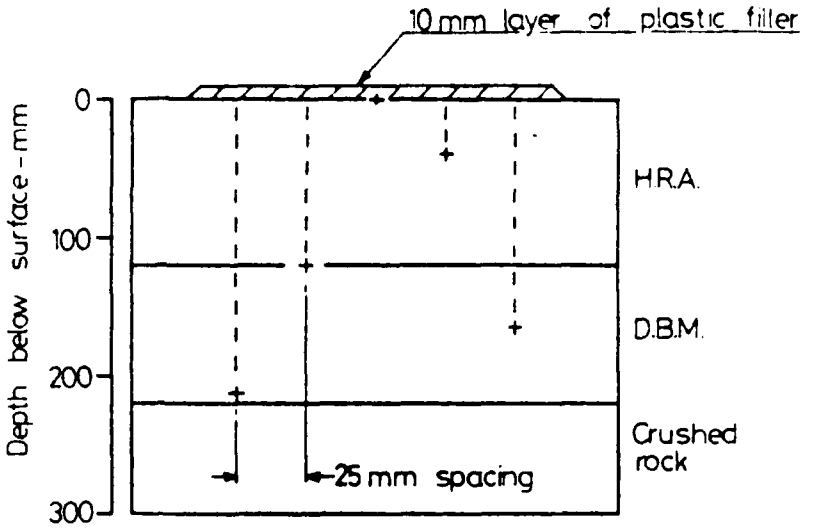

SECTION X-X
(not to scale)

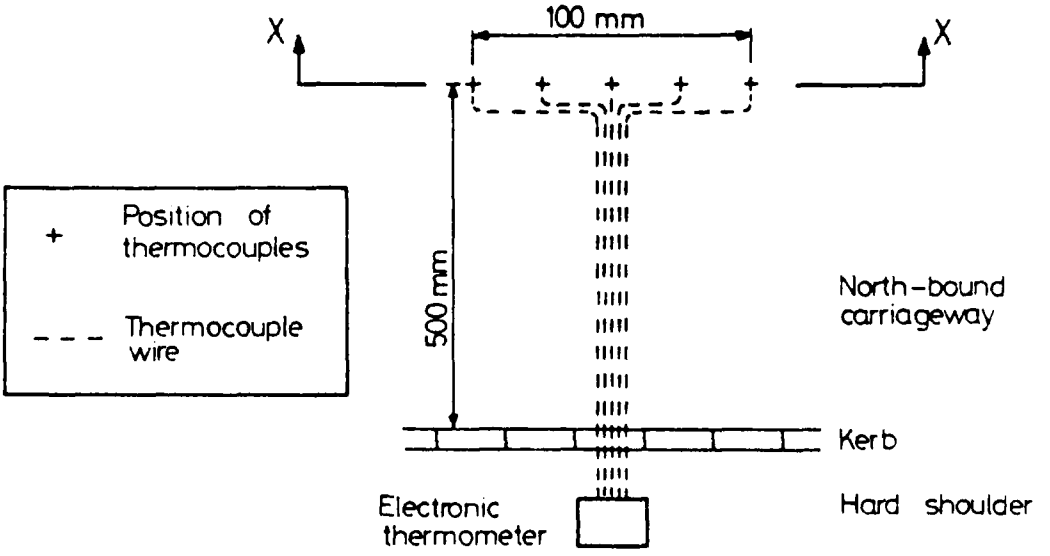

PLAN
(not to scale)

LAY-OUT OF THERMOCOUPLES AT HILLSBOROUGH TEST SECTION

FIG. 38

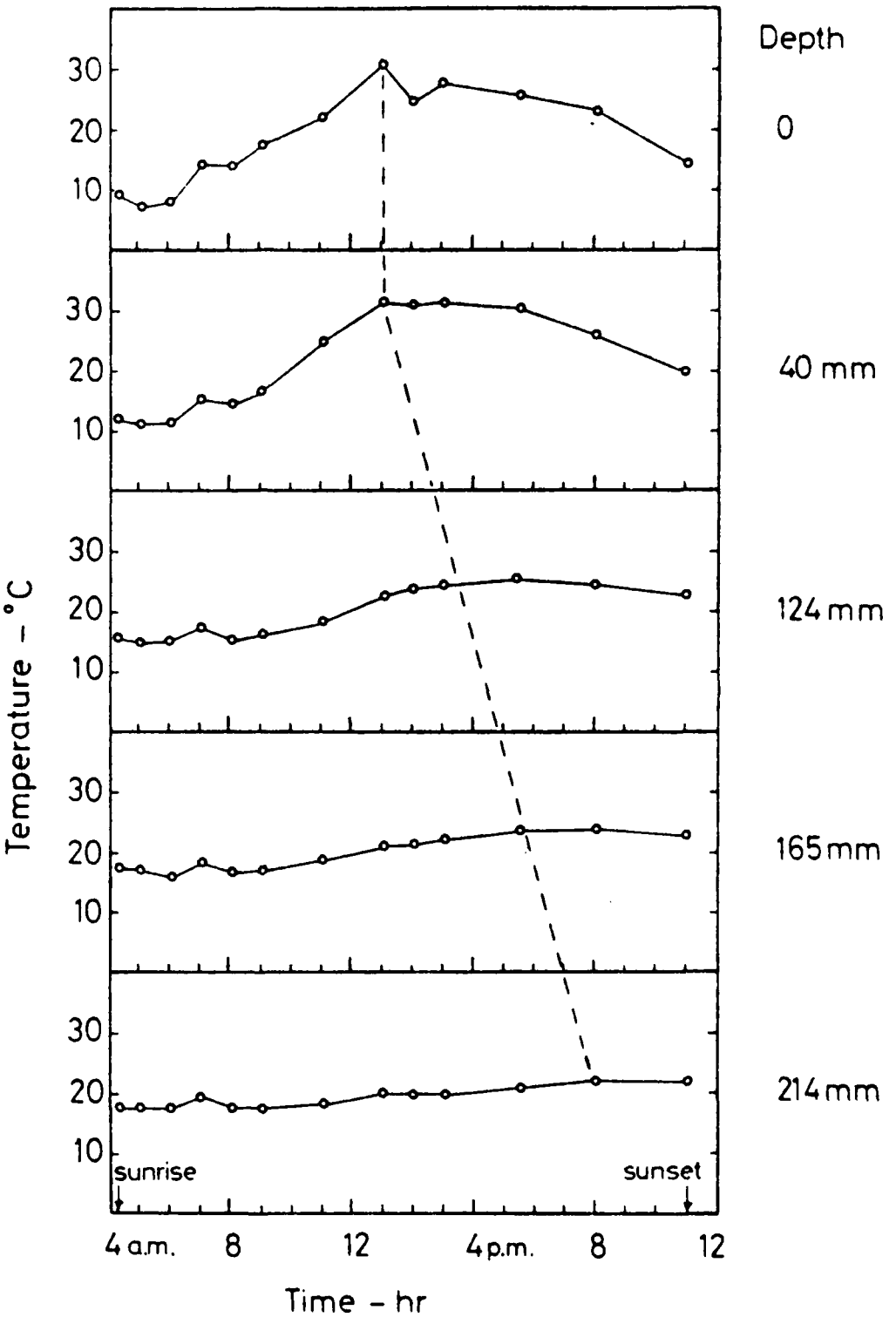

PAVEMENT TEMPERATURES RECORDED AT HILLSBOROUGH TEST SECTION ON JUNE 21, 1977

FIG. 39

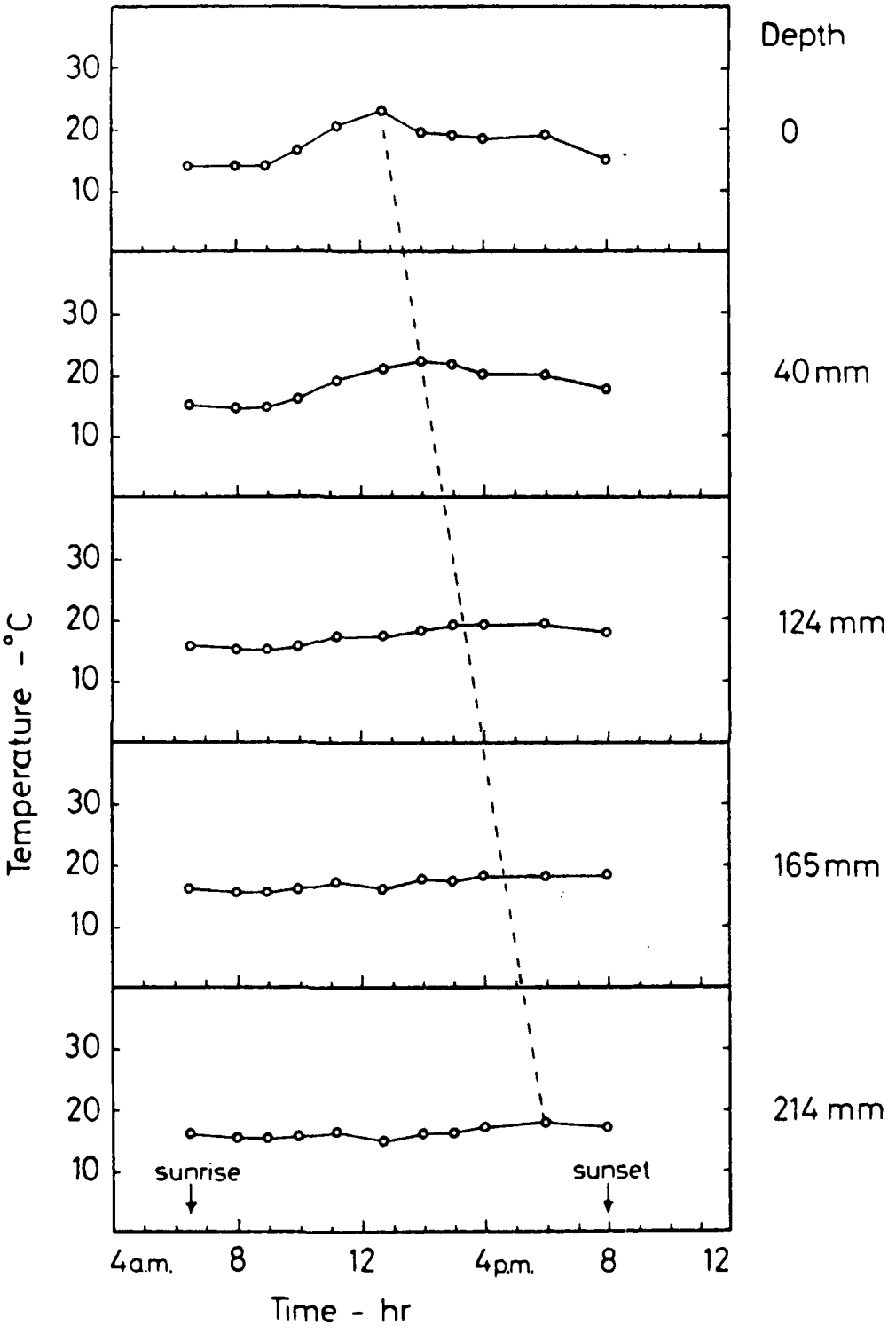

PAVEMENT TEMPERATURES RECORDED AT HILLSBOROUGH TEST SECTION ON SEPT. 15, 1977.

FIG. 40

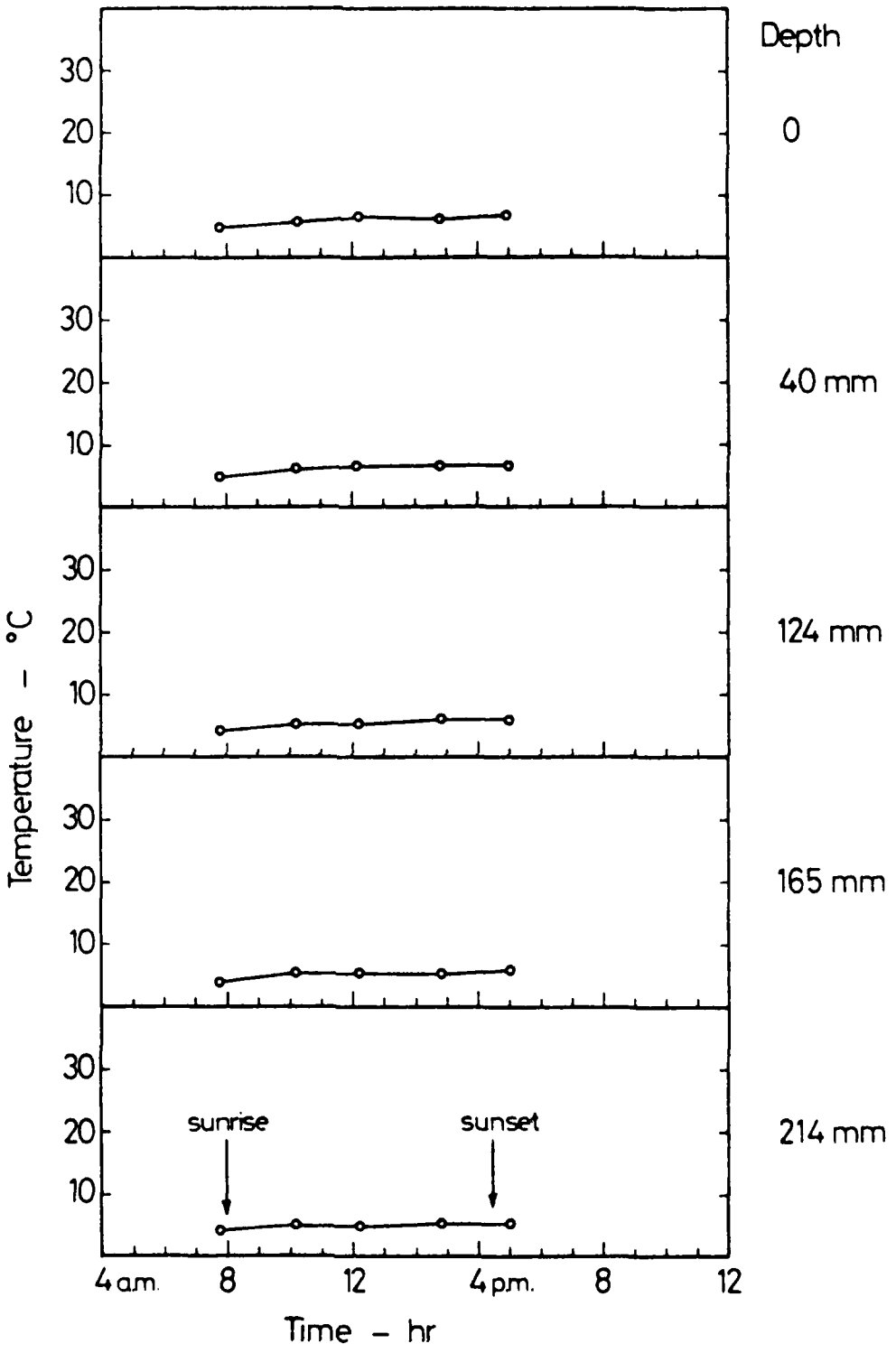

PAVEMENT TEMPERATURES RECORDED AT HILLSBOROUGH TEST SECTION ON DEC. 5, 1977.

FIG. 41

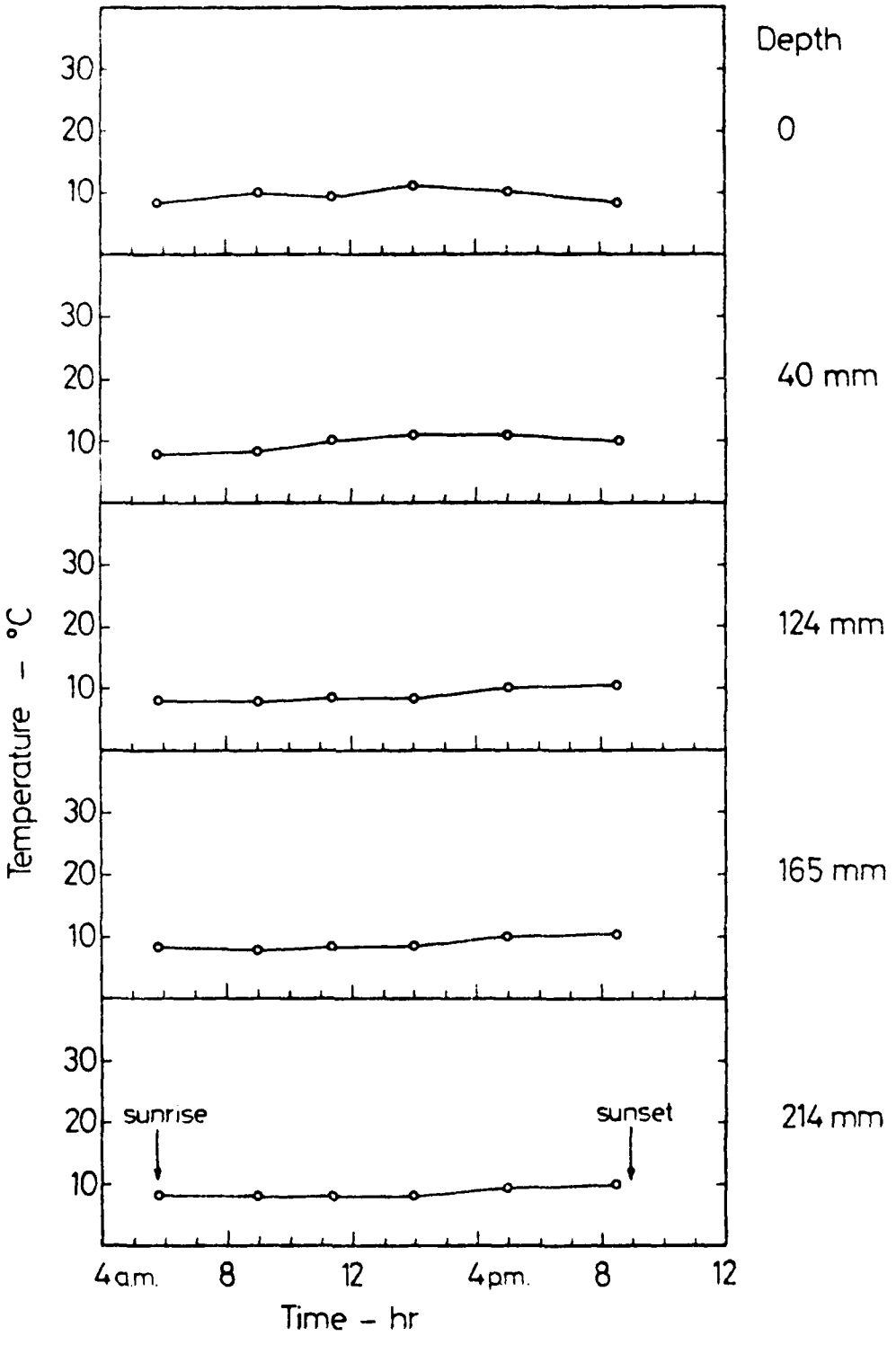

PAVEMENT TEMPERATURES RECORDED AT HILLSBOROUGH TEST SECTION ON APRIL 19, 1978.

FIG. 42

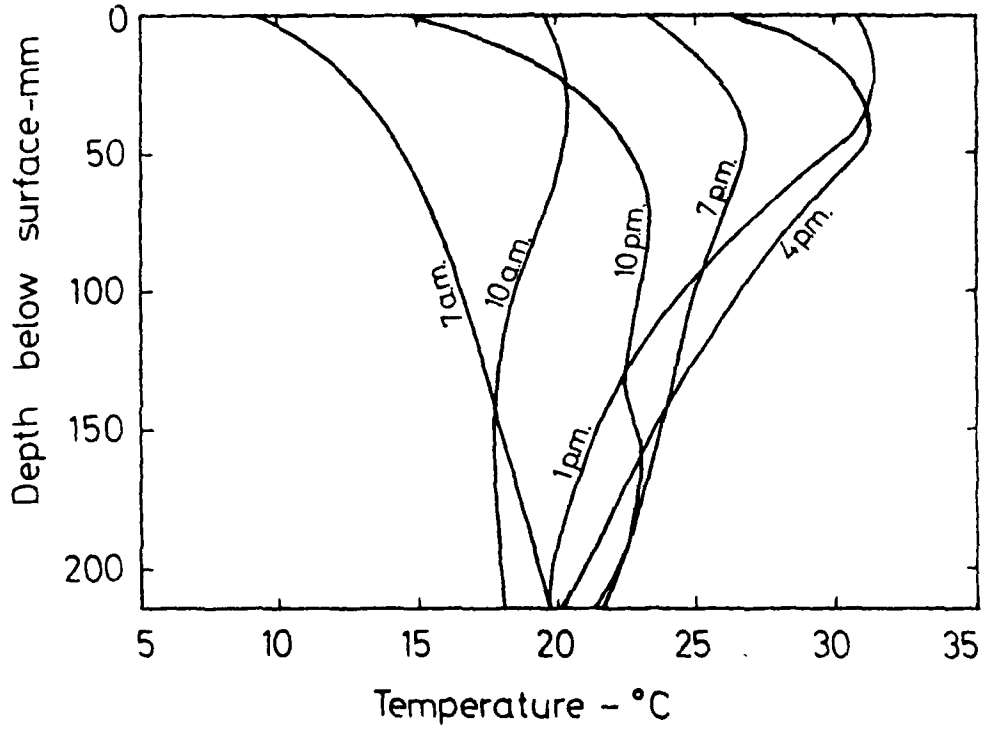

TEMPERATURE GRADIENTS IN PAVEMENT ON JUNE 21, 1977

FIG. 43

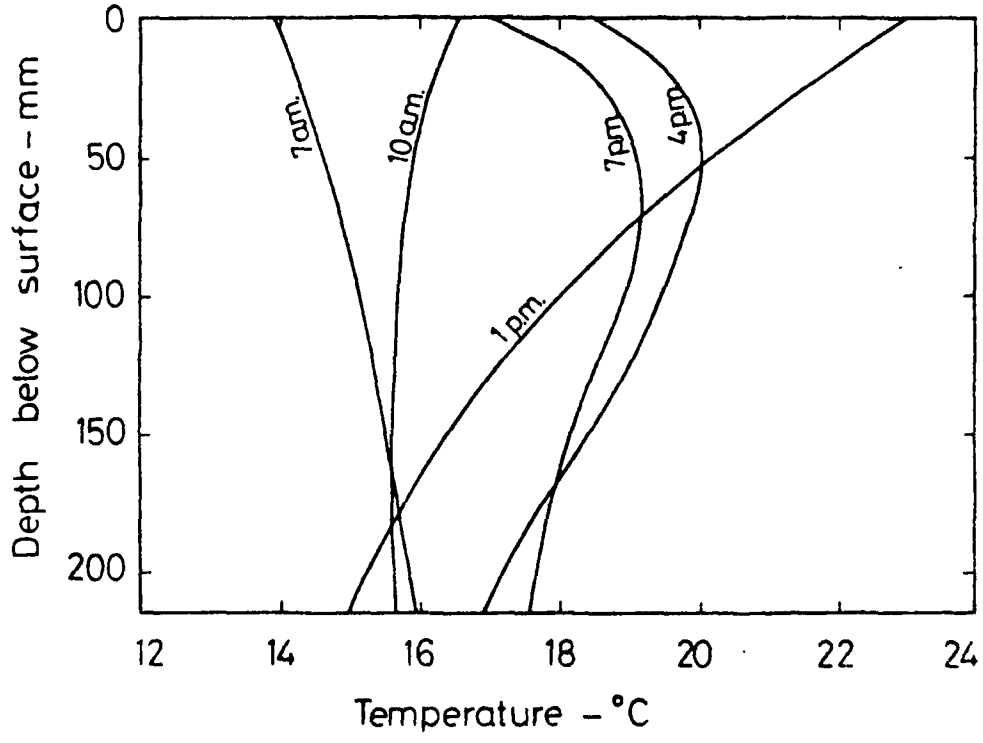

TEMPERATURE GRADIENTS IN PAVEMENT ON SEPTEMBER 15, 1977.

FIG. 44

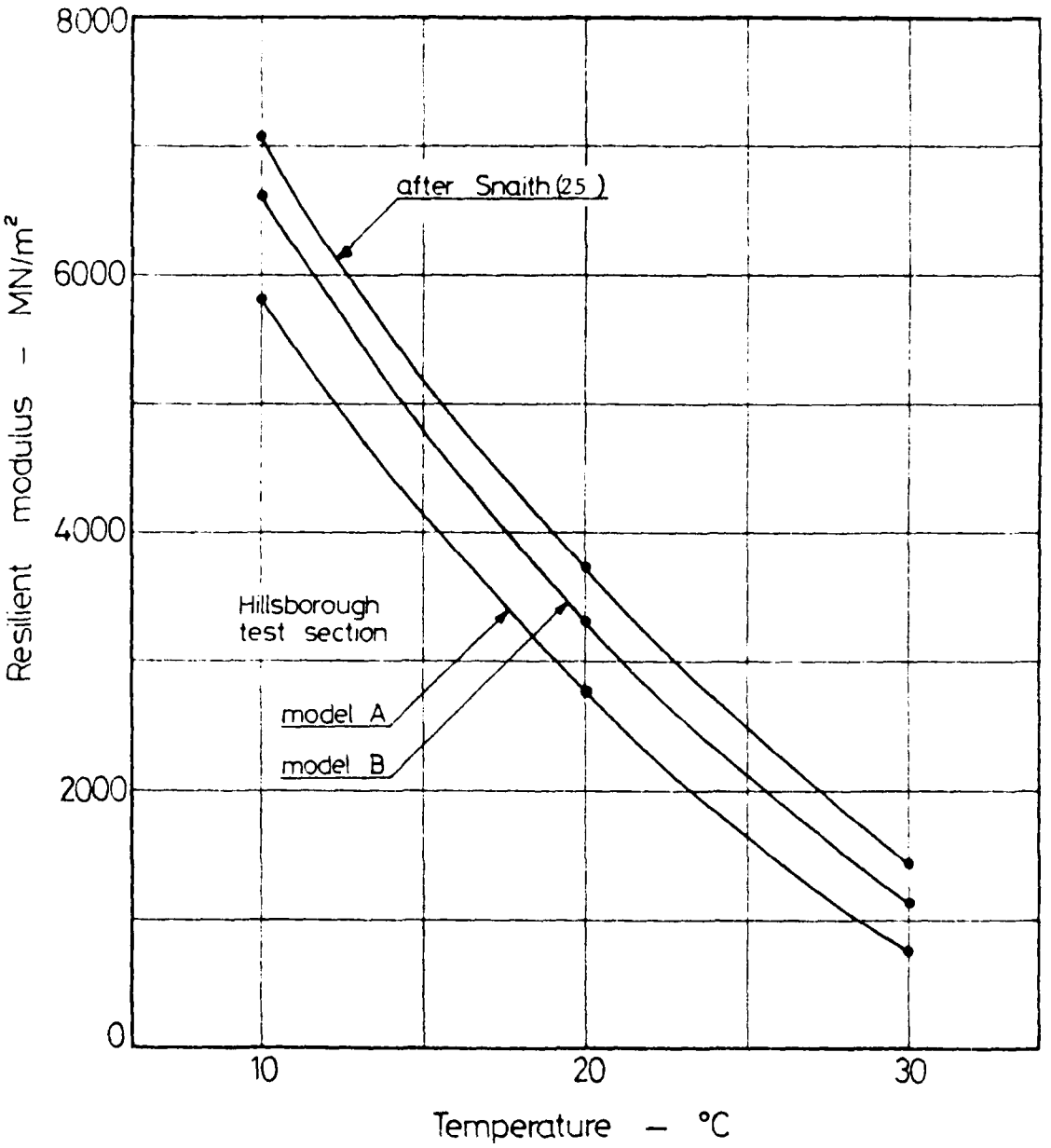

VARIATION OF RESILIENT MODULUS OF BITUMINOUS MATERIAL WITH TEMPERATURE

FIG. 45

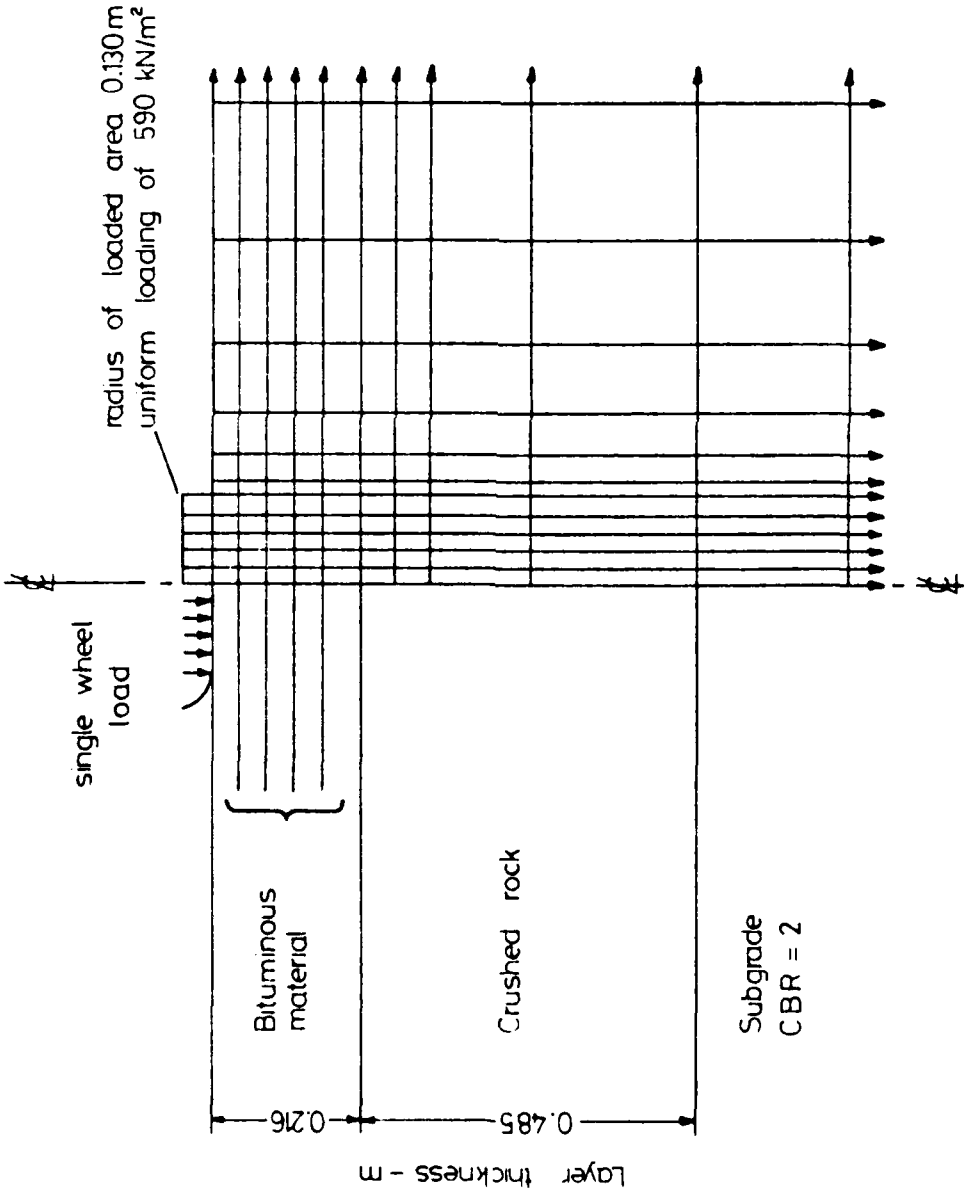

FINITE ELEMENT REPRESENTATION OF HILLSBOROUGH TEST SECTION AFTER OVERLAYING
(BITUMINOUS MATERIAL MODELLED AS FIVE SUB-LAYERS)

FIG. 46

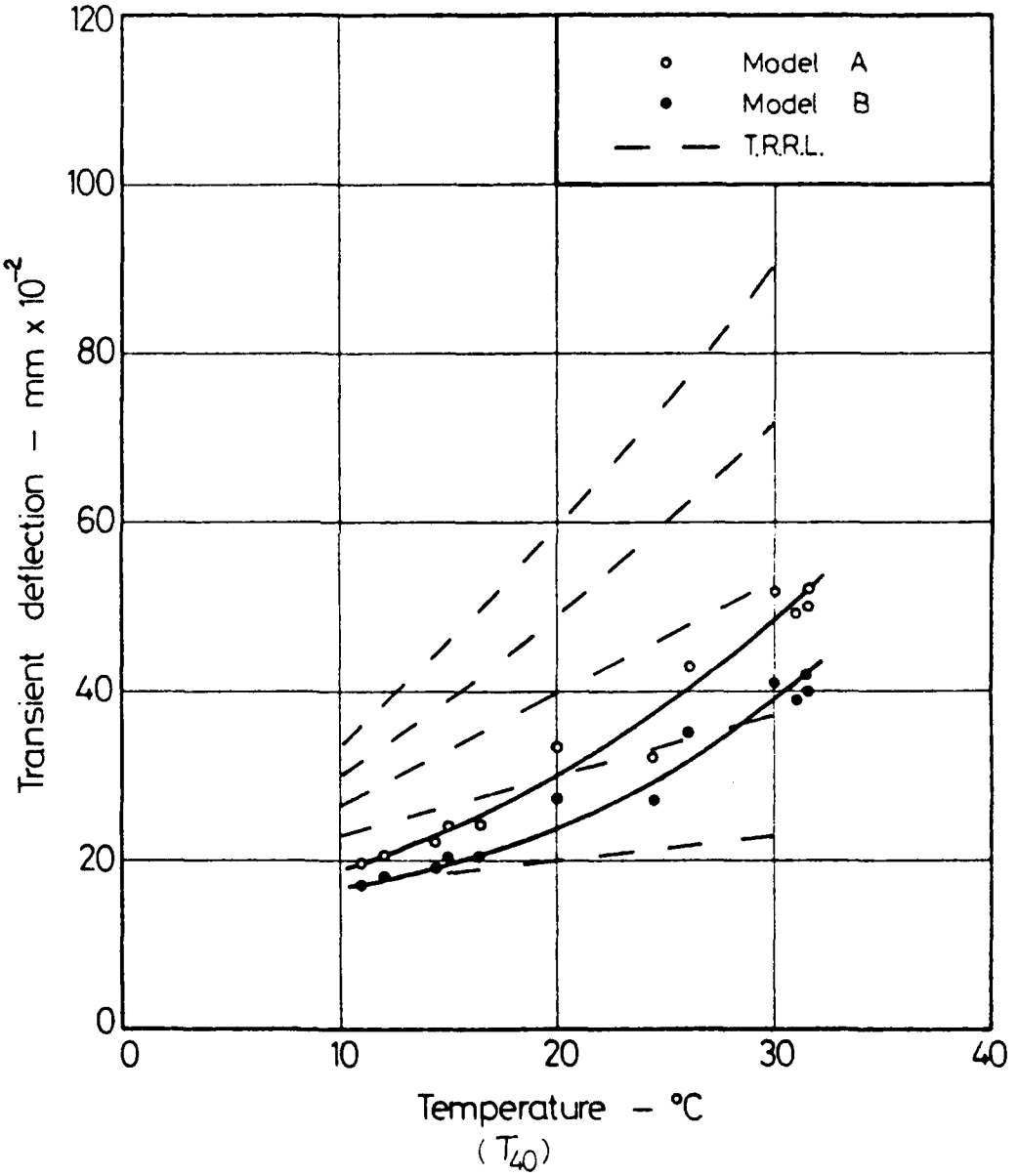

VARIATION OF TRANSIENT DEFLECTION WITH TEMPERATURE (BITUMINOUS MATERIAL MODELLED AS FIVE SUB-LAYERS)

FIG. 47

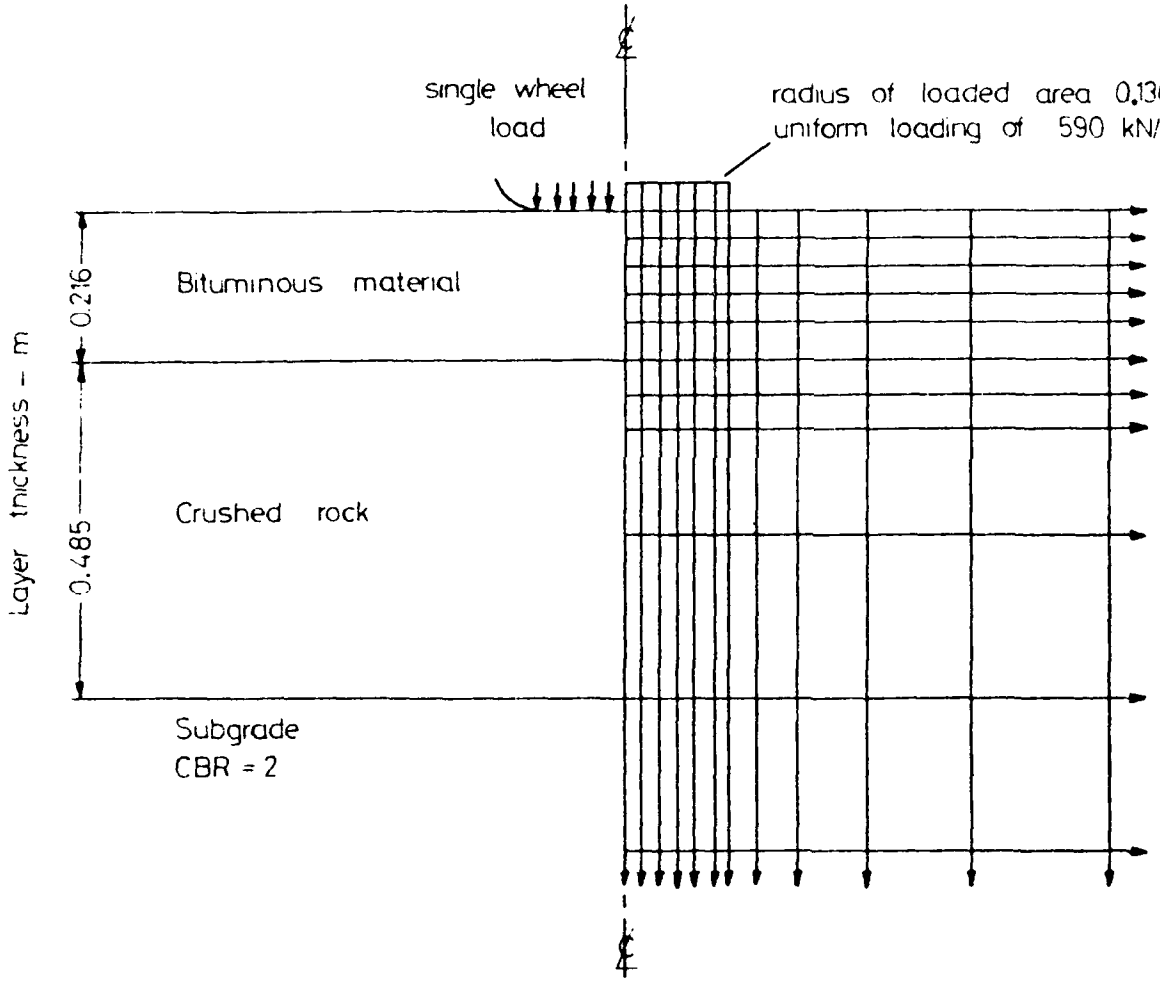

FIG. 48

FINITE ELEMENT REPRESENTATION OF HILLSBOROUGH TEST SECTION AFTER OVERLAYING (BITUMINOUS MATERIAL MODELLED AS ONE LAYER)

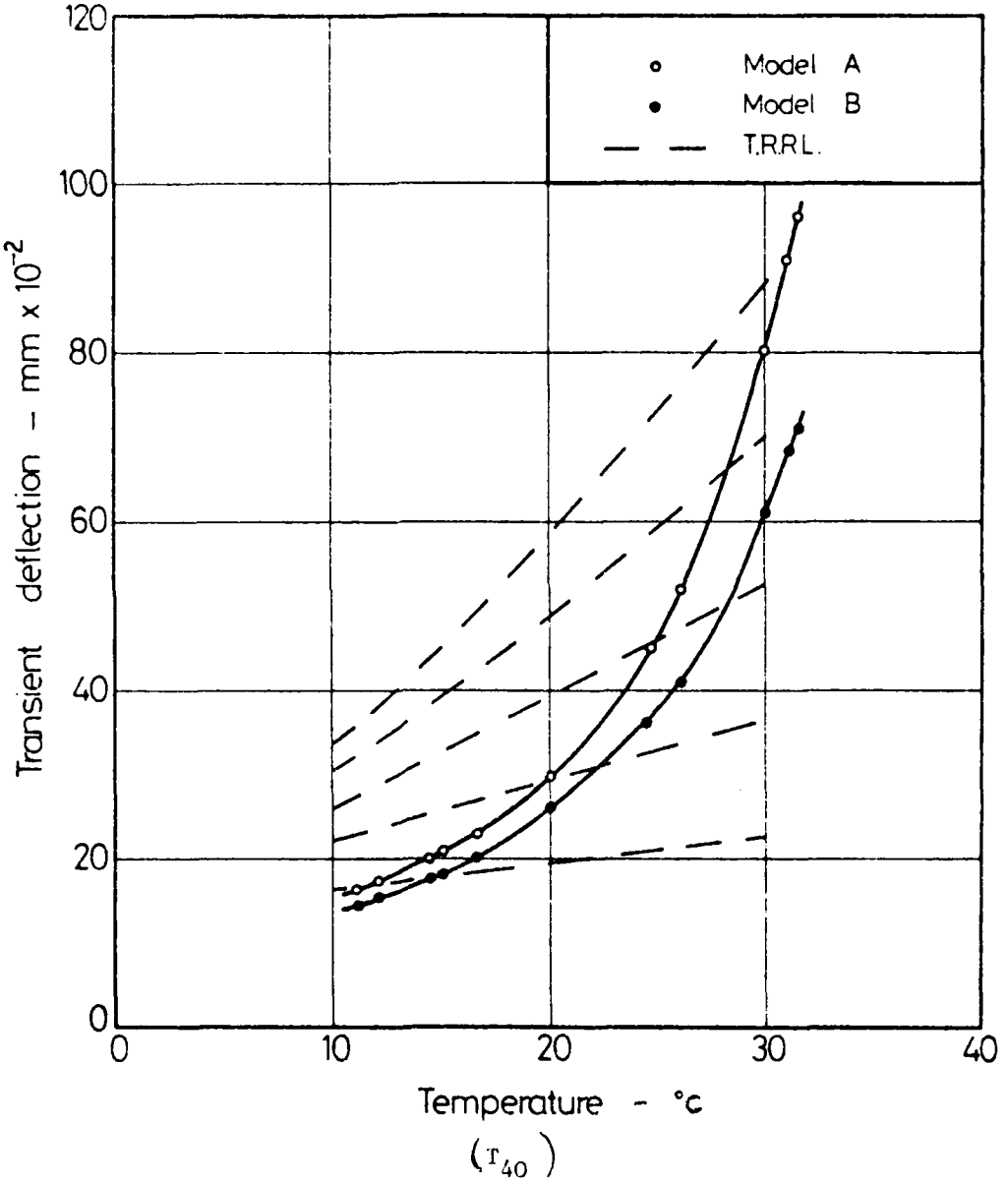

VARIATION OF TRANSIENT DEFLECTION WITH TEMPERATURE (BITUMINOUS MATERIAL MODELLED AS ONE LAYER)

FIG. 49

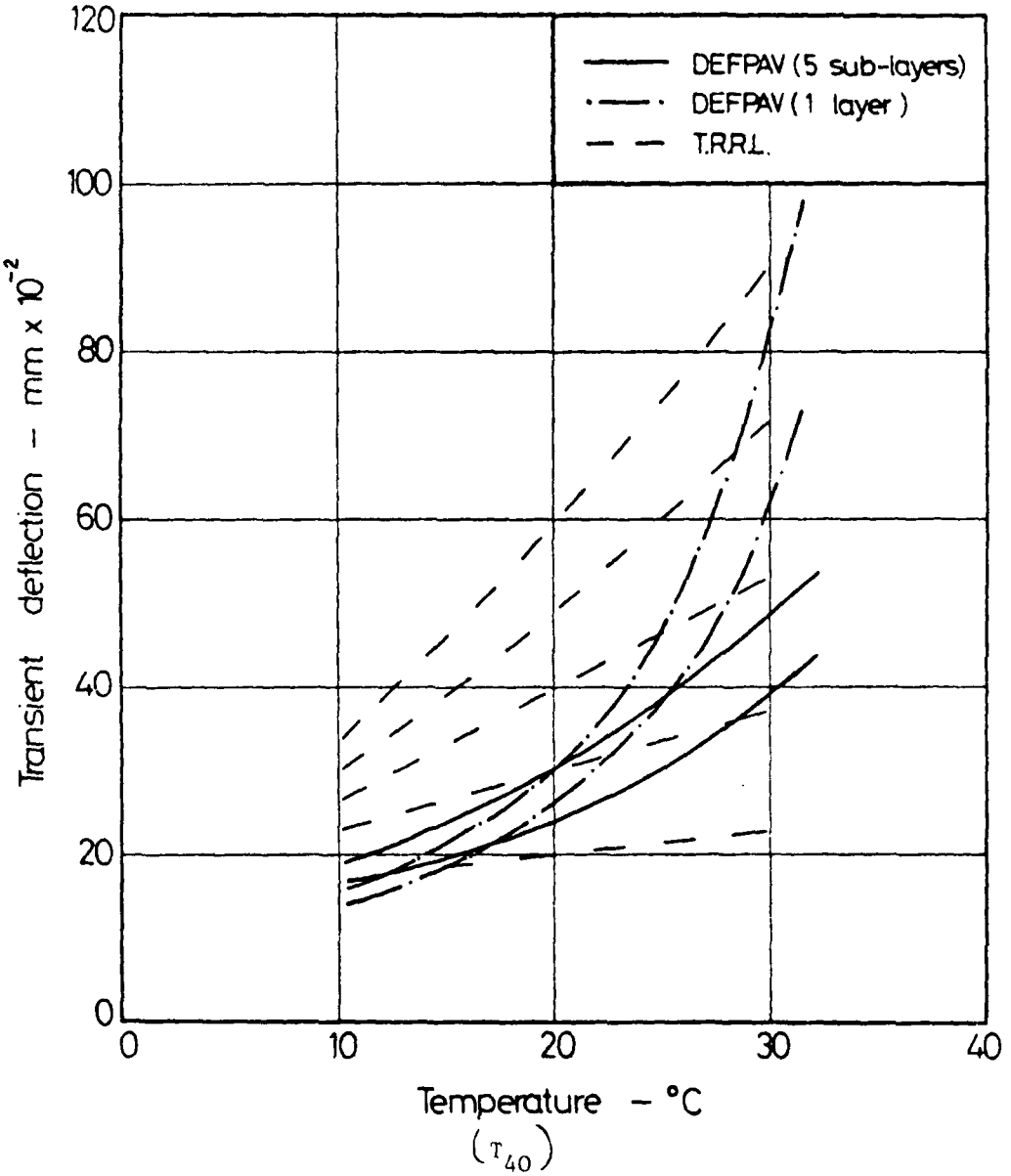

COMPARISON OF DEFLECTION/TEMPERATURE RELATIONSHIPS

FIG. 50

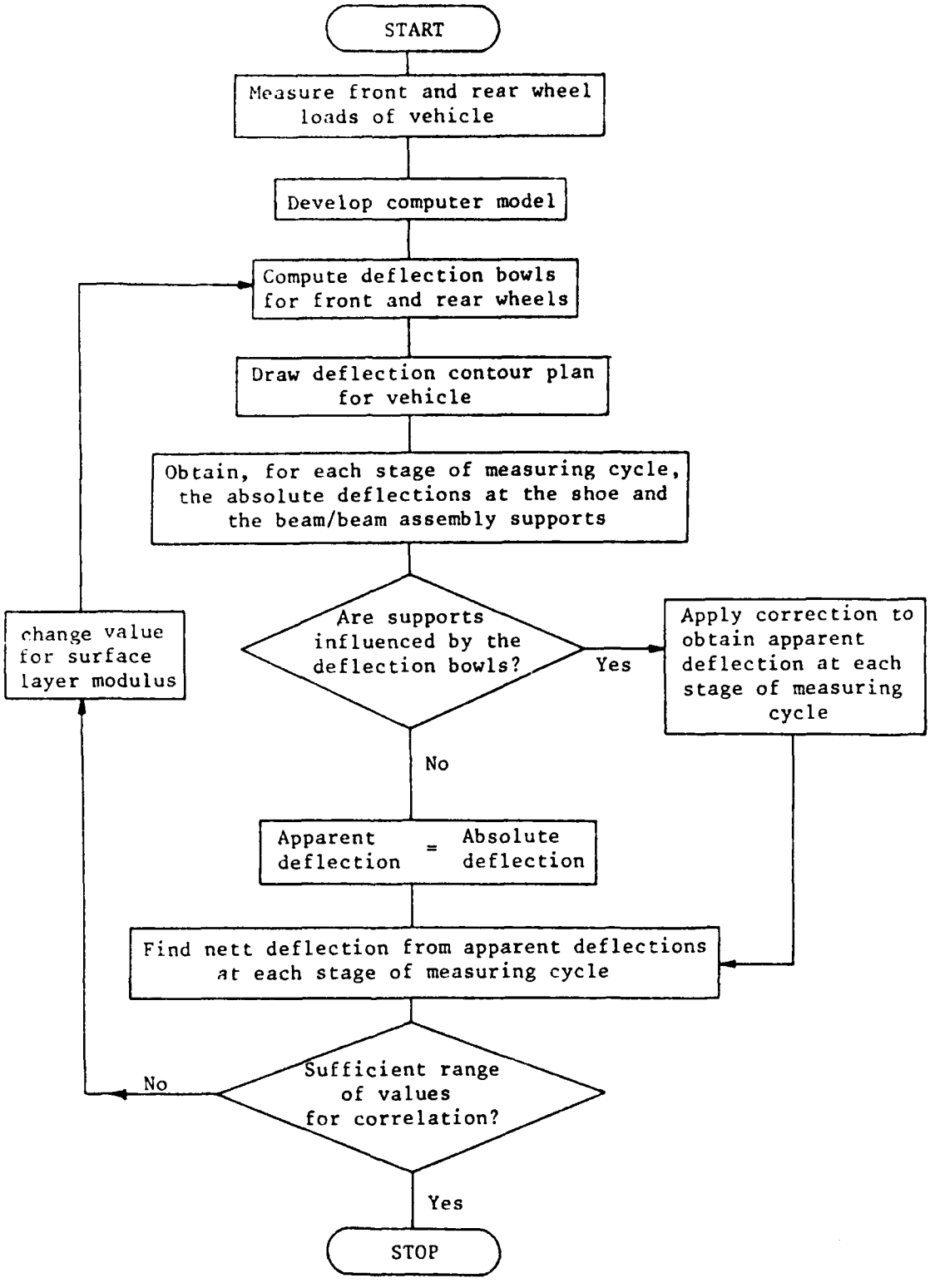

PROCEDURE FOR THE PREDICTION OF MEASURED DEFLECTIONS

FIG. 51

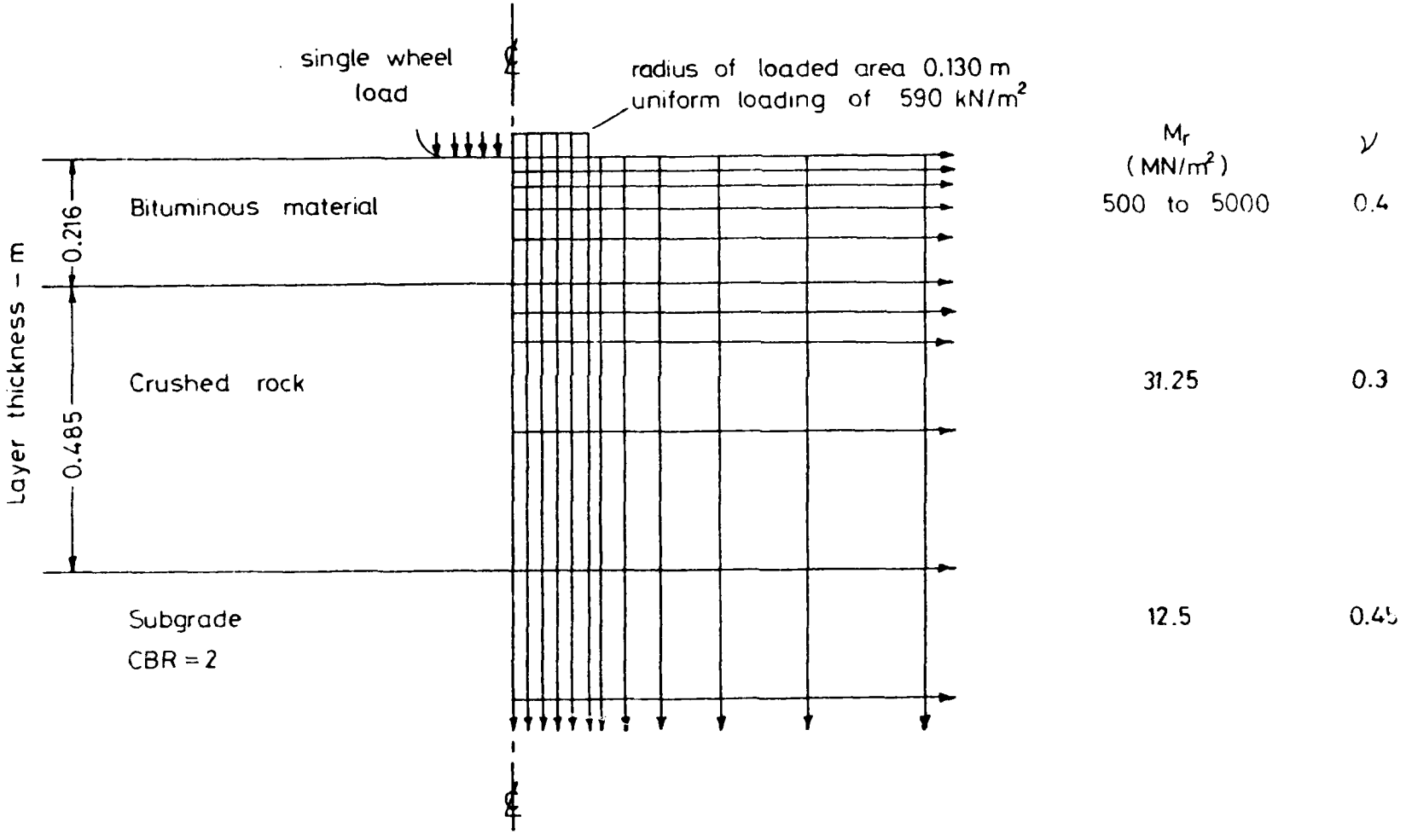

FIG. 52

FINITE ELEMENT REPRESENTATION OF HILLSBOROUGH TEST SECTION AFTER OVERLAYING -SIMULATING REAR WHEEL LOAD OF BENKELMAN BEAM VEHICLE.

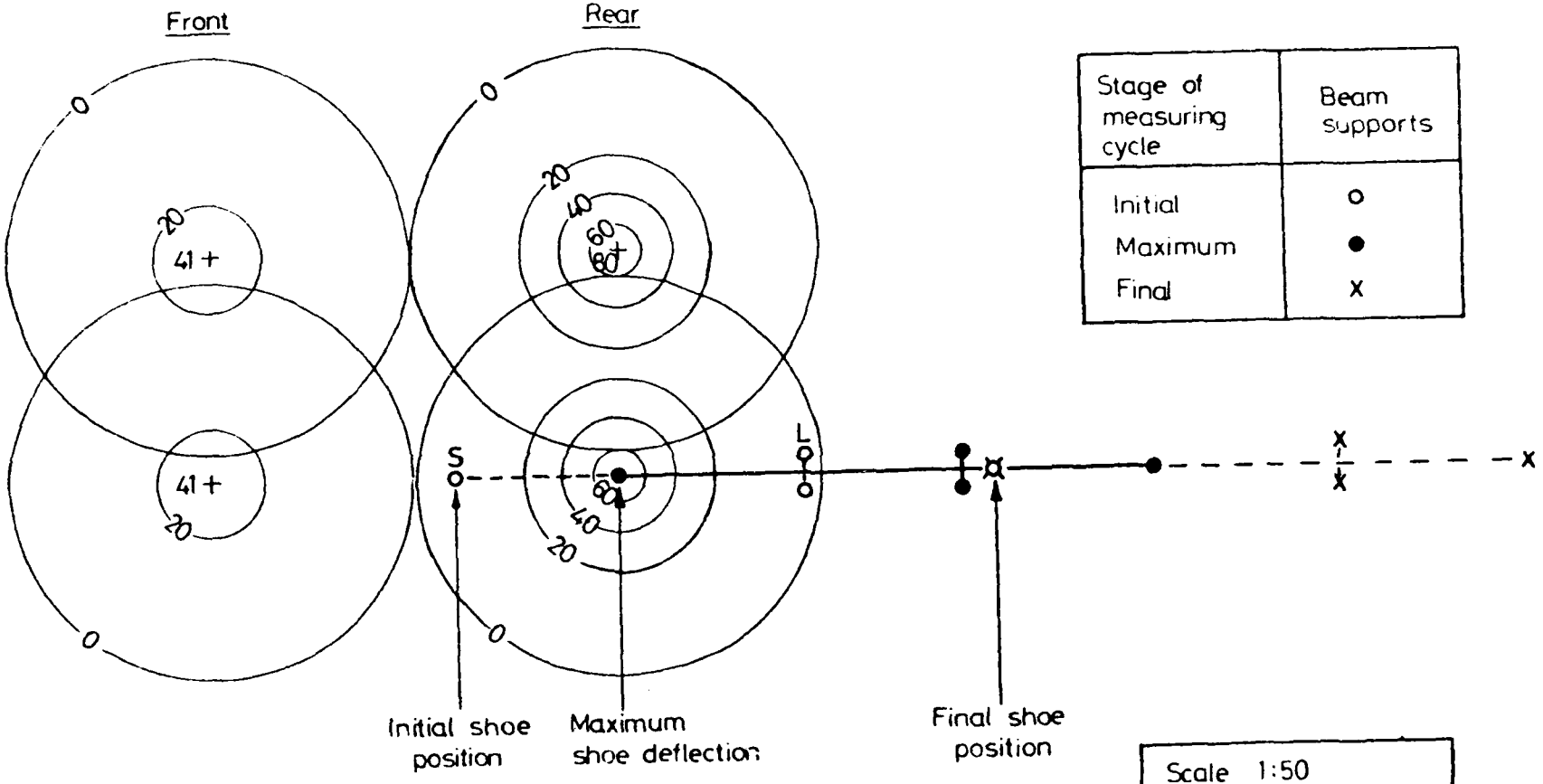

FIG. 53

PREDICTION OF MEASURED DEFLECTIONS FROM DEFLECTION CONTOUR PLAN FOR BENKELMAN BEAM VEHICLE (M_{r_1} =750 MN/m^2).

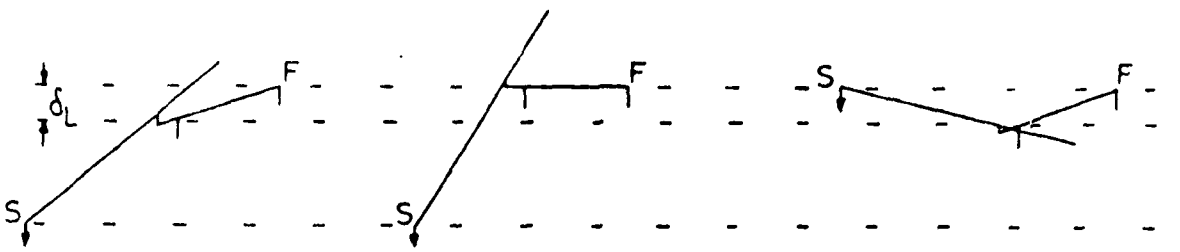

Apparent shoe deflection = Absolute shoe deflection - δ_{S_L}

where δ_{S_L} = equivalent deflection at shoe S due to a vertical displacement δ_L at front legs.

Evaluation of δ_{S_L}

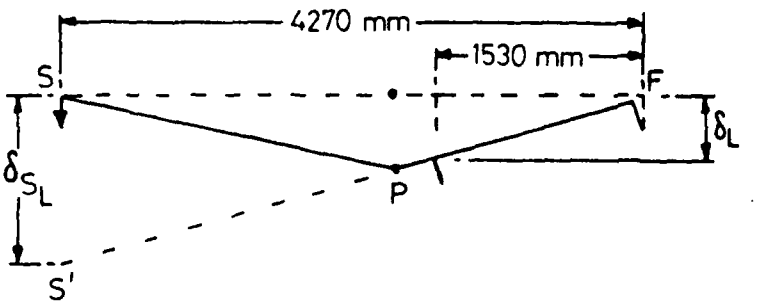

F : Rear foot
P : Pivot
S : Shoe

Assume front legs are given a vertical displacement δ_L.

This is equivalent to rotation of PS' about P to PS.

Assuming negligible movement at F,

$$\delta_{S_L} = \frac{4270}{1530} \delta_L = 2.8 \delta_L$$

Thus

Apparent shoe deflection = Absolute shoe deflection - 2.8 δ_L.

EFFECT OF FRONT LEG DISPLACEMENT ON MEASURED BENKELMAN BEAM DEFLECTION

FIG. 54

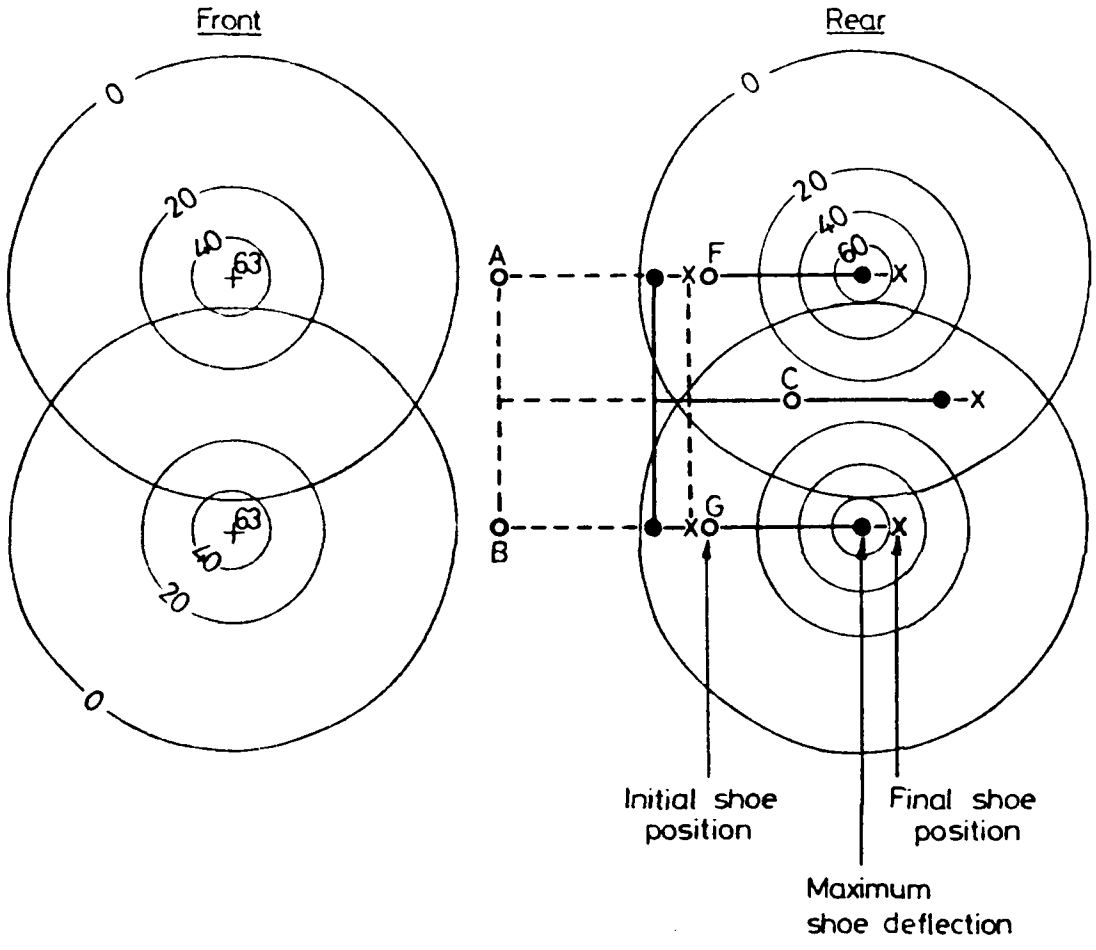

Stage of measuring cycle	Beam assembly supports
Initial	o
Maximum	●
Final	x

Scale 1:50

Contours at intervals of 20×10^{-2} mm

FIG. 55

PREDICTION OF MEASURED DEFLECTIONS FROM DEFLECTION CONTOUR PLAN FOR DEFLECTOGRAPH ($M_{r_1} = 750$ MN/m^2).

Evaluation of δ_{G_B}

δ_{G_B} = equivalent deflection at shoe G due to a vertical displacement δ_B at support B

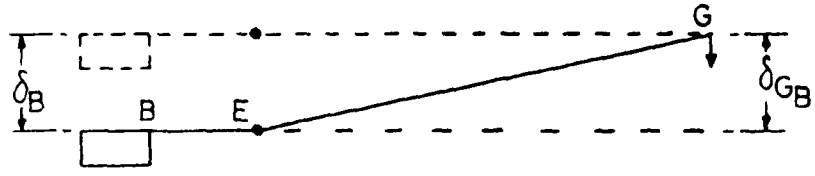

B : Recording head support
E : Pivot
G : Shoe

Assume support B (recording head support) is given a vertical displacement δ_B, then, assuming no rotation at B, BE will deflect as shown.

Vertical deflection of BE is equivalent to an upward deflection δ_B at shoe G. Thus

$$\delta_{G_B} = \delta_B$$

EFFECT OF VERTICAL DISPLACEMENT AT RECORDING HEAD SUPPORT ON MEASURED DEFLECTOGRAPH DEFLECTION

FIG. 56

Evaluation of δ_{G_C}

δ_{G_C} = equivalent deflection at shoe G due to a vertical displacement δ_C at support C.

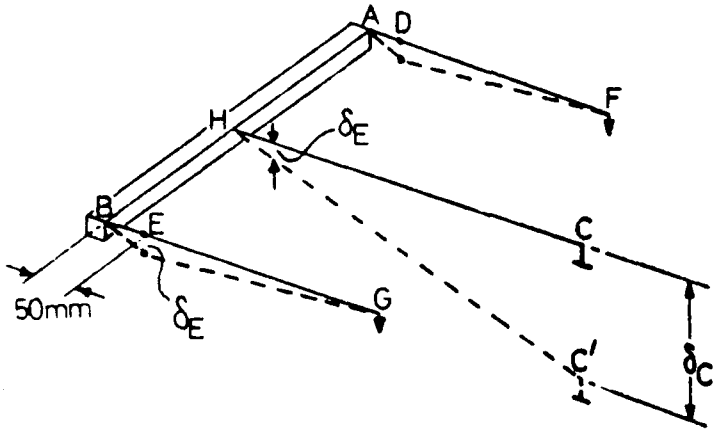

Assume support C (T-frame support) is given a vertical displacement δ_C, then support B will rotate about its rear corner.

Vertical displacement δ_E at pivot E equals that at a point 50 mm along HC.

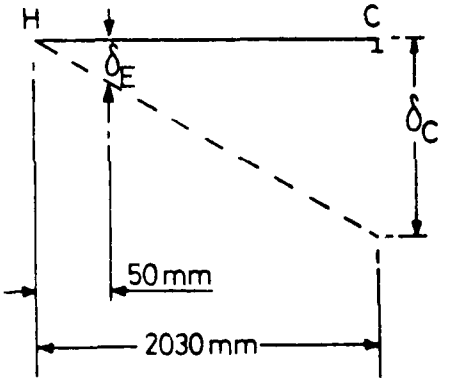

Consider length HC of T-frame. Assuming negligible movement at H,

$$\delta_E = \frac{50}{2030} \delta_C \qquad (1)$$

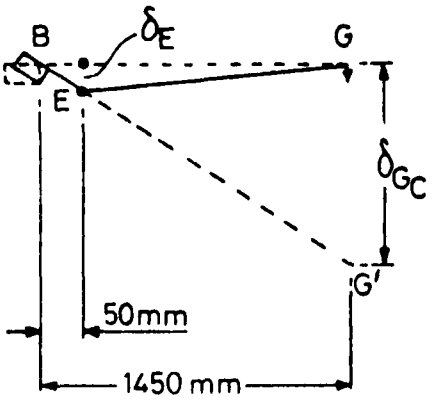

Consider beam assembly BEG. Vertical displacement δ_E at pivot E is equivalent to rotation of EG' about E to EG.

Assuming negligible movement at B,

$$\delta_{G_C} = \frac{1450}{50} \delta_E \qquad (2)$$

Substituting (1) in (2) gives

$$\delta_{G_C} = 0.7\, \delta_C$$

NOT TO SCALE

EFFECT OF VERTICAL DISPLACEMENT AT T-FRAME SUPPORT ON MEASURED DEFLECTOGRAPH DEFLECTION

FIG. 57

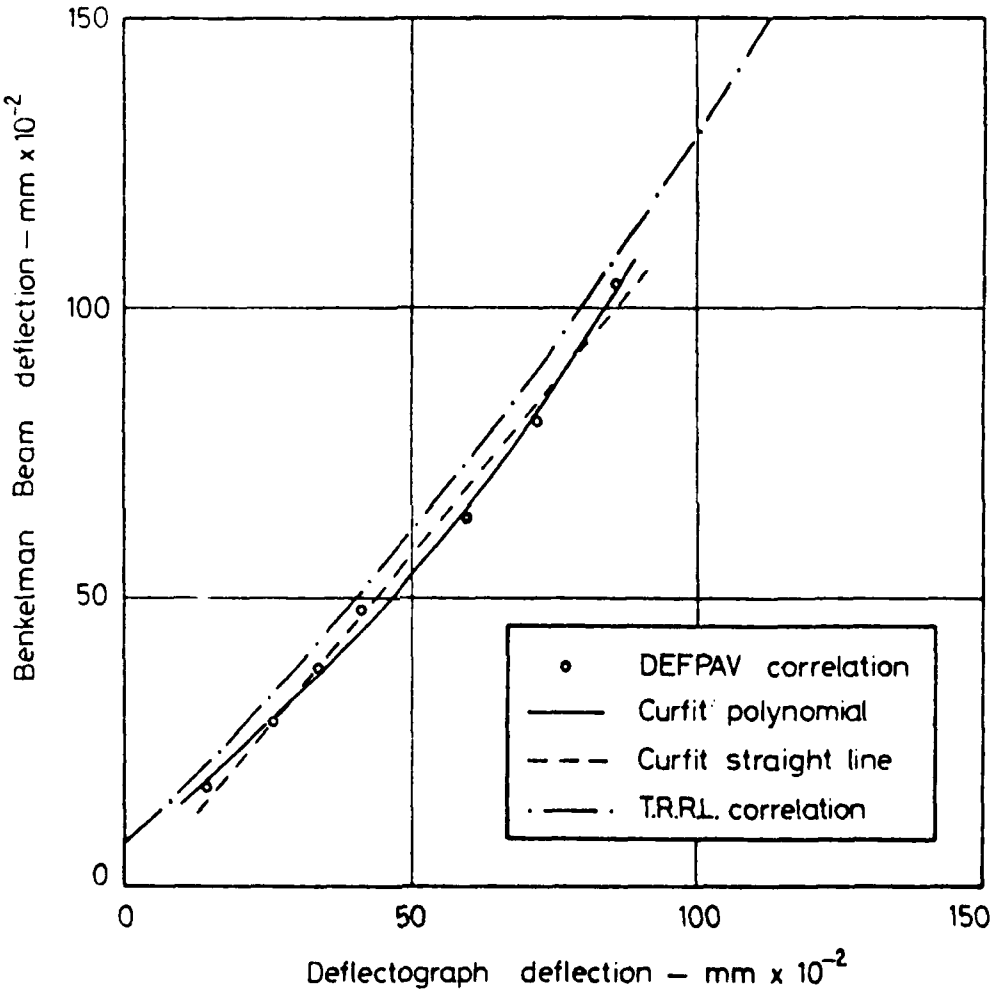

COMPARISON OF T.R.R.L. CORRELATION CURVE AND THAT DERIVED USING THE COMPUTER PROGRAM DEFPAV.

FIG. 58

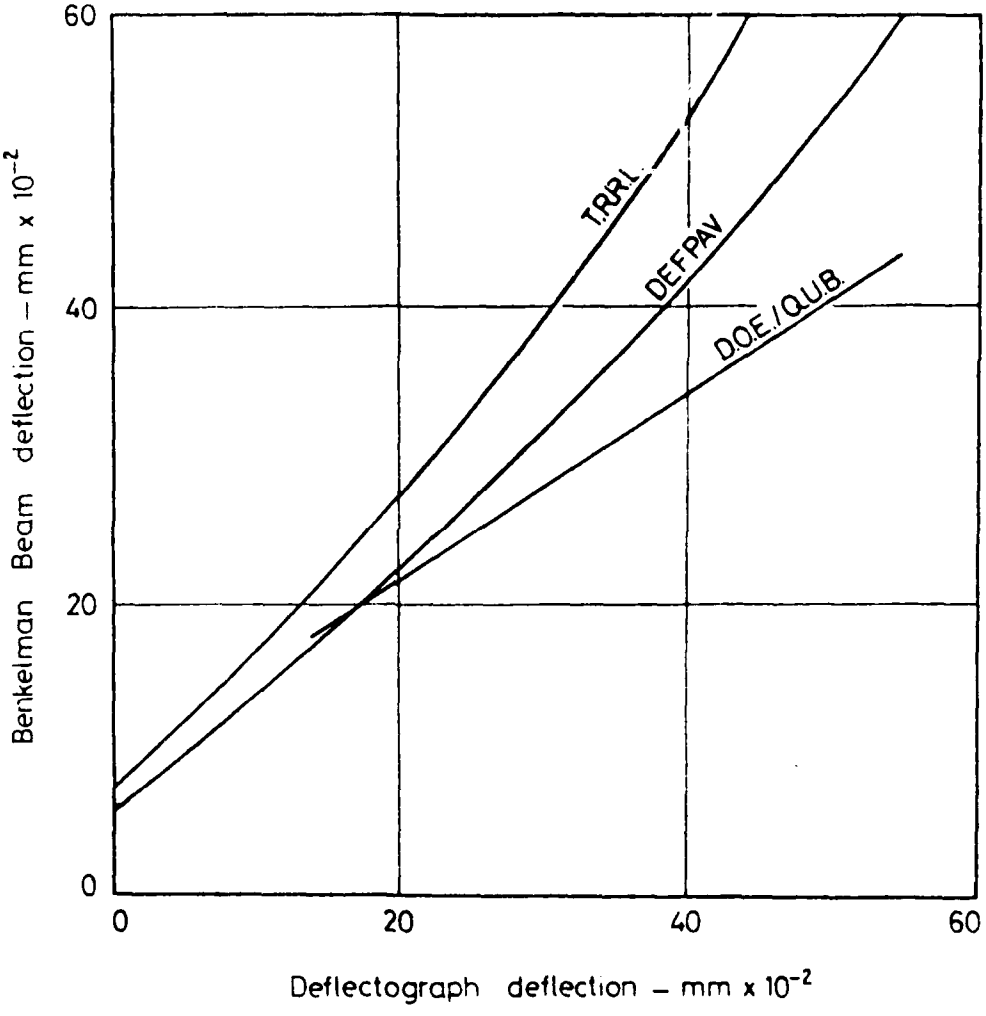

COMPARISON OF T.R.R.L., D.O.E./Q.U.B. AND DEFPAV CORRELATION CURVES (AFTER SHAW ET AL(42)).

FIG. 59

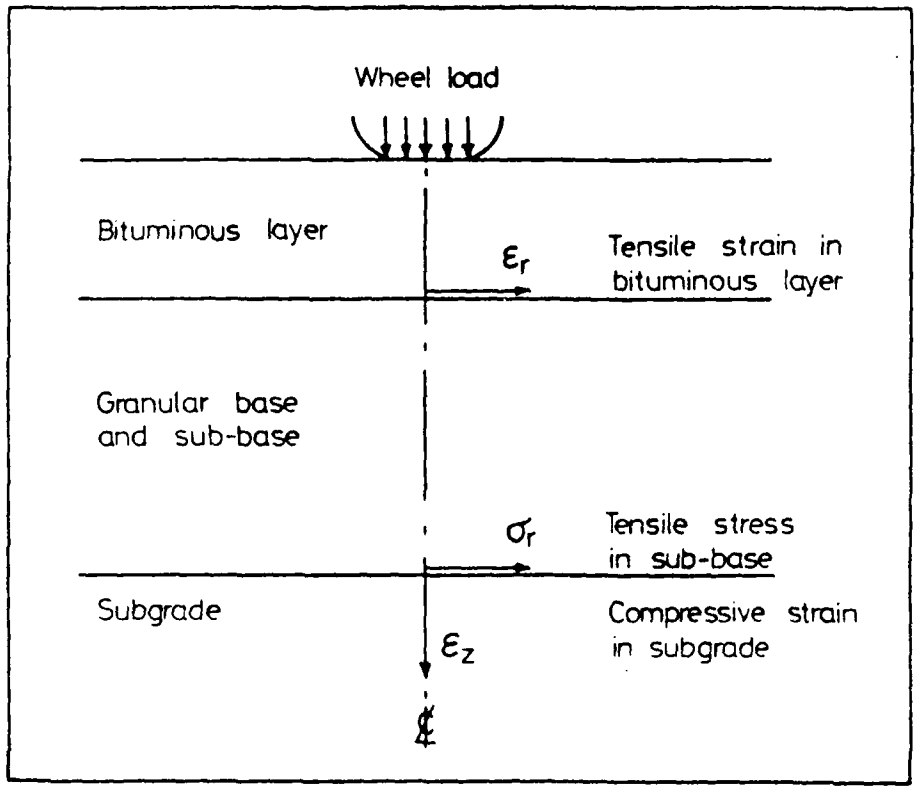

FAILURE PARAMETERS USED IN THEORETICAL PAVEMENT ANALYSIS

FIG. 60

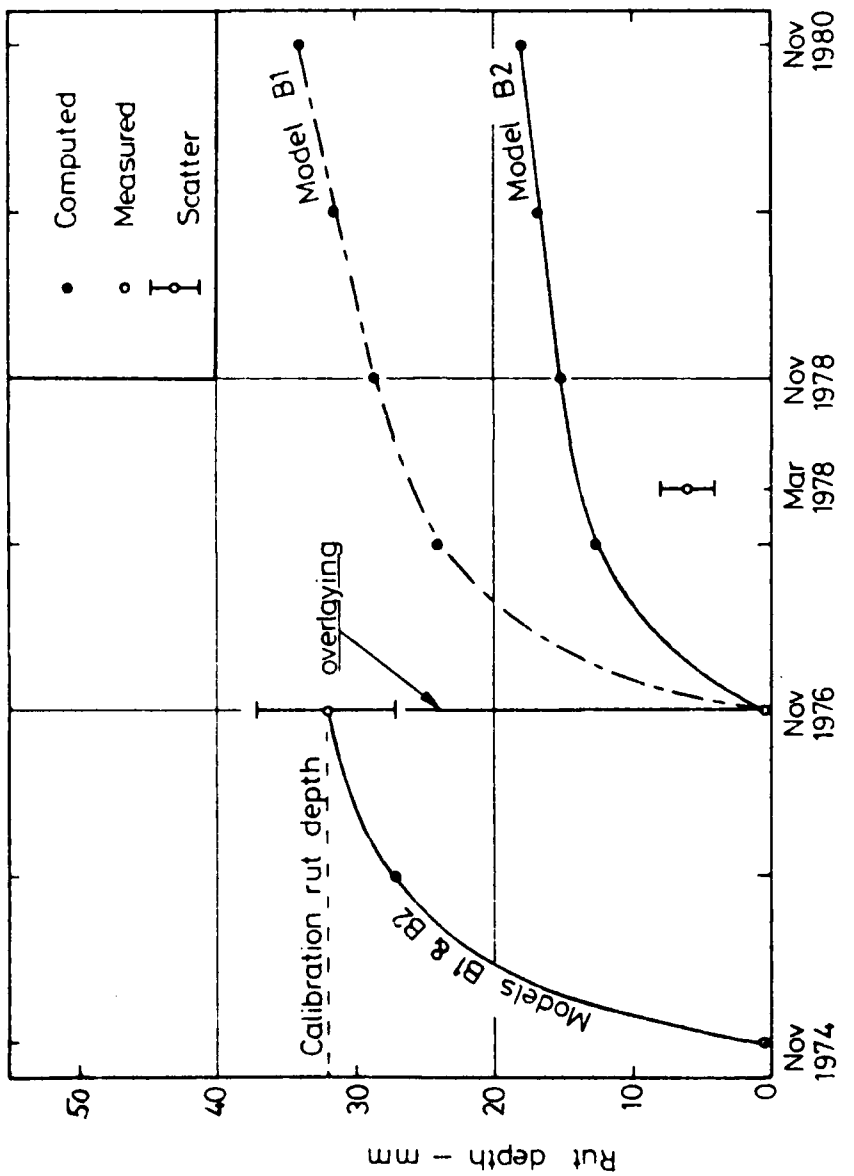

PREDICTED GROWTH OF RUT DEPTH AT HILLSBOROUGH TEST SECTION

FIG. 61

AD-A090 827 BIRMINGHAM UNIV (ENGLAND) DEPT OF TRANSPORTATION AND--ETC F/G 13/2
FLEXIBLE PAVEMENT ANALYSIS.(U)
MAY 80 M S SNAITH, D MCMULLEN
DA-ERO-78-G-125
UNCLASSIFIED
NL

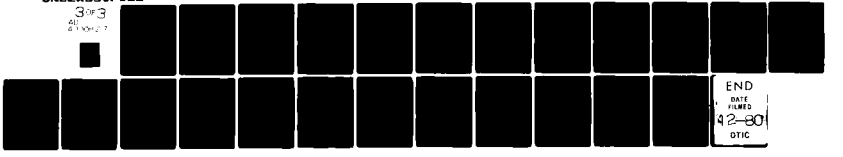

END
DATE FILMED
12-80
DTIC

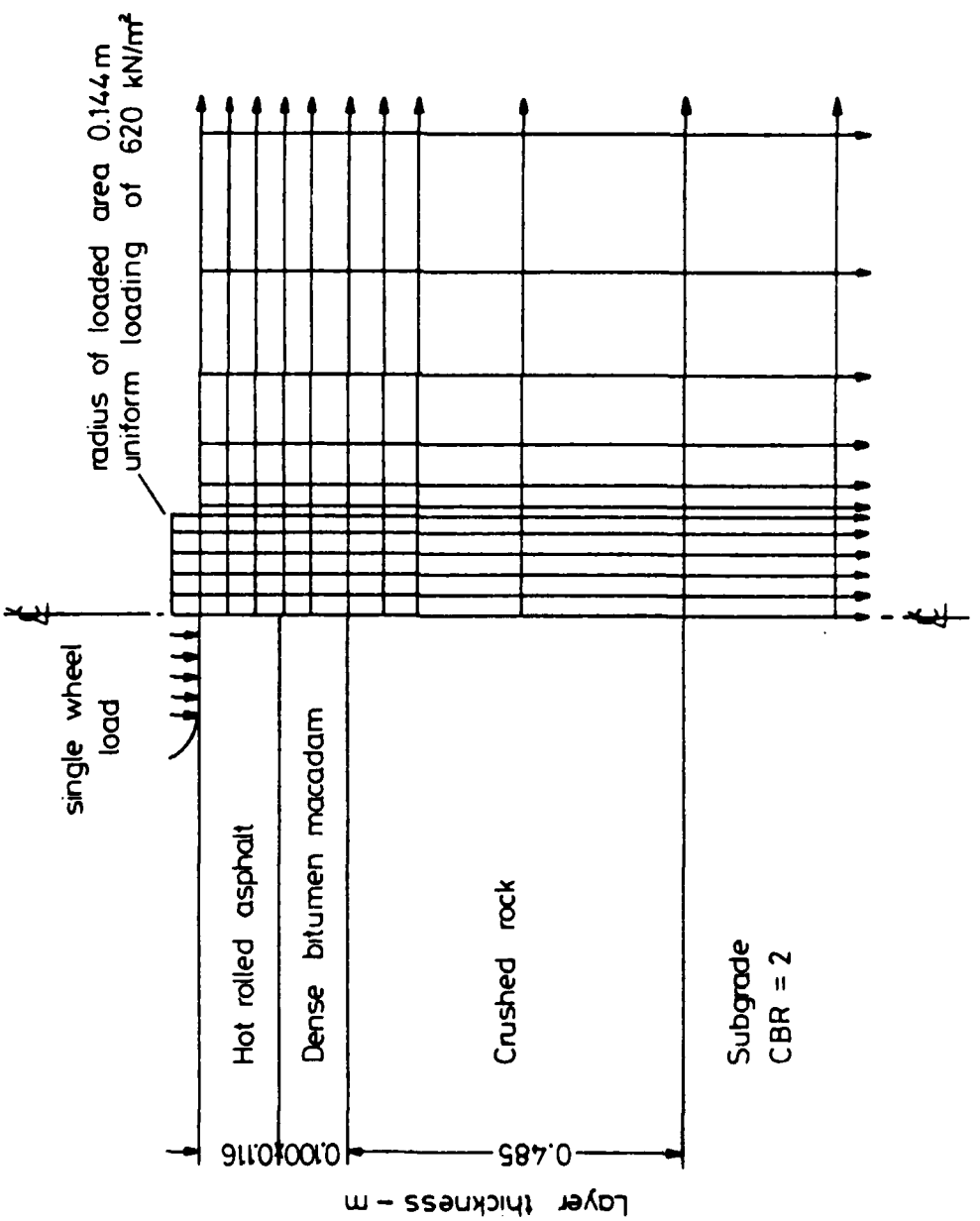

FINITE ELEMENT REPRESENTATION OF HILLSBOROUGH TEST SECTION AFTER OVERLAYING (MODEL B - 150 m TEST LENGTH) - SIMULATING STANDARD AXLE WHEEL LOAD

FIG. 62

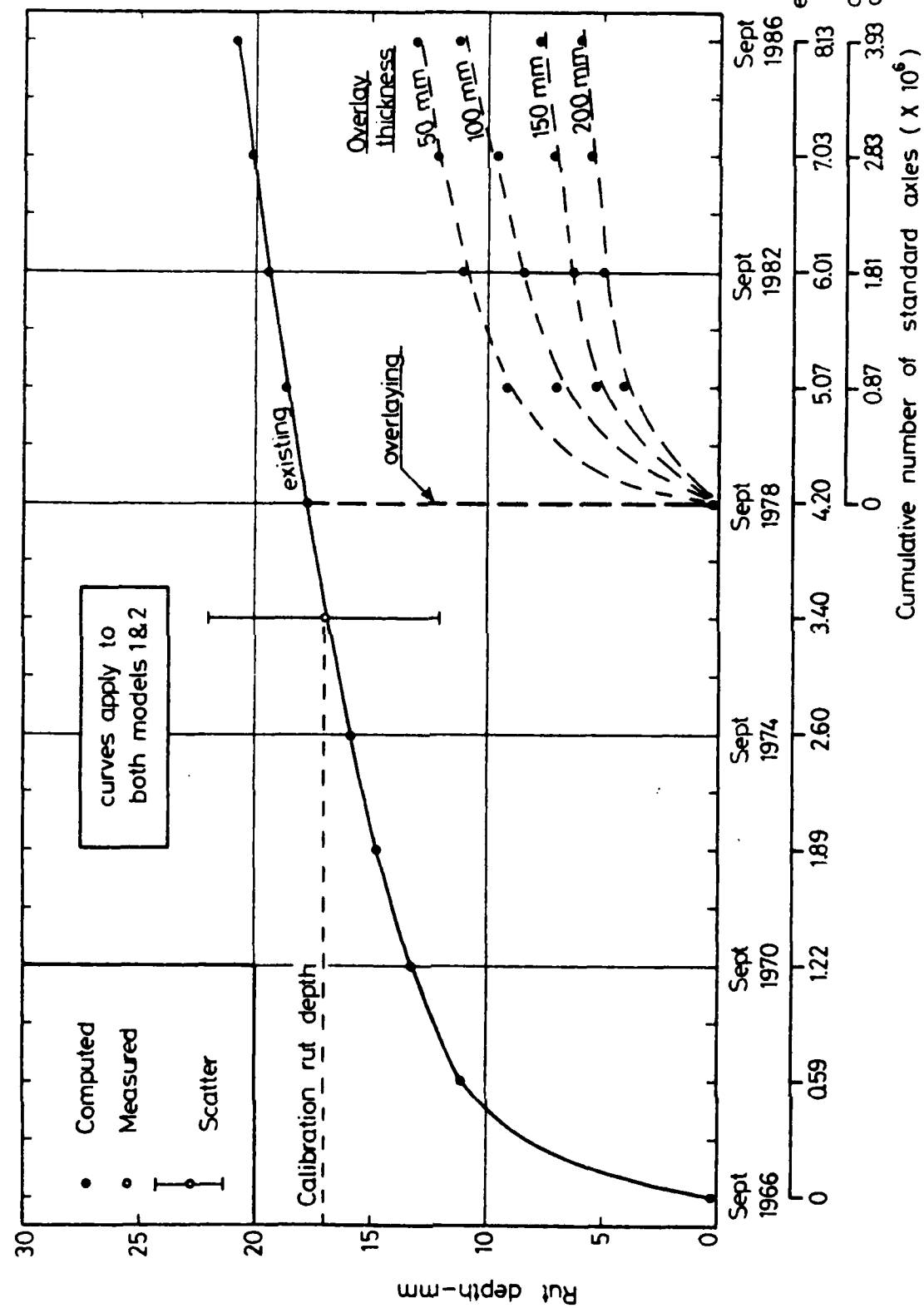

PREDICTED GROWTH OF RUT DEPTH AT M1 MOTORWAY TEST SECTION

FIG. 63

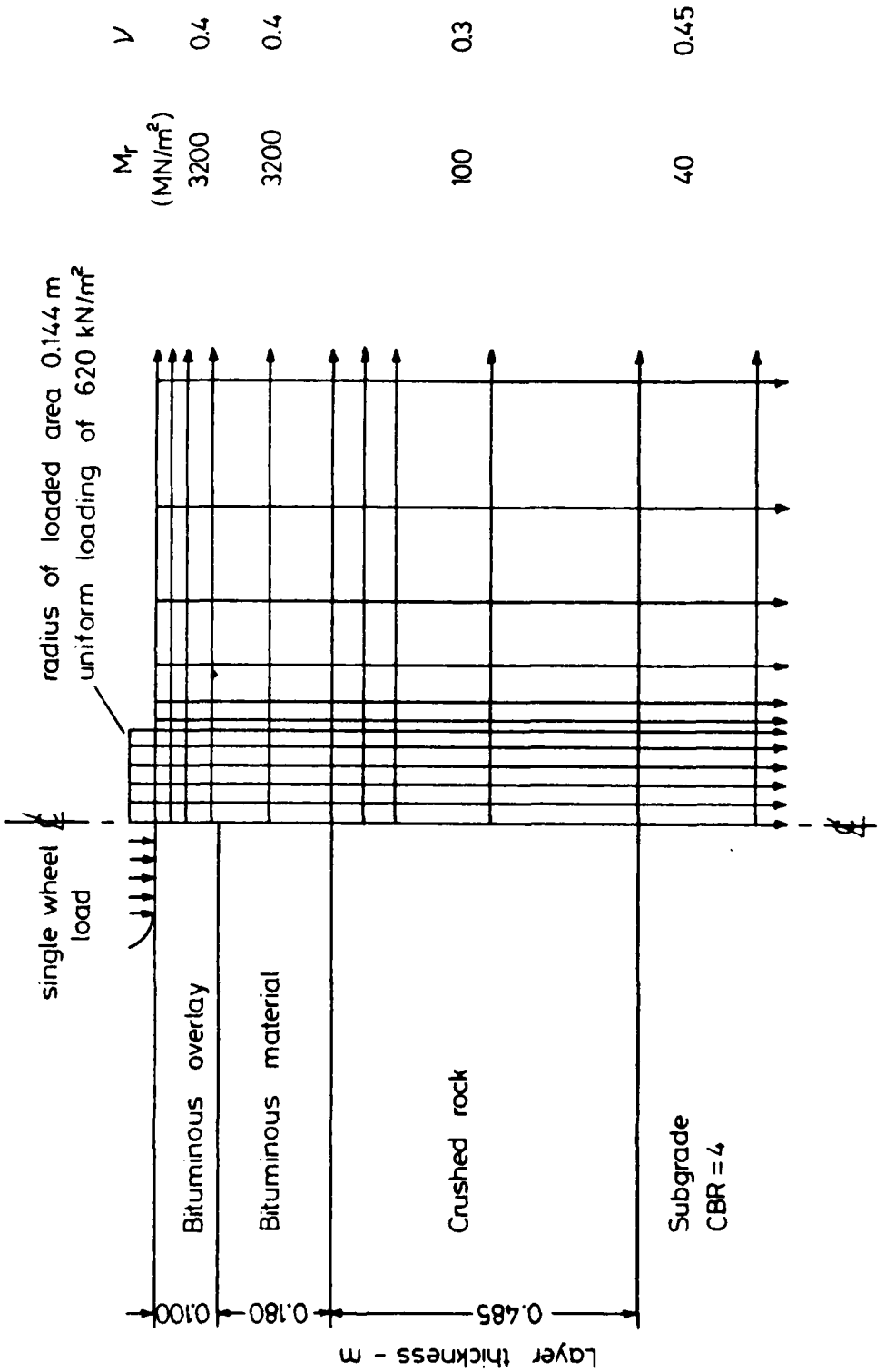

FINITE ELEMENT REPRESENTATION OF M1 MOTORWAY TEST SECTION WITH OVERLAY THICKNESS OF 100 mm – SIMULATING STANDARD AXLE WHEEL LOAD

FIG. 64

Temperature (°C)	10	20	30
Snaith (99)	7070	3720	1440
Model A	5800	2750	750

Modulus values — MN/m^2

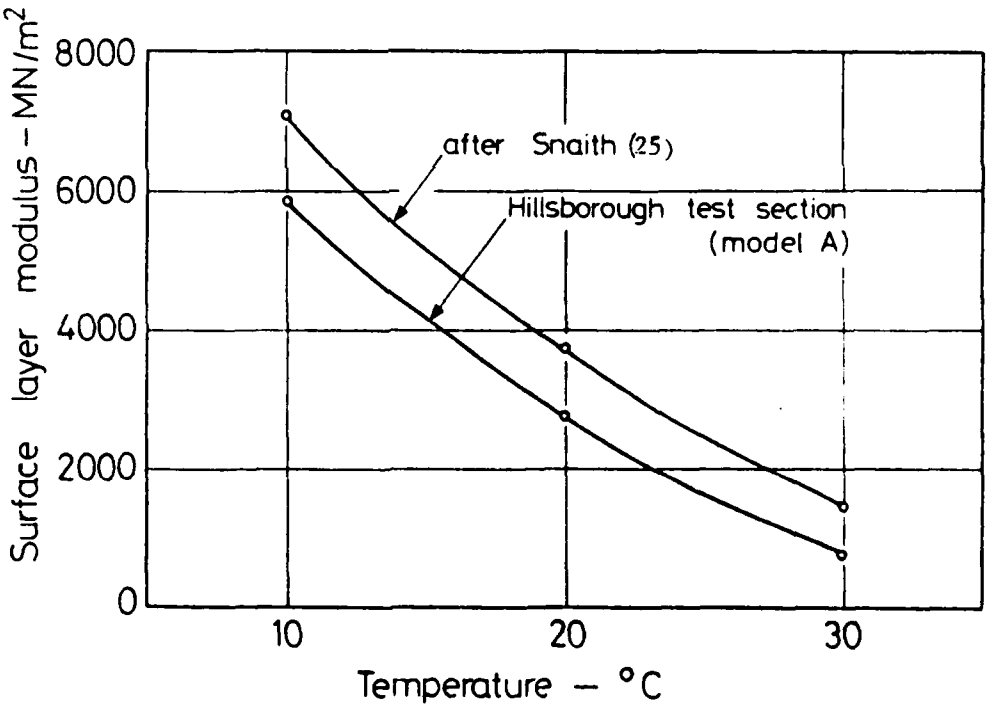

DETERMINATION OF RESILIENT MODULUS OF SURFACE LAYER AT HILLSBOROUGH TEST SECTION FOR VARIOUS TEMPERATURES

FIG. 65

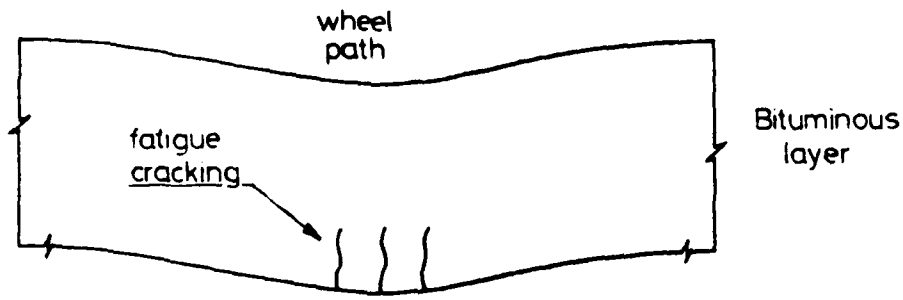

(a) Assumed mode of failure

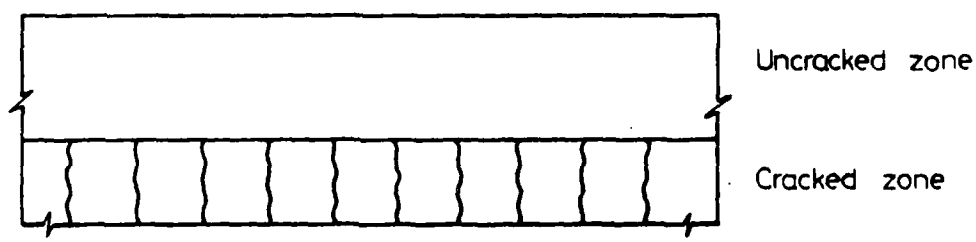

(b) Computer model

SIMULATION OF CRACK PROPAGATION THROUGH THE BITUMINOUS LAYER

FIG. 66

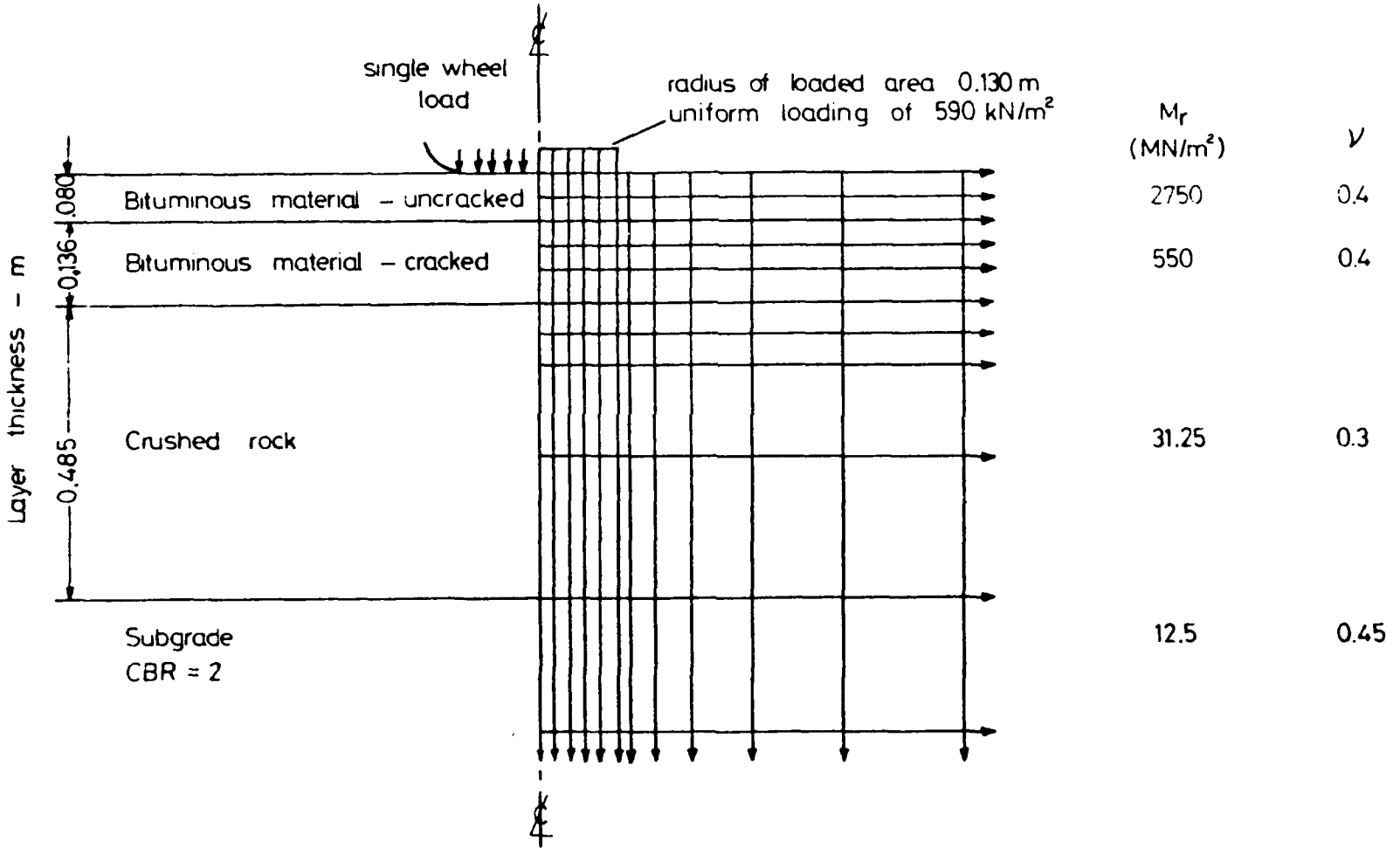

FIG. 67

FINITE ELEMENT REPRESENTATION OF HILLSBOROUGH TEST SECTION AFTER OVERLAYING (MODEL A – 20 m TEST LENGTH) WITH CRACKING RATIO 63% -SIMULATING REAR WHEEL LOAD OF BENKELMAN BEAM VEHICLE

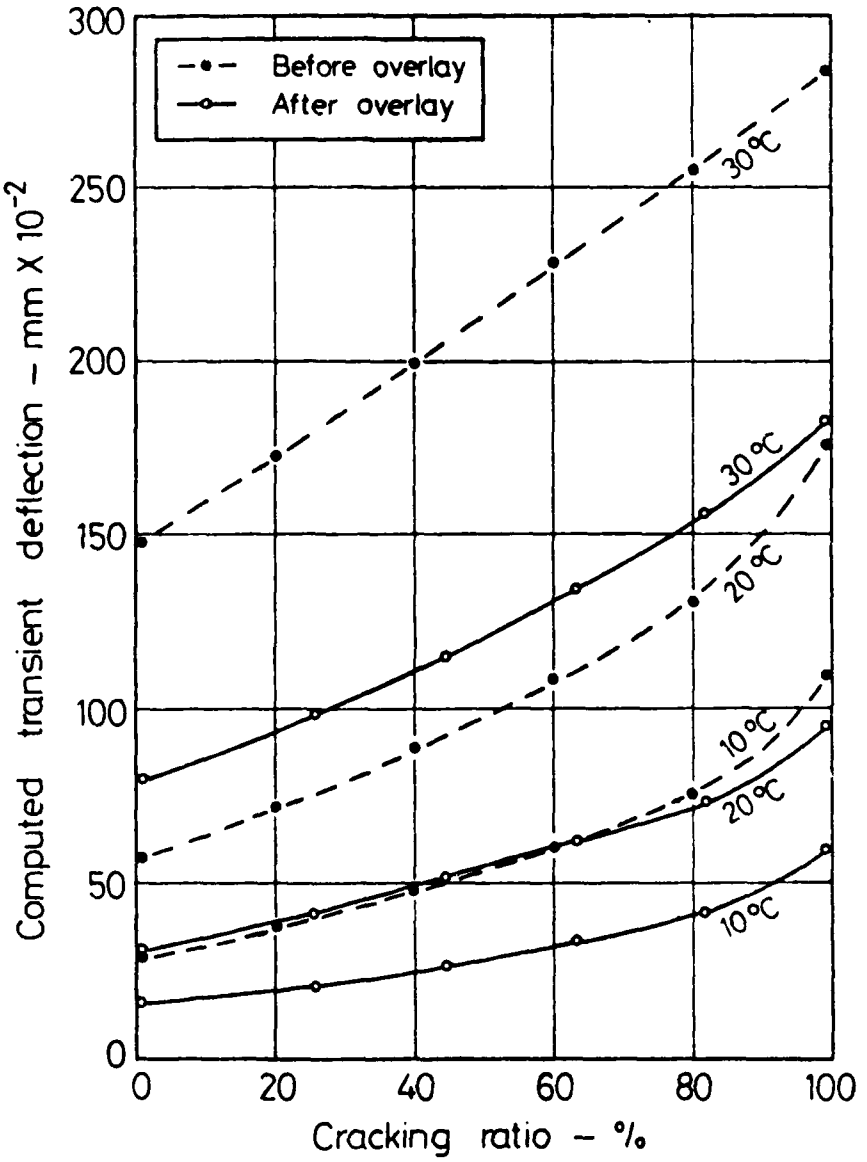

VARIATION OF COMPUTED TRANSIENT DEFLECTION WITH CRACKING RATIO

FIG. 68

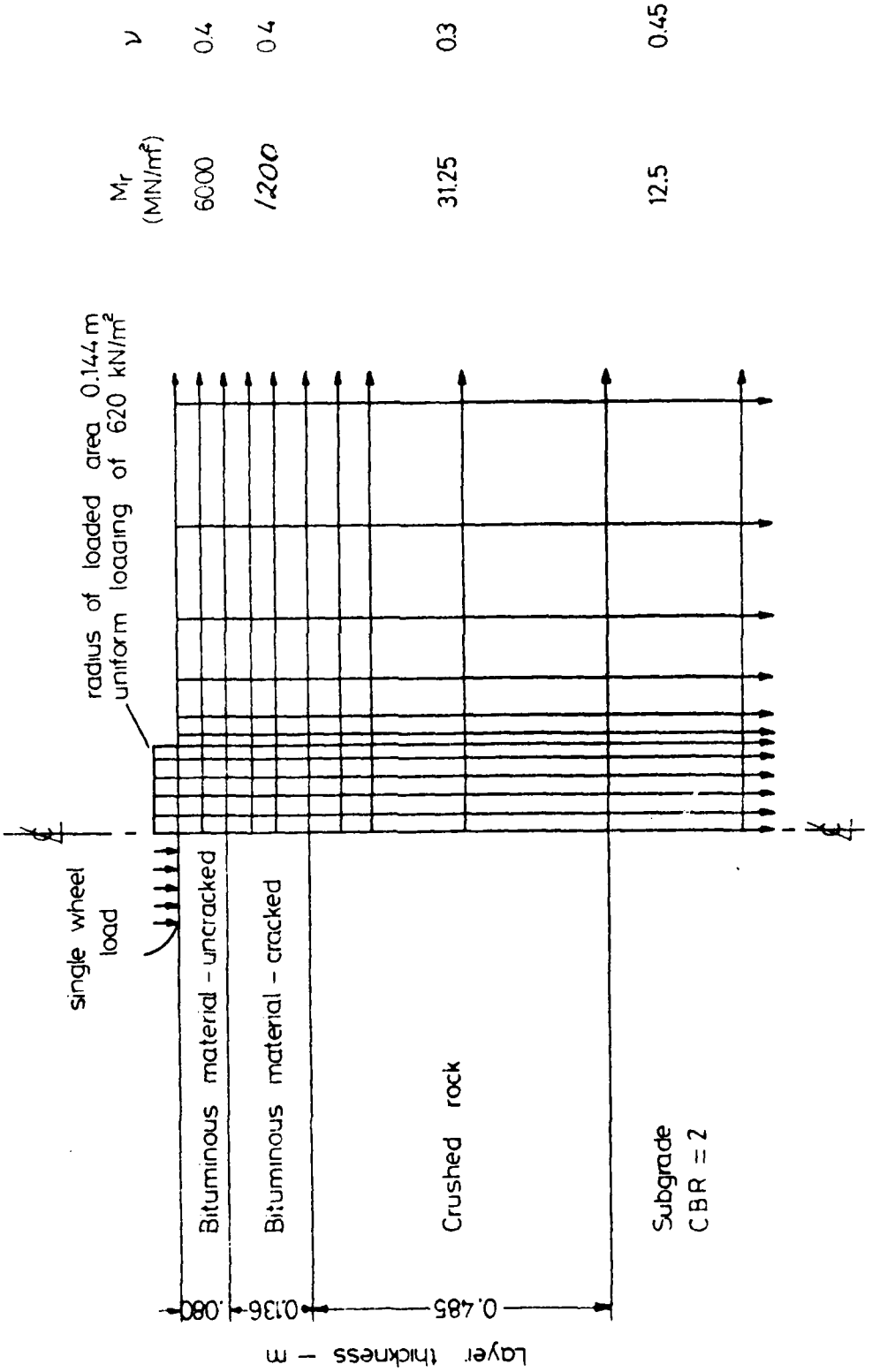

FINITE ELEMENT REPRESENTATION OF HILLSBOROUGH TEST SECTION AFTER OVERLAYING (MODEL A - 20 m TEST LENGTH) WITH CRACKING RATIO 63 % -SIMULATING STANDARD AXLE WHEEL LOAD

FIG. 69

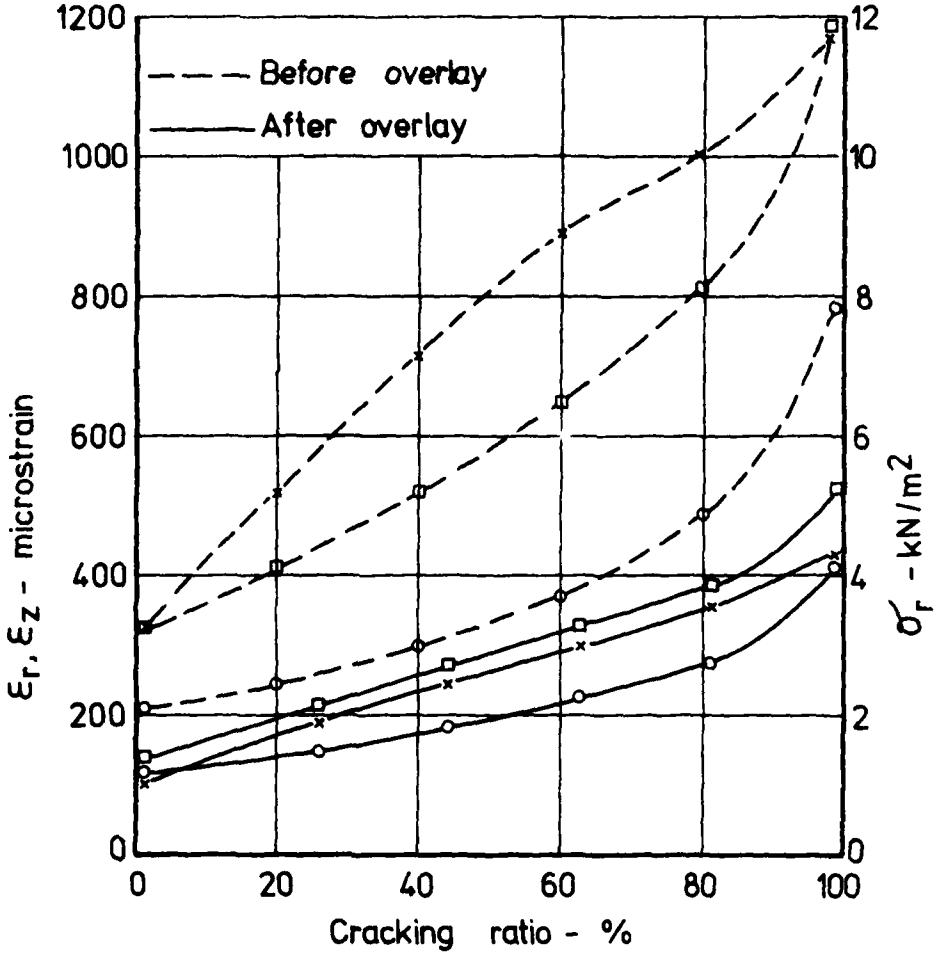

× Tensile strain in bituminous layer, ε_r

o Compressive strain at top of subgrade, ε_z

□ Tensile stress in granular layer, σ_r

VARIATION OF PAVEMENT STRESSES AND STRAINS WITH CRACKING RATIO

Fig. 70

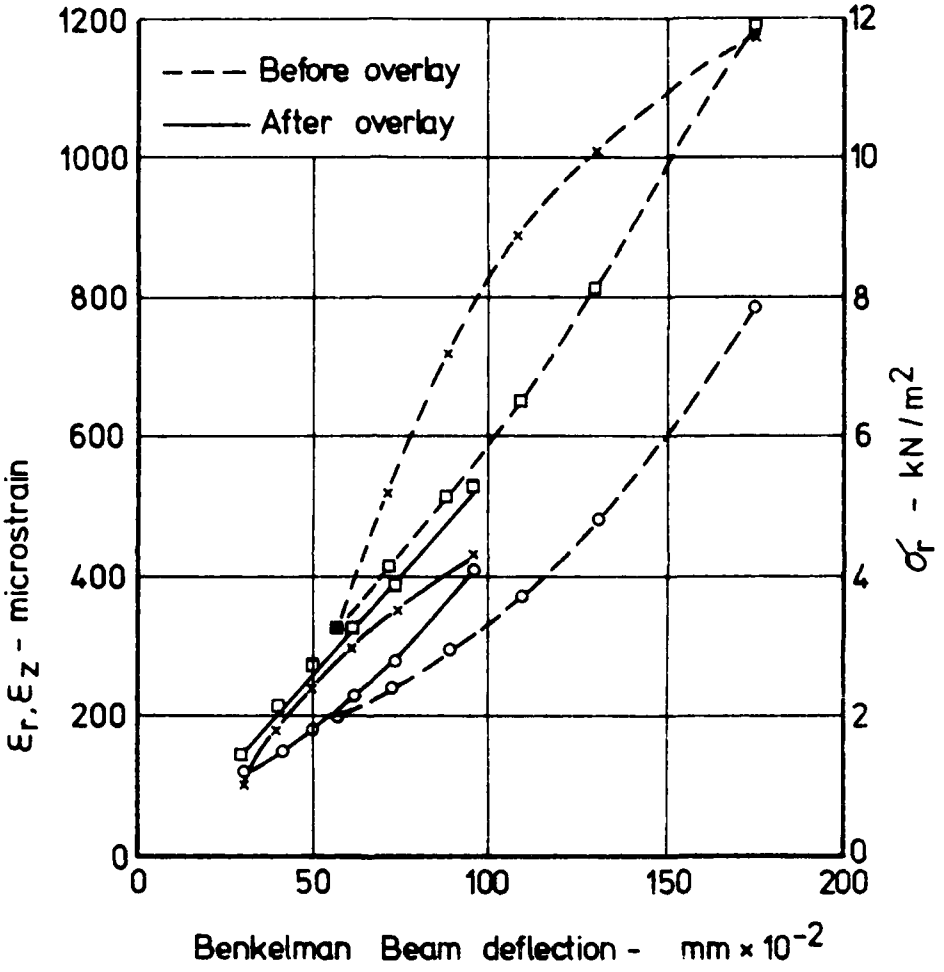

× Tensile strain in bituminous layer, ε_r

o Compressive strain at top of subgrade, ε_z

□ Tensile stress in granular layer, σ_r

VARIATION OF PAVEMENT STRESSES AND STRAINS WITH BENKELMAN BEAM DEFLECTION

Fig. 71

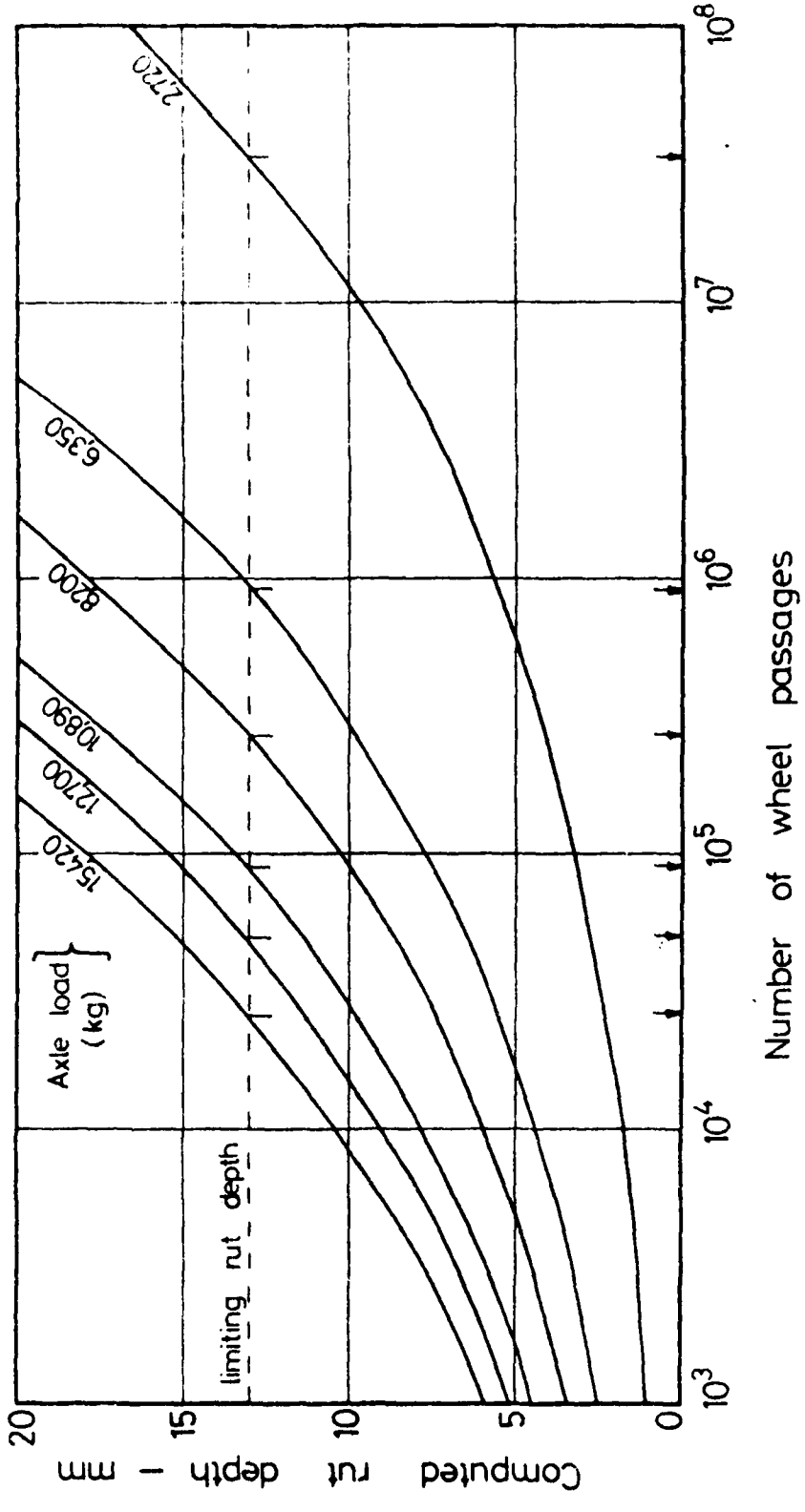

COMPUTED GROWTH OF RUT DEPTH AT THE HILLSBOROUGH TEST SECTION

FIG. 72

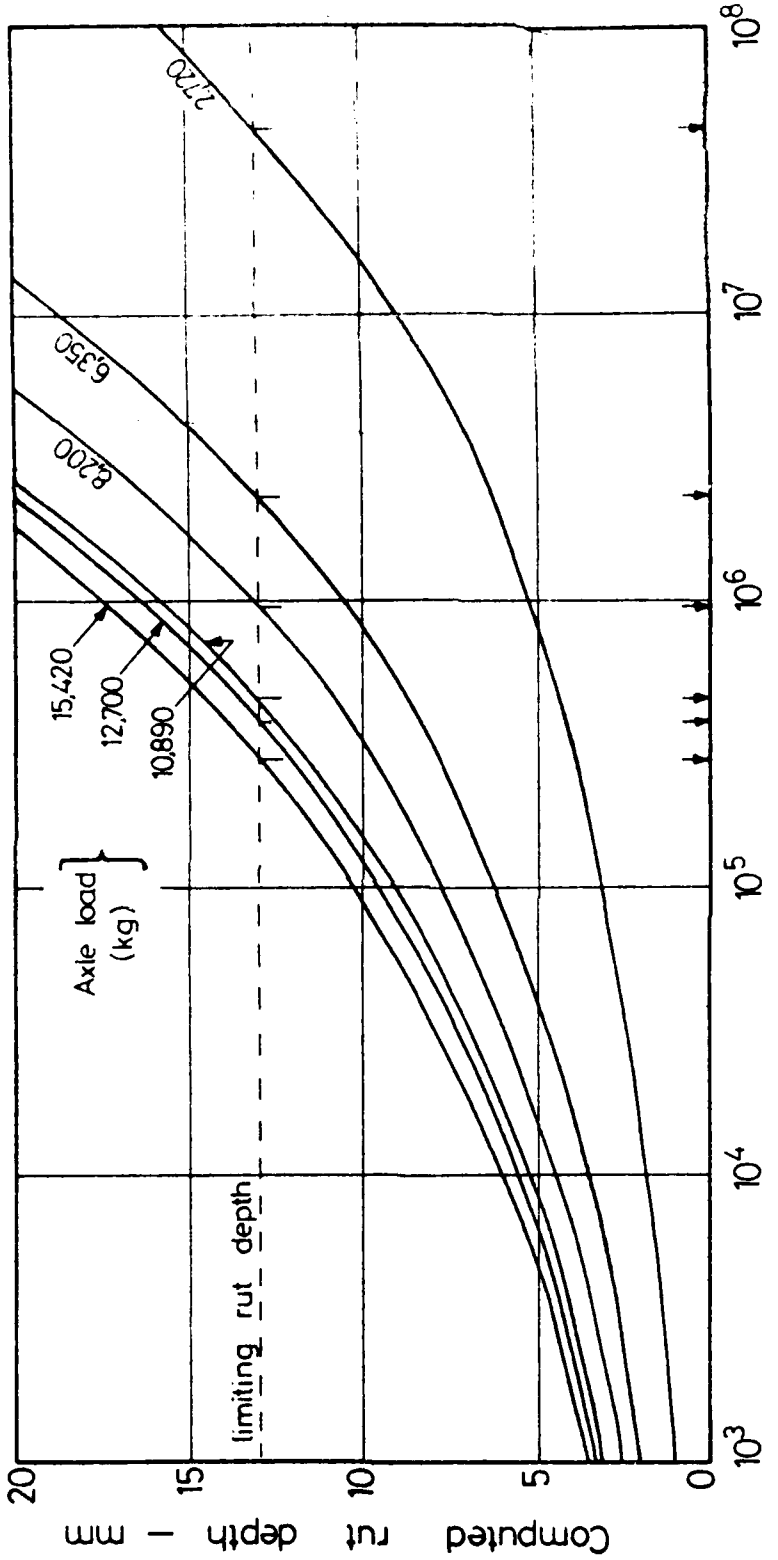

COMPUTED GROWTH OF RUT DEPTH AT THE M1 MOTORWAY TEST SECTION

FIG. 73

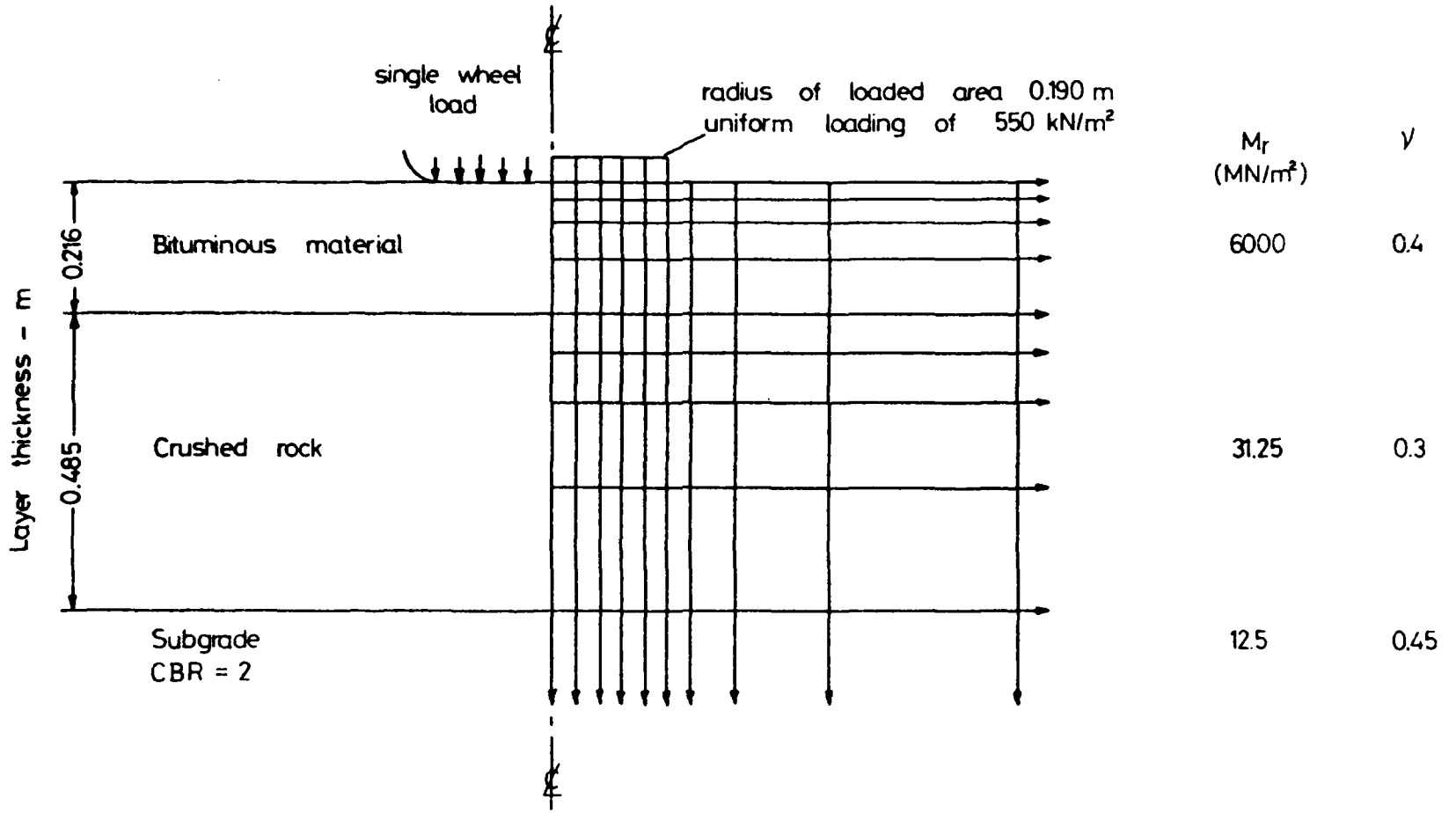

FIG. 74

FINITE ELEMENT REPRESENTATION OF HILLSBOROUGH TEST SECTION AFTER OVERLAYING – SIMULATING 6350 kg WHEEL LOAD

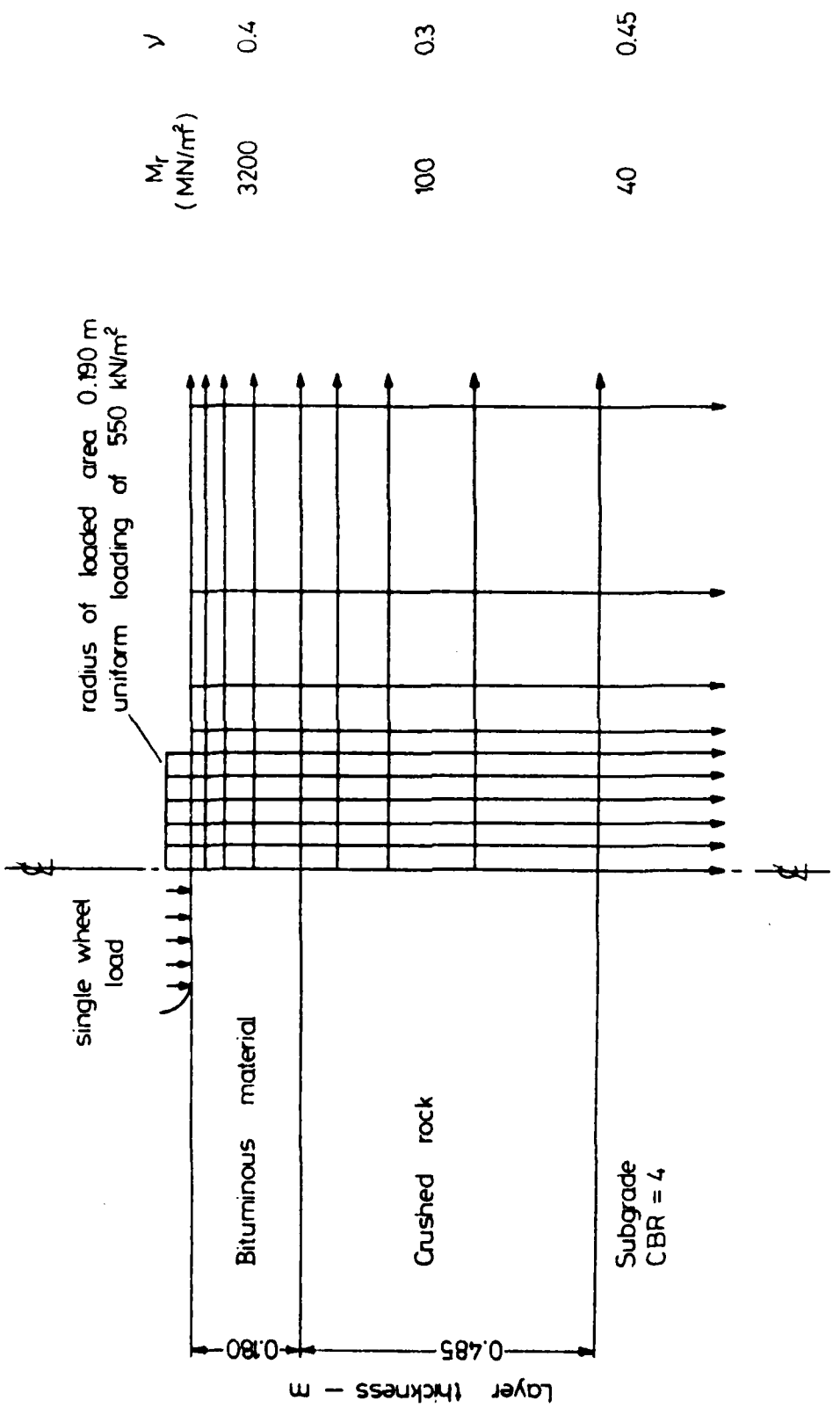

FINITE ELEMENT REPRESENTATION OF M1 MOTORWAY TEST SECTION
– SIMULATING 6350 kg WHEEL LOAD

FIG. 75

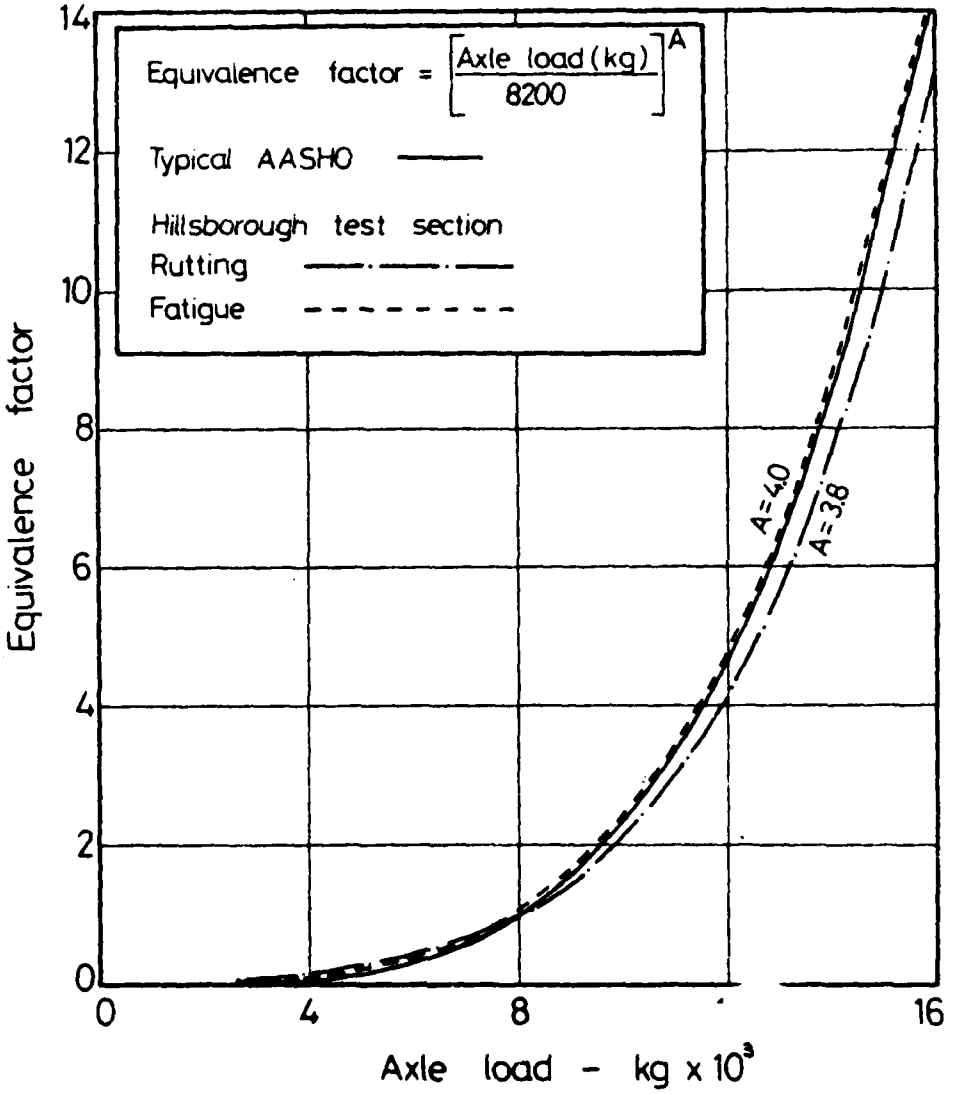

LOAD EQUIVALENCE FACTORS DERIVED FOR THE HILLSBOROUGH TEST SECTION

FIG. 76

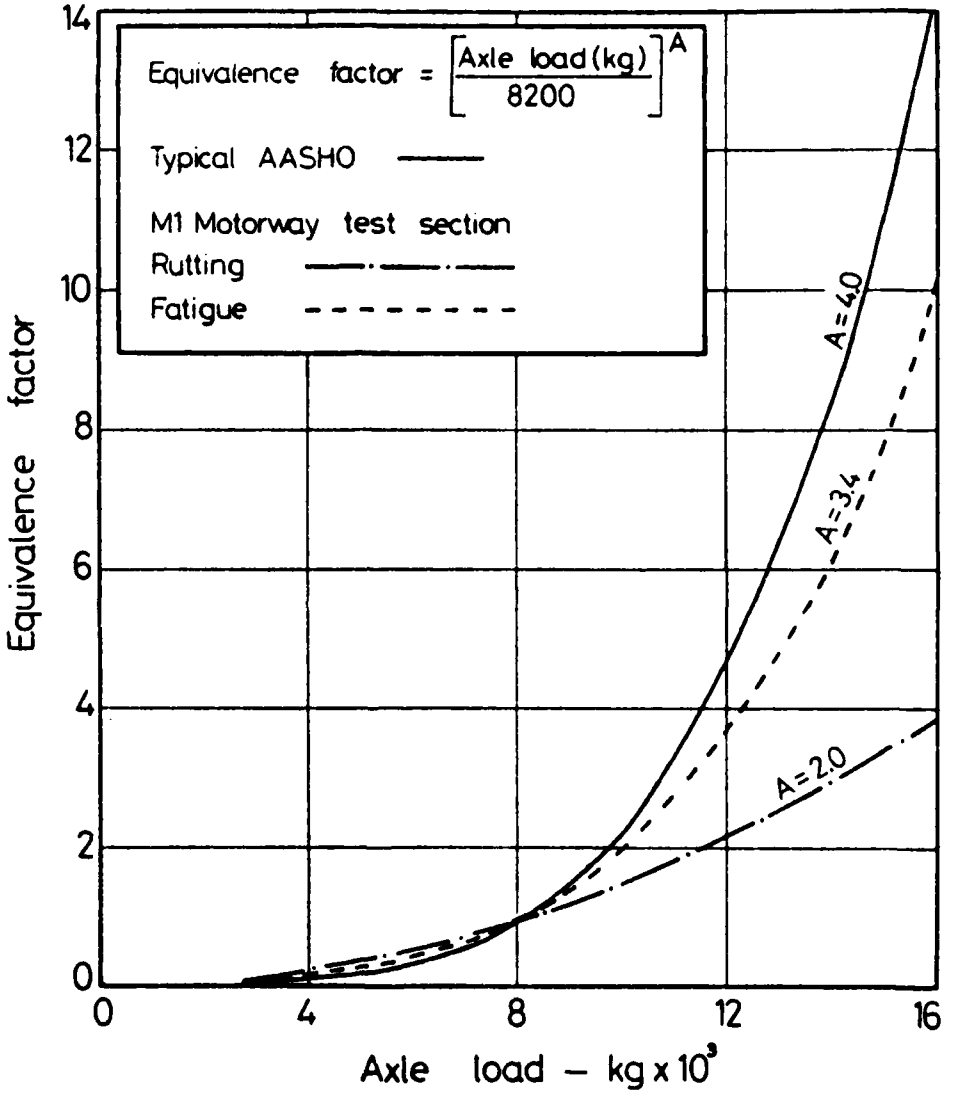

LOAD EQUIVALENCE FACTORS DERIVED FOR THE M1 MOTORWAY TEST SECTION

FIG. 77

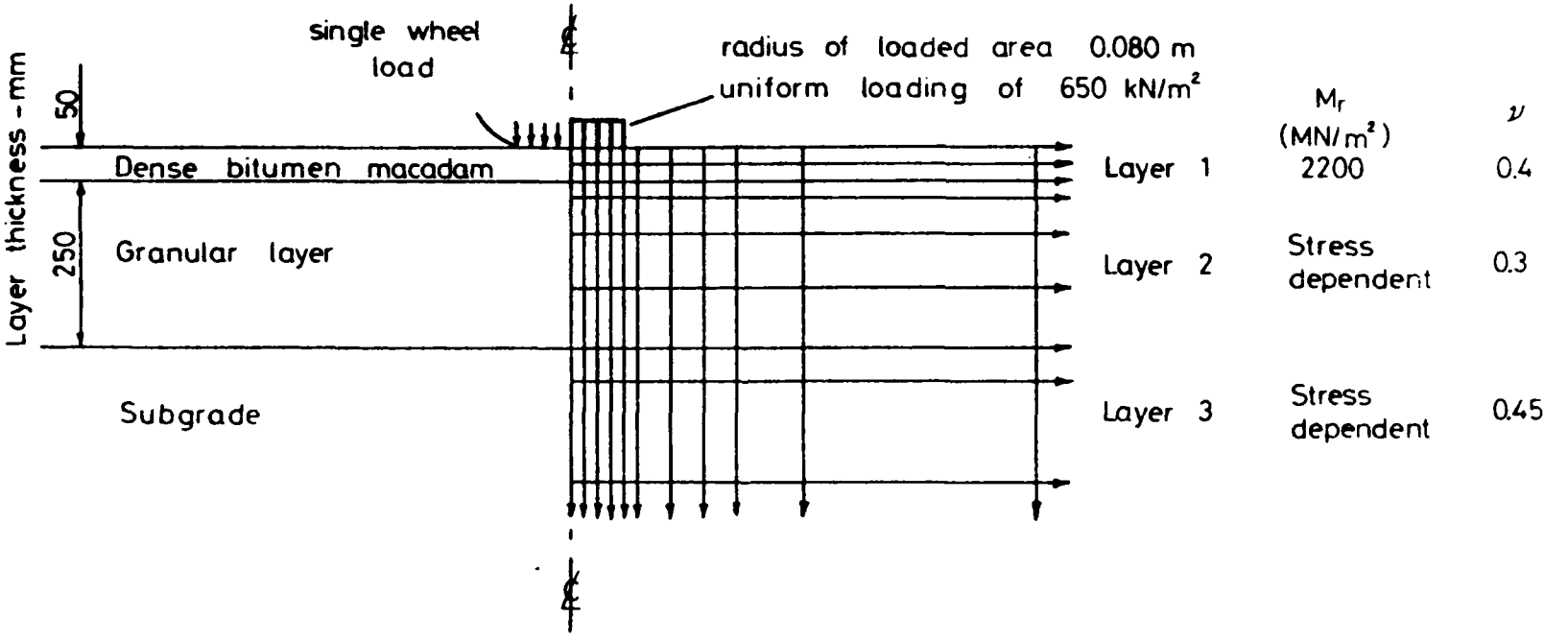

FIG. 78

FINITE ELEMENT REPRESENTATION OF PAVEMENT WITHOUT FABRIC

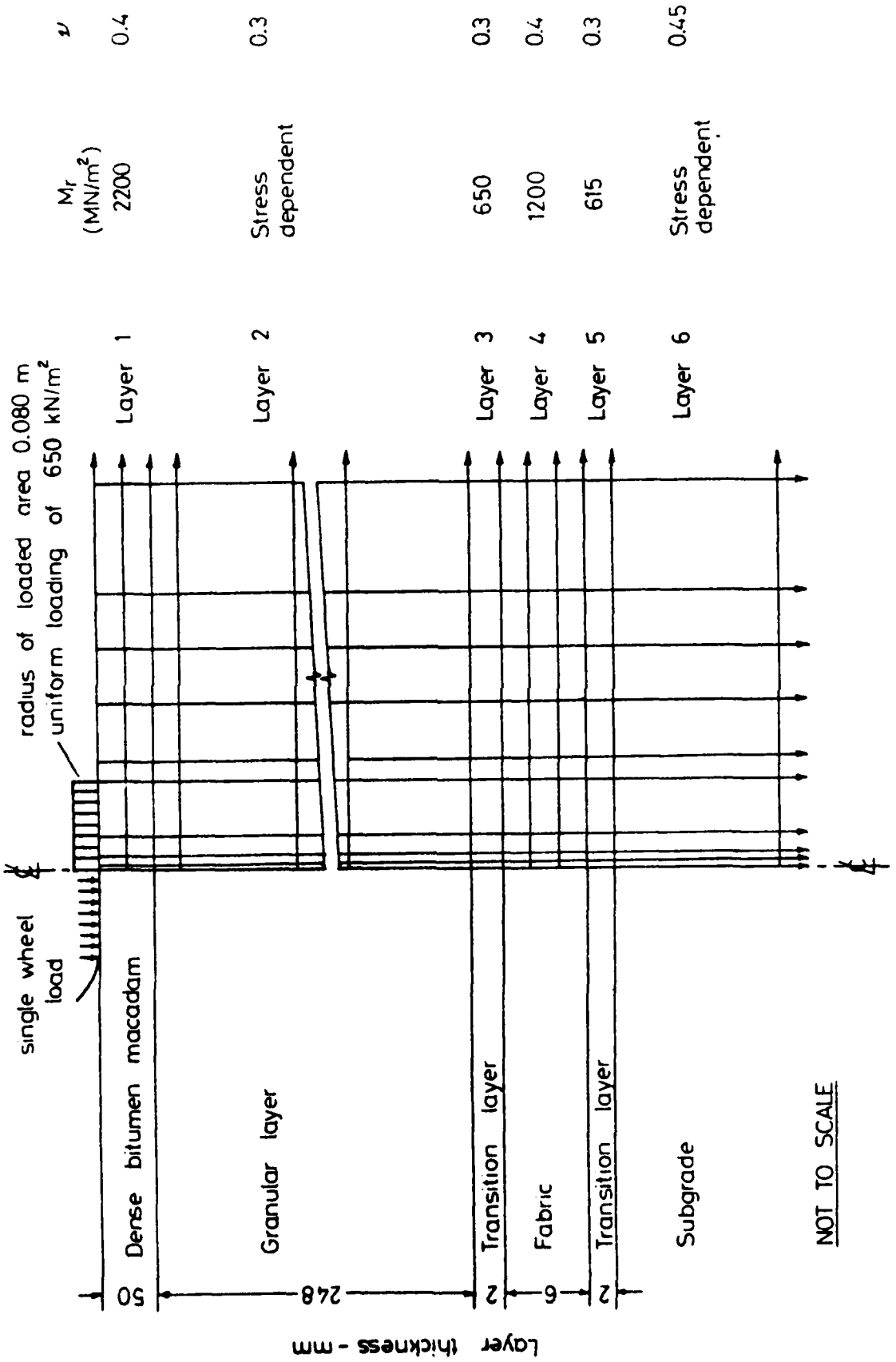

FINITE ELEMENT REPRESENTATION OF PAVEMENT WITH FABRIC

FIG. 79

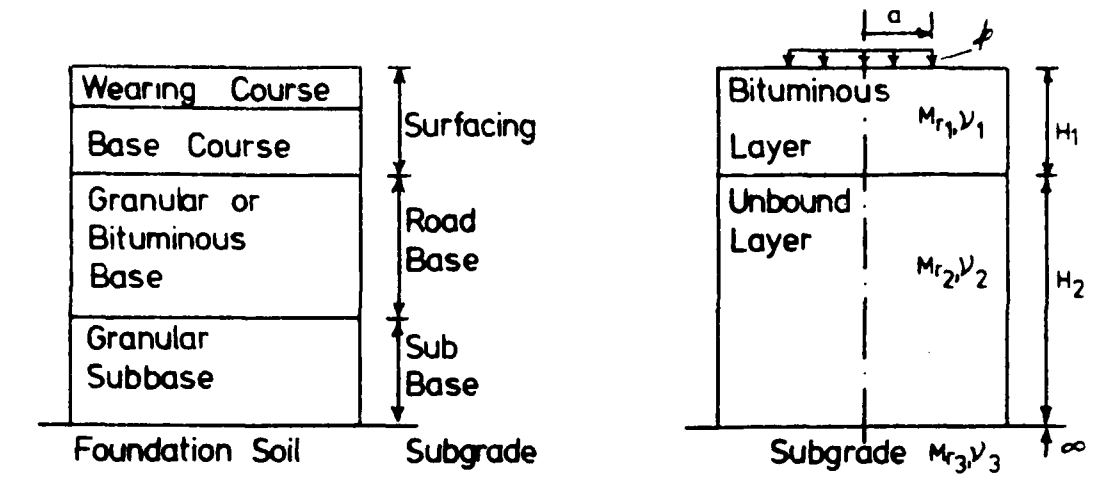

(a) Typical Pavement Construction (b) Analytical Model

Figure 80 THREE-LAYER MODEL OF A FLEXIBLE PAVEMENT

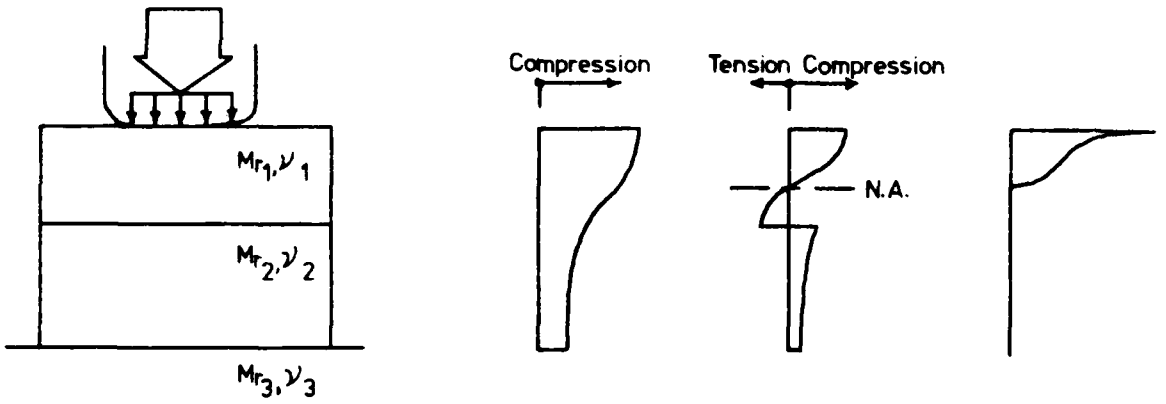

(a) Pavement Layers (b) Distribution of vertical stress under centre line of wheel loads (c) Distribution of radial stress under centre line of wheel loads (d) Surface deflection bowl

Figure 81 GENERAL RESPONSE OF A PAVEMENT SUBJECTED TO A TRAFFIC LOAD

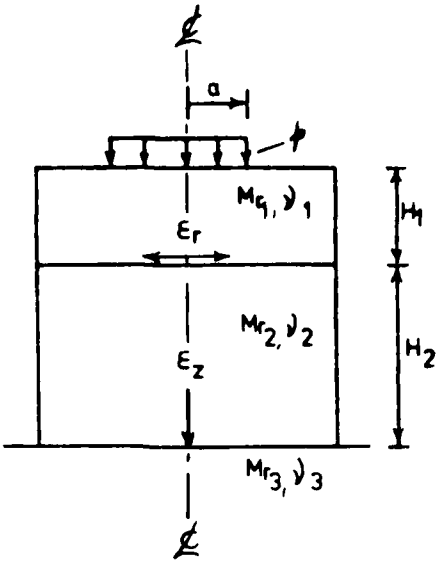

Figure 82 DEFINITION OF CRITICAL STRAINS

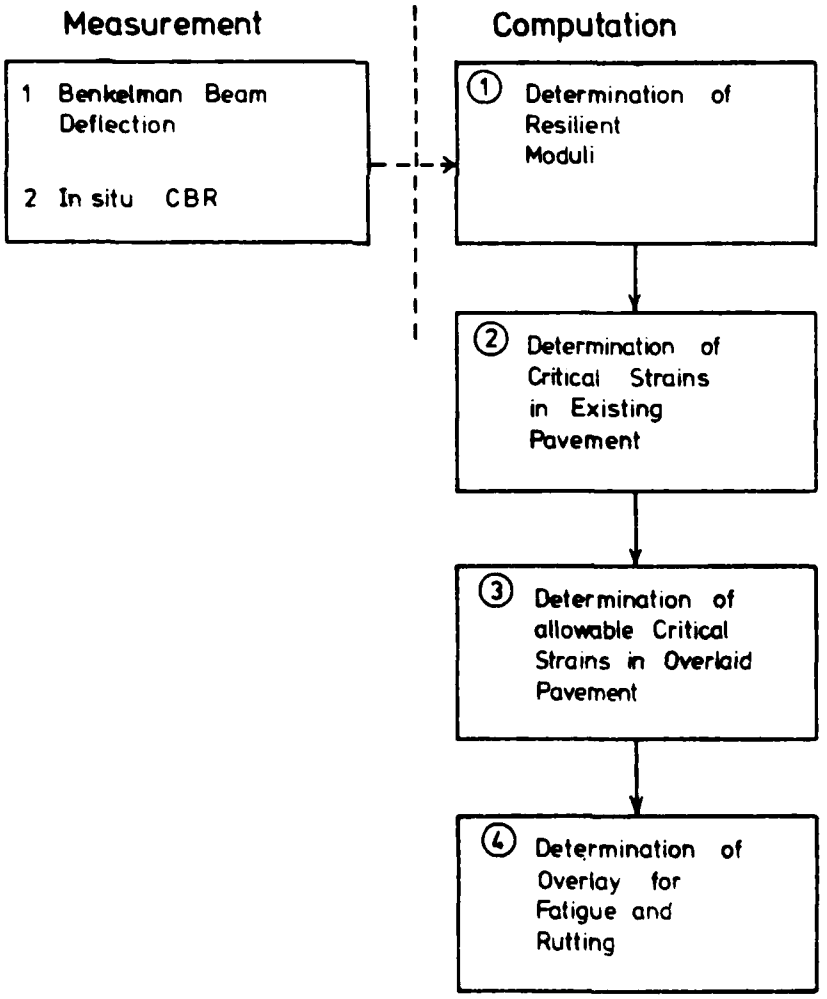

Figure 83 FLOW CHART ILLUSTRATING THE PROPOSED METHOD

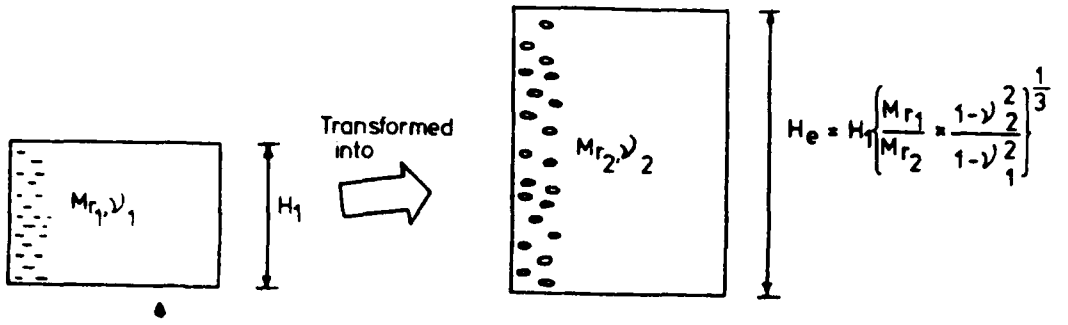

Figure 84 EQUIVALENT THICKNESS CONCEPT

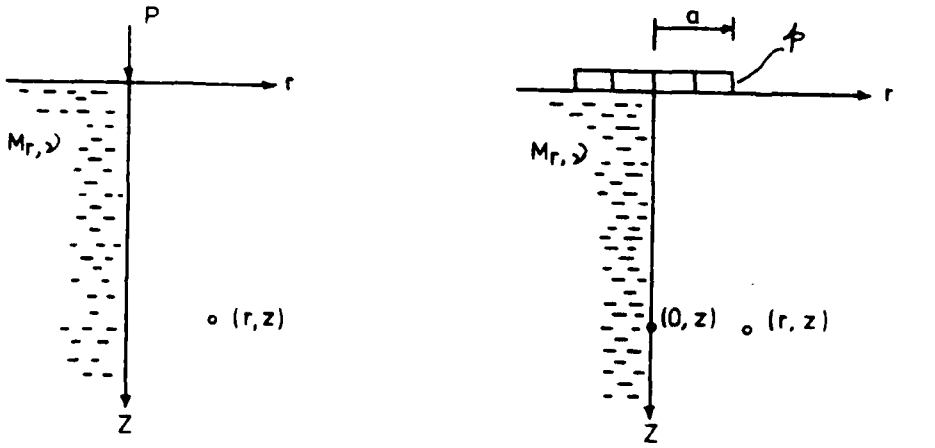

(a) A Point Load (b) A Uniformly Distributed Load

Figure 85 LOAD ON THE SURFACE OF A SEMI-INFINITE MASS

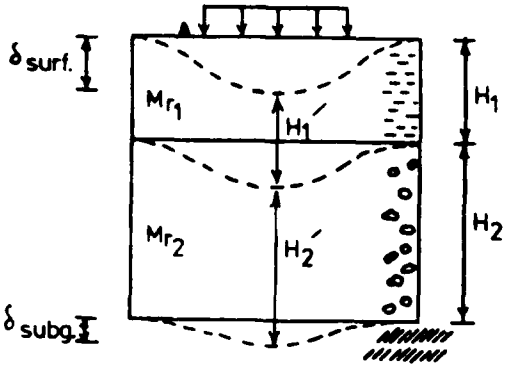

$$\delta_{surf.} = \delta_{subg.} + c_2 + c_1$$

$$c_2 = H_2 - H_2'$$

$$c_1 = H_1 - H_1'$$

(a) Pavement Layered System

$c_2 = H_2 - H_2 = \delta_1 - \delta_2$

$c_1 = H_1 - H_1' = \delta_3 - \delta_4$

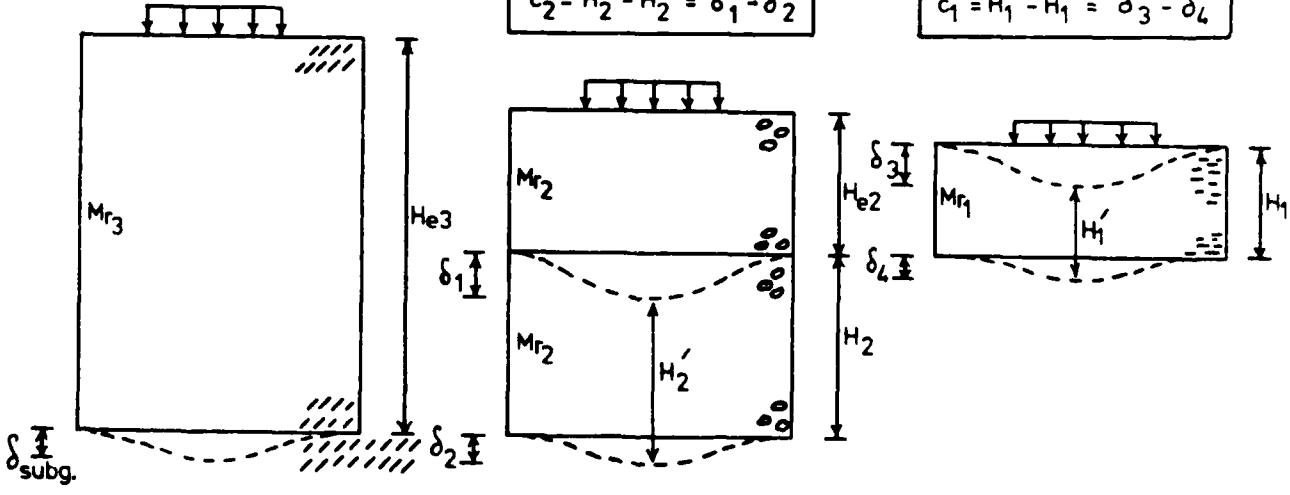

(b) Equivalent Subgrade Thickness Layer

(c) Equivalent Unbound Thickness Layer

(d) Bituminous Layer

Figure 86 COMPONENTS OF A SURFACE DEFLECTION

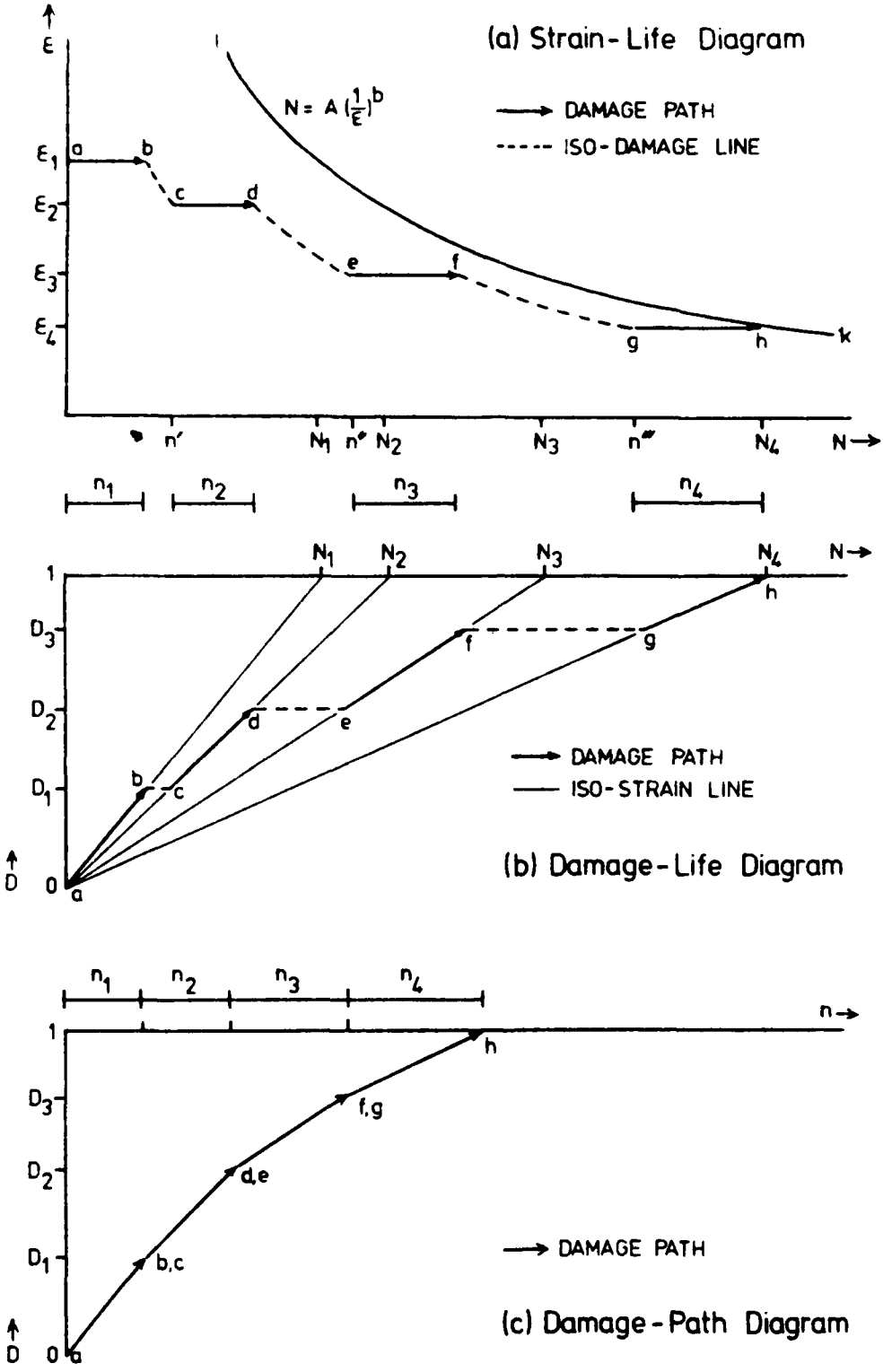

Figure 87 GRAPHICAL PRESENTATION OF CUMULATIVE DAMAGE THEORY

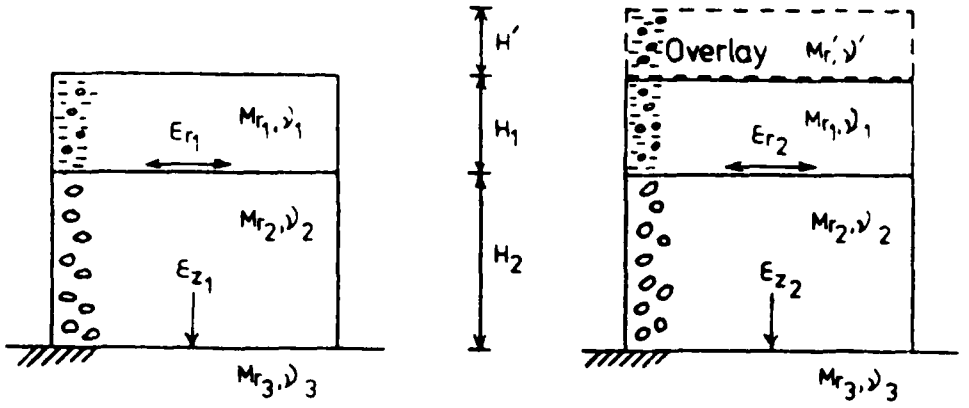

Figure 88 CHANGES IN STRAIN LEVELS DUE TO OVERLAY

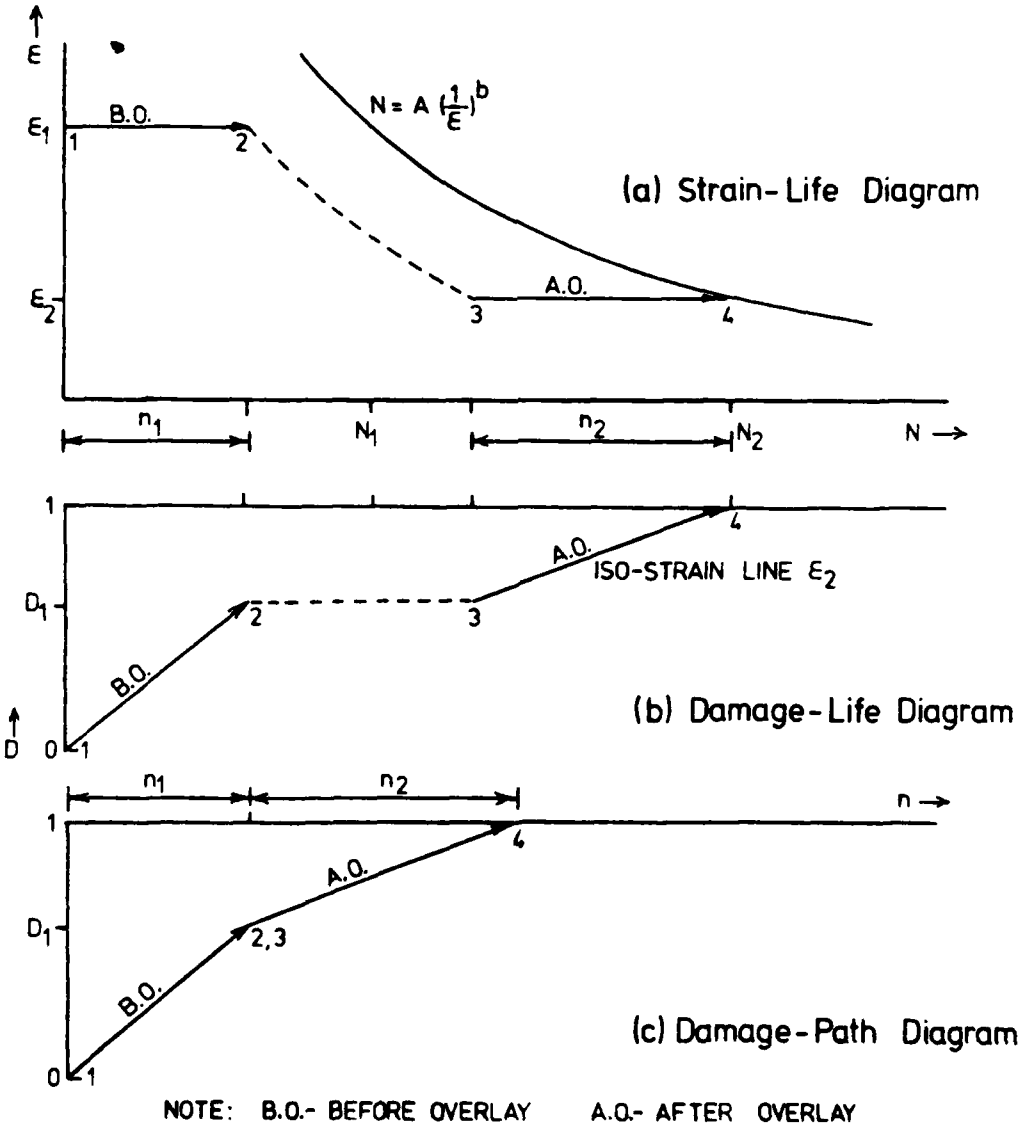

NOTE: B.O.- BEFORE OVERLAY A.O.- AFTER OVERLAY

Figure 89 DAMAGE PROCESS IN A PAVEMENT STRUCTURE WITH A SINGLE OVERLAY


FILME